Nonalcoholic steatohepatitis (NASH): Animal Studies of Interactive Hepatoxicity

Vivian Clarkson
UCT Division of Anatomical Pathology

MSc. Supervised By
Professor Pauline de la Motte Hall, Division of Anatomical Pathology
Professor David Marais, Lipid Laboratory, Internal Medicine
Professor Enid Shephard, Liver Unit, Groote Schuur Hospital

DECLARATION

I, **Vivian Clarkson**, hereby declare that the work on which this thesis is based is my original work (except where acknowledgements indicate otherwise) and that neither the whole work nor any part of it has been, is being, or is to be submitted for another degree is this or any other University.

I empower the University to reproduce for the purpose of research either the whole or any portion of the contents in any manner whatsoever.

_____ 17.11.04

SIGNATURE DATE

♠ *Thank you* ♠

I would like to express my sincerest gratitude to the long list of technical assistants, friends, supervisors and excellent scientists, without whom the project would not have been possible

Financial

University of Cape Town Postgraduate Funding Office – for a much-appreciated scholarship

Supervisors

Professor Pauline Hall – for setting up the project and making it possible for me to spend two lovely years in Cape Town

Professor David Marais – for making space for me in his lab, making me feel welcome, teaching me about lipids and having time to answer my questions

Professor Enid Shephard – for support, encouragement, and stimulating scientific discussions; also for making inroads for me in the labs of Professors Bernard Ryffel and Frank Brombacher

I would also like to thank the supervisors for going over the thesis many times, despite demanding schedules.

Technical

My incredible sacrifice team

Marilyn Tyler (thanks also for cutting paraffin sections)

Zoe Lotz (thanks also for measurement of aminotransferases)

Lizette Fick (thanks also for lessons in immunocytochemistry and cryosectioning, and free antibodies)

Trevor Finch (thanks for excellent animal care)

Nolan Hendrix

Willem Reyneveldt

The Immunolab – for H&E, D/PAS and SR stains

Trish Papier – for teaching me immunohistochemistry

Christl Honiball – for TNFS SR stains, and for cutting sections for 4-HNE

Heather McLeod

Nafiesa Ali

Jaap Visser and the SPF Animal Unit – for excellent animal care during the TNFS

Dee Blackhurst, Marietje Levy, Pam Byrnes, Bhati Ratanje, and the Lipid Lab – for teaching me techniques, answering questions, and always having materials ready when I needed them

The Ryffel Lab – for allowing me to work in your lab and use your antibodies

Professor Frank Brombacher, Mark Simpson, Debroski Herbert and the Brombacher Lab – for making room for me in your lab, allowing me liberal use of your ELISA materials, and your fluorescent microscope

Vivienne Woodburne, Lester Davies and the helpful staff at the GSH Liver Unit

Ray Kriel – for help with computer problems of every kind…

Medical Graphics

Other

Richard Kirsch – for kindly "breaking me into" NASH
Mpho Tlali – for patiently grading and staging the STS and LTS slides with me, and for all those conversations and laughs over afternoon coffee
Hannes Holm (for being a great officemate, making me laugh, providing me with inexhaustible amounts of hot beverages, and free muffins)**, the Anatomical Pathology Registrars**
Maureen Duffield – for rekindling my passion for running

The Clarksons

My parents – for never compromising on education, and giving me opportunities to travel

Chris Clarkson (technical assistant, Grand Master of Cool, true scientist, partner in crime and fellow globetrotter) – thanks for your friendship

The NASH community

Table of Contents

Abstract

The term "Nonalcoholic steatohepatitis" (NASH) describes a form of liver disease indistinguishable from alcoholic liver disease, but present in persons who consume insignificant amounts of alcohol. The spectrum of non-alcoholic liver disease ranges from non-progressive steatosis, through to NASH and sometimes to cirrhosis. Risk factors predisposing to NASH include obesity, diabetes mellitus, hypertriglyceridemia and procedures leading to rapid and profound weight loss such as gastric bypass and bulimia. Given the high incidence of type II diabetes, obesity and various types of hyperlipidaemia in the Western Cape, NASH has become one of the most commonly encountered liver diseases in the Liver Clinic, Groote Schuur Hospital. Statistics also suggest nonalcoholic fatty liver disease underlies most cases of elevated liver enzymes in many other parts of the world. The exact pathogenic mechanisms involved are not well understood, and no effective treatment options are currently available. However, animal models of NASH now provide unique opportunities for study of this disease in the laboratory setting.

This thesis employs a dietary animal model, which restricts methionine and choline intake, to replicate aspects of the injurious process in human NASH. Two lines of inquiry are pursued. The first involves an assessment of the effect of alcohol consumption on fatty liver of non-alcoholic aetiology. Elevated liver enzymes, altered levels of lipid peroxides, and increased cytochrome P450 activity recorded in this study, suggest alcohol may exacerbate nonalcoholic fatty liver disease.

The second line of inquiry is an exploration of the role of Tumor Necrosis Factor alpha (TNFα), a cytokine implicated in pathogenesis of alcoholic liver disease and thought to be pivotal in NASH pathogenesis. The role of TNFα in the dietary model of NASH is investigated using mice lacking functional TNFα genes, as well as wild type mice in which expression of this cytokine is induced by endotoxin challenge. Endotoxin challenge does

elicit a marked inflammatory response and enhanced generation of lipid peroxides in the fatty liver, both of which may contribute to injury. However, as knockout mice still develop experimental NASH, TNFα cannot be considered the sole driving force required for the development of NASH.

This strength of the project lies in the use of a variety of techniques (in the fields of Pathology, Immunology and Lipid Biochemistry) to investigate a range of aspects of NASH. The results of the alcohol study may provide the first empirical evidence supporting the need to restrict alcohol intake in patients with NASH, while the data on TNFα is vital for illuminating the complex, (potentially) counter-intuitive role of this cytokine in NASH. Where definitive conclusions cannot be drawn from the data, the questions posited may constitute the basis for future research.

List of Abbreviations

4-HNE: 4-hydroxynonenal

ADH: Alcohol dehydrogenase

ALDH: Acetaldehyde dehydrogenase

ALT: Alanine aminotransferase

ASH: Alcoholic steatohepatitis

AST: Aspartate aminotransferase

ATP: Adenosine triphosphate

BHP: Butylated hydroperoxide:

BMI: Body mass index

C/EBP: CCAAT/enhancer binding protein

CD: Conjugated dienes

CDP-choline: Cytidine phosphocholine

CE: Cholesterol ester

CoA: Coenzyme A

CT: Computerized tomography

Ctrl: Control

CYP2E1: Cytochrome P450 2E1

CYP450: Cytochrome P450

D/PAS: Periodic acid-Schiff stain with diastase predigestion

DMII: Diabetes mellitus II

ECM: Extracellular matrix

EDTA: Ethylenediamine tetraacetic acid

FA: Fatty acid

FasL: Fas Ligand

FC: Free cholesterol

FFA: Free fatty acid

fTBARS: Free thiobarbituric acid reactive substances

G3P: Glycerol 3-phosphate

GSH: Groote Schuur Hospital

H&E: Hematoxylin and eosin

HDL: High density lipoprotein

HFE: Human leukocyte antigen class I-like

HPA: Hypothalamic-pituitary-adenocortical axis

HSC: Hepatic stellate cell

HSDI: 11β hydroxysteroid dehydrogenase I

IκKβ: Inhibitor kappa kinase beta

ICAM-I: Adhesion molecule

IFNγ: Interferon gamma

IKβ-α: Inhibitor of NFκβ

IL: Interleukin

IR: Insulin resistance

IRS: Insulin receptor substrate

ko: Knockout

LBP: Lipopolysaccharide binding protein

LCBC: Lipase-colipase-bile salt complex

LDL: Low density lipoprotein

LOOH: Lipid hydroperoxides

LP: Lipid peroxidation

LPS: Lipopolysaccharide

LPSS: Lipopolysaccharide study

LTS: Long term study

MCD: Methionine and choline deficient

MCDD: Methionine and choline deficient diet

MDA: Malondialdehyde

MnSOD: Manganese superoxide dismutase

MRC: Medical Research Council

MRI: Magnetic resonance imaging

MTP: Mitochondrial triglyceride transfer protein

NAD/NADH: Nicotinamide adenine dinucleotide, oxidised and reduced forms

NAFLD: Nonalcoholic fatty liver disease

NASH: Nonalcoholic steatohepatitis

NFκβ: Nuclear factor kappa beta

NO: Nitric oxide

$O_2^{\bullet-}$: Superoxide anion

Ob-Rb: *Ob* receptor

OH•: Hydroxyl radical

PBS: Phosphate buffered saline

PC: Phosphatidylcholine

PDGF: Platelet derived growth factor

PE: Phosphatidylethanolamine

PL: Phospholipid

PMN: Polymorphonuclear lymphocytes

PPARα: Peroxisome proliferator-activated receptor alpha

PUFA: Polyunsaturated fatty acids

RO•: Alkoxy radical

ROO•: Peroxy radical

ROS: Reactive oxygen species

SAH: *S*-adenosylhomocysteine

SAMe: *S*-adenosylmethionine

SPF: Specific pathogen free

SR: Sirus red

STS: Short term study

TBA: Thiobarbituric acid

TBARS: Thiobarbituric acid reactive substances

TCA: Tricarboxylic acid

TG: Triglyceride

TGFβ: Transforming growth factor beta

TGLp: Triglyceride lipase

TNFα: Tumor necrosis factor alpha

TNFS: Tumor necrosis factor study

tTBARS: Total thiobarbituric acid reactive substances

UCP-2: Uncoupling protein 2

UCT: University of Cape Town

UDCA: Ursodeoxycholic acid

VLDL: Very low density lipoprotein

wt: Wild type

Chapter One

Introduction I: Overview of Nonalcoholic steatohepatitis

1.1 Introducing Nonalcoholic Steatohepatitis: Definition and Scope

Ludwig *et al.* (1980) first coined the term non-alcoholic steatohepatitis (NASH) to describe a form of liver disease then considered indistinguishable from alcoholic liver disease, but present in persons who consume "insignificant" amounts of alcohol. Under numerous synonyms such as fatty liver hepatitis, non-alcoholic steatonecrosis and alcohol-like liver disease in non-alcoholics, a number of the pathological findings had been described as early as the 1950s, at a time when ileal bypass surgery was a treatment option for morbid obesity (Ludwig *et al.*, 1997). However, what would later become known as "NASH" remained obscure in the spectrum of liver disease for decades, and relevant investigations were confounded by prevailing opinions such as those ascribing characteristic hepatic lesions to post-surgical complications of bacterial overgrowth. This was in spite of findings such as those of Thaler (1971), in which the existence of a fatty liver disease resembling that of alcoholic aetiology but present in non-alcoholic, non-surgical patients, was described. The progression of nonalcoholic fatty liver to a place of prominence was further hampered by the absence of established and consistent terminology, and the fact that published features such as the Mallory body were previously considered pathognomic for alcoholic liver disease. Consequently, patients who denied a history of alcohol abuse were often dismissed as closet drinkers (Ludwig *et al.*, 1997).

Devising the descriptive term "NASH" brought the condition into sharper focus. Ludwig *et al.* (1980) defined for the first time a real and separate entity ("a hitherto unnamed disease"), and established the classical profile of the NASH patient as typically middle aged, female and moderately obese, often with obesity-related diseases such as diabetes mellitus. Patients in this study denied alcohol abuse and most consumed on average less than one drink per week. In this landmark paper (Ludwig *et al.*, 1980), macrovesicular

fatty change "fatty cysts" were noted in all patients, primarily in zones 2 and 3 of Rappaport.

It has since become clear that the histopathological definition of NASH is subject to a wider range of interpretation than originally thought. The essential requirements for a diagnosis of NASH, relating to steatosis (quantity and location), ballooning degeneration of hepatocytes, inflammation (localization, composition and quantity), and the presence of fibrosis and Mallory bodies, still foster some debate. In many studies, mild focal macrovesicular steatosis (with steatosis defined as triglycerides exceeding 5% of liver weight [Mach, 2000]), and lobular inflammation (composed mainly of mononuclear cells) have been considered sufficient for diagnosis of NASH. Others have insisted on the presence of ballooning degeneration, and others still required neutrophils with or without fibrosis (Brunt *et al.*, 1999; Brunt, 2001). The quantity of alcohol considered to be "insignificant" also varied, ranging from <20g/day to 210g weekly (Bacon *et al.*, 1994; Teli *et al.*, 1995; Brunt *et al.*, 1999; Brunt, 2001). This final point presents a challenge if one must determine how much, if any, of the damage observed and attributed to NASH is actually the result of alcohol-mediated hepatoxicity.

Clearly, a moderate consensus must be reached, for if the requirements for consideration are too broad, patients may be inappropriately diagnosed. If requirements are too strict, only the severest cases would be considered eligible, presenting a narrow and misleading picture. Criteria continue to differ between publications, which may offer one reason for differing observations among various investigations. The term nonalcoholic fatty liver disease (NAFLD) may come to represent a more comprehensive and useful description, and subdivided into categories it takes into consideration the range of disorders encompassing everything from bland steatosis, to the features commonly identified with

NASH (i.e. NAFLD types 3 and 4), as shown below (Matteoni *et al.*, 1999):

Type 1: Steatosis
Type 2: Steatosis plus lobular inflammation
Type 3: Steatosis, lobular inflammation plus ballooning degeneration
Type 4: Steatosis, ballooning degeneration, Mallory bodies, ± fibrosis

For the purpose of this study, we have adapted the definition of Brunt *et al.* (1999), Matteoni *et al.* (1999) and Brunt (2001), in which NASH is viewed as **an idiopathic, chronic form of liver disease present in persons who consume an insignificant amount of alcohol (<20g/day), characterised by steatosis, lobular inflammation (including polymorphonuclear leukocytes), and ballooning degeneration.** Mallory bodies and fibrosis may or may not be present. Other features which may occur but are not largely considered helpful in diagnosis include fatty cysts, glycogenated nuclei, lipogranulomas, granular iron pigment and intrahepatocellular mega-mitochondria (Brunt, 2002). Substantial alcohol consumption must be ruled out by a detailed history, and sometimes by random blood assays for estimation of ethanol levels, and serum desialylated transferrin, a marker of alcohol consumption. Other potential causes of fatty liver such as metabolic/hereditary liver disease must also be appropriately excluded (Lonardo, 1999).

Histological evaluation for NASH can be conducted on routinely processed liver biopsies, and should include hematoxylin and eosin (H&E) stained sections of two or more levels for overall assessment of inflammation, hepatocyte injury and fibrosis. Fibrosis should be assessed by Masson's trichrome, sirus red or other stains for collagen; and Gordon and Sweet's silver stains are useful for assessment of the recticulin framework (Brunt, 2002). The periodic-acid Schiff stain after diastase predigestion (D/PAS) will show debris in Kupffer cells, and eosinophilic globules in periportal hepatocytes (Brunt, 2001). An iron stain, such as Prussian blue, evaluates hepatocellular granular iron, but is not necessary for diagnosis. If specific fat stains are required, samples must be preserved accordingly,

as lipid is lost as a result of exposure to organic solvents during processing and paraffin embedding.

The microscopic and macroscopic aspects of NASH have been described. It is noteworthy that while histological features of NASH, as originally described (Ludwig *et al.*, 1980; Brunt, 2002), are largely homogeneous, they are not necessarily indicative of aetiology. Furthermore, no single pathological feature is pathognomic for NASH; diagnosis is based rather on a variety of microscopic findings.

Microscopic aspects

Steatosis in NASH is typically macrovesicular. At the light microscopic level, the lipid presents as a single large droplet within the hepatocyte cytoplasm, displacing the nucleus to the periphery of the cell. In some of the more severe cases, however, mixed macro-microvesicular steatosis has been observed. Fatty change and ballooning degeneration are accentuated in (but not necessarily exclusive to) zone 3. Steatosis and necroinflammation may no longer be apparent in late-stage, so-called burned out NASH with cirrhosis (Brunt, 2001).

Inflammation is typically lobular (although portal inflammation has been recorded and may represent advanced stages of NASH (Bacon *et al.*, 1994; Marceau *et al.*, 1999), and, according to the definition used here, must necessarily include polymorphonuclear leukocytes (PMN). In severe NASH, PMN may be noted in association with ballooned hepatocytes (Brunt, 2001). Immunohistochemical typing of the inflammatory infiltrate typically shows mild to moderate quantities of CD4 and CD8 positive T cells (Marceau *et al.*, 1999; Lefkowitch *et al.*, 2002), present in roughly equal quantities. B cells are only rarely present. The infiltrate contains a large number of macrophages/Kupffer cells. In perivenular regions, aggregates of these are visible even at low magnification, characterized by enlarged, rounded cell bodies, often containing numerous densely

stained intracellular particles. Along sinusoids in zones 1 and 2, they tend to be nonaggregated, individual cells with elongated, tapering appearances identical to those in normal liver (Lefkowitch *et al.*, 2002). If confirmation of the Kupffer cell magnitude is required, it may be necessary to perform D/PAS and/or immunohistochemical stains for detection of CD68 (or immunocytochemical detection of F4/80), as the unexpected potential exists for misidentification of these cells as lymphocytic or endothelial in routine light microscopy (Lefkowitch *et al.*, 2002). Lipogranulomas have occasionally been reported in portal tracts or lobules (Bacon *et al.*, 1994; Brunt, 2001). They are typically small and may comprise collections of fat-laden Kupffer cells, as well as surrounding lymphocytes.

Hepatocellular injury manifests primarily as ballooning degeneration, with or without apoptosis or necrosis (Brunt, 2001). Ballooning degeneration, the result of microtubule dysfunction and accumulated intracellular fluid, is characterized by swollen hepatocytes with finely granular cytoplasm, usually in zone 3 (Burt *et al.*, 1998). Collections of ballooned hepatocytes often co-exist near steatotic counterparts. Other features of note include vacoulated glycogenated nuclei; enlarged mitochondria ("megamitochondria") containing "true" crystals of as yet unknown composition, which occur as linear bundles displacing, or continuous with, the cristae (Caldwell, 2002); and Mallory's hyaline (perinuclear, ropy inclusions consisting of aggregated cytoskeletal peptides, heat shock and tau proteins) found in ballooned hepatocytes of adult but not paediatric cases of NASH. Small, densely staining, eosinophilic fragments in the sinusoids (acidophil bodies) represent remnants of apoptotic cell death (Brunt, 2001).

The incidence of fibrosis associated with NASH ranges from 41-100% in various studies (Ludwig *et al.*, 1980; Itoh *et al.*, 1987; Pinto *et al.*, 1996). Fibrotic severity is thought to correlate with steatosis and age, but not with inflammation or glycogenated nuclei (Marceau *et al.*, 1999). Initial collagen deposition occurs in perivenular regions and

perisinusoidal spaces of zone 3. In some areas, single cells become surrounded by collagen in a pericellular pattern referred to as "chicken wire fibrosis". These features have also been described in alcohol-induced steatohepatitis (ASH), and serve to distinguish ASH and adult (but not paediatric [Lavine, 2002]) NASH from other forms of liver disease, in which initial fibrosis shows a portal distribution (Brunt, 2001; Angulo, 2002a). As NASH progresses, fibrosis may become periportal, then bridging. The latter is considered the final stage preceding cirrhosis (Angulo *et al.*, 1999; Brunt, 2001). A staging for fibrosis in NASH is shown below (Brunt *et al.*, 1999; Brunt, 2002):

Stage 1: Zone 3 perisinusoidal/pericellular fibrosis, focal or extensive
Stage 2: Zone 3 perisinusoidial fibrosis, focal or extensive periportal fibrosis
Stage 3: Perisinusoidial and portal fibrosis, bridging fibrosis
Stage 4: Cirrhosis, with or without residual perisinusoidal fibrosis

Finally, the degree of iron deposition is of continuing interest. Although the role of iron in NASH remains the subject of some controversy, various studies have noted elevated serum ferritin (iron-storage protein) and mild hepatic iron deposition in hepatocytes and Kupffer cells of patients with NASH (Ludwig *et al.*, 1980; Bacon *et al.*, 1994). Raised serum ferritin is also thought to be a component of the insulin resistance syndrome (Fernández-Real *et al.*, 1998), which shares many epidemiological features and metabolic derangements with NASH (Cigolini *et al.*, 1996; Lonardo, 1999). A mixed pattern of iron deposition in hepatocyes and sinusodial cells – decreasing in a gradient from Rappaport zones 1 to 3 – has also been described in patients with insulin resistance (Turlin *et al.*, 2001). The relationship between iron and fibrosis in NASH remains unresolved, however, with some studies reporting a positive correlation (George *et al.*, 1998) while others report none (Brunt *et al.*, 1999; Younossi *et al.*, 1999).

Macroscopic and laboratory findings

Patients with NASH are often identified incidentally during investigations of asymptomatic elevations of liver enzymes, i.e. aspartate aminotransferase (AST) and alanine aminotransferase (ALT), which are indicative of liver injury. It has been

suggested that an AST/ALT ratio lower than 1 is highly suggestive of NASH (Zamin *et al.*, 2002), although some patients may have normal liver enzymes (Garcia-Monzon *et al.*, 2000). A high AST/ALT ratio appears to be a good indicator of patients at risk for fibrosis (Angulo *et al.*, 1999; Shimada *et al.*, 2002). The use of high mean corpuscular Hb, gamma glutamyl transferase, desialyated transferrin (Harrison *et al.*, 2002) and serum thioredoxin, a stress-inducible thiol-containing protein (Sumida *et al.*, 2003), have been suggested as supplementary indicators of NASH, but data remains scant.

Lipid profiles indicate 90% of patients with NASH have some form of dyslipidaemia. Plasma fasting triglycerides (TG) are elevated (mean 4.0 mmol/L), with or without low levels of high density lipoprotein (HDL) and raised total cholesterol, in 73% (Knobler *et al.*, 1999). It noteworthy, however, that half the patients in this study had type 1 NAFLD liver only (i.e. steatosis without inflammation). In a more recent study, LDL-cholesterol was found to be significantly elevated while ApoAI was decreased in patients with NASH (Koruk *et al.*, 2003). Surprisingly, this study also reported elevated levels of Apo B, though another study (Charlton *et al.*, 2002) reported reduced levels.

Finally, the presence of metabolic derangements such as hyperinsulinemia, insulin resistance, obesity, hypertension and glucose intolerance may also be indicative of NASH.

1.2 Prevalence

It is surprisingly difficult to comment accurately on the prevalence of NASH. Since most patients are asymptomatic at the time of diagnosis and thus discovered "accidentally", it is possible only to speculate on the number of unreported cases. The methods employed in reaching a diagnosis also vary between studies, ranging from computerized tomography (CT), ultrasound, autopsy findings, liver biopsy (Yu and Keefe, 2002),

magnetic resonance imaging (MRI) and ^{1}H magnetic resonance spectroscopy (^{1}H MRS) (Garg and Misra, 2002). Table 1.2.1 shows the prevalence of NAFLD and NASH documented by some of these techniques. It is worth mentioning that CT and MRI may be falsely affected by oedema, glycogen accumulation and inflammation. Ultrasonography, which picks up echogenicity ("liver brightness") as a result of ultrasound scatter by fat droplets, will not detect the presence of inflammation. Furthermore, this screening technique is likely to pick up hepatic fat only when it exceeds 25-30% (Lonardo, 1999; Saadeh *et al.*, 2002), vastly underestimating the actual prevalence. Liver biopsy, an invasive procedure, is not generally conducted unless deemed necessary, and thus introduces a selection bias. Errors may also arise from variations in reproducibility of findings/differences of interpretation among pathologists. A study showed substantial or moderate concordance in evaluation of extent of steatosis, grade and location of fibrosis, vacuolated nuclei and ballooning degeneration, but poor agreement in assessment of parameters of inflammation (Brunt, 2002). In addition, it may not highlight cases of so-called cryptogenic cirrhosis, which may be burned out NASH in which the features characteristic of the disease are no longer apparent (Ludwig *et al.*, 1997; Brunt, 2001; Ayata *et al.*, 2002). Finally, demographics emphasised in various studies differ considerably, focusing on specific sectors of a given population. Table 1.2.2 gives a summary of some of the landmark papers.

Table 1.2.1: Prevalence of NAFLD and NASH assessed by various techniques (Yu and Keefe, 2002)

Technique	NAFLD	NASH
LFTs (NHANES)	28%	-
Liver biopsy	15-39%	1-32%
Autopsy	16-24%	2.1-2.4%
Ultrasound	16-23%	-
Computerised tomography	9.7%	-

Table 1.2.2: Demographics of patients with NASH (Yu and Keefe, 2002)

Author	Year	Number in Study	Per cent female (%)	Per cent obese (%)	Per cent with diabetes mellitus (%)	Per cent with elevated triglycerides (%)
Ludwig	1980	20	65	90	50	67
Itoh	1987	16	75	100	5	63
Diehl	1988	39	81	71	55	20
Lee	1989	49	78	95	51	-
Powell	1990	42	83	95	36	81
Bacon	1994	33	42	39	21	21
Laurin	1996	40	73	70	28	-
Pinto	1996	32	75	47	34	28
Matteoni	1999	132	53	70	33	92
Angulo	1999	144	67	60	28	27

In spite of these pitfalls, it is possible to speculate on the prevalence of NAFLD. NAFLD Type 1 has been estimated at 14-25% of eastern and Italian populations in clinical surveys, 10% in a Saudi Arabian radiological series (Lonardo, 1999) and 14% in Japanese non-drinkers (Harrison *et al.*, 2002). The prevalence of NAFLD in the United States appears to average about 20%, while the prevalence of NASH (NAFLD types 3 and 4) is approximately 3%, making these conditions the most common liver diseases in that country (Harrison *et al.*, 2002; Yu and Keefe, 2002).

1.3 Risk Factors and Associations

The factors associated with/predisposing to development of NASH appear to be age, gender, type II diabetes mellitus and insulin resistance, hyperlipidemia, obesity, surgical procedures for obesity (gastroplasty) and other factors causing profound and rapid weight loss (e.g. bulimia), and inherited abnormalities.

Age

Although NASH has been documented in children (Moran *et al.*, 1983; Rashid and Roberts, 2000; Lavine , 2002) and adults of all ages, it appears to be most common in individuals in their fourth to sixth decades of life (Reid, 2001; Harrison *et al.*, 2002).

Gender

The classical patient with NASH is female, middle aged and obese (Ludwig *et al.*, 1980; Chitturi and Farrell, 2001; Ludwig, 1997), and many authors have been compelled to describe this as a condition affecting primarily individuals with these features. It is noteworthy, however, that as shown in Table 1.2.1, many studies display a paucity of male subjects, which raises questions of sampling bias. Furthermore, it has been noted that in studies of paediatric NASH, boys outnumber girls 2:1, although it is not known whether this ratio is representative of the overall paediatric population (Lavine, 2002). Finally, in a revolutionary study by Bacon *et al.*, (1994), results indicated that NASH was also frequently seen in young, lean males.

In spite of this, it is interesting that a relationship between gender and sustained liver damage has been described in two animal models of NASH (Tessitore *et al.*, 1995; Kirsch *et al.*, 2003).

Type II diabetes mellitus (DMII) and insulin resistance (IR)

The association of DMII and IR with NASH is neither surprising nor coincidental, since many aspects of importance in DMII (hyperinsulinemia, obesity and hyperlipidemia) also factor prominently in NASH. In one study, a history of DMII was reported to increase the risk of NASH 2.6-fold (Wanless and Lentz, 1990), while a review concluded that up to one third of patients with NASH have diabetes or fasting hyperglycemia at the time of diagnosis (James and Day, 1998). More recently, it has been estimated that IR is present in almost all patients with NAFLD, irrespective of the co-existence of impaired glucose tolerance or obesity (Day, 2002a).

Hyperlipidemia

It is estimated that 20-90% of patients with NASH have concurrent abnormalities of lipid metabolism. Elevations of triglyceride, sometimes accompanied by increases in total cholesterol, have been noted (Knobler *et al.*, 1999; Chitturi and Farrell, 2001). Abnormal triglyceride storage and impaired metabolism are thought to be crucial to development and pathogenesis of NASH, since corrections of this lead to improved liver function tests.

Obesity

According to Ludwig *et al.* (1997), "fat people have fat livers." Steatosis occurs in 70% of those 10% above ideal body weight and 100% of the morbidly obese (body mass Index [BMI] greater than $30kgm^{-2}$). 40-100% of patients with NASH in clinical studies are also obese; furthermore, when adjusted for age and gender, obesity and diabetes are more prevalent in patients with cryptogenic cirrhosis than in individuals with liver diseases due to other, well-defined causes (Ratziu *et al.*, 2000; Gholam *et al.*, 2002; Harrison *et al.*, 2002; Yu and Keefe, 2002).

Recent reports suggest, however, that fat distribution rather than mere quantity is of importance (Shaffer, 2002). Thus abdominal obesity, defined as a waist/hip ratio of >0.95 in males and >0.8 in females (Lean *et al.*, 1995), identifies those more likely to be at risk of developing NASH.

Gastric modification procedures

For patients unable to commit to a lifetime of caloric restriction, for whom all other alternatives have failed, surgery lends itself as a treatment for morbid obesity. Given the prominent place of obesity in NASH, one would expect combating obesity to improve steatohepatitis. Indeed, although steatosis regresses after gastroplasty (Ranlov and Hardt, 1990), most reports find that lobular inflammation is increased (Peters *et al.*, 1975; Luyckx *et al.*, 1998; Luyckx *et al.*, 2000; Chitturi and Farrell 2001). Complications

following gastric bypass surgery are similar to those found in ASH, are probably mediated by endotoxin, and have been known to progress to cirrhosis and liver failure. A comparison of various surgical treatments for morbid obesity observed the most critical complication in patients submitted to jejuno-ileal bypass (JIB), and the best clinical outcomes with bilio-intestinal bypass (BIB) and laparoscopic adjustable gastric banding (Doldi, 1998).

NASH is also associated with other causes of rapid and profound weight loss such as bulimia and fasting (Chitturi, 2001).

Genetics

Inherited disorders may predispose individuals to NASH. Classes of candidate genes thought to be involved include

♦**Genes influencing patterns and quantity of adipose tissue deposition** such as *ob* (which codes for the satiety factor leptin, and is thought to be involved in genetic lipodystrophy syndromes), the genes for anti-insulin hormone resistin, apolipoprotein E, (involved in hepatic lipid storage), microsomal triglyceride transfer protein (MTP), and apolipoprotein B, both of which are involved in hepatic lipid transport by very low density lipoprotein (VLDL) (Bernard *et al.*, 2000; Charlton *et al.*, 2002; Day, 2002a; Day, 2002b; Garg and Misra, 2002).

♦**Genes affecting the nature and rate of fatty acid oxidation** such as genes involved in mitochondrial β-oxidation (e.g. peroxisome proliferator alpha, PPARα), leptin, and genes for the drug and steroid metabolising enzymes of the P450 class (Leclercq *et al.*, 2000; Barzilai , 2002; Day, 2002b).

♦**Genes affecting the body's ability to cope with oxidative stress**, such as genes coding for mitochondrial manganese superoxide dismutase (MnSOD, which inactivates superoxide anion $O_2^{\bullet-}$), uncoupling protein 2 (UCP2), copper/zinc superoxide dismutase, aldehyde oxidase, and catalase. A 5kb gene deletion which is associated with Kearns-Sayer mitochondrial myopathy has been rarely described in mitochondrial DNA of patients with NASH and may affect hepatocyte susceptibility to oxidative damage (Caldwell *et al.*, 1999; Caldwell, 2002; Cortez-Pinto and Diehl, 2002; Day, 2002b; Sreekumar *et al.*, 2003).

♦**Genes directly or indirectly affecting insulin sensitivity and action** such as glucose-6-phosphatase, hepatocyte-derived fibrinogen-related protein and leptin (Sreekumar *et al.*, 2003).

♦**Genes encoding cytokines, or otherwise involved in immunomodulation**

Raised serum, hepatic and peripheral fat tumour necrosis factor alpha (TNFα) have been reported in patients with NASH, linked directly to elevated levels of transcription. Patients with NASH are also thought to express significantly higher levels of TNFα type I cellular receptor (p55) than normal controls (Crespo *et al.*, 2001; Wigg *et al.*, 2001), and have higher prevalence of the so-called 238 or TNFA allele. The presence of this or a second polymorphism (308 or TNF2) is also associated with higher IR indices (Valenti, 2002). Animal models of hepatotoxicity also suggest a role for other proinflammatory cytokines such as interleukins (IL) 12 and –18 (Tsutsui *et al.*, 1997; Li *et al.*, 2002).

Leptin, recently also identified as a potential modulator of immunity, may play a role (Diehl, 2002).

♦**Genes involved in iron metabolism**

A potential role for iron in the pathogenesis of NASH has been described (Fargion, 2001), though this remains controversial (Younossi *et al.*, 1999; Chitturi *et al.*, 2002). Significant associations between C282Y – a missense mutation in the gene encoding a human leukocyte antigen class I-like molecule (HFE) – and NASH, have been reported (Fargion *et al.*, 2001; Chitturi *et al.*, 2002).

Drugs

Although sometimes listed as a cause of NASH, drug-related complications resulting in fatty liver are more appropriately called drug-induced steatohepatitis. Some drugs which cause this include amiodarone, perhexiline and coralgil (cardiovascular drugs), bleomycin (cytotoxic anti-tumour), chloroquine (anti-malarial), estrogens and estrogen receptor ligands, and methotrexate (psoriasis), (Burt *et al.*, 1998; Chitturi and Farrell 2001; Langman *et al.*, 2001).

1.4 Diagnosis

Diagnosis of NASH should be based on a battery of tests, the results of which must conform to certain requirements (see **1.1**), since most patients are asymptomatic at time of presentation. Some patients complain of generalized fatigue, lethargy, mild epigastric or right upper quadrant pain. Hepatomegaly may be found in up to 25% of patients (Bacon *et al.*, 1994; Harrison *et al.*, 2002). Laboratory examination would usually indicate raised serum liver enzymes and should ideally be negative for blood ethanol and markers of ethanol exposure. These biochemical findings can be correlated with ultrasonography, CT or MRI scans, though the pitfalls of these have been described (see **1.2**). Liver biopsy remains the gold standard for accurate diagnosis, grade and stage of liver injury and determination of prognosis (Brunt, 2001), however whether it should be undertaken for all suspected cases is controversial. Some authors argue it is required to confirm

abnormalities consistent with NASH, thus eliminating the risk of assuming a patient has uncomplicated, benign steatosis (Talwalkar, 2002). Others (Laurin, 2002) argue that NAFLD and NASH are "diseases of exclusion" which can often be identified with reasonable accuracy once laboratory findings are correlated with risk factor assessment. Furthermore, although there is <1% risk of serious post-biopsy complications, up to 5% may require hospitalization (sometimes days or weeks later). The procedure fails to obtain tissue in 2% of cases (Laurin, 2002), and how indicative biopsy-sized specimens are of overall liver condition is unknown. Finally, the high cost of the procedure makes it inaccessible to individuals unable to finance it. ^{1}H MRS has been recommended as a specific, accurate and non-invasive method for estimation of generalized hepatic fat: methylene proton signals are specific for mobile triglycerides *in vivo* and create a clear resonance peak. However, it gives no indication of inflammatory status or stage of fibrosis (Garg and Misra, 2002).

Recently, a scoring system has been proposed as a simple means of diagnosing NASH (Dixon *et al.*, 2003). The HAIR system combines the presence of hypertension, elevated ALT (>40 IU) and raised IR index (>5.0) as a simple sum. Each component is equally weighted and assigned a value of 1, for example

HAIR score 1: Obesity, ALT <40 IU, IR index <5.0
HAIR score 2: Obesity, ALT >40 IU, IR index <5.0
HAIR score 3: Obesity, ALT >40 IU, IR index >5.0

The authors speculate that a score of 3 "virtually assures the presence of NASH".

1.5 Natural History

Retrospective studies with prolonged follow-up show that steatosis is a benign condition in the absence of pre-existing fibrosis or steatohepatitis (Teli *et al.*, 1995; Matteoni *et al.*, 1999). Factors affecting the progression of steatosis to steatohepatitis and fibrosis are not clear, but appear to include the initial degree of fat accumulation, and any number of superimposed, exacerbating variables or "hits" (Day and James, 1998). Patients

circumscribed by the constellation of risk factors for NASH (see **1.3**) have also been identified as potential candidates for progressive NAFLD. Once NASH develops, there is the potential for development of cirrhosis in 19-50% (Brunt, 2001; Angulo, 2002a; Day, 2002c; Harrison *et al.*, 2002). NASH is believed to be a common underlying causes of cryptogenic cirrhosis, the end stage of chronic hepatic disorders in which the underlying aetiology is unknown (Ayata *et al.*, 2002).

Some authors suggest hepatic steatosis is a premalignant condition in animal models (Goshal and Farber, 1993; Yang *et al.*, 2001). More recently, features suggestive of advanced NASH have been linked to hepatocellular carcinoma (HCC) in humans, strongly suggesting that HCC may be part of the natural history of the disease (Bugianesi *et al.*, 2002; Shimada *et al.*, 2002b).

1.6 Therapy

Where possible, treatment of NASH should aim to combat the factors considered crucial to development of the disease. Liver transplantation for treatment of end stage liver disease resulting from advanced NASH, without treatment of initiating factors, simply results in recurrent NASH and even cirrhosis (Molloy *et al.*, 1997). Diet regulation and exercise remain the cheapest, safest forms of therapy where NASH is associated with obesity, and studies have recorded reduction of liver enzyme levels and improvement of histology, so long as the rate of weight loss does not exceed 1.6kg/week. Where weight loss and/or exercise are impossible and hyperlipidemia is present, an antihyperlipidemic medication such as a fibrate may be of benefit. Fibrates are ligands for the nuclear receptor hormone, peroxisome proliferator-activated receptor alpha (PPARα). The liganded PPARα dimerises with its receptor RXR, and the complex acts on promoters of genes involved in lipid metabolism (Schoon *et al.*, 1996). In general, β-oxidation of fatty

acids is increased, plasma triglyceride is decreased, and high density lipoprotein (HDL) is increased (D. Marais, personal communication).

Cytoprotective agents such as ursodeoxycholic acid (UDCA), which are thought to have membrane stabilizing and antiapoptotic activity, are safe, have few drug interactions, and show promise in four preliminary studies (Angulo, 2002c; Neuschwander-Tetri and Caldwell, 2003). The use of antioxidant agents has been equally promising in adult and paediatric studies. Of note are betaine (a normal component of the metabolic cycle of methionine, which indirectly increases levels of the cellular antioxidant glutathione), and vitamin E or α-tocopherol (which is known to protect against membrane lipid peroxidation and suppress a host of cytokines, including TNFα).

Where NASH is associated with IR, antidiabetic medications may be helpful. Metformin (a biguanide that sensitises to insulin, diverts fatty acids from triglyceride production to mitochondrial β-oxidation, and decreases hepatic TNFα) has been used with success in animal models and human studies. It has been known, however, to produce lactic acidosis in patients with liver disease (Lin *et al.*, 2000; Angulo, 2002c; Lieber, 2002; Mehta *et al.*, 2002; Neuschwander-Tetri and Caldwell, 2003).

In conclusion, NASH has emerged over the past two decades as a chronic form of liver disease associated with obesity and DMII but also present in lean, nondiabetic individuals. A variety of techniques are available for diagnosis, however liver biopsy remains the gold standard. Treatment options should be tailored to combat factors considered crucial to disease development and progression, and to counteracting relevant pathogenic mechanisms, which are discussed in detail in the following chapter.

Chapter Two

Introduction II: Pathogenic Mechanisms in NASH

2.1 Animal Models in NASH Research

Much of what is now known of the pathogenesis of NASH has been obtained from animal models of the disease. In order to put the current body of knowledge in context, an overview of the most frequently used models is presented (Koetish and Diehl, 2002).

Models of lipotrope deficiency

An extensively documented model for acquired steatohepatitis is a dietary one, which restricts lipid-clearing compounds (lipotropes) such as choline (Ghoshal and Farber, 1993). Hepatic triglyceride trapping in this model is believed to be the result of deficient very low density lipoprotein (VLDL) synthesis. Choline is required for synthesis of phosphatidylcholine (PC), a major component of VLDL, which in turn is the medium for hepatocyte secretion of triglyceride and cholesterol ester. The cytidine diphosphocho (CDP)-choline pathway, which is vital to all mammals, is the major pathway for PC biosynthesis. It is summarized below:

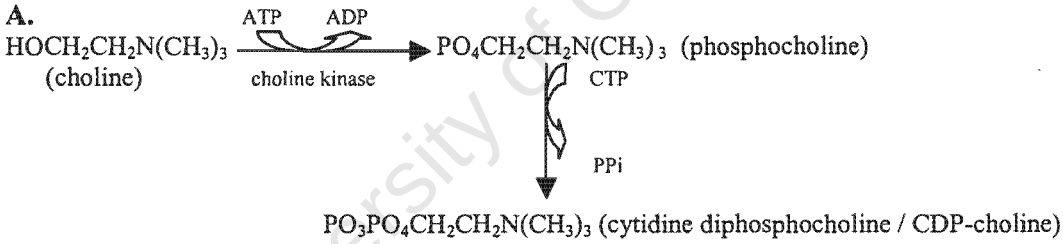

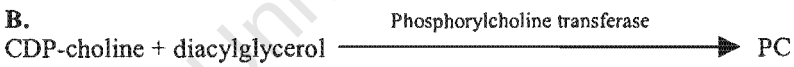

An alternative pathway for phophatidylcholine synthesis relies on sequential methylation of phosphatidylethanolamine (PE). The enzymes primarily involved are phosphatidylethanolamine N-methyltransferase I (located on the endoplasmic reticulum) and II (associated exclusively with liver mitochondria-associated membrane). The methyl group donor in this pathway is S-adenosylmethionine (SAMe). Therefore, if both pathways for PC synthesis are blocked by dietary restriction of the relevant precursors (methionine and choline), hepatic triglyceride accumulates rapidly.

The model is straightforward and relatively inexpensive. Rodents rapidly develop fatty change and inflammation, along with necrosis and compensatory hepatocyte proliferation (Ghoshal *et al.*, 1983; Ghoshal and Farber, 1993; Kirsch *et al.*, 2003). As discussed later, models of methionine and choline deficiency (MCD) have illuminated aspects of importance in pathogenesis of NAFLD such as the role of oxidative stress and lipid peroxidation. SAMe, to which methionine must be converted in order to partake in many metabolic functions, plays pivotal roles in metabolic transmethylation, transsulfuration and aminopropylation. Via transmethylation reactions, SAMe serves as a primary universal donor to a variety of acceptors, including nucleic acids, proteins, phospholipids and amines. The common product in these reactions is S-adenosylhomocysteine (SAH). As a result of SAH's inhibitory effect on SAMe-mediated reactions, its rapid and efficient removal from the system is essential. It is hydrolyzed to homocysteine and adenosine by SAH hydrolase at a rate directly proportional to the rate at which these products can, in turn, be expelled from the system. Metabolism of homocysteine proceeds via two pathways, remethylation and transsulfuration, both of which are also regulated by SAMe. An ultimate product of transsulfuration reactions is cysteine, one of three amino acids found in glutathione, the systemic proctectant against oxidative stress. It is believed that oxidative stress in the MCD model is at least partially the result of depletion of this vital antioxidant (Lieber, 2002; Lieber and Packer, 2002).

Over prolonged periods, MCD-generated steatohepatitis progresses to fibrosis and cirrhosis (Ghoshal and Farber, 1993). In this regard, the model lends itself well to investigations of the mechanisms predisposing to fibrosis and cirrhosis in human NASH. Regrettably, however, animals subjected to a MCD diet (MCDD) lose rather than gain weight, and are not known to be insulin resistant. At this juncture, the MCD model parts with human NASH, and other models bearing these important features must be looked to for answers.

Genetically obese mice

Several genetic alterations have been described which lead to steatosis, obesity and hyperinsulinemia in rodents. The models described here share in common mutations affecting expression or activity of leptin. First identified as a satiety hormone, which inhibits feeding behaviour and increases energy expenditure by interaction with receptors (Ob-Rb) on hypothalamic neurons, leptin is now known to regulate diverse phenomena. These include immune modulation, angiogenesis and matrix deposition during wound healing. The wide range of cells (endothelia, macrophages, lymphocytes and hepatic stellate cells) and tissues (lungs, pancreas, kidney) expressing Ob-Rb, may suggest many other unknown functions (Ikejima *et al.*, 2001; Diehl, 2002).

The *ob/ob* model utilizes mice with a null mutation in the *ob* gene, preventing leptin synthesis. Zucker rats (*fa/fa*) and diabetic *db/db* mice (Lee *et al.*, 1996; Takaya *et al.*, 1996) have mutations in the leptin receptor, leading to leptin resistance. Recently, three new spontaneous mutations ($Lepr^{db\text{-}rtnd}$, $Lepr^{db\text{-}dmpg}$, $Lepr^{db\text{-}rlpy}$) have also been described (Kim *et al.*, 2003). These models appear to be a more realistic approximation of human NAFLD/NASH. However, it has been observed that functional leptin may be pivotal in progression to fibrosis (Ikejima *et al.*, 2001; Leclercq *et al.*, 2002; Saxena *et al.*, 2002). Consequently, genetically obese mice appear to be protected from fibrosis resulting from exposure to hepatotoxic agents. A full understanding of the pathogenesis of NAFLD (steatosis to cirrhosis) will therefore require detailed investigations of both the MCD and genetically obese models of fatty liver.

Lipoatrophic mice

Strains of genetically altered mice lacking adipocytes or with impaired adipocyte differentiation have generalized lipoatrophy. Since leptin is produced primarily by adipose tissue, these mice are leptin deficient. They also display similar phenotypic features to those found in genetically obese mice which are characteristic of

NAFLD/NASH such as fatty liver disease, IR, and elevated TNFα. These models are invaluable because they stress that obesity is not mandatory for development of NAFLD, which rather is the result of a complex interplay involving cytokines, leptin and disturbances of lipid metabolism.

In conclusion, it is noteworthy that no animal model is an ideal representation of NASH. A comprehensive understanding of the pathogenesis of the disease will probably be best served by combining findings from the various models.

2.2 Pathogenic Mechanisms in NASH

2.2.1 Lipids and lipid metabolism

Dietary lipids consist of about 90% triglyceride (triacyglycerols or TG). The rest is made up of free and esterified cholesterol (FC, CE), phospholipids (PL), and some plant sterols. The highly apolar nature of lipids presents a unique problem if they are to be accessed and utilized in a highly polar solvent system such as the human body. Dietary lipid must therefore undergo a number of changes during digestion and absorption (Mead *et al.*, 1986; Gurr and Harwood, 1991).

Entry of food into the duodenum from the stomach stimulates the secretion of enteric hormones, which in turn stimulate the gallbladder to deliver stored bile, and the liver to secrete fresh hepatic bile. Enteric hormones also stimulate secretion of pancreatic juice, which contains TG lipase (TGLp) and colipase. The lipase-colipase-bile salt complex (LCBC) is regarded as the enzyme unit responsible for interaction with the digestive fat emulsion. Pancreatic lipase (TGLp), which acts at an oil-water interface, is specific for water-insoluble TG containing long-chain fatty acids, as shown below. It will also

hydrolyze water soluble TG, but such reactions lead to rapid and irreversible inactivation of the enzyme, thus are dependent on bile acid salt conjugates for stability.

As part of the LCBC, bile salts are also responsible for promoting emulsification of monoacylglycerols, free fatty acids and even unhydrolyzed TG, and later, for the formation of mixed micelles with monoacylglycerols and fatty acids. In spite of this, at high concentrations (0.3-0.8M) these salts form a strong complex with TGLp, displacing it to the aqueous phase and inhibiting action of the enzyme. The role of colipase is therefore to act as a counteracting influence by forming a tight complex with TGLp and maintaining its interfacial recognition.

As mentioned above, it is believed that emulsified TG entering the duodenum from the stomach are subjected to the actions of TGLp, which releases monoacylglycerols and free fatty acids (FFA). The fate of PL is similar, with hydrolysis at the 2-acyl group by a phospholipase being the initial and relevant step preceding absorption. The products of hydrolysis, with bile acids, form water-soluble mixed micelles that shuttle lipids between the intraluminar emulsion and the absorptive surface of intestinal epithelium. At the surface, glycerol, being water soluble, diffuses through the cell membrane. Bile salts leave the micelle and are resorbed from the ileum, from where they return to the liver. The intestinal uptake of lipolytic products from the micellar phase into the mucosal cell may be mediated by a non-energy-dependent passive process. Short chain fatty acids are then transported directly into the portal blood, partly in solution or as albumin-bound fatty acid. Medium chain fatty acids pass directly through the cells into portal circulation or are occasionally re-esterified into triglycerides within the absorptive cells. Long chain

fatty acids are re-esterified into triglycerides and become part of chylomicrons. The re-esterification process is associated with the endoplasmic reticulum of the mucosal cells, and may occur either by (1) sequential acylation of 2-monoacyglycerol from earlier TG hydrolysis (the fate of 85% re-esterified TG), or (2) the action of glycerol kinase and acyltransferases on glycerol liberated from TG hydrolysis or glycolysis.

Chylomicrons and VLDL function vitally to transport and provide fatty acids derived from dietary lipids for metabolic purposes. In order for this to happen, longer chain fatty acids (now mainly as reconstituted TG) are packaged into a lipoprotein complex with apolipoproteins (APO B48 for chylomicrons, APO B100 for VLDL). From the enterocyte, lipoproteins diffuse to the central lacteals, and through the lymphatic endothelium. They are then transported via the lymphatic system to the blood, to be taken to sites for utilization or storage. During passage through the blood, the action of lipoprotein lipase progressively hydrolyses the TG component of chylomicrons or VLDL, progressively leaving denser particles depleted in TG and more enriched in PL, C and CE. Remnants of chylomicrons and VLDL return to the liver.

♦ β-Oxidation

Fatty acids (FA) resulting from the processes detailed above are carried to requisite cells where they are transferred to binding sites on the cell membrane. The non-esterified FA are transferred across the bilipid membrane and transported through the cytoplasm complexed to low molecular weight fatty acid binding proteins (FABP), which present them at the outer mitochondrial membrane. Here, FA are converted to their coenzyme A (coA) derivatives by acyl-coA synthetase. Translocation of these derivatives across the inner membrane must be assisted by carnitine acyltransferases (I and II, located on the inner and outer surfaces of the membrane respectively) and a translocase, since the inner membrane is poorly permeable to long chain fatty acyl-coA derivatives. Once the acyl-

coA is on the inner face of the second mitochondrial membrane, the first steps of β-oxidation take place. In short, this pathway consists of a spiral of events culminating in thiolytic cleavage of the β-keto carbon of acyl-coA, thus:

$RCH_2CH_2\ COSCoA \longrightarrow RCOSCoA + CH_3COSCoA$ (acetyl-coA)
**where R represents an alkyl functional group*

generating acetyl-coA and the coA derivative of the fatty acid (now two carbons shorter) at each completion of the cycle until the entire fatty acid chain has been degraded. The acetyl-coA produced may go on to be oxidized in the tricarboxylic acid (TCA) cycle, or two molecules of acetyl-coA may condense to ultimately form acetoacetate, although this is not efficiently used as an energy source in liver mitochondria.

The energy yield from β-oxidation is considerable, making it the foremost pathway for generation of useful energy from fatty acid. Five ATP molecules are generated for each spiral of the pathway, and if the acetyl-coA is subsequently oxidized through the TCA cycle, up to 12 ATP molecules may be generated per turn. The high yield oxidation of FA through these means are, however, entirely dependent on the availability of oxaloacetate, obtained from carbohydrate metabolism; thus, at least in the liver, the response to an increasing or exclusive fat diet is decreased energy yield per fat molecule.

Slightly modified β-oxidation also takes place in peroxisomes and glyoxysomes, collectively termed "microbodies". These are of particular import in liver and kidneys. In the healthy liver, it appears mitochondria and peroxisomes collaborate in overall fatty acid oxidation (~50% from each), with microbodies oxidizing very long chain fatty acids (which are impermeable to the inner mitochondrial membrane) to medium chain products before transport to mitochondria for complete breakdown (Gurr and Harwood, 1991). Hypolipidemic drugs such as clofibrate, high fat diets, starvation and diabetes all markedly upregulate peroxisomal oxidation.

Other pathways for generation of energy from fatty acid include

♦**α-Oxidation**, a method for degrading FA which, for structural reasons, prove difficult or impossible with β-oxidation. The degradation process is 1 carbon at a time (rather than the 2-carbon process of β-oxidation). In the presence of a peroxide-generating system (NADP(H), oxygen and 2 cytosolic factors), α-oxidation converts a long chain FA to an aldehyde with one less carbon.

♦**ω-Oxidation**

This microsomal pathway oxidizes medium-chain fatty acids to dicarboxylic acids (i.e. there is oxidation of the terminal methyl carbon). In the liver microsomal system, the system is very similar to the drug and steroid hydroxylating systems and requires cytochrome P450, NADPH, cytochrome c reductase, phosphatidlycholine (PC) and oxygen. The precise roles of ω-oxidation are believed to be concerned with oxidation of hydrocarbon chains when other systems are incapable, unavailable or overwhelmed. For example, it is essential in liver microsomes of aged animals where coAse and ATPase prevent the normal activation of fatty acids; and in the oxidation of highly substituted derivatives where it is essential before β-oxidation can proceed.

♦**Lipid peroxidation**

A final degradative process affecting fatty acids is **lipid peroxidation** (LP), the introduction of a functional group containing two catenated oxygen atoms, O-O, into unsaturated fatty acids in a free radical chain reaction (Wheatly, 2000). Although saturated and monounsaturated fatty acids may undergo peroxidation, the rates of such reactions on these substrates are much slower and usually require high temperatures and catalysts (Mead *et al.*, 1986). However, the double bonds present in polyunsaturated fatty acids (for example the commonly occuring 1,4-polyenes) renders them highly susceptible to oxidative attack.

The first indicator of a peroxidative process is considered to be the conjugation of methylene-interrupted dienes, forming conjugated dienes (CD). An example of this would be the movement of the double bond in a 1,4-polyene to generate a 1,3-polyene. Strictly speaking, these are not products of LP, as the oxidative state remains the same. But as they are easily measured, they are considered a good hallmark for an imminent peroxidative process or an oxidative stress. True LP begins with an *initiation* process involving the formation

of a carbon-centred radical by hydrogen abstraction from the lipid:

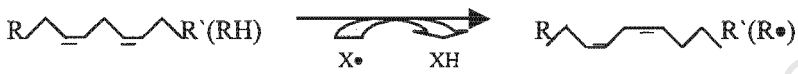

These initiation reactions are of particular importance, since it has been shown that highly purified polyunsaturated fatty acids are stable for long periods *in vitro*, even in the presence of oxygen. Different initiation processes (protolysis, γ-radiation, singlet oxygen, transition metal ions M^{n+}, alkyl radicals R•) produce different radicals. Furthermore, although the initiating event controls the *extent* of the following chain reaction, the subsequent chemistry is essentially the same regardless of the event.

Once LP has been initiated, it is *propagated* by resonance stabilized free radicals that react readily with oxygen to form peroxy radicals (ROO•). If the peroxidative process is enzymatic, dioxygen addition is regiospecific and the conversion of the alkyl radical, first to a peroxy radical and then a hydroperoxide, is catalyzed by lipoxygenases. If the peroxidative process is non-enzymatic (autoxidation), addition is not regiospecific (Mead *et al.*, 1986; Gurr and Harwood 1991; Wheatly, 2000).

Thus:

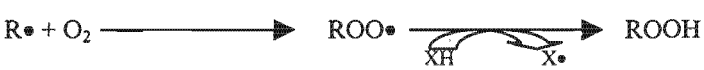

The hydroperoxides (ROOH or LOOH) formed may decompose under certain conditions, giving rise to peroxy and alkoxy (RO•) radicals which can initiate and propagate new chains, such that

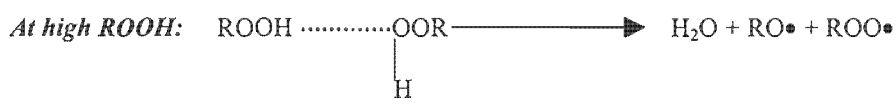

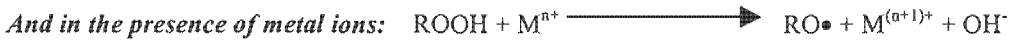

The final step of LP is termination. It involves reactions between radicals producing dimers and higher polymers. Apart from these cross-linking reactions, β-scission can occur, generating small products such as malondialdehyde (MDA). The end products of LP differ, depending on and reflecting the fatty acid composition of the starting material. Other common products include ketones, and aldehydes such as 4-hydroxynon-2-enal (4-HNE) and hex-2-enal.

2.2.2 Lipid metabolism and the pathogenesis of NASH

It is clear that the pathogenesis of NAFLD/NASH must be somehow linked to disordered lipid metabolism. The accumulation of fat within TG is believed to be the result of increased hepatic uptake of FA, increased endogenous synthesis of FA, and/or decreased disposal of FA. Certainly, IR, which is frequently associated with NASH (see **1.3**), favours increased mobilization of FA from adipocytes (Chitturi and Farrell, 2002). High insulin levels are also known to increase degradation of apoplipoprotein B100, a component of VLDL (Neuschwander-Tetri, 2001; Harrison and Diehl, 2002), while suppressing mitochondrial β-oxidation (Chitturi and Farrell, 2002; Neuschwander-Tetri, 2001). Since lipid accumulation in nonadipose sites (lipotoxicity) is itself known to be cytotoxic (Chitturi *et al.*, 2002) – causing mitochondrial swelling, increased lysosomal

fragility and impaired membrane integrity (Harrison, 2002) – suppression of homeostatic mechanisms which safeguard against this would naturally be deleterious. Furthermore, when mitochondrial β-oxidation is overwhelmed or compromised, it may be compensated for by other mechanisms such as peroxisomal β-oxidation and ω-oxidation (Chitturi and Farrell, 2002). Hydrogen peroxide produced through peroxisomal oxidation may react with chelates of copper and iron to yield hydroxyl radical (OH•), and thus may predispose to oxidative stress (i.e. the outcome of oxidative damage to biologically relevant macromolecules, which occurs when oxidative stress-related molecules exceed cellular antioxidant defense mechanisms). By reacting with, crosslinking and modifying them, OH• may cause inactivation of cellular proteins (Wolff *et al.*, 1986; Farrell *et al.*, 2002). Members of the cytochrome P450 class of proteins (CYP), which are essential for ω-oxidation as well as hepatic drug hydroxylation, have been implicated as catalysts of LP in liver microsomes (Leclercq *et al.*, 2000).

Reactions that generate and dispose of highly reactive LP products are usually restricted to specific subcellular compartments, thus limiting cross-reaction with cellular components. Understandably, it is therefore difficult to estimate accurately the level (and consequently, implication) of meaningful LP occurring during the course of fatty liver disease, since at least in most animal studies, tissue must necessarily be disrupted to assess markers of peroxidation. Nevertheless, measurements of breath alkanes (an accepted index of *in vivo* LP [van Gossum and Decuyper, 1989]) have reported increased LP *in vivo* in hepatic steatosis resulting from treatment with various hepatotoxic agents (Lettéron *et al.*, 1996). Experimentally, ROOH, RO• and ROO• are known to cause crosslinkage and fragmentation of proteins closely associated with the peroxidizing lipid. MDA and 4-HNE are capable of modifying APO B of lipoproteins. LP products are also capable of initiating LP in membrane phospholipids, which may be transformed to signalling compounds such as 2,4-decadienal, that induce apoptosis (Spiteller, 2002). LP

products form adducts with DNA at low doses, and induce strand breakage and genotoxicity at high doses (Wolff *et al.*, 1986; Parola and Robino, 2001). In these ways, LP become direct affecters of hepatic lipid transport, signal transduction pathways, proliferation and function in target cells.

In the context of fatty liver disease (both alcoholic and nonalcoholic), LP are also relevant because they stimulate expression of collagen α_1 gene expression in cultured cells and livers from animal models of hepatocellular injury (Parola *et al.*, 1993; Bedossa *et al.*, 1994). 4-HNE helps drive the fibrogenic response further by upregulating transforming growth factor β (TGFβ) in human monocyte/macrophage cell lines and in rat Kupffer cells isolated from fibrotic livers. Evidence of LP is concomitant with or precedes activation of hepatic stellate cells, which are instrumental in collagen deposition during fibrosis. These effects may be prevented or reversed early on by addition of antioxidants to the experimental system. 4-HNE may also be able to elicit apotosis in liver cell cultures, though this aspect remains unexplored (Parola and Robino, 2001). Finally, LP products cause aggregation of cytokeratins, thus being instrumental in development of the Mallory body (Pessayre *et al.*, 1999).

The enhanced oxidative stress generated by means discussed above results in various mitochondrial adaptations. For example, increased expression of uncoupling protein 2 (UCP-2) has been reported. UCP-2 leads to dissipation of the proton gradient that normally exists across the inner mitochondrial membrane, resulting in re-oxidation of NADH and $FADH_2$ as well as the production of heat rather than synthesis of ATP. This is believed to reduce mitochondrial oxidant production; however, because this involves limitations of ATP production, this coping mechanism may encourage hepatocellular necrosis (Day, 2002a; Harrison and Diehl, 2002).

The role of lipids and perturbations of lipid metabolism in NASH cannot be over-emphasized. In addition to direct damage, the products of disordered metabolism enter into a negative feedback loop, which drives other factors involved in pathogenesis of NASH such as IR, inflammation and cytokine induction. Since excessive oxidant production depletes hepatocytes of necessary antioxidants such as glutathione (Harrison and Diehl, 2002), excessive oxidative stress becomes a self-reinforcing phenomenon.

2.2.3 Role of inflammation and cytokine production

LP products upregulate adhesion molecules and are potent chemoattractants for neutrophils (Pessayre *et al.*, 1999), which may explain the PMN infiltrate observed in NASH. Superoxide anion ($O_2^{\bullet-}$) and nitric oxide (NO) produced by PMN in turn induce further lipid peroxidation, and play a direct role in progression of liver injury by stimulating collagen synthesis in HSC, propelling the liver to a fibrotic state (Casini, 1997). It has been hypothesized that 4-HNE is also a potent activator of Kupffer cells (Luckey and Petersen, 2001), which in turn produce reactive oxygen and nitrogen species (Videla *et al.*, 2003).

Much of the damage recorded in liver injury is mediated by recruited and resident inflammatory cells. The role of Kupffer cells is gaining prominence. In a carbon tetrachloride (CCl_4) model of liver cirrhosis, inactivation of Kupffer cells by gadolinium chloride ($GdCl_3$) decreased serum aminotransferases, lipid peroxidation and collagen deposition (Muriel and Escobar, 2003). In an animal model of alcoholic liver disease (Järveläinen *et al.*, 2000), $GdCl_3$ alleviated steatosis and induction of cytochrome P450 2E1 (CYP2E1). It is believed the deleterious effect of Kuppfer cells is mediated in part through disordered cytokine production. Cytokines are pleiotropic regulatory peptides that may be produced by virtually every nucleated cell to modulate its local environment in response to inflammatory or immunological challenge (Tilg and Diehl, 2000; Raeburn *et al.* 2002). Evidence in support of the role of cytokines in NAFLD/NASH may lie in

the fact that numerous pathological features associated with NAFLD/NASH, and attributable to LP, may also be caused by cytokines (Day, 2002a). Thus cytokines may cause hepatocyte injury, necrosis and apoptosis (tumour necrosis factor alpha [TNFα]), are chemotactic for neutrophils (interleukin 8 [IL-8]), may activate hepatic stellate cells (TNFα, transforming growth factor beta [TGFβ]) and may facilitate formation of Mallory bodies (TGFβ).

There are a number of stimuli or "hits" capable of setting in place the cytokine cascade relevant to NAFLD/NASH. As discussed above, LP linked to high levels of free fatty acids (FFA) mobilized from a large adipose mass (as seen in NASH associated with obesity) may be chemotactic for, and activate, PMN and Kupffer cells. Kupffer cells may also be activated by circulating endotoxin or lipopolysaccharide (LPS). Elevated levels of LPS have been noted in patients with NASH, and may be a consequence of intestinal bacterial overgrowth as encountered in patients who have undergone surgical treatment for morbid obesity (Wigg *et al.*, 2001). LPS represents the main outer membrane component of gram negative bacteria, which is released during bacterial replication and lysis. Its structure, shown below, is amphiphillic and tripartite. *Lipid A*, which is responsible for LPS biological activity, is a β1,6-linked D-glucosamine disaccharide backbone with six or seven attached acyl residues to anchor the structure to the membrane (though the length, position and number of these fatty acids may vary). The minimal requirement for lipid A bioactivity (i.e. the cytokine inducing capacity) is a molecule having two *gluco*-configurated hexosamine residues, two phosphoryl groups and six fatty acids (as seen in *Escherichia coli*). *Core polysaccharide* is a branched polysaccharide of 9-12 sugars, which is essential for bacterial viability; it is the same within any gram negative bacterial species. *O-antigen* is a linear sequence of repeating oligosaccharine units which distinguishes baterial serotypes (Ulmer *et al.*, 2002).

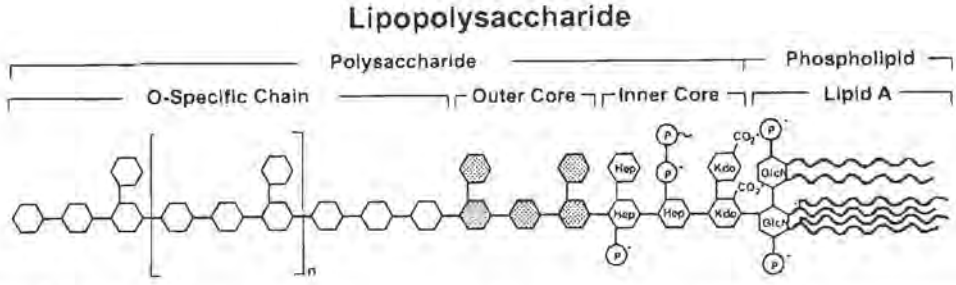

Fig 2.2.1: Structure of LPS. Reprinted with permission from Ulmer *et al.*, © 2002 Trends Glycosc. Glycotech **14(76):** 53-68.

After penetration of LPS through the intestinal barrier, it is transported to the liver bound to LPS binding protein (LBP). Kupffer cells are primarily responsible for hepatic clearance of LPS, mainly via interactions of LBP with CD14 receptors, but also via Toll-like receptors, possibly assisted by activated nuclear factor-κβ (NFκβ). Other factors involved in LPS binding which are beyond the scope of this chapter are shown in figure 2.2.2.

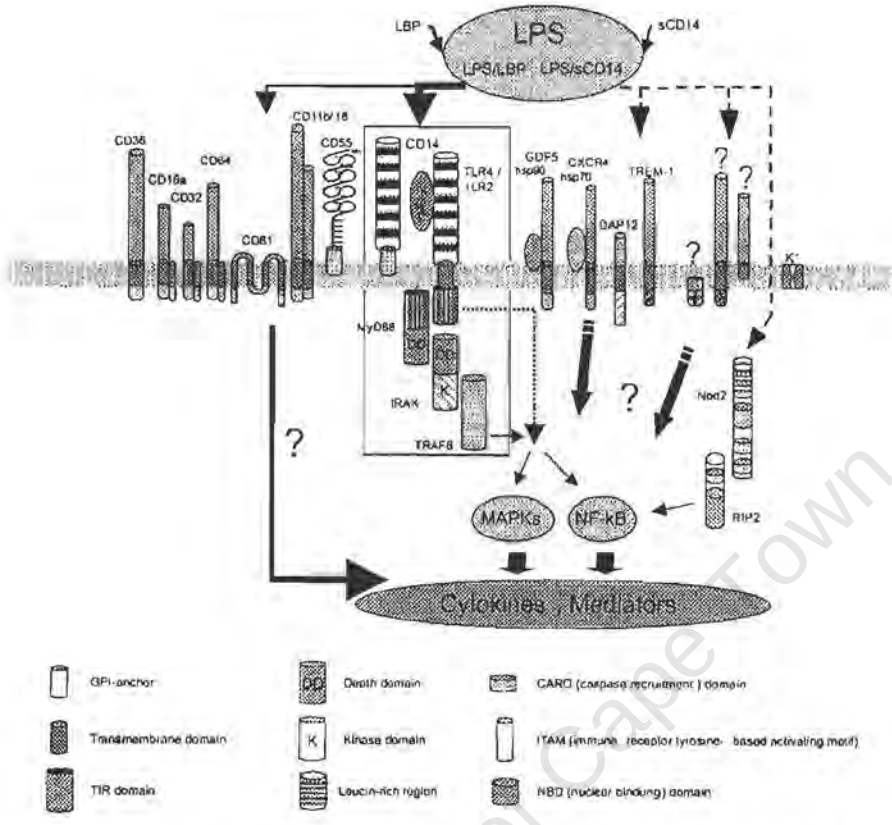

Fig. 3. **Endotoxin recognition and signaling in monocytes/macrophages by the *raft*-associated LPS- receptor complex.** The main LPS signaling pathway through TLR is boxed.

Fig. 2.2.2: Monocyte/macrophage endotoxin recognition and signalling. Reprinted with permission from Ulmer *et al.*, © 2002 Trends Glycosc. Glycotech **14(76):** 53-68.

Binding and endocytosis of LPS activates Kupffer cells and results in the synthesis and secretion of cytokines such as TNFα, which promotes apoptosis and is pro-inflammatory via a feedback induction of more TNFα, IL-1β and chemokines (Casini, 2002; Raeburn *et al.*, 2002; Ulmer *et al.*, 2002). IL-1β is proinflammatory via induction of itself, TNFα, COX-2 and inducible nitrogen oxide (iNOS), which upregulates NO synthesis. NO may react with macromolecules, free metal ions and free radicals (Morio *et al.*, 2001; Parolo and Robino, 2001) to generate harmful reactive nitrogen intermediates (RNI). IL-1β also induces expression of adhesion molecule (ICAM-I). In addition, TNFα and IL-1β induce the pro- / anti-inflammatory cytokine IL-6 (which is crucial for induction of acute phase

proteins and the pro-fibrogenic cytokine TGFβ, which activates hepatic stellate cells), as well as IL-18, which is proinflammatory, synergistic with IL-1β, and instrumental in induction of IL-12. The induction of IL-12 is essential for induction of interferon gamma (IFNγ) and increased expression of Fas ligand (FasL). IFNγ enters a TNFα-augmenting positive feedback loop. In addition, it induces expression of major histocompatibility complex I and II, stimulates synthesis of adhesion molecules on endothelial cells and inhibits Th2 responses. FasL induces apoptosis in cells expressing Fas receptor (Tsutsui *et al.*, 1997; Raeburn *et al.*, 2002).

These and other data suggest a pivotal role for TNFα in liver injury. TNFα is in fact known to activate caspase 8, which activates caspase 3 downstream, inducing apoptosis. It also induces sphingomyelinase, which increases ceramide, an inhibitor of the electron transport chain; by this means TNFα promotes ROS formation and consequent lipid peroxidation. It is interesting to note, however, that the normal outcome of TNFα exposure is hepatocyte proliferation (not cell death [Tilg and Diehl, 2000]), indicating that mechanisms normally exist (and are absent in NASH) which modulate the effect of TNFα. These mechanisms remain to be elucidated, though it is suspected that transcription of certain protective factors is necessary (Tilg and Diehl, 2000). Indeed, although freshly isolated healthy mouse hepatocytes are essentially insensitive to TNFα, TNFα-induced apoptosis *in vitro* and *in vivo* becomes dose-dependent when cultured hepatocytes or normal mice are first treated with transcriptional inhibitors such as actinomycin D, D-galactosamine and α-amanitin (Leist, 1994). Some authors (Tilg and Diehl, 2000) speculated that the protective mechanisms against TNFα cytotoxicity may involve activity of TNF-induced nuclear factor-κβ (NFκβ). The induction of NFκβ by TNFα is believed to depend on upregulation of LP by TNFα (Bowie *et al.*, 1997). NFκβ is a transcription factor which encodes, among other things, anti-apoptotic products, which block activation of caspases and release of mitochondrial oxidants. The role of

NFκβ remains controversial, however, since it has now been documented in *ob/ob* mice that fatty liver remains vulnerable in an animal model of hepatotoxic challenge using LPS, despite inhibition of caspase 3 and induction of NFκβ (Yang *et al.*, 2001). This, however, does not necessarily nullify the validity of a "two hit" hypothesis of cytokine-mediated hepatic injury where a first hit increases exposure of hepatocytes to TNFα (see **1.3**), while a second alters hepatocyte ability to protect itself from TNFα induced cell death (Tilg and Diehl, 2000). In support of this, although baseline levels of TNFα and IL-6 are increased in unchallenged genetically obese rodents, expression of these cytokines is actually attenuated following LPS challenge in genetically obese *fa/fa* and *ob/ob* mice (which bear many resemblances to the clinical NASH profile, see **2.1**); yet these strains are highly vulnerable to hepatic damage in response to LPS (Loffreda *et al.*, 1998; Diehl, 2002). This may be the result of increased vulnerability to necrosis (via reduced ATP production), rather than apoptosis (Yang *et al.*, 2001). Furthermore, TNFα-mediated hepatocellular damage is mitigated in various animal models where pro-inflammatory cytokines are knocked out (Tilg and Diehl, 2000).

2.2.4 IR and the pathogenesis of NASH

IR refers to resistance to the effects of insulin on glucose uptake, metabolism and/or storage (Kahn and Flier, 2000). IR in obesity and type 2 diabetes mellitus is manifested by decreased insulin-stimulated glucose transport and metabolism in adipocytes and skeletal muscle, and by impaired suppression of hepatic glucose output.

A link between IR and obesity is not unexpected, since insulin is a critical regulator of most aspects of adipocyte biology, and adipocytes in turn are among the most highly responsive of cells to insulin (Khan and Flier, 2000). Given the correlation between obesity and NAFLD/NASH, it follows that a link between IR and NAFLD/NASH also exists; indeed, it is now estimated that IR is almost universal in patients with NASH

(regardless of diabetic state), when measured by glucose tolerance or clamp methods (Day, 2002a; Chalasani *et al.*, 2003). It has also been shown that subjects with histologically proven fatty liver as well as those with precirrhotic stages of NASH fail to suppress lipolysis (a crucial function of insulin) during a two-step hyperinsulinemic euglycemic clamp (Sanyal, 2001). Finally, NASH has also been found localized to peripheral subcapsular regions of the liver in patients receiving insulin in peritoneal dialysis fluid, and focal NASH has been observed in liver hilum of patients with an abnormal pancreatic vein that drains insulin-rich blood directly into the hilum rather than to the prehepatic portal circulation (where insulin concentrations are lowered by dilution [Neuschwander-Tetri, 2001]). This raises the intriguing and important question of whether IR plays a causal role in the development of NAFLD/NASH.

Adipocytes have long been known for their role as energy storage depots for triglycerides (from which energy is obtained in times of need in the form of free fatty acids [FFA] and glycerol), their role as endocrine cells has only recently become evident. Adipocytes express and secrete many peptide hormones and cytokines, most notably TNFα. Levels of circulating serum and adipose tissue TNFα are elevated in obese humans, correlate with BMI, and decrease with weight reduction (Day, 2002a). In mice with TNFα mutations, insulin sensitivity is improved in both diet and genetically induced obesity. In addition, insulin sensitivity has also been significantly restored in Zucker rats using a soluble TNF-receptor IgG protein that neutralized TNFα (Cheung *et al.*, 1998). Unsurprisingly, it is believed IR concomitant with obesity is directly linked to TNFα. TNFα downregulates insulin signalling, in part through impairment of glucose transporters such as GLUT4. In addition, activation of inhibitor kappa kinase beta (IκKβ) by TNFα in adipocytes and hepatocytes increases serine phosphorylation of insulin receptor substrates (IRS), which reduces tyrosine phosphorylation and tyrosine kinase activity, events normally initiated by insulin receptor binding. Serine phosphorylation of

IRS1 and IRS2 thus markedly reduces ability of IRS molecules to dock at the insulin receptor and interact with downstream pathways essential for insulin signalling. Impaired anti-lipolytic (and pro-glycogenic) effects of insulin in adipose tissue then lead to increased FFA release. FFA are capable of inducing IR in skeletal muscle via IκKβ, thus they may be involved in a self-perpetuating cycle of peripheral IR. Since transcription of TNFα also engages in a positive feedback loop with IκKβ, this cytokine also establishes a self-reinforcing, self-propagating cycle of IR (Khan and Flier, 2000; Le Roith and Zick, 2001; Day, 2002a).

Impaired insulin sensitivity is a harbinger of many troubles. Visceral adipocytes are more prone to lipolysis than their peripheral equivalents, due to increased production of anti-insulin hormone resistin, a greater complement of adrenergic receptors, and potentially increased production of cortisol (due to their higher activity of 11β hydroxysteroid dehydrogenase I, 11β HSDI). Any FFA released from these visceral adipocytes drains directly to the liver via the portal vein. Although it has been demonstrated that FFA-induced, IκKβ-mediated IR does not occur in liver (Day, 2002a), FFAs may exert deleterious effects relevant to NASH in other ways. The ability of polyunsaturated fatty acids (PUFA) to regulate metabolic processes at the transcriptional level, and through changes in membrane fatty acid composition resulting in altered hormonal signalling, has been described (Clarke, 2001). PUFA, particularly those of the n-3 family, are essential "fuel partitioners" that upregulate expression of genes encoding proteins involved in FA oxidation, directing FA away from triglyceride storage. In this way they may reduce risk of lipotoxicity as a result of excessive cellular triglyceride accumulation. However, PUFA-mediated suppression of lipogenic gene expression occurs, in part, via reduction of nuclear abundance and DNA binding affinity of transcription factors responsible for imparting insulin and carbohydrate control to lipogenic and glycolytic genes. Accumulated FA metabolites such as long-chain acyl-CoAs also increase protein kinase C

activity, enhancing serine phosphorylation of IRS1 (Kim, 2003). It has also been hypothesized that increased fatty acid concentration results in elevation of intramitochondrial cetyl CoA/CoA and $NADH/NAD^+$ ratios, leading to inactivation of pyruvate dehydrogenase. This causes increased citrate concentrations, leading to inhibition of phosphofructokinase. Subsequent increases in cellular glucose –6-phosphate concentration inhibit hexokinase II activity, which result in increased intracellular glucose concentration and decreased muscle glucose uptake (Randle *et al.*, 1963). However this model has been increasingly challenged (Schulman, 2000) in favour of the IRS phosphorylation model described above. In any case, it is possible to speculate on a role for excessive FFA on development of hepatic IR. In addition, PUFA (probably via active metabolites such as eicosanoids) direct activation of peroxisome proliferator-activated receptor alpha (PPARα).

2.2.5 PPARs

PPARs are members of the nuclear hormone receptor superfamily, a group of nuclear proteins which mediate the effects on DNA of small lipophilic compounds such as steroids, retinoids, bile and fatty acids, oxidized phopholipids, fibrates and thiazolidinediones (Kersten, 2002). The three isotypes so far identified (denoted α, β and γ) are grouped together based on a common structural motif consisting of a central DNA-binding domain containing two zinc fingers and a large C-terminal domain that binds ligand (Aranda and Pascual, 2001). Only PPARα activates DNA transcription in response to peroxisome proliferators.

Activation of PPARα generally leads to induction of a host of genes encoding proteins for lipid transport, oxidation (β- form, but also ω-oxidation, possibly through CYP4A) and thermogenesis. The importance of PPARα cannot be overemphasized, therefore, and nullizygous $PPAR\alpha^{-/-}$ mice develop fatty liver, elevated blood triglycerides and

hyperglycemia, linked to their inability to increase rates of FA oxidation during periods of starvation. Also, although PPARα is only weakly expressed in white adipose tissue, PPARα null mice suffer from a delayed onset form of obesity noted particularly in females (Costet *et al.*, 1998). In an animal model of type 2 diabetes using dominant negative muscle specific insulin growth factor I receptor, Kim *et al.* (2003) showed that treatment with a PPARα agonist improved lipotoxicity by driving FA oxidation. Rao *et al* (2002) also showed prevention or reversal of choline defiency induced steatohepatitis when rats were given a choline-deficient diet with clofibrate, a potent PPARα ligand. Recently, these findings have been corroborated by Ip *et al.* (2003). In a study utilizing the same rodent nutritional model of NASH, these investigators protected MCD mice against steatohepatitis, utilizing Wy-14,643 (a PPARα agonist). Nevertheless, the story may become less favourable when FFA accumulate, leading to excessive PPARα induction, excessive FA oxidation, and subsequent generation of reactive oxygen species which may generate oxidative stress, promote lipid peroxidation, and contribute to upregulation of TNFα.

Finally, PPARα is now known to inhibit expression of the glucose transporter, GLUT4, in adipose tissue (Kersten, 2002), thus potentially contributing directly to peripheral IR. The central role of GLUT4 was highlighted by elegant experiments on lean, normoglycemic, IR offspring of diabetic parents illuminate additional players in the IR arena. Such studies show a 50% reduction in the rate of insulin-stimulated whole-body glucose metabolism (Schulman, 2000). This dysfunction presents before the onset of diabetes and is not secondary to complications of the disease such as glucose toxicity. The rate of insulin delivery is comparable between experimental subjects and controls (Schulman, 2000), and changes in concentration of intracellular glucose are proportional to those of

glucose-6-phosphate (see below).

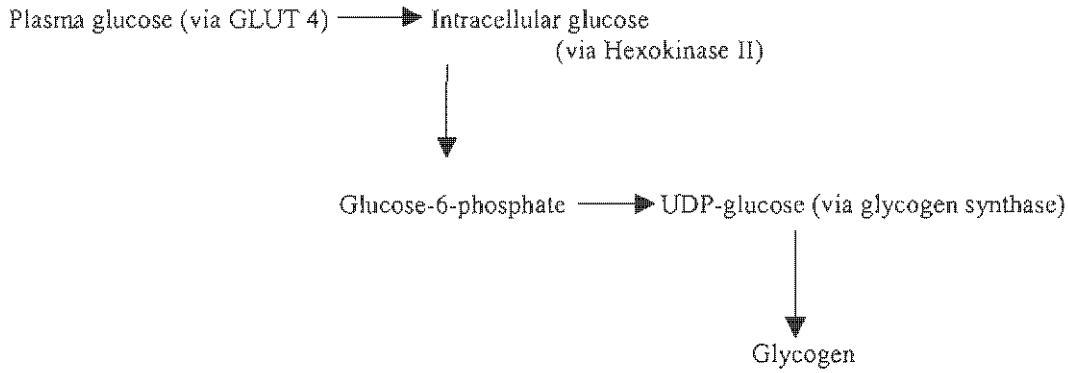

It has therefore been suggested that in affected subjects, impaired plasma glucose transport into the cell (conducted by glucose transporters, mainly GLUT4) rather than phosphorylation (catalyzed by hexokinase II) is predominantly responsible for control of muscle glycogen synthesis in IR and diabetes. GLUT4 expression is normal in skeletal muscle of obese and diabetic patients, and it is believed that defects in glucose transport may be as the result of impaired translocation, docking or fusion of GLUT4 containing vesicles with the plasma membrane. This may result from increased activity of PPARα, TNFα, and/or increased plasma fatty acid concentrations, tying the mechanisms at play in IR once again to those also involved in development of steatosis. Differences in delivery of substrate or insulin to the tissue bed are not believed to have a role in IR (Schulman, 2000; Kersten, 2002).

The role of other PPARs in IR is less clear. It is possible that PPARβ could also play a role, as it has been implicated in lipid metabolism (primarily in nerve cells) and differentiation of pre-adipose tissue (Kersten, 2002). However, since this PPAR isotype still remains an enigma, any role in NAFLD can only be speculated upon.

PPARγ regulates genes involved in insulin action and adipogenesis (differentiation of pre-adipocytes into mature fat cells or adipocytes), inhibits leptin and TNFα (Le Roith and

Zick, 2001; Kersten, 2002). At the current time, there appear to be no studies investigating the role of PPARγ in NASH pathogenesis, although it was the subject of a recent clinical trial (Neuschwander-Tetri *et al.*, 2003).

2.2.6 Leptin

Another hormone of increasing and mesmerising importance in NASH pathogenesis is leptin. This 16 kilodalton product of the *ob* gene was first isolated from mouse choroid plexus and identified as a satiety factor which played a role in energy balance and food intake (Ikejima *et al.*, 2001; Saxena *et al.*, 2002). Accordingly, rodents deficient in leptin expression or signalling (see **2.1**) display hyperphagia and obesity. Early signs of genetic obesity in these animals is evident even in the first week of life, in the absence of hyperphagia (Boulangé *et al.*, 1979). It seems tempting to assume that the principal function of leptin is, therefore, to control appetite and thus protect against obesity. But leptin levels are low in the lean and elevated in the obese, and diet-induced obesity is not essentially corrected in hypoleptinemic mice by restoration of plasma leptin levels (i.e. weight loss as a result of reduced food intake occurs, but food-restricted *ob* mice still deposit excess adipose tissue compared to wild type controls). Leptin levels do not increase significantly after a meal, and leptin by itself, does not lead to the termination of a meal (Friedman and Halaas, 1998). Furthermore, there is no evidence that nutritional abundance has been a prominent feature in the evolution of life, thus negating the need for a system protecting against it (Lee *et al.*, 2001; Chitturi *et al.*, 2002). Some authors have argued that the role of leptin may have evolved as a "thrifty gene" which, as a satiety factor, conferred an advantage during periods of deprivation. Given the toxic effects of fatty acid overload, it also seems likely, however, that leptin (which is expressed mostly in adipose tissue) may have evolved to prevent lipotoxicity by blocking lipogenesis and stimulating FFA oxidation, thus regulating triglyceride accumulation (Chitturi *et al.*, 2002; Day, 2002a). Accordingly, in addition to hypertriglyceridemia, genetically obese rodents (with defective leptin expression or signalling) also have functional impairment of

pancreatic β-cells, and IR. Further, the major site of leptin action is in selected nuclei of the ventrobasal hypothalamus, and hypothalamic lesions in these areas produce IR. Conversely, leptin treatment in *ob/ob* mice causes a rapid drop in insulin levels, even before changes in food intake occur (Khan and Flier, 2000; Lee *et al.*, 2001).

The potential roles of leptin have now been expanded to include immunomodulation and matrix deposition during wound healing (Chitturi *et al.*, 2002; Leclercq *et al.*, 2002; Saxena *et al.*, 2002).

Leptin is upregulated in the obese NASH patient, which may seem paradoxical since the functions of leptin described above (suppression of lipogenesis and TG accumulation, and upregulation of FA oxidation) are in fact compatible with, and drive, improved insulin sensitivity. Yet increased leptin levels must likely occur in the obese patient with NASH, since leptin is synthesized by adipocytes. It has been suggested that this increase may represent a corrective (albeit inadequate) response to steatosis, with which its expression correlates (Diehl, 2002; Chitturi, 2002). Other authors speculate that this increase in leptin may indicate leptin resistance (Friedman and Halaas, 1998), though currently there appears to be no evidence in support of this.

Leptin is also required for development of fibrosis: leptin upregulates profibrogenic TGFβ (Ikejima *et al.*, 2001), leptin deficiency decreases collagen production, and leptin deficient rodents do not develop fibrosis (Leclercq *et al.*, 2002; Saxena *et al.*, 2002). This fits neatly with elevated levels of leptin noted in patients with NASH, although it is noteworthy that leptin expression did not correlate with fibrotic severity in this study (Chitturi *et al.*, 2002). It should also be pointed out that in this study, leptin levels were assessed in serum. This assay does not distinguish between free leptin and leptin bound to the soluble form of the receptor, Ob-Re (Friedman and Halaas, 1998). It is possible

that an association between fibrosis and leptin levels may emerge if there was some mechanism to exclude bound leptin from the assay.

Many theories on the role of leptin in NASH come from genetically obese models of the disease (see **2.1**). Based on the impaired phagocytic ability of macrophages and increased "resting" levels of TNFα and IL-6 (but decreased levels after LPS challenge) in leptin deficient/resistant rodents, the immunomodulatory capacity of leptin has been established (Loffreda *et al.*, 1998). This has led some authors to speculate that part of the pathogenic mechanism of NASH, as it relates to the constellation of obesity/IR/leptin, involves decreased macrophage phagocyte activity, resulting in increased exposure of peripheral adipocytes to gut-derived endotoxin. Escape of bacterial endotoxin into the systemic circulation would then trigger ectopic expression of proinflammatory cytokines such as TNFα, explaining increased expression of this cytokine in peripheral fat (Loffreda *et al.*, 1998). This increased expression, in turn, would play a role in NASH pathogenesis, as described above.

But theories based on results from animal models of NASH should be constructed with caution. The fact that genetically obese models display defective expression or signalling of leptin, in contrast to the human scenario where this hormone is increased, could set in motion a cascade of events that would be misleading and inappropriate for a pathogenic model of human NASH. In addition, unlike in rodents, leptin action in humans has little effect on the hypothalamic-pituitary-adenocortical (HPA) axis; as such, humans with leptin or leptin receptor mutations and obesity do not appear to have extraordinary degrees of IR, and none with diabetes have been described (Khan and Flier, 2000). Perhaps a more informative understanding of the role of leptin in hepatocellular injury may be acquired from investigations of tissue-specific knockouts, or of normal mice treated with hepatotoxic agents, where addition of exogenous leptin to the cocktail

significantly augments inflammatory and profibrogenic responses (Ikejima *et al.*, 2001). On the basis of such studies as these, it is conceivable that the role of leptin in NASH may revolve around (among other things) generation of ROS (by its ability to drive FA oxidation), and propulsion of the steatotic liver towards fibrosis.

2.2.7 Cytochrome P450 2E1 (CYP2E1)

The cytochrome P450 class of proteins (CYP450) were first identified as a cellular pigment having an unusual red-shifted visible absorption maximum (at about 450nm), when present as the reduced-carbon monoxide complex. Later investigations revealed CYP450 to be *b*-type cytochromes containing iron-protoporphyrin IX as the prosthetic group. Since then, it has been established that CYP450 serve numerous functions besides the electron carrying (as a terminal oxidase in mitochondrial and microsomal pathways) for which they were named. The roles of these remarkable enzymes include "mixed" monoxygenation (hydroxylation, by which they incorporate one atom of molecular oxygen into their substrate and another into water), peroxygenation, epoxidation, N- and S-oxidation, desulfuration, reduction of nitro and azo groups, oxides, peroxides and epoxides; deamination and dehalogenation; N-, S- and O-dealkylation, and nonhydrolytic carbon-carbon bond cleavage (Black and Coon, 1987). Through these reactions they are vital for drug metabolism and synthesis of cholesterol and steroids. For many of the reactions, regioselectivity and stereoselectivity are observed. The CYP450 enzymes are therefore highly versatile, unique catalysts among biological oxidizing systems. In humans, there are at least 18 families of CYP450 (with a "family" defined as sequences with >40% amino acid identity) and 43 subfamilies (sequences with >55% identity). The identified human CYP450 are shown in Table 2.2.1.

Table 2.2.1: Human CYP450 (from Nelson, 2001)

CYP450	Function	Encoded by; known subfamilies
CYP1	Drug metabolism	3 genes, 1 pseudo; 3 subfamilies
CYP2	Drug and steroid metabolism	16 genes, 16 pseudo; 13 subfamilies
CYP3	Drug metabolism	4 genes, 2 pseudo; 1 subfamily
CYP4	Arachidonic acid or fatty acid metabolism	11 genes, 10 pseudo; 5 subfamilies
CYP5	Thromboxane A2 synthase	1 gene; 1 subfamily
CYP7A	Bile acid biosynthesis; 7-alpha hydroxylase of steroid nucleus	1 subfamily
CYP7B	Brain specific 7-alpha hydroxylase	1 subfamily
CYP8A	Prostacylclin synthase	1 subfamily
CYP8B	Bile acid biosynthesis	1 subfamily
CYP11	Steroid biosynthesis	3 genes; 2 subfamilies
CYP17	Steroid biosynthesis	1 gene; 1 subfamily
CYP19	Steroid biosynthesis	1 gene; 1 subfamily
CYP20	Unknown	1 gene; 1 subfamily
CYP21	Steroid biosynthesis	1 gene, 1 pseudo; 1 subfamily
CYP24	Vitamin D degradation	1 gene; 1 subfamily
CYP26A	Retinoic acid hydroxylase, important in development	1 subfamily
CYP26B	Probable retinoic acid hydroylase	1 subfamily
CYP26C	Probable retinoic acid hydroxylase	1 subfamily
CYP27A	Bile acid biosynthesis	1 subfamily
CYP27B	Vitamin D3 1-alpha hydroxylase; activates vitamin D	1 subfamily
CYP27C	Unknown	1 subfamily
CYP39	Unknown	1 subfamily
CYP46	Cholesterol 24-hydroxylase	1 subfamily
CYP51	Cholesterol biosynthesis	1 gene, 3 pseudo; 1 subfamily

CYP450-dependent systems are widely distributed through most tissues of the human body, though the liver has by far the highest content. Where the system is present, it can be detected in virtually all subcellular membranes, with endoplasmic reticulum and mitochondria comprising the richest sources. Induction of CYP450 is typically by drugs and toxins (e.g. ethanol, phenobarbital, clofibrate, DDT, halothane and CCl_4 among many), which are detoxified to less pharmacologically potent molecules. Occasionally, however, CYP450 toxify xenobiotics. For example, the relatively harmless aryl hydrocarbon, benzo[*a*]pyrene (a component of charred organic material such as flame-grilled meat), is converted to a highly mutagenic, carcinogenic diol-epoxide derivative by the joint action of CYP450 and epoxide hydrolase (Black and Coon, 1987; Nelson, 2001).

A key function of CP450 is lipid metabolism: they catalyse ω and ω-1 hydroxylation of fatty acids during ω-oxidation, as well as isomerization and hydroxylation of prostaglandins at terminal positions. Such functions suggest a role for CYP450 induction in fatty liver disease: indeed, due to its extensive capacity for detoxification of drugs, solvents and metabolism of alcohol, CYP2E1 is believed to be vital in alcoholic liver injury. CYP2E1 is now known to be a key player in one of the three major pathways through which ethanol is metabolized (the alcohol dehydrogenase [AHD] and catalase systems being the other two [Boggan, 2003]). CYP2E1 catalyses the reaction

$$CH_3CH_2OH + NADPH + O_2 \longrightarrow CH_3CHO + NADP^+ + H_2O$$

During chronic alcohol consumption, levels of the enzyme are rapidly elevated, though they return to normal quickly if ethanol is withdrawn (Takahashi *et al.*, 1993; Roberts *et al.*, 1995).

Because CYP2E1 is also induced by pathophysiological states such as diabetes, prolonged starvation and morbid obesity (probably due to elevated ketone levels associated with these states [Takahashi *et al.*, 1993; Robertson *et al.*, 2001; Woodcroft *et al.*, 2002; Emery *et al.*, 2003]), it comes as no surprise that it factors in NASH, as well. Evidence from animal models shows increased hepatocyte CYP2E1 expression and activity in MCDD mice (Weltman *et al.*, 1996), and increased CYP2E1 immunostaining has been noted in patients with NASH (Weltman *et al.*, 1998). Distribution of CYP2E1 protein is in zone 3, corresponding to sites of maximum hepatocellular damage in human NASH.

It is believed that the pathogenic effects of this increased activity are tied to the ability of CYP2E1 to act as a catalyst of microsomal LP, and thus a source of oxidative stress. CYP2E1 is a major microsomal source of hydrogen peroxide (H_2O_2) and consequently, NADPH-dependent LP. If activity of this enzyme is abrogated, members of the CYP4A

subfamily present as suitable catalytic alternatives, and are also capable of reducing oxygen to superoxide ($O_2^{\bullet-}$) and H_2O_2 (Leclercq, 2000; Robertson *et al.*, 2001).

It is likely the full explanation for the effects of CYP2E1 is not yet known. The regulation of this enzyme is complex, taking place through transcriptional activation (as with ethanol and MCDD), messenger RNA (mRNA) stabilization, increased mRNA translatability and decreased protein degradation – which also plays a role in ethanol-mediated regulation (Koop and Tierney, 1990; Roberts *et al.*, 1995; Weltman *et al.*, 1996). Enzyme activity is to some extent independent of transcriptional activity (Rodriguez-Antona *et al.*, 2001), thus it would be intriguing to elucidate all the factors that regulate both in NASH. In models of alcohol-induced hepatotoxicity, it has been noted that inactivation of Kupffer cells alleviates CYP2E1 induction (Järveläinen *et al.*, 2000); perhaps this interaction plays a role in NASH, too. Investigations of primary cultured rat hepatocytes also show that "normal" insulin activity suppresses CYP2E1 transcription in a dose-dependent fashion, and half-life of CYP2E1 mRNA is decreased from ~48h to ~15h at 10nmolL^{-1} insulin (Woodcroft *et al.*, 2002). It is likely that this interaction is relevant in the context of IR and elevated CYP2E1 in NASH.

2.3 Progression to Hepatic Fibrosis

Although there is disparate information regarding risk factors for fibrosis and rate of fibrosis progression in NASH (see **1.1**), the molecular and morphological changes that herald fibrosis are fairly well understood. It is appreciated that the overall increase in hepatic extracellular matrix (ECM) is vital, revolving mainly around changes in matrix composition within the subendothelial space of Disse (see Fig. 2.3.1). In normal liver, this space contains constituents that are not electron dense, a mesh of ECM that provides cellular support, allows unimpeded transport of growth factors and provides signals to maintain the differentiated function of surrounding cells (Friedman, 2003). However in

injured liver this may be replaced by a matrix filled with elevated levels of fibril-forming collagen (types I and III) and fibronectin (Friedman, 1993). Fibrosis may underlie impaired hepatocyte function, loss of endothelial fenestra and the activation of matrix-producing hepatic stellate cells (HSC, formerly also termed lipocyte, fat-storing or Ito cell). The HSC is now established as the main cell type involved in hepatic fibrosis. In the normal liver, HSCs are the primary storage depot for hepatic retinoids, and are distinguished by intracellular fat droplets containing vitamin A. In most species they also express a cystokeletal intermediate filament characteristic of muscle cells called desmin, and α-smooth muscle actin. With progressive injury, HSC are transformed into myofibrolast-like cells with scant vitamin A and active secretory apparatus for collagen production.

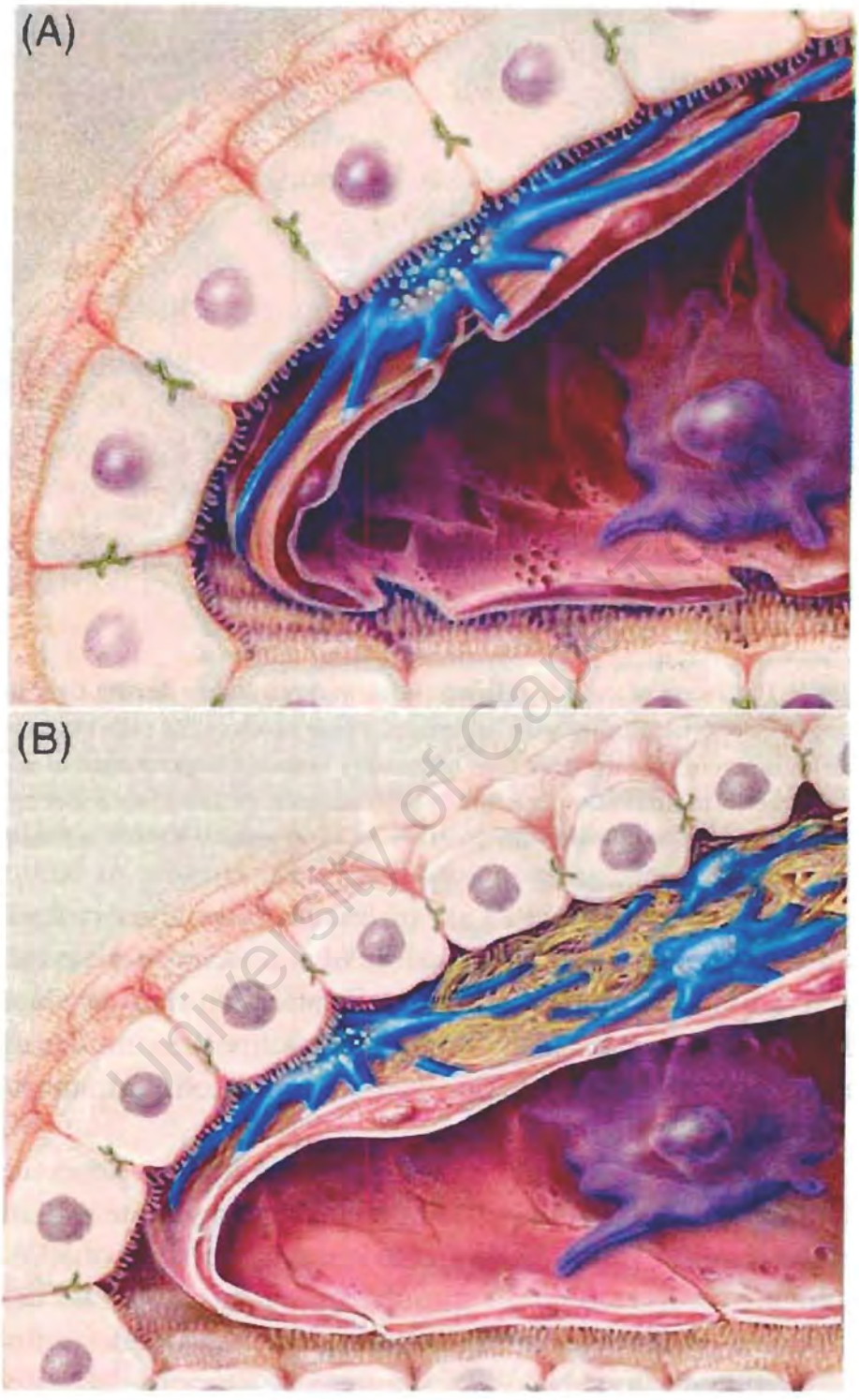

Figure 2.3.1: Changes during fibrosing liver injury. (A) Normal sinusoidal architecture with HSC (blue) containing vitamin A. Hepatocytes (pale pink) possess microvilli, and endothelial fenestrae (endothelial cells in dark pink) are still present. (B) During fibrosis, HSC proliferate and are surrounded by fibrillar matrix. Endothelial fenestrae and hepatocyte microvilli are lost.
Reprinted with permission of the European Association for the Study of the Liver. Friedman, © 2003 J. Hepatology **38:** S38-S53.

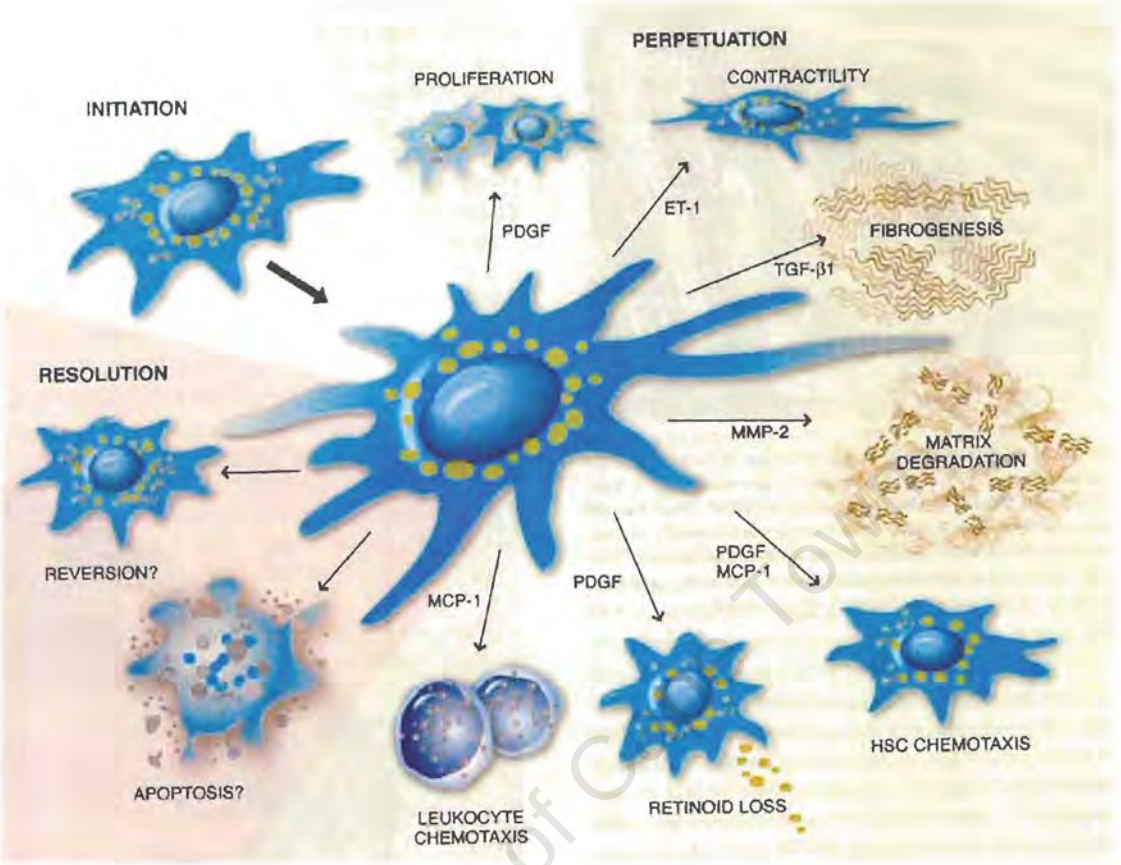

Figure 2.3.2: Pathways of HSC activation and pathways to resolution. Response to injury is HSC activation by a two-step process of initiation and perpetuation. Resolution of fibrosis may occur by reduction of HSC number by apoptosis, and reversal of activated HSC to quiescent phenotype. Reprinted with permission of the European Association for the Study of the Liver. Friedman, © 2003 J. Hepatology **38:** S38-S53.

The critical event in early hepatic fibrosis is HSC ***activation***, the conversion of quiescent vitamin-A storing cells into proliferative, fibrogenic and contractile myofibroblasts (Friedman, 2003). Its features include cell enlargement, increased rough endoplasmic reticulum, loss of vitamin A, proliferation, increased expression of smooth muscle-type features (such as α-smooth muscle-specific actin), and increased production of matrix constituents. Activated HSC express elevated receptors for proliferative and

profibrogenic cytokines such as platelet derived growth factor (PDGF), and TGFα respectively, making them even more responsive to these peptides. Kupffer cells are thought to be the main source of these cytokines in this event. Kupffer cell activation coincides with appearance of HSC activation markers. Kupffer cells stimulate matrix synthesis, cell proliferation and release of retinoids by HSC through the action of lipid peroxidation products, reactive oxygen intermediates, matrix metalloproteinase 9 and cytokines, most notably TGFβ (Friedman, 2003). *In vitro*, exposure of HSC to medium from Kupffer cell cultures accelerates the process of activation. Hepatocytes and leukocytes may also be sources of initiating factors. For example, neutrophils produce reactive species when activated, which may directly promote collagen synthesis (Casini, 1997). Lymphocytes such as CD4+ T helper cells (Th) are also potent sources of cytokines, although their role has been largely overlooked in fibrogenesis associated with liver disease. Available information however appears to indicate that Th2, the subclass of Th cells which produce cytokines such as IL-4, IL-5, IL-6 and IL-13, and promote humoral immunity, favour fibrogenesis in liver injury over Th1 (which secrete proinflammatory cytokines and play a role in cell-mediated immunity [Shi *et al.*, 1997]).

The activated HSC are ***perpetuated*** by direct effects of autocrine and paracrine mediators. PGDF and TGFβ continue to play major roles, as may LP products, and, at least in alcoholic liver injury, toxic metabolites such as acetaldehyde (which stimulates collagen production). Changes in the microenvironment may also perpetuate the activated state. It is known that HSC cultured on gel resembling normal subendothelial matrix remain inactivated for prolonged periods; activation occurs rapidly, however, if they are cultured on gel containing type I collagen. Some authors also suggest changes in the microenvironment of the space of Disse may be promoted by degradation of collagen type IV (matrix component of the space in uninjured liver). This occurs as a result of secretion of type IV collagenase by activated HSC. Although activated HSC are depleted in

vitamin A, it is unclear whether the loss of retinoids is a contributing cause of activation/perpetuation, or a consequence (Friedman, 1993; Friedman, 2003).

HSC activation clearly involves morphological and biochemical changes which require reprogramming of HSC gene expression, a phenomenon which must be orchestrated by changes in activity and expression of key transcriptional factors. A number of these been identified (Mann and Smart, 2002). Among the most prominent is NFκβ, which shows increased activity in non-quiescent HSC. In the context of fibrosis, activation of this transcription factor is distinct from the classical NFκβ response, as it is characterized by persistent elevation of NFκβ, leading to expression of responsive genes such as IL-6 and ICAM-1. Normally, NFκβ is regulated by inhibitor of NFκβ (IKβ-α), which interacts with NFκβ to form inactive cytoplasmic complexes. If NFκβ activation is required, a signal transduction cascade culminates in degradation of IKβ-α, allowing nuclear translocation and subsequent DNA binding of the released NFκβ. This binding results in transcription of responsive genes, which include that for IKβ-α (thus there is a negative feedback loop). It is believed that aberrant expression of NFκβ in activated HSC involves expression of a hyperphophorylated form of IKβ, IKβ-β. This interacts competitively with NFκβ, but lacks the inhibitory properties of IKβ-α. Instead, it serves to keep NFκβ in a transcriptionally active state. The reasons for this remain unknown.

Other transcription factors expressed in activated HSC include members of the AP-1 family, which are required for IL-6 induction; Kruppel-like transcription factors, which have recognition sequences in the genes for α1(I) collagen, TGFβ and TGFβ receptors; CCAAT/ enhancer binding protein (C/EBP), which also regulates α1(I) collagen gene expression; and E-box transcription factors, which have been shown to regulate smooth muscle-specific α actin expression. Interestingly, one transcription factor present in quiescent HSC but diminished in their active counterparts, is PPARγ, cousin to PPARα

(the inducer of lipid transport and oxidation genes, as described under ***2.2.5***). PPARγ regulates genes involved in insulin action and adipogenesis (differentiation of pre-adipocytes into mature fat cells or adipocytes), inhibits leptin and TNFα (Le Roith and Zick, 2001). Although a PPARγ agonist has been used to improve IR by reducing IRS1 phosphorylation in cultured cells and Zucker rats, and rosiglitazone (a PPARγ ligand) shows promise in a recent NASH clinical trial (Jiang *et al.*, 2003; Neuschwander-Tetri *et al.*, 2003), there appears to be no data on investigations which may shed light on its role, if any, in the mechanisms involved in progression to fibrosis.

Indeed, studies specific to the fibrogenic response in NASH are scant. A recent study showed that connective tissue growth factor (CTGF) is over-expressed in liver of patients with NASH, that this expression correlated with degree of fibrosis, and was upregulated by insulin (Paradis *et al.*, 2001). The absence of a correlation between leptin levels and the severity of fibrosis in patients with NASH (Chitturi *et al.*, 2002) is also very interesting; this probably indicates a role for other mediators in the fibrogenic response. Recently, a study in *ob/ob* mice showed the necessity for norepinephrine (a leptin-inducible neurotransmitter which in turn regulates leptin, and is also secreted by HSC) in the development of fibrosis, even in leptin sufficiency (Oben *et al.*, 2003). The emerging picture is still obscure, and highly complex. Much remains to be understood about the factors that drive a steatotic liver to the fibrotic state in the context of NASH.

The pathogenesis of NASH appears increasingly complex. It may be summarized by a "two hit model", as described by Day and James (1998), and elaborated upon by Day (2002). The first "hit" would be development of steatosis, and could be the result of factors such as increased fatty acid flux to the liver due to increased lipolysis, a consequence of peripheral IR. If the available adipose mass is large (as in obesity), the quantity of fatty acids delivered would not be insignificant. Increased FFA supply to an initially insulin-sensitive liver would still result in FFA esterification to TG, leading to steatosis. Resulting progressive lipotoxicity would further drive IR, in part through PUFA control of gene expression. IR could also contribute to initial steatosis by other means: insulin-mediated degradation of VLDL and inhibition of mitochondrial fatty acid oxidation could encourage hepatic triglyceride trapping. These factors could drive increased TNFα expression and thus enhance IR, via IκKβ.

Once steatosis is established, the fatty liver becomes vulnerable to damage. Increased LP, TNFα, CYP2E1, insulin, leptin (probably initially upregulated as a protective mechanism against lipotoxicity, but capable of contributing to the downward spiral of NASH), resulting mitchondrial abnormalities and other factors (described in detail in the sections above) could serve as second hits driving the steatotic liver to steatohepatitis. It has also been hypothesized that NASH pathogenesis can be summarized in terms of a first "hit" which exposes the liver to TNFα, followed by a series of second "hits" which sensitize the liver to the effects of this cytokine (Tilg and Diehl, 2000). However, the central role of TNFα in NASH is debatable, and could well have been overestimated in the past.

In this thesis, some of the factors at play in a rodent nutritional model of NASH are investigated. The basic metabolic derangements resulting from methionine and choline deficiency have been described, however there are limited studies examining the pathogenic alterations occurring in *interactive* hepatoxicity. As discussed earlier, there is

great inconsistency with regard to the amount of alcohol considered "insignificant" during a diagnosis of NASH (see **1.1**). The central aim of this project was, therefore, to investigate the effect of low and high dose alcohol on a fatty liver.

The role of TNFα (which is known to be pivotal in alcoholic liver injury) has also been speculated upon (Tilg and Diehl, 2000; Day, 2002a). As discussed previously (see **2.2.3**, **2.2.4**), TNFα is in many ways the ultimate pro-inflammatory cytokine. It is vital in propagation of the inflammatory process, drives oxidative processes (both beneficially and detrimentally), regulates metabolic processes by interacting with transcription factors, and is instrumental in development of IR by this means. However, although the utility of TNFα suggests a central role for this cytokine in NASH, the question of redundancy has not (to the knowledge of this investigator) been critically addressed in the literature. Two studies (using TNFα knockout mice and LPS as a second hit, respectively) were conducted to address the possibility that TNFα (though vital) may not be an absolute driving force behind the pathogenesis of NASH.

Chapter Three

Materials and Methods

Materials

Animals

Young adult male C57BL6 mice for all studies were obtained from National Health and Laboratory Services, South Africa. For assessment of effect of differing storage conditions on CYP2E1 activity, male C57BL6 mice were obtained from the Hatter Institute, UCT.

Diets

Both the MCDD and Control diets were from ICN Biomedicals. Composition of both diets is detailed in Appendix 1.

Chemicals

Unless otherwise specified, all reagents and chemicals were of analytical grade. Reagents for which company names are not indicated were obtained from other laboratories and were products of internationally established companies.

10% neutral formalin
Aniline – Sigma
Anti F/480 – BMA
Anti-4-HNE – Oxis Research
Anti-CD 19 – PharMingen International
Anti-CD 8 – PharMingen International
Anti-CD4 – PharMingen International
Anti-rat IgG conjugated with Texas Red – PharMingen International
Aspartic acid
Avidin Biotin complex – Vector Laboratories, DAKO Corporation
Biotinylated NK1.1 – PharMingen International
***t*-Butyl hydroperoxide** – Sigma
Butylated hydroxytoluene –Sigma
Chloramine T trihydrate– Merck
Chloroform – BDH
Citric acid – BDH
$CuSO_4.5H_20$ – BDH
Cyclohexane – BDH
DAB – DAKO Corporation
Entellar® Mounting Medium – Merck
Ethanol – Scharlau
Ethylenediamine tetracetic acid (EDTA) – BDH
$(NH_4)_2Fe(SO_4)_2$ (Ferrous ammonium sulphate) – Saarchem, Merck
$FeCl_3$ – Fluka

FITC conjugated rabbit anti-mouse IgG – PharMingen International
Fluorescent mounting medium – DAKO Corporation
Folin-Colciteau phenol reagent – Merck
Glacial CH_3COOH – Merck
Glucose 6-phosphate – Sigma
Glucose 6-phosphate dehydrogenase – Wellington
Glycerol – Sigma
Glycine – BDH
HCl – BDH
Human serum albumin – Sigma
Hydrogen peroxide 30% (w/w) solution – Sigma
Hydroxyproline
K_2HPO_4 – Merck
KCl – Saarchem, Merck
KH_2PO_4 – Merck
Lactate dehydrogenase
L-alanine
Malate dehydrogenase
Methanol – BDH
$MgCl_2$ – Saarchem
Na_2CO_3 – Saarchem
NaCl – Saarchem, Merck
NADH (Nicotinamide Adenine Dinucleotide, reduced form) – Sigma
NaH_2PO_4 – Merck
NaN_3 – Sigma
NAOH – BDH
Nicotinamide adenine dinucleotide phosphate (NADP) – Sigma
***n*-propanol** – Merck
OCT compound – Sakura
Oxaloacetic acid
***p*-Aminophenol** – Merck
***p*-Dimethlyaminobenzaldehyde (Erhlich's reagent)** – Sigma
Perchloric acid – Merck
Phenol – Merck
Phospholipid by choline kit – Roche
Polyclonal rabbit anti-mouse TNFα – PharMingen International
Rat anti-mouse/rat TNFα – PharMingen International
Recombinant TNFα – PharMingen International
Sodium dodecyl sulphate (SDS) – BDH
Streptavidin Cy3 – Sigma
2-Thiobarbituric acid – Sigma
Trichloroacetic acid – Merck
Triglyceride kit – Roche
Triton X-100 – Merck
Vectastain ABC *Elite* kit – Vector Laboratories
Xylenol orange – Sigma
Xylol/Xylene

3.1 Measurement of Aminotransferases

Aminotransferase refers to the class of enzymes that catalyze interconversions of amino acids and α-oxoacids by transfer of amino groups. Hepatic injury results in release of these enzymes, often even before symptoms of liver disease become apparent (Tietz, 1987). Aminotransferases were measured as described by Tietz (1987), as an indication of ongoing hepatic injury.

3.1.1 Sample preparation

Serum was obtained at time of sacrifice by centrifugation of collected blood in a Jouan MR-1812 centrifuge at 857g for 15min.

3.1.2 Alanine aminotransferase (ALT)

ALT catalyses the transfer of an amino group from L-alanine to α-oxoglutarate (with help of pyridoxal-5'-phosphate, P-5'-P), to generate pyruvate and L-glutamate. Since activity of aminotransferases is difficult to measure directly, this assay assesses activity indirectly by quantitation of pyruvate via lactate, as shown:

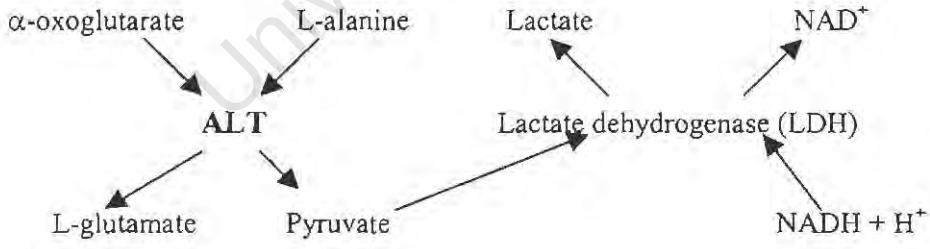

Aminotransferase buffer (13.6g KH_2PO_4, 3.3g NaOH in 1 litre distilled H_2O, pH 7.4) and oxaloacetic acid (0.73g oxaloacetic acid in 30ml buffer, pH 7.4, adjusted to a final volume of 50ml) were prepared and stored at 4^0C and -20^0C, respectively.

A cocktail of 36mg NADH, 19ml buffer, 50µl lactate dehydrogenase (25mg/2.5ml H_2O) and L-alanine (7.6g L-alanine in 100ml buffer, pH 7.4) was prepared fresh. 650µl cocktail was mixed with 50µl serum. The mixture was left at room temperature for 15min to allow NADH-dependent reduction of endogenous oxoacids. Thereafter, 50µl oxaloacetic acid was added, samples were vortexed, and absorbance was read at 340nm every 30sec for 5min. The catalytic activity (quantity of enzyme that catalyzes reaction of 1µml substrate per min) was represented as U/L.

3.1.3 Aspartate aminotransferase (AST)

The principle underlying measurement of AST is similar to that for ALT (Tietz, 1987). However, AST catalyzes the transfer of amino groups from L-aspartate to α-oxoglutarate, generating oxaloacetate and L-glutamate. The assay therefore indirectly measures AST activity by quantitation of oxaloacetate via L-malate production, as shown:

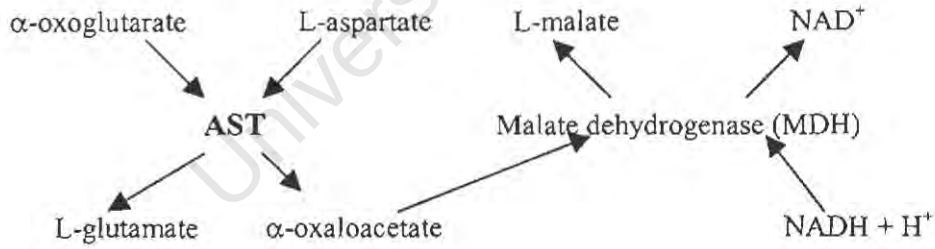

AST was measured only for LTS samples. Aspartic acid solution (pH 7.4) was prepared by dissolving 2.66mg aspartic acid in 100ml aminotransferase buffer. Malate dehydrogenase (MDH) was prepared to a concentration of 5mgml^{-1} in distilled water. Oxaloacetic acid solution was prepared by dissolution of 0.735g oxaloacetic acid in 50ml buffer; this was stored in 5ml aliquots at -20^{0}C.

The reaction cocktail was 36mg NADH, 19ml buffer, 4.5ml aspartic acid solution and 50µl MDH. 650µl of cocktail were mixed with 50µl serum and equilibrated at room temperature for 15min. Subsequently, 50µl oxaloacetic acid was added, the mixture was vortexed and absorbance was read at 340nm every 30sec for 5min. Catalytic activity was represented as U/L.

3.2 Light Microscopy

Tissue processing

Tissue was processed at 37^{0}C. A slice from the left lobe of the liver was immersed in two changes of 10% neutral formalin for 2h and 1h, respectively. Tissue was then dehydrated in two changes of 96% ethanol (1h each), followed by four 1h changes of 100% ethanol. Dehydrated tissue was immersed in three changes (1h each) of xylol. Subsequently, tissue was passed through four changes of embedding wax (three changes at 45min each, one at 1h). The tissue was then embedded in paraffin wax.

Stains were conducted by standard techniques. They included hematoxylin and eosin (H&E) for overall assessment of liver injury and architectural disturbance, periodic-acid Schiff after diastase digestion (D/PAS) for assessment of debris-containing Kupffer cells, and sirus red (SR) for fibrosis.

Sections were coded so they could be assessed and scored "blind", according to the system proposed by Brunt *et al.* (1999), with some modifications. The following factors were assessed:

♦ **Steatosis**
0: None
1: Fat droplets in <33% of hepatocytes
2: Fat droplets in 33-66% of hepatocytes
3: Fat in >66% of hepatocytes

♦**Inflammatory foci (focus defined as ≥5 inflammatory cells)**
0: 0-3
1: 4-9 in 20 high power fields (hpf, 40x)
2: 10-19 in 20 hpf
3: >20 in 20 hpf

♦**Macrophages (as assessed by D/PAS)**
0: 0-3
1: 4-9 aggregates in 20 hpf
2: 10-19 aggregates in 20 hpf
3: >20 aggregates in 20 hpf

♦**Fibrosis**
0: None
1: Zone 3 pericellular fibrosis
2: As above, plus portal fibrosis
3: As above, with bridging fibrosis
4: Cirrhosis

3.3 Immunofluorescence

3.3.1 Tissue preparation

A thin slice of tissue from the left lobe was placed with the cut surface down in a Tissue Tek® cryomold containing a thin layer of OCT compound (Sakura). Thereafter, tissue was covered carefully with OCT, allowed to freeze on dry ice, wrapped in tin foil and stored at –80°C. Prior to staining, tissue was cut 5µm thick at –20°C using a Leica CM 1850 eryostat, and affixed to APES coated slides. Tissue was air dried overnight and marked by circling with a diamond pencil.

3.3.2 Staining for natural killer cell (NK)-specific surface markers (NK1.1)

Sections were acetone fixed and air dried for 10min each. Non-specific binding due to endogenous biotin was blocked with 1% avidin for 15min. Excess avidin was shaken off, and additional blocking was carried out with 0.01% biotin for 15min. After excess biotin was removed by shaking, tissue was incubated for 60min with 100µl of 1:100 biotinylated NK1.1. Unbound antibody was removed by gentle washing with PBS at the end of the incubation period. Thereafter, tissue was incubated with 100µl of 1:100 Streptavidin Cy3

for 60min in the dark. When the incubation period elapsed, tissue was gently washed with PBS and mounted with Fluorescent Mounting Medium.

3.3.3 Macrophage-specific staining (F4/80)

Tissues were fixed in acetone and dried as described (**3.3.2**). Blocking was carried out using normal goat serum100µl (1:200) for 15min. Subsequent staining was carried out in the dark for 60min using 100µl of a 1:100 dilution of rat anti-mouse F4/80. After incubation, tissue was washed with PBS and incubated for 30min with goat anti-rat IgG conjugated with Texas Red (long term study, see **4.5**). As this antibody was unavailable for later investigations, FITC conjugated rabbit anti-mouse IgG was used for fluorescent detection of macrophages in the LPS study (see **5.5**). After incubation, tissue was mounted and viewed as above.

3.3.4 Staining for CD4, CD8 and CD 19 positive cells

Tissue was fixed and dried as above. Non-specific binding was blocked with 5% bovine serum albumin for 15min, after which tissue was incubated for 90min in the dark with either FITC conjugated anti-CD4 for detection of T helper cells, anti-CD8 for detection of T cytotoxic cells or anti-CD19 for detection of B cells.

3.4 Biochemical Quantitation of Collagen by Hydroxyproline

Collagen was measured biochemically by quantitation of hydroxyproline (an imino acid found exclusively in collagen) essentially according to the method of Reddy and Enwemeka (1996). 100µl of liver homogenate (see Materials and Methods **3.5.1**) previously washed in 2:1 methanol/chloroform, and hydroxyproline standards (Table 3.1), were hydrolysed in 50µl of 2N NaOH by autoclaving for 20min at 120^{0}C. Liberated hydroxyproline was subsequently oxidized to the pyrrole by addition of 450µl 0.56M

chloramine T (prepared in 20ml 50% n-propanol and 80ml acetate citrate buffer (120g sodium acetate trihydrate; 46g citric acid; 12ml acetic acid; 34g sodium hydroxide) no more than two days before use, and stored in the dark), followed by 25min incubation at room temperature. Development of a chromophore was encouraged by addition of 500µl freshly prepared Ehrlich's Reagent (15g p-dimethylaminobenzaldehye in 100ml 2:1 v/v n-propanol/perchloric acid) and incubation at 65^{0}C for 20min.

Table 3.1: Hydroxyproline Standards
Stock: D-Hydroxyproline [1µgµl^{-1}], though assay not stereospecific

Vol. Stock [µl]	Vol. Water [µl]	Vol. 4N NaOH [µl]	Total Vol [µl]	Mass of Hydroxyproline [µg]
0	25	25	50	0
5	20	25	50	5
10	15	25	50	10
20	5	25	50	20
25	0	25	50	25

3.5 Measurement of Hepatic and Serum TG, Phosphatidylcholine and Lipid Peroxidation

3.5.1 Tissue processing

Liver samples were thawed on ice, after which approximately 70mg of each liver sample was homogenised on ice in 2ml chilled SEAP (0.15M NaCl, 0.002M NaH_2PO_4, 0.01g% NaN_3, 0.001M EDTA) using a Virtis Handishear®. Subcellular structure was completely destroyed in the resulting homogenate with sonication (twenty 1sec bursts) using a Virtis Virsonic®. 0.8ml of homogenate which was utilised for measurement of lipid peroxidation, and the remainder was aliquoted (600µl per tube) and stored at -70^{0}C.

3.5.2 Lipid extraction

Hepatic lipids were extracted according to a modification of the Folch technique (Bligh and Dyer, 1959). The method is an improvement on the original method described by

Folch (1957), which used large volumes and was time-consuming, making it inappropriate for lipid peroxidation studies. The principle underlying the technique is that tissue in a monophasic solution of chloroform and methanol separates into a biphasic system when diluted with chloroform and an aqueous solvent. The lipid fraction remains in the non-aqeous phase (chloroform), while the aqueous methanol eontaining phase holds non-lipid impurities

To 0.8ml homogenised liver or rodent chow was added 2ml ehilled methanol and 1ml chilled chloroform. The mixture was vortexed for 20sec and subjected to centrifugation for 15min (2 056g, 4^0C) in a Beckman GS-6R centrifuge. The resulting supernatant was transferred to a clean tube on ice. The remaining pellet was then washed by addition of 2ml methanol, 1ml chloroform and 0.8ml SEAP, vortexed and subjected to centrifugation as described above. A phase split was effected to remove non-lipid impurities from the pooled supernatant by addition of 2ml chloroform and 2ml SEAP. The mixture was vortexed and subjected to centrifugation for 10min (2 056g, 4^0C). The upper (aqueous) phase was removed by suction, leaving an organic phase that was dried at room temperature under nitrogen gas in a Pierce Reacti-therm module. The dried extract was then re-suspended in 200µl chloroform and aliquoted into tubes containing 20µl each. The solvent was dried completely (in the dark) to prevent contamination of subsequent assays by chloroform. The measured mass of lipid extracted was often influenced by protein dust and other insoluble debris, which collected on the walls of tubes, and could not be removed. As a result of this, the coefficient of variation (measure of consistency) for the mass of extracted lipid ranged from 6-19%; the presumed mass of lipid extracted from each liver has therefore not been recorded for any study.

3.5.3 Hepatic and serum TG

Hepatic TG were measured according to the method of McGowan *et al.* (1983), using a commercial kit. Hydrolysis of TG is catalyzed by lipase to produce glycerol and free

fatty acids. The glycerol generated is then phosphorylated to glycerol 3-phosphate (G3P) by adenosine 5'-triphosphate, in the presence of glycerol kinase. Subsequent oxidation of G3P to produce hydrogen peroxide and dihydroxyacetone phosphate is catalyzed by L-α-glycerophosphate oxidase. The chromogenic indicator is a quinoneimine formed from a reaction between hydrogen-peroxide, 4-aminophenoazone and 4-chlorophenol, under the influence of a peroxidase.

Standards were prepared by mixing an appropriate amount of commercial standard ($200mgdl^{-1}$) with requisite volumes of 0.9% NaCl, as described in Table 3.2. Standards were then mixed with 50μl ethanol and 15μl 1% Triton X-100. Experimental samples were prepared by adding 10μl homogenate to 50μl ethanol, 15μl 1% Triton X-100 and vortexing for ten seconds each. Thereafter, 490μl 0.9% NaCl was added to the mixture. After a final vortex, the mixtures were spun for 1min in a Jouan MR-1812 centrifuge (13 709g, 4^0C) to pellet the powdery sediment, and 125μl of the clear supernatant was carefully transferred to a microtitre plate. To this was added 125μl of the provided enzyme reagent, with mixing. The reaction was considered complete after twenty minutes, and absorbance was read at 500nm. The quantity [μg] of TG in each sample (in duplicate) was extrapolated from a linear regression curve of the standards.

The process for measurement of serum TG was essentially identical. Serum was obtained as described (**3.1.1**). 20μl of serum and 480μl 0.9% NaCl were used for the triglyceride assay, which in all other respects was conducted as described above. Coefficient of variation for the TG assay was 5%.

Table 3.2: Triglyceride standards
Stock solution: 200mgdl^{-1}

Vol. Stock solution [µl]	Vol. 0.9% NaCl [µl]	Triglyceride content [µg]
0	500	0
1	499	2
2.5	497.5	5
5	495	10
10	490	20
20	480	40
25	475	50
40	460	80
50	450	100

†*Precinorm® U*, a commercially provided standard with a TG range of 111-153mgdl^{-1} was used as a positive control.

3.5.4 Phosphatidylcholine

Measurement of phosphatidylcholine was according to instructions of a commercial kit. Phosphatidylcholine, in the presence of phospholipase D, is broken down to choline and phosphatidic acids. The choline generated is oxidised by choline oxidase to betaine and hydrogen peroxide; the latter reacts with 4-aminophenazone and phenol in the presence of a peroxidase to yield the chromogen, 4-(p-benzoquinone-mono-imino)-phenazone, the quantity of which is assessed spectrophotometrically.

Due to technical limitations, this assay was conducted only on LTS samples. The protocol for preparation of samples for the assay was identical to that described for TG, though dried lipid extract was used as the substrate (EDTA in the homogenate interferes with activity of calcium-dependent phospholipases). Standards and enzyme reagent were provided with the kit (Roche). Enzyme reagent was prepared by mixing 40ml of the provided buffer with the enzyme reagent. Details of the standards used are given in Table 3.3.

Table 3.3: Phospholipid Standards
Stock solution: Choline chloride [54.1mgdl^{-1}]

Vol. Stock solution [µl]	Vol. 0.9% NaCl [µl]	Choline content [µg]
0	500	0
1	499	0.54
7	493	3.79
14	486	7.57
28	472	15.10

†*Precinorm® U*, a commercially provided standard with a PL range of 80-134mgdl^{-1} was used as a positive control.

3.5.5 Measurement of conjugated dienes

Pure, unoxidized cyclohexane has an optical density of 0.049 at 234nm. A GBC UV/VIS 916 spectrophotometer was used to set the baseline with distilled water and the absorbance of a cyclohexane blank was measured to ascertain purity. Cyclohexane with an OD within 0.02 was assumed to be sufficiently pure for the assay.

Conjugated dienes (CD) were measured as previously described (Vasankari *et al.*, 1995). The assay operates on the understanding that molecules containing conjugated dienes are characterized by an intense absorption (K band) which ranges, with respect to its peak, from 215-250nm, depending on nearby substituent groups (Recknagel and Glende, 1984). The spectra of lipids containing CD are characterised by an intense K band near 233nm, with a lesser secondary absorption maximum due to ketone dienes, in the range of 260-280nm.

CD content of each sample was measured by addition of 1ml cyclohexane to the lipid extract and vortexing for ten seconds to encourage dissolution. Immediately after, the absorbance of each sample was measured at 234nm. Each sample was assayed in duplicate. The concentration of conjugated dienes in each sample was calculated using a molar extinction coefficient (Σ^M) of 2.95×10^4 $M^{-1}cm^{-1}$. The coefficient of variation for the assay was 12%.

3.5.6 Lipid hydroperoxides

Lipid hydroperoxides were measured indirectly according to principles outlined by Jiang *et al.* (1991, 1992), in which the oxidation of Fe^{2+} to Fe^{3+} by peroxides is described. In the presence of xylenol orange, a dark brown Fe^{3+}-xylenol orange complex is formed which absorbs maximally at 560nm.

Dried lipid extract was re-dissolved in 100µl chloroform, mixed with 350µl methanol and the mixture vortexed to generate a monophase. To each tube was then added 50µl nanopure water and 600µl FOX 2 Mix†. Standard reactions were prepared by mixing bland chloroform with methanol (as described above) and 50µl of the relevant standard (Table 3.2, 3.3). The reaction was allowed to proceed for 20min, then all tubes were spun at 13 709g in a Jouan MR-1812 centrifuge for 1min. Absorbance was read thereafter at 560nm. The concentration of lipid hydroperoxides in each sample (measured in duplicate) was determined by extrapolation from a non-linear regression curve of the t-butyl hydroperoxide (BHP) standards. The consistency of the assay was assessed by coefficient of variation (11%), and by calculating the ratio of BHP to $FeCl_3$ at absorbance of 1.00, which had a value of 8.62±0.27.

†***FOX 2 Mix:*** *1 part FOX 2A (2.5mM ferrous ammonium sulphate, 2mM Xylenol Orange in 0.25mM H_2SO_4) to 4.5 parts FOX 2B (0.88mM BHT in methanol), always prepared fresh.*

Table 3.4: $FeCl_3$ Standard Curve
Stock solution†† = 4mM $FeCl_3$

Stock Solution [µl]	Water [µl]	Concentration of working solution [mM]	Quantity of ferric chloride in assay [nMol]
20	980	0.08	4
40	960	0.16	7
80	920	0.32	15
100	900	0.40	18
400	600	1.6	73
500	500	2.0	91

††*Prepared fresh weekly*

Table 3.5: BHP Standard Curve
Stock solution = 6.96mM BHP
Working solution (W.S.) = 1000µl stock solution + 9000µl nanopure water

W.S. [µl]	Water [µl]	Concentration of working solution [mM]	Mass of butylated hydroperoxides in assay [nMol]
40	960	0.028	1
100	900	0.070	3
200	800	0.140	6
300	700	0.278	9
400	600	0.557	13
800	200	0.696	25

3.5.7 Thiobarbituric acid reactive substances (TBARS)

Measurement of TBARS was done according to the method of Asakawa and Matsushita (1979), with minor modifications. The assay measures the pink chromogen formed when aldehydes and other late products of lipid peroxidation react with thiobarbituric acid. Therefore, although the assay is often used as a tool for detection and measurement of the late, so-called secondary scission product malondialdehyde, it is not specific for this.

To all tubes were added 50µl 0.27% $FeCl_3$, and 100µl ethanol (for measurement of "total" TBARS, i.e. those present at time of death and those generated subsequently during tissue handling) or 100µl containing 0.22% butylated hydroxytoluene, an antioxidant (for measurement of "free" TBARS, i.e. the amount of TBARS present at time of death). To experimental tubes was then added dried lipid extract dissolved in 50µl chloroform. Chloroform and water blanks were prepared by adding 50µl bland chloroform and 50µl nanopure water respectively. The mixtures were vortexed for five seconds each, mixed with 750µl glycine buffer, pH 3.6 (0.2M glycine HCl) and 750µl TBA reagent (0.5% thiobarbituric acid, 0.3% SDS), and vortexed again. The tubes received a glass bead each, were capped with marbles and boiled at 100^{0}C. After exactly 15min, the tubes were

removed, cooled to room temperature and mixed with 500µl glacial acetic acid and 500µl chloroform. The mixture was vortexed and spun for 15 min

(2 056g, 4^0C). Two hundred fifty microlitres (250µl) of the pink aqeous phase of each sample was used to determine the concentration of TBARS by measuring absorbance at 540nm; the value of Σ^M used was $1.09x10^5$ $M^{-1}cm^{-1}$. All samples were assayed in duplicate. The coefficient of variation for the free TBARS assay was 6%, while that for the total TBARS assay was 11%.

3.6 Histological Assessment of 4-Hydroxy-2-nonenal (4-HNE)

Protein adducts of the late LP product, 4-HNE, were detected on routine formalin fixed, paraffin embedded sections according to a modification of the method described by Zheng (1998), using the avidin-biotin-peroxidase complex (ABC). Sections were dewaxed for 5min in xylene, then rehydrated with 100% ethanol, 95% ethanol, 70% ethanol and water respectively. Antigen retrieval was subsequently conducted in 10mM citric acid (pH 6.0) by warming for 1min and then boiling for 10min in a microwave. Sections were allowed to return slowly to room temperature and then washed and allowed to soak in distilled water (5min).

Endogenous peroxidase activity was quenched by soaking for 20min in freshly prepared 3% hydrogen peroxide in 60% methanol. All subsequent incubations were carried out in a humidified chamber. Endogenous biotin was blocked with a commercially available kit (DAKO) by incubating in avidin and biotin solutions (15min each). Tissue was washed with Buffer B (10mM phosphate buffered saline, 0.3% triton X-100) and final blocking was conducted for 40min using 1 drop normal horse serum in 2.5ml Buffer B. Blocking serum was drained and tissue was incubated for 60min with 50µl freshly prepared anti 4-HNE ($10\mu g\mu l^{-1}$) in 10mM phosphate buffered saline (PBS, 8g NaCl, 0.2g KCl, 1.44g

Na_2HPO_4, 0.24g KH_2PO_4, pH 7.4). After incubation, the sections were washed 3 times and incubated with ~100µl of a universal secondary antibody for 40min. During the incubation, ABC mix was prepared and allowed to stand for 30min before use. Secondary antibody was washed off 3 times and tissue was incubated with ABC mix for 40min. At this time, DAB was mixed as recommended by the supplier, with 1 drop of nickel solution to obtain a dark stain. Tissue was washed once with water, then incubated with DAB for 7min. The stain was drained, and sections were couterstained with hematoxylin (10sec) and Scott's solution (10sec). Sections were then mounted with Entellar® mounting medium.

3.7 Measurement of Total Protein

Total protein was measured according to the method of Lowry *et al.* (1951), as modified by Markwell *et al.* (1978). This modification incorporates an increased quantity of a copper tartrate reagent, which allows the use of tissue homogenates containing EDTA, a chelating agent which interferes with Lowry's method.

Two distinct steps underlie the principle of the assay: the chromogenic reaction of proteins with copper (which generates the initial faint blue tint), and the reduction of phosphomolybdic-phosphotungstic reagent (Folin Ciocalteu) by the copper treated protein, which intensifies the colour (Lowry *et al.*, 1951).

40µl of 1/10 dilution for homogenate and 1/50 dilutions for microsomes (see **3.8**) were utilized. The substrate was brought to a final volume of 250µl with nanopure water, to which was added 750µl Solution $C^{†††}$. The mixture was vortexed and left to stand for 15min. Thereafter, 75µl Folin C solution (1:1 Folin Ciocalteu/water) was added forcefully to the mixture. Due to the short half-life of the reagent (Lowry, 1951), the

mixture had to be vortexed immediately; it was then left to stand for 45min to encourage development of full colour. Human serum albumin was used as a standard and prepared as detailed in Table 3.6.

[†††]***Solution C:*** *100:1 Solution A/Solution B*

Solution A: *2% anhydrous Na_2CO_3; 0.4% NaOH; 0.16% $Na_2CO_4O_6$; 1% SDS*

Solution B: *4% $CuSO_4.5H_2O$*

Table 3.6: Protein Standards
Stock: Human serum albumin [1µgµl^{-1}]

Vol. Stock solution [µl]	Vol. water [µl]	Protein content [µg]
0	250	0
5	245	5
10	240	10
15	235	15
20	230	20
25	225	25
30	220	30
50	200	50
90	160	90
150	100	150
250	0	250

3.8 Comparison of Cytochrome P450 2E1 (CYP2E1) Activity

The production of *p*-aminophenol (4-hydroxyaniline) from aniline was used as a measure of CYP2E1 activity, as originally described by Imai *et al.* (1966). To maximise microsomes, the remains of the left lobe and the whole middle lobe of the liver were used.

Microsomes were extracted according to the method of Donato *et al.* (1999) with minor modifications. Tissue was homogenized in 2ml CYP homogenization mix (50mM Tris HCl, 150mM KCl and 1mM EDTA, pH 7.4). The homogenate was then transferred to microfuge tubes and spun at 10 000g for 20min at 4°C. The supernatant was transferred to 11x60mm Beckmann Ultra-clear® polyallomer tubes and brought to a final volume of

6ml with homogenization mix. This was spun at 100 000g for 40min at 4°C in a Beckman L-80 ultracentrifuge, using a SW65 (swing-out) rotor.

The supernatant was decanted and the microsomal pellet was suspended with three short pulses of a sonicator in 200µl CYP solublization mix (CYP homogenization mix with 10% glycerol), separated into 50µl portions and snap frozen in liquid nitrogen. Aliquots were stored at -80°C until required.

Reports of loss of cytochrome activity during cold storage (Pearce *et al.*, 1996) prompted a set of experiments prior to measurement of enzyme activity in microsomes from LTS and TNFKO studies. Briefly, wild type C57BL6 mice were sacrificed using carbon monoxide. Livers were rapidly removed, and divided into lobes. The left and middle lobes were used for each experiment. Each was divided into half, and one half was snap frozen and stored at -80°C. The second half was homogenized as described previously, 1ml was used for immediate microsomal extraction and the other 1ml of homogenate was stored at -80°C. The extracted microsomes were snap frozen and stored. Two weeks later, microsomes were also extracted from frozen liver and homogenate.

The assay was conducted on all samples to determine whether CYP2E1 activity was retained regardless of storage by assessing a time course of enzyme activity, and enzyme activity at a fixed time point.

To 50µl microsomes was added 450µl Cyp Reaction mix (16mM aniline, 0.64mM NADP, 6mM glucose 6-phosphate and 5mM $MgCl_2$)in 0.1M phosphate buffer (13.97g K_2HPO_4, 2.7g KH_2PO_4 in 1litre of water, pH 7.4). The temperature of the mixture was equilibrated by incubation at 37°C for 10min. The reaction was started by addition of 500µl substrate mix containing 1.3U glucose 6-phosphate dehydrogenase in phosphate

buffer. The standards were 0-100nmol *p*-aminophenol (Table 3.7), prepared to a final volume of 600µl. Since the standards were the expected end product of aniline hydroxylation, they were incubated in the absence of reaction and substrate mixes. All mixtures were incubated for 40min at 37°C. The reaction (samples but not standards) was stopped by addition of 250µl 20% trichloroacetic acid, and spun at 857g for 10min at 4°C to pellet precipitated protein. 600µl of the resulting supernatant was transferred to a fresh tube. Chromophore development was encouraged in samples and standards by addition of 200µl 10% Na_2CO_3 and 2% phenol, respectively, followed by 40min incubation in the dark. Absorbance was read at 590nm.

The assay procedure was identical for LTS and TNFKO samples, except that prior investigations showed the reaction to be complete at ~60min. The mass of *p*-aminophenol generated from the microsomal system was determined from a non-linear regression of standards, and expressed per mg microsomal protein, per minute.

Table 3.7: *p*-Aminophenol standards
Stock: 0.1456g *p*-aminophenol in 1ml H_2O [1M]
Working solution (w.s.): 100µl stock + 9900µl phosphate buffer [0.01M]

Vol. W.s. [µl]	Vol. Phosphate buffer [µl]	Initial Conc. [µM]	Conc. in assay [µM]	Mass of *p*-aminophenol in reaction [nmol]
0	600	0	0	0
0.5	599.5	8.3	5	5
1	599	16.7	10	10
2	598	33.3	20	20
4	596	66.7	40	40
6	594	100	60	60
10	590	166.7	100	100

3.9 Measurement of Serum TNFα

TNFα was measured in serum from the LPSS, according to the method of Coligan *et al.* (1994). All resources were kindly supplied by the laboratory of Professor Frank Brombacher.

Coating

Nunc-maxisorp plates were coated with purified rat anti-mouse/rat TNFα diluted to 1:1000 in 10mM PBS (see **3.6**) with 1% v/v bovine serum albumin and 0.02% w/v sodium azide ("TNF dilution buffer"). 50µl was added to each well. The plate was sealed with cling film and incubated overnight at 4°C.

Blocking

Plates were washed four times with 200µl/well of 10mM PBS containing 0.02% w/v sodium azide and 1% v/v Tween. Blocking was thereafter conducted y adding 200µl/well of 2% w/v low fat milk in 10mM PBS. Plates were re-sealed and incubated overnight at 4°C. The following day, plates were washed as described above.

Assay

Standards were recombinant TNFα, diluted 3-fold with TNF dilution buffer (to a total of 60µl) in a range of 0.001 to 100ng (see Table 3.8). The dilutions were conducted in a non-coated plate.

Table 3.8: Recombinant TNFα standards
Working solution (w.s.): Recombinant TNFα [1.67ngμl^{-1}]

Standard	Vol. [μl] relevant solution (brackets)	Vol. dilution buffer [μl]	Final volume [μl]	Mass of TNFα [ng]
1	90 (w.s.)	0	60	100
2	30 (standard 1)	60	60	33.33
3	30 (standard 2)	60	60	11.11
4	30 (standard 3)	60	60	3.70
5	30 (standard 4)	60	60	1.23
6	30 (standard 5)	60	60	0.41
7	30 (standard 6)	60	60	0.14
8	30 (standard 7)	60	60	0.05
9	30 (standard 8)	60	60	0.02
10	30 (standard 9)	60	60	0.005
11	30 (standard 10)	60	60	0.002
12	30 (standard 11)	60	60*	0.001

*30μl of original 90μl discarded to equalise volume

Serum samples were diluted ½, $^1/_3$, and $^1/_9$ in dilution buffer to a total volume was 50μl. When all samples had been added to the coated and blocked assay plate, 50μl of each standard was transferred. The top and bottom rows and the first and last column of each plate were not utilised, as evaporation is fastest in these regions. Plates were sealed with cling film and incubated at 37^{0}C for 3h. Thereafter, plates were washed four times with distilled water.

Secondary antibody was 1/1000 biotinylated IgG fraction of polyclonal rabbit anti-mouse TNFα, prepared in dilution buffer. 50μl was added to each well and incubated for 3h at 37^{0}C. Plates were washed four times at the end of the incubation period with distilled water.

Conjugation was carried out with 50μl/well of alkaline phosphatase labelled streptavidin in dilution buffer (1/1000). Incubation was for 1h at 37^{0}C, after which plates were washed four times with distilled water. Substrate (*p*-nitrophenol phosphate) was prepared

at a concentration of $1mgml^{-1}$ in substrate buffer (0.02% w/v sodium azide, 0.08% $MgCl_2.6H_2O$, 9.7% v/v di-ethanolamine, liquified in water bath). 50µl was added to each well, the plates were covered with tin foil (substrate is photosensitive) and incubated at 37^0C. Readings were taken at 405nm after 30min and 1h incubations.

3.10 Statistical Analyses

Statistical analyses were conducted in GraphPad Prism. Comparisons between 2 treatment groups (e.g. Ctrl versus MCD) were conducted with non-parametric, 2-tailed t-tests (Mann-Whitney). To compare the effect of one treatment within groups (e.g. comparing effect of alcohol in Ctrl or MCD groups), comparisons were conducted using non-parametric single variable analyses of variance (Kruskall-Wallis test). Differences were considered statistically significant when $p<0.05$.

Chapter Four

Animal Studies of Interactive Hepatoxicity I:

Effect of Alcohol on Fatty Liver

All studies were conducted with the approval of the UCT Ethics Committee for Research on Animals, and in compliance with the standards of the Medical Research Council (MRC), South Africa.

4.1.1 Pilot Short Term Study (STS): Role of short term alcohol consumption in the MCD model of NASH

Biochemical and histological assessment for this study was conducted on tissue harvested at the end of a previous study in which liver tissue was generated using the MCD model of NASH. The study had been previously conducted by colleagues in the UCT NASH Research Group (Principal investigator Professor P. Hall); the aim of the study was to assess the effect of low (4% v/v) and intermediate (8% v/v) dose alcohol in the methionine-choline deficient animal model of NASH (see **2.1**). For 4 weeks, animals were maintained on a high fat, methionine and choline deficient diet (MCDD) or control (Ctrl) diet supplemented with choline bitartate (2g/kg) and DL-methionine (3g/kg). The effect of alcohol was tested in mice by allowing free access to water, 4% ethanol and 8% ethanol (all supplemented with 0.025%w/v saccharine from Sigma, and started before commencement of the diets), as shown below. Mice were placed on a diurnal 12h light/dark cycle. At termination, segments of liver tissue were frozen for subsequent studies, as well as for quantitation of hepatic TG and assessment of lipid peroxidation (LP) to investigate the effect of low dose alcohol on liver injury due to the MCDD.

Experimental design of the short term study

Water +0.025% (w/v) saccharine + Ctrl diet
4% ethanol +0.025% (w/v) saccharine + Ctrl diet
8% ethanol +0.025% (w/v) saccharine + Ctrl diet
} n=6/group

Water +0.025% (w/v) saccharine + MCDD
4% ethanol +0.025% (w/v) saccharine + MCDD
8% ethanol +0.025% (w/v) saccharine + MCDD
} n=6/group

4.1.2 Long Term Study (LTS): The effect of long term alcohol intake in the MCD model of NASH

This formed the definitive study in the program, and was conducted to

- Induce a hepatic environment resembling advanced human NASH, including structural alterations such as fibrosis
- Assess the effect of the MCDD plus alcohol given over prolonged periods on lipid accumulation and LP, hepatic injury and activity of cytochrome P450 2E1 (CYP2E1)
- Characterize the nature of the inflammatory infiltrate present in this late stage of hepatic dysfunction
- Determine the effect, if any, of intermediate (8% v/v) and high (20% v/v) dose alcohol consumption on a steatotic liver.

The study was conducted in duplicate (denoted in Appendix 3 as "Group 1" and "Group 2", conducted simultaneously). The first group was utilised for assessment of liver pathology, biochemical assays and measurement of aminotransferases; the second group was used for measurement of serum TG. Plans were set in place to utilise the second group in future analysis of cytokine profiles.

Two groups of 48 male C57BL6 mice were allowed two weeks to acclimatise in the UCT Animal Facility, before being placed on water + 0.025% (w/v) saccharine. For animals on alcohol + 0.025% (w/v) saccharine, the concentration of ethanol was raised by 2% every second day until the desired concentration (see below) was achieved. Only after all animals had been on their requisite concentrations of ethanol for a minimum of 4 days, were Ctrl and MCDD dietary regimens begun. All animals were placed on a diurnal 12h light/dark cycle.

Experimental design of the LTS

Water + 0.025% (w/v) saccharine + Ctrl diet
8% ethanol + 0.025% (w/v) saccharine + Ctrl diet
20% ethanol + 0.025% (w/v) saccharine + Ctrl diet
} n= 8/group

Water + 0.025% (w/v) saccharine + MCDD
8% ethanol + 0.025% (w/v) saccharine + MCDD
20% ethanol + 0.025% (w/v) saccharine + MCDD
} n= 8/group

Ctrl animals were maintained on the diet for 57 days (due to unanticipated shortage of diet), MCDD animals were maintained on the diet for 63 days. During this period animals were allowed food and drink *ad libitum*. Drink was refreshed every second day, and once weekly all animals were weighed.

Sacrifice was by cardiac puncture and exsanguination under ether anaesthetic. Blood was collected in eppendorf tubes for measurement of aminotransferases, serum TG and blood alcohol, though the latter was ultimately not measured due to a technical mishap. At the time of sacrifice, body weight and liver weight were also recorded. Livers were divided into the (A) left lobe (for routine stains, immunohistochemical stains of LP-protein adducts, immunocytochemistry, lipid peroxidation and electron microscopy), (B) median lobe (for measurement of cytochrome P450 2E1 activity), (C) right and posterior lobes. Once portions had been suitably allocated, tissue was wrapped in tin foil and snap frozen in liquid nitrogen. All tissue was subsequently stored at -80^{0}C until required.

Results

4.2 Body and Liver Weight

All animals on the MCDD experienced weight loss and lethargy compared to controls (Figure 4.1), although this state did not appear to be a consequence of inadequate food intake. Conversely, Ctrl mice experienced steady weight gain and remained active for the duration of the study. At sacrifice, the livers of MCD animals were distinguished by a pale pink

appearance. In LTS rodents, MCD livers also had a slight greasy consistency and granular appearance, and infrequently some specimens developed small nodules. Livers of MCD animals were significantly smaller than control counterparts in all studies. When adjusted to body weight (i.e. liver weight per gram body weight) to correct for weight loss on the MCDD, liver:body weight was similar in all groups (Figure 4.2). Raw data of LTS weights may be found in Appendix 2.1.

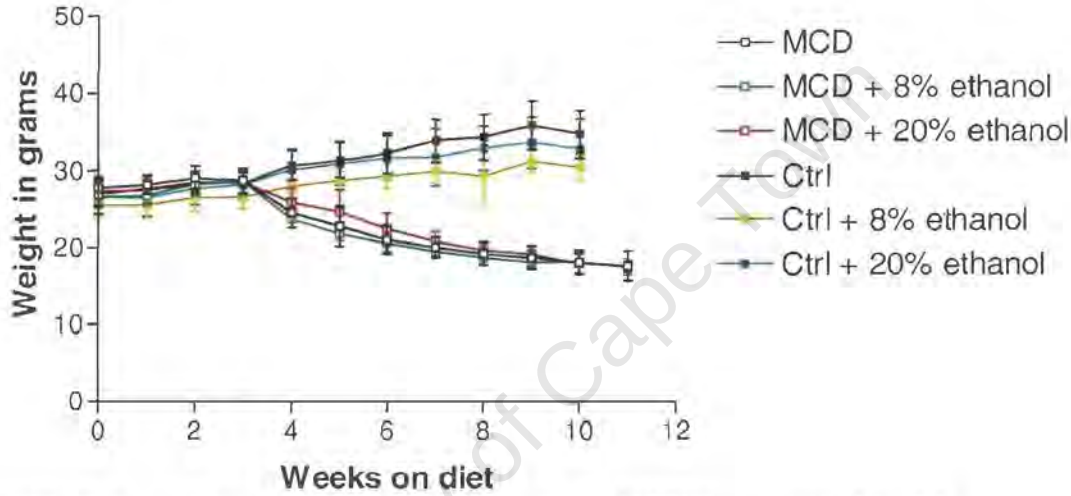

Figure 4.1: Body weight over the course of LTS. Mice on the MCDD lose weight while Ctrl counterparts gain weight.

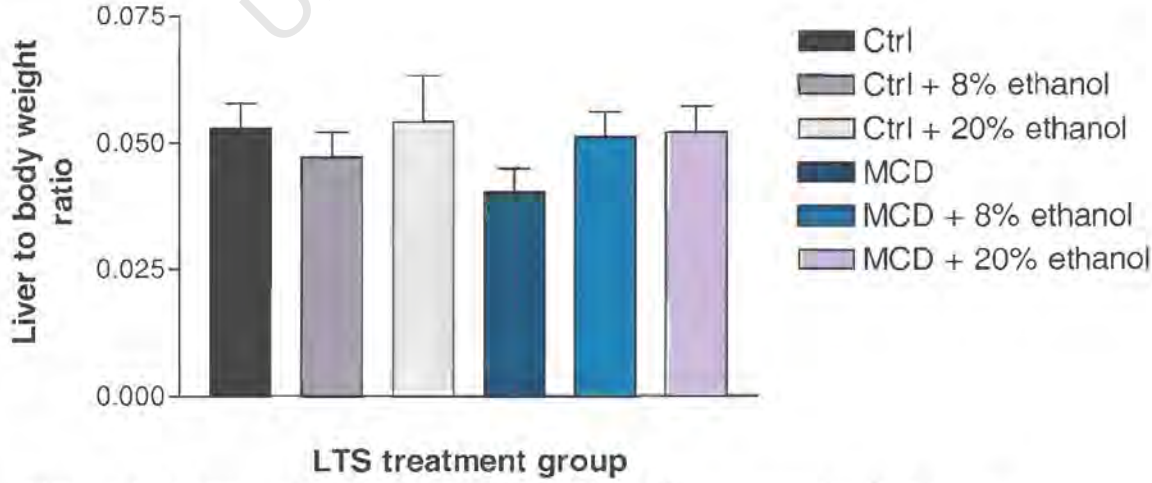

Figure 4.2: The ratios of liver weight:body weight in the LTS are comparable for all groups.

4.3 Aminotransferases

Alanine aminotransferase (ALT) levels were measured for all studies. In LTS animals, alanine aspartate transferase (AST) levels were also measured; however due to concerns regarding the influence of ether anaesthesthesia on AST levels (E. Shepard, private communication) this assay was excluded in subsequent studies.

In LTS rodents, aminotransferase levels were significantly raised in MCD versus Ctrl (ALT p=0.0109; AST p=0.0031). Both ALT and AST levels were affected by alcohol intake in MCDD groups, though the changes did not reach statistical significance (ALT p=0.1973; AST p=0.3768). Aminotransferases showed no significant change with alcohol intake in Ctrl samples. The ratio of AST to ALT was slightly greater than 1 in Ctrl, Ctrl plus 8% ethanol and MCDD, but was roughly 1 in all other groups (Figure 4.3). Raw data is presented in Appendix 2.3.

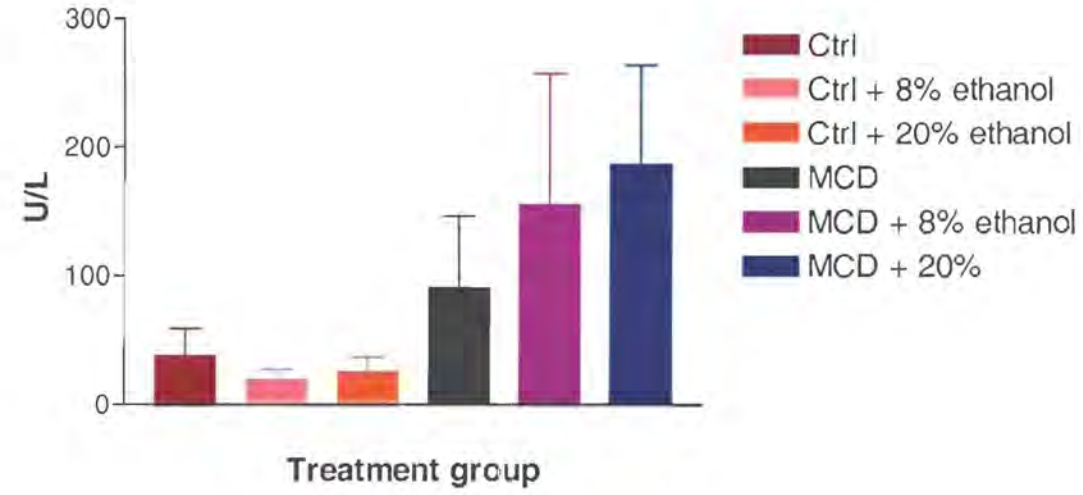

A

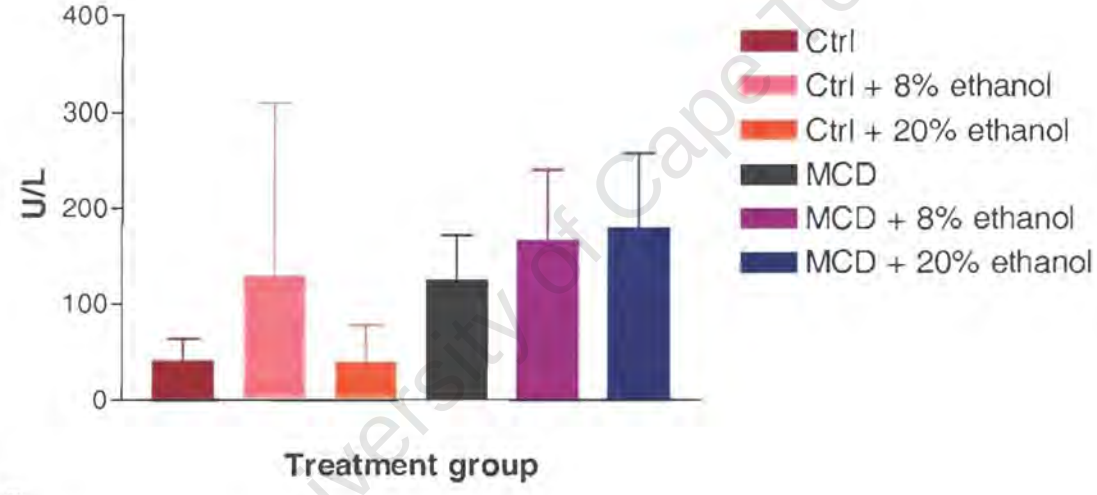

B

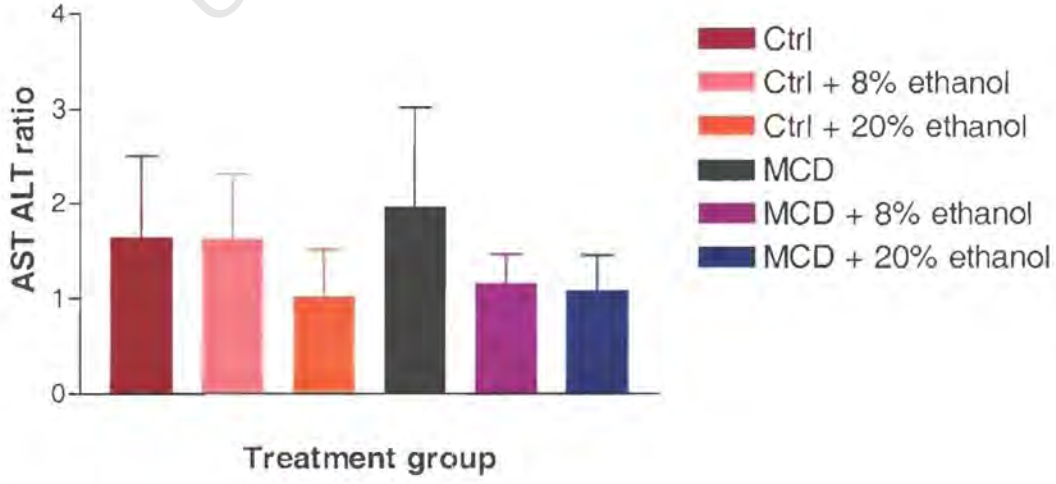

C

Figure 4.3: (A) ALT (B) AST (C) AST/ALT of LST treatment groups. Although alcohol consumption enhanced aminotransferase levels, only differences in MCD vs Ctrl were significant (ALT p=0.0109; AST p=0.0031).

4.4 Histopathology

4.4.1 Steatosis

All animals on MCDD developed macrovesicular steatosis (Figure 4.4), with lipid in ~70-90% of hepatocytes. In some LTS MCDD animals on alcohol, steatosis was mixed (micro and macrovesicular). Other than this, there was no apparent difference at the level of light microscopy with regard to steatosis, between MCD animals on water and MCD animals on either dose of alcohol. In the LTS, one animal on Ctrl diet and 8% ethanol also developed steatosis (Appendix 2.4, mouse no.15), though other animals sharing the same cage showed no fatty change.

In all studies, steatosis was marked in zones 1 and 2, often with some zone 3 sparing (Figure 4.5) which was due in part to hepatocyte dropout as a consequence of necroinflammation.

4.4.2 Inflammation

Lobular inflammation was a prominent feature in all MCDD groups of the LTS (Figure 4.5), and foci were typically at sites of small foci of confluent hepatocyte necrosis. The necroinflammatory foci were always prominent in zone 3 but were also seen in zones 1 and 2. These foci contained both mononuclear cells and polymorphonuclear leukocytes (PMN). D/PAS positive Kupffer cells were also prominent in all MCD mice in the LTS group (Figure 4.6).

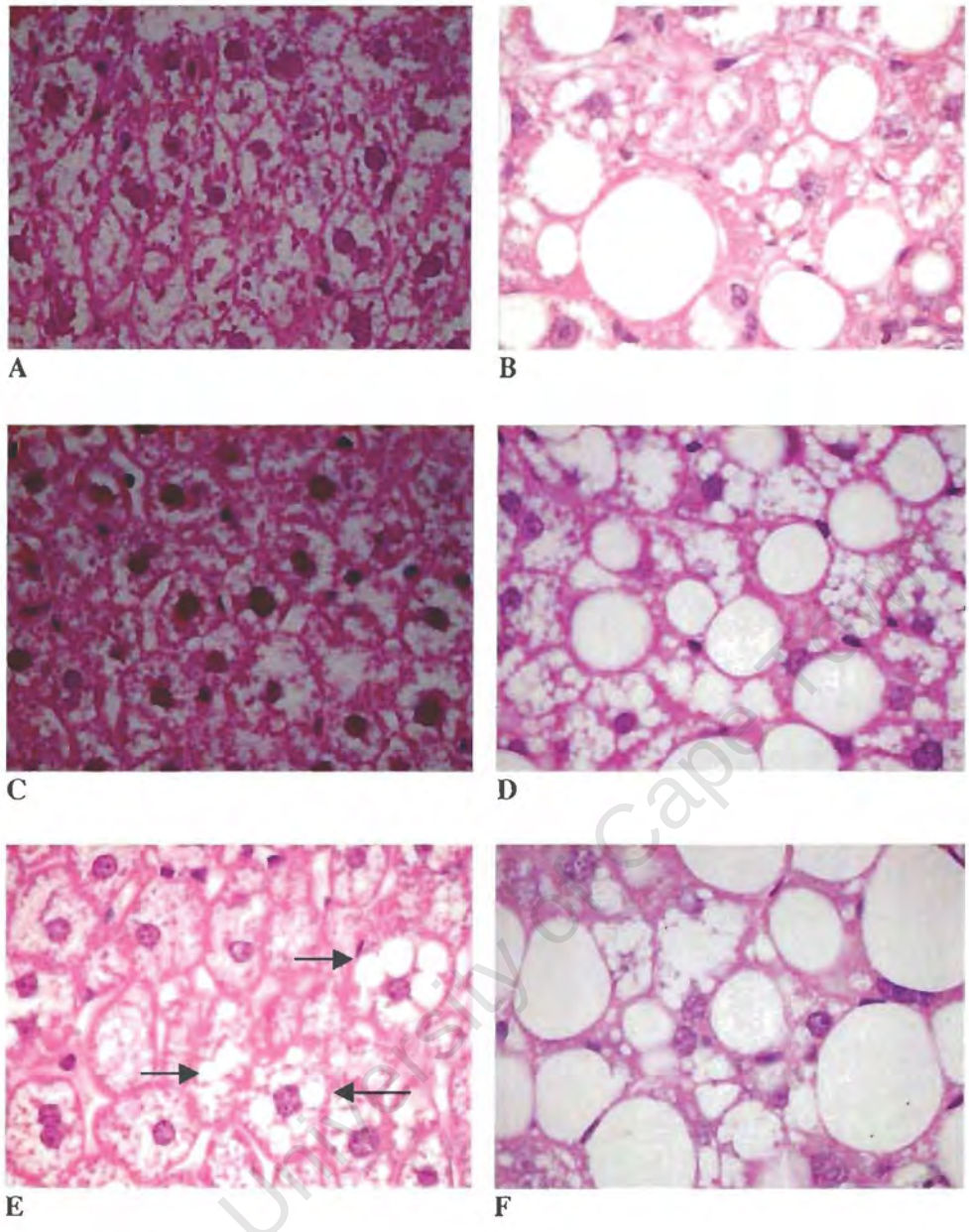

Figure 4.4: H&E sections from LTS show (A) Ctrl on water, i.e. normal liver (B) MCD on water, with macrovesicular fatty change and mild microvesicular steatosis (C) Ctrl +8% ethanol, which is histologically indistinguishable from normal liver (D) MCD + 8% ethanol, with some mixed micro- and macrovesicular steatosis (E) Ctrl + 20% ethanol, with arrows indicating early signs of ethanol-induced steatosis (F) MCD + 20% ethanol, also with a mixed pattern of steatosis. 40x objective.

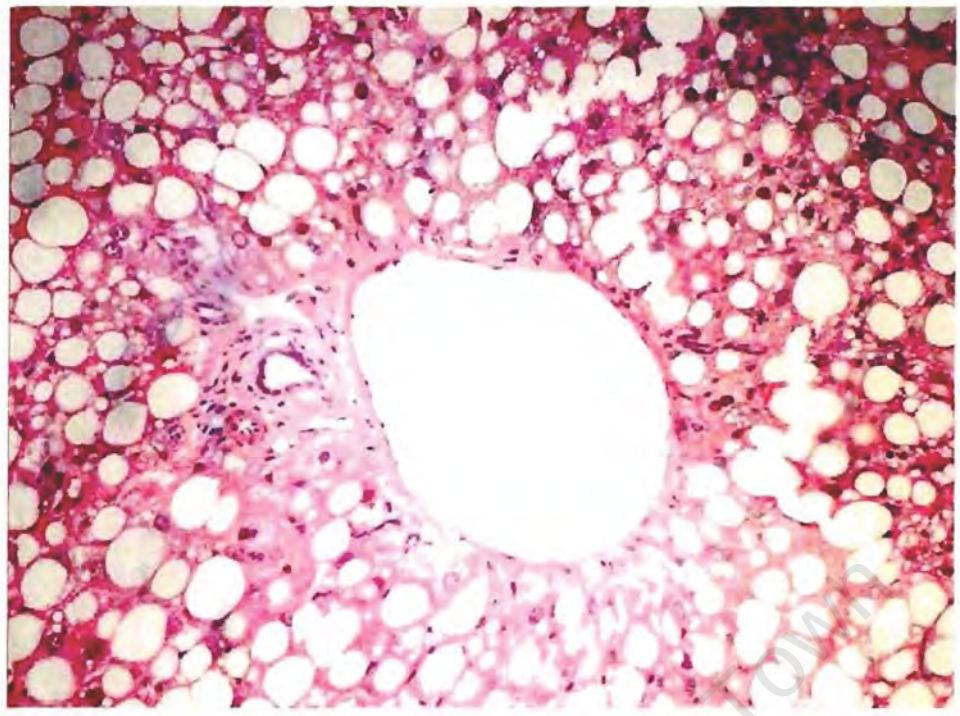

A

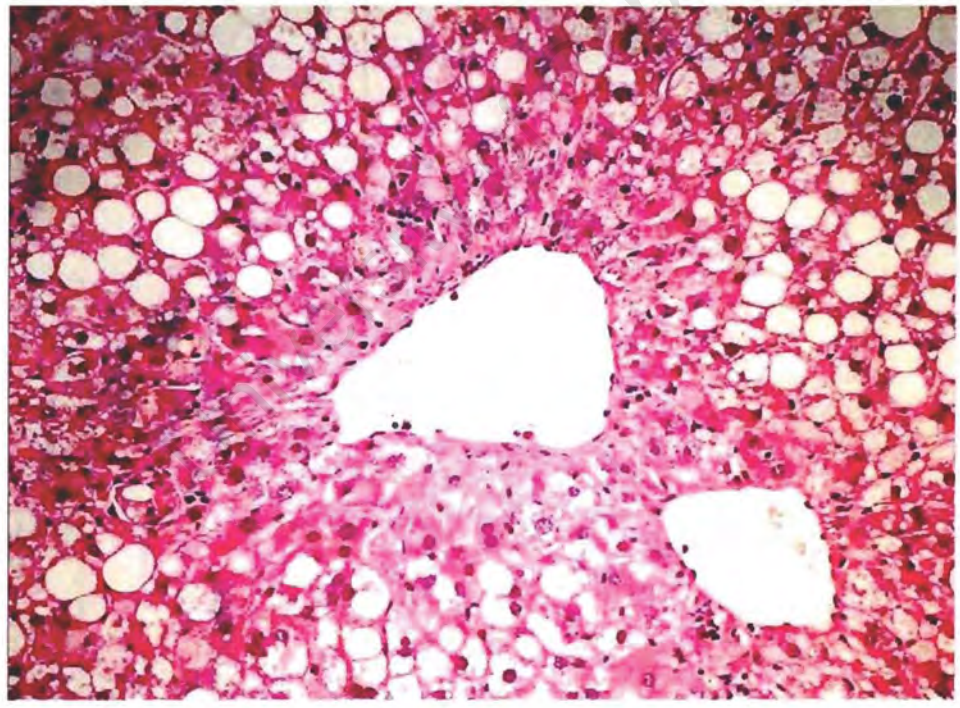

B

Figure 4.5: (A) In mice receiving the MCDD, steatosis occurs even in zone 1 hepatocytes adjacent to the limiting plate, while (B) some zone 3 hepatocytes are spared. H&E, 40x objective.

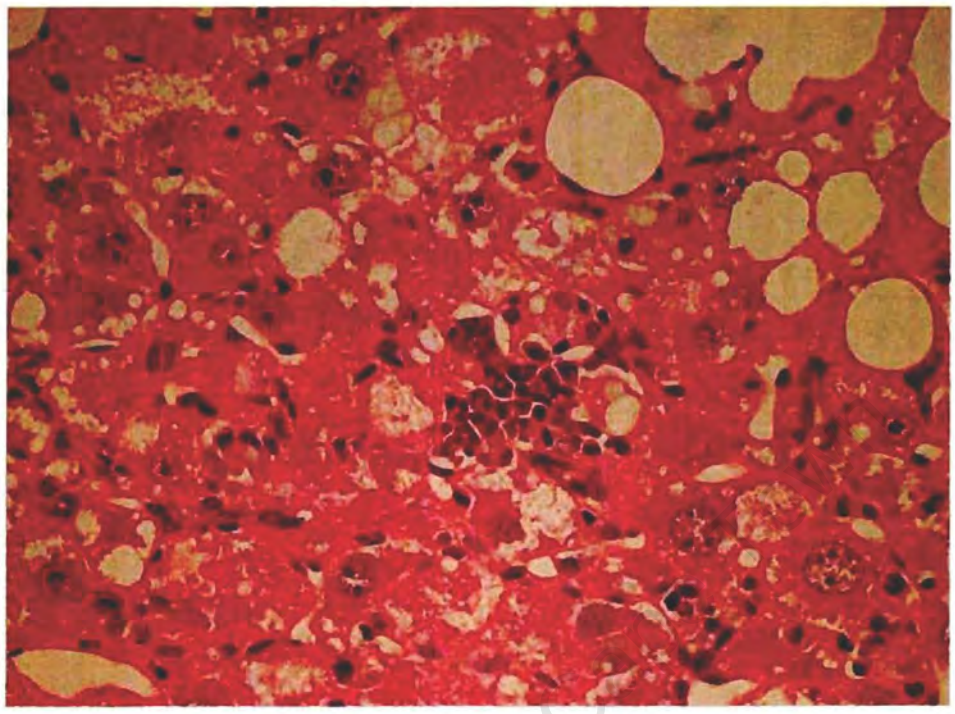

Figure 4.6: (A) Typical lobular necroinflammatory focus in MCDD liver, composed of mononuclear cells and PMNs. H&E, 40x objective.

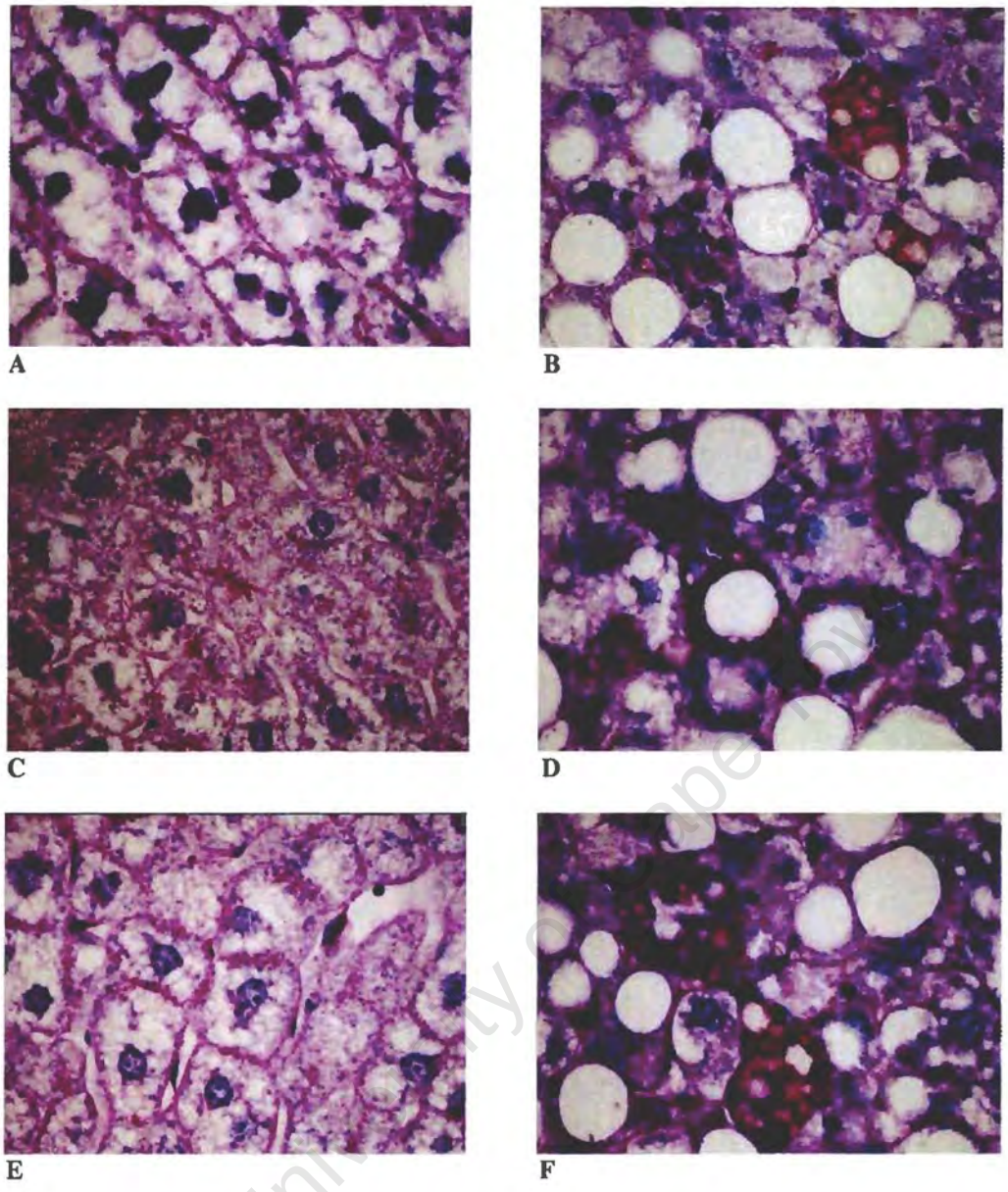

Figure 4.7: Livers from LTS. Kupffer cells containing phagocytosed lipid and cellular debris (scarlet positive stain), are present only in MCDD samples. There is no apparent difference with added alcohol. (A) Ctrl (B) MCD (C) Ctrl + 8% ethanol (D) MCD + 8% ethanol (E) Ctrl + 20% (F) MCD + 20% ethanol. D/PAS, 40x objective.

4.4.3 Fibrosis and other features

In LTS MCDD animals, SR stains (Figure 4.8) showed pericellular fibrosis in zone 3 regions; fibrosis was similar and mild in all MCDD treatment groups. Other features noted in all MCD groups included the presence of mega-mitochondria, glycogenated nuclei, binucleate hepatocytes, and multiple nucleoli. Histopathological features are summarised in Table 4.1. It is noteworthy that in the absence of ballooning degeneration and significant fibrosis, the features described for the LTS are more consistent with NAFLD type 2 (steatosis plus lobular inflammation [Matteoni, 1999]) than with classic human NASH (NAFLD types 3 and 4).

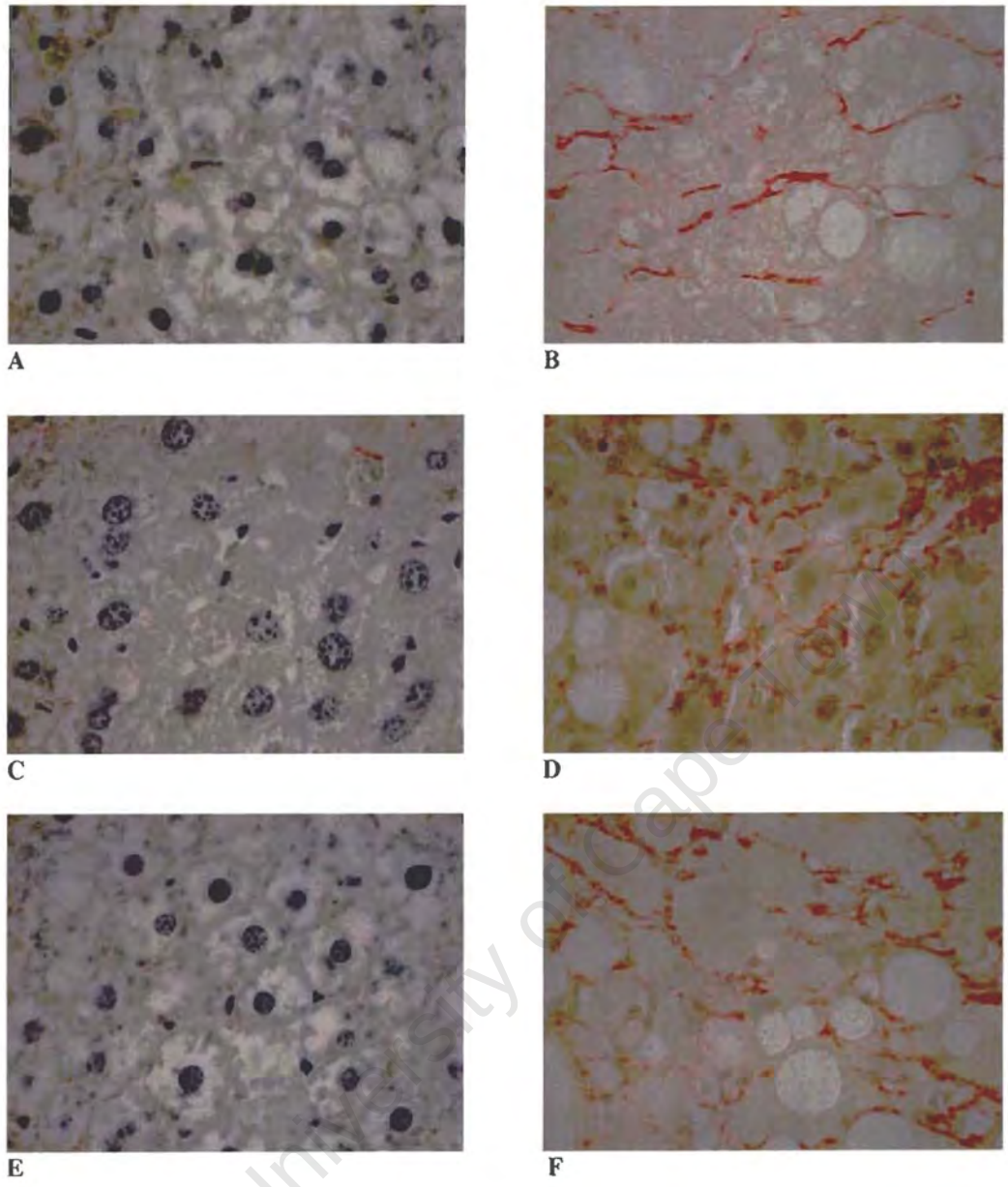

Figure 4.8: Livers from (A) Ctrl (B) MCD (C) Ctrl + 8% ethanol (D) MCD + 8% ethanol (E) Ctrl + 20% (F) MCD + 20% ethanol. Pericellular fibrosis is seen in MCDD treated animals, but this was a mild feature restricted to zone 3 regions, and did not appear to be enhanced by ethanol. SR, 40x objective.

Table 4.1: Histological features in LTS livers

Treatment	Fat score	Fat (distrb.)	Inflammatory foci (score)	Inflammatory foci (number)	D/PAS macrophage (score)	D/PAS macrophage (number)	Fibrosis (score)
Ctrl	0.0±0.0	-	0.13±0.35	1.38±1.41	0.0±0.0	0.0±0.0	0.0±0.0
Ctrl + 8% ethanol*	0.38±1.06	Random**	0.25±0.46	2.0±1.85	0.0±0.0	0.0±0.0	0.0±0.0
Ctrl + 20% ethanol	0.86±0.38	Random**	0.43±0.53	2.86±1.57	0.0±0.0	0.0±0.0	0.0±0.0
MCD	2.8±0.45	Zones 1-3***	3.0±0.0	46.25±16.52	3.0±0.0	87.0±55.89	0.60±0.55
MCD + 8% ethanol	3.0±0.0	Zones 1-3***	2.83±0.41	34.67±7.76	3.0±0.0	68.83±25.61	0.71±0.49
MCD + 20% ethanol	3.0±0.0	Zones 1-3***	2.78±0.44	44.56±11.59	3.0±0.0	98.44±34.67	0.88±0.35

*Mouse #15 (Appendix 2.4) always excluded due to the presence of fatty liver of uncertain aetiology
**Droplets too sparse to determine zonal distribution
***Fat droplets in zones 1 and 2; variable numbers of hepatocytes in zone 3 showed steatosis
Classification terms: **Distr:** Zonal distribution; **Score:** Mean score (± standard deviation) per group, as outlined in **3.3**; **Number:** Refers to average number (± standard deviation) of inflammatory foci or enlarged macrophages in 20hpf.

4.5 Characterization of the Inflammatory Infiltrate

Immunofluorescent stains were performed for detection of natural killer cells (NK, NK1.1), B cells (CD 19), T helper cells (Th, CD4), cytotoxic T cells (Tc, CD8) and macrophages (F4/80) in the inflammatory infiltrate of the LTS. Spleen was used as positive control. No frozen sections were available from the STS.

No staining was obtained for NK cells, even in positive control samples. Similar to human NASH, B cells were not detected in frozen sections (Figure 4.9). However, unlike in human NASH (Lefkowitch, 2002), Th and Tc cells were also absent (Figures 4.10 and 4.11). It is noteworthy that immunofluorescent methods are of limited sensitivity, thus if these cell types were present in small numbers, they may have escaped detection. On the other hand, Kupffer cells were a finding in all liver sections (Figure 4.12). In Ctrl samples, these were small, of irregular shape, and sparsely distributed. MCDD samples were distinguished by the presence of dense collections of enlarged Kupffer cells containing lipid droplets and lipofuscin.

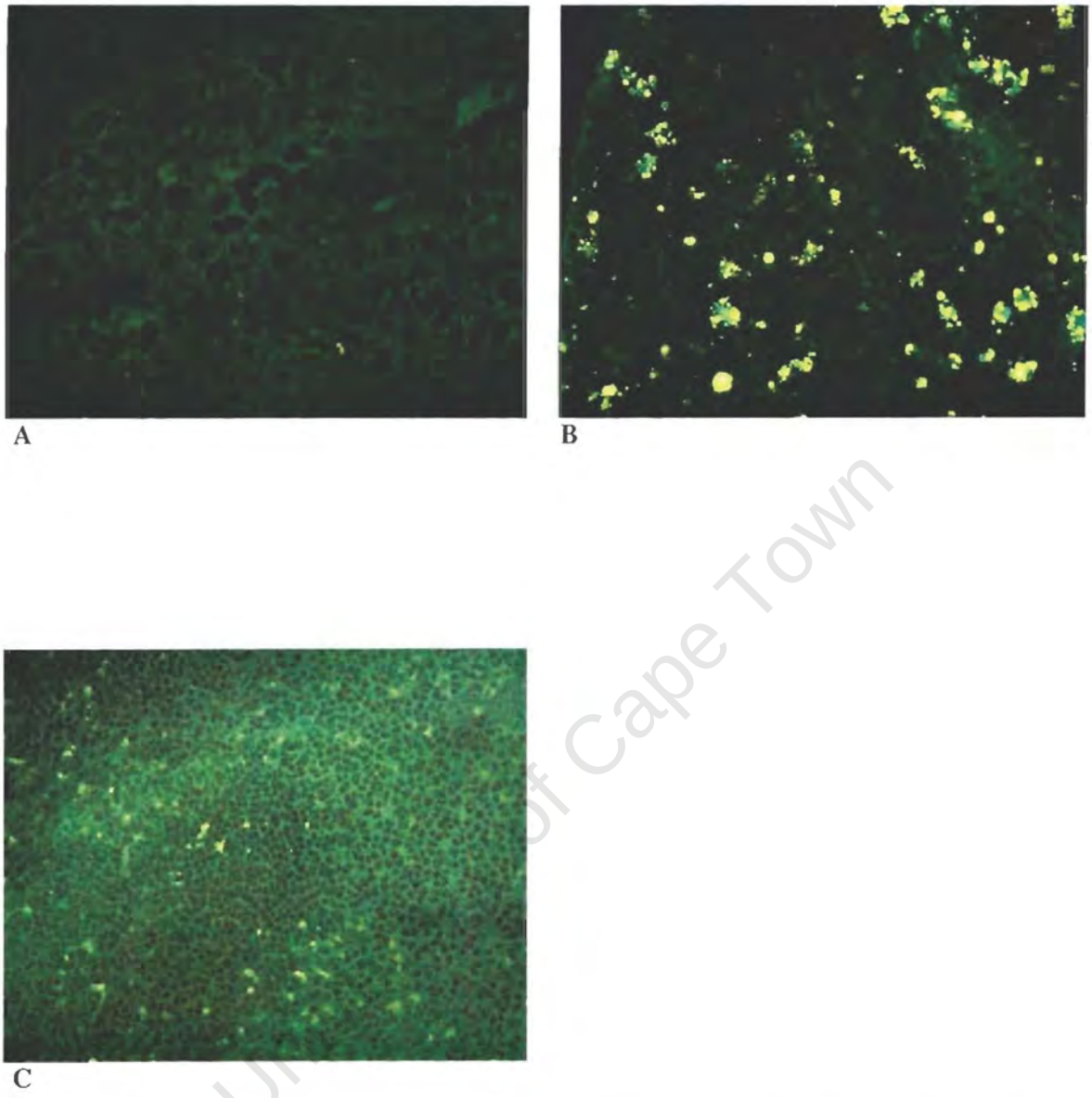

Figure 4.9: B cells are absent in (A) Ctrl and (B) MCDD livers, though prolific in murine spleen (C), used as positive control. Autofluorescence in (B) is due to lipofuscin in Kupffer cells. Immunofluorescent stains using antibody to CD19, 40x objective.

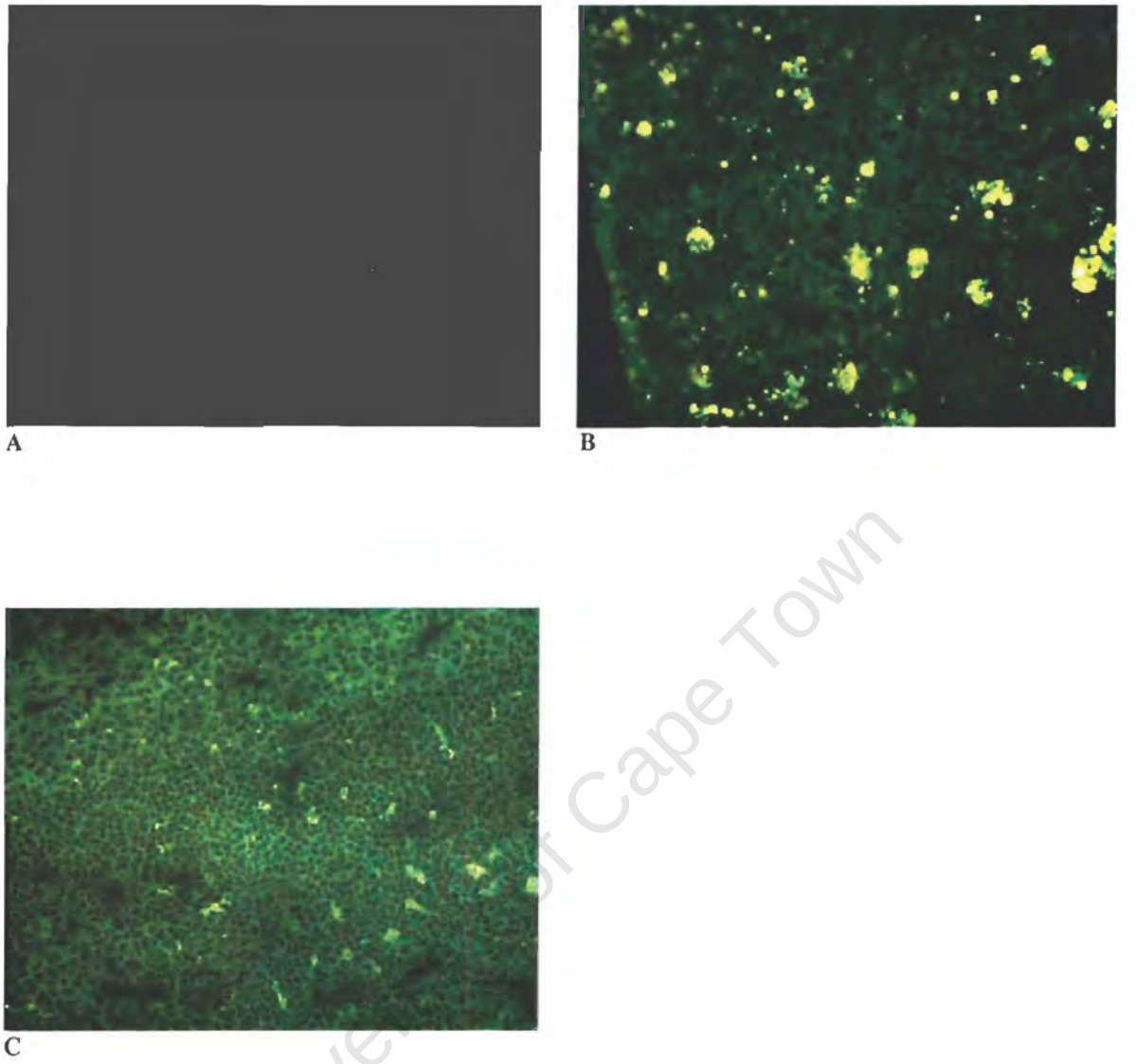

Figure 4.10: CD 4+ cells are absent in (A) Ctrl and (B) MCDD livers
(C) Murine spleen serves as a positive control. Immunofluorescent stains using antibody to CD4, 40x objective.

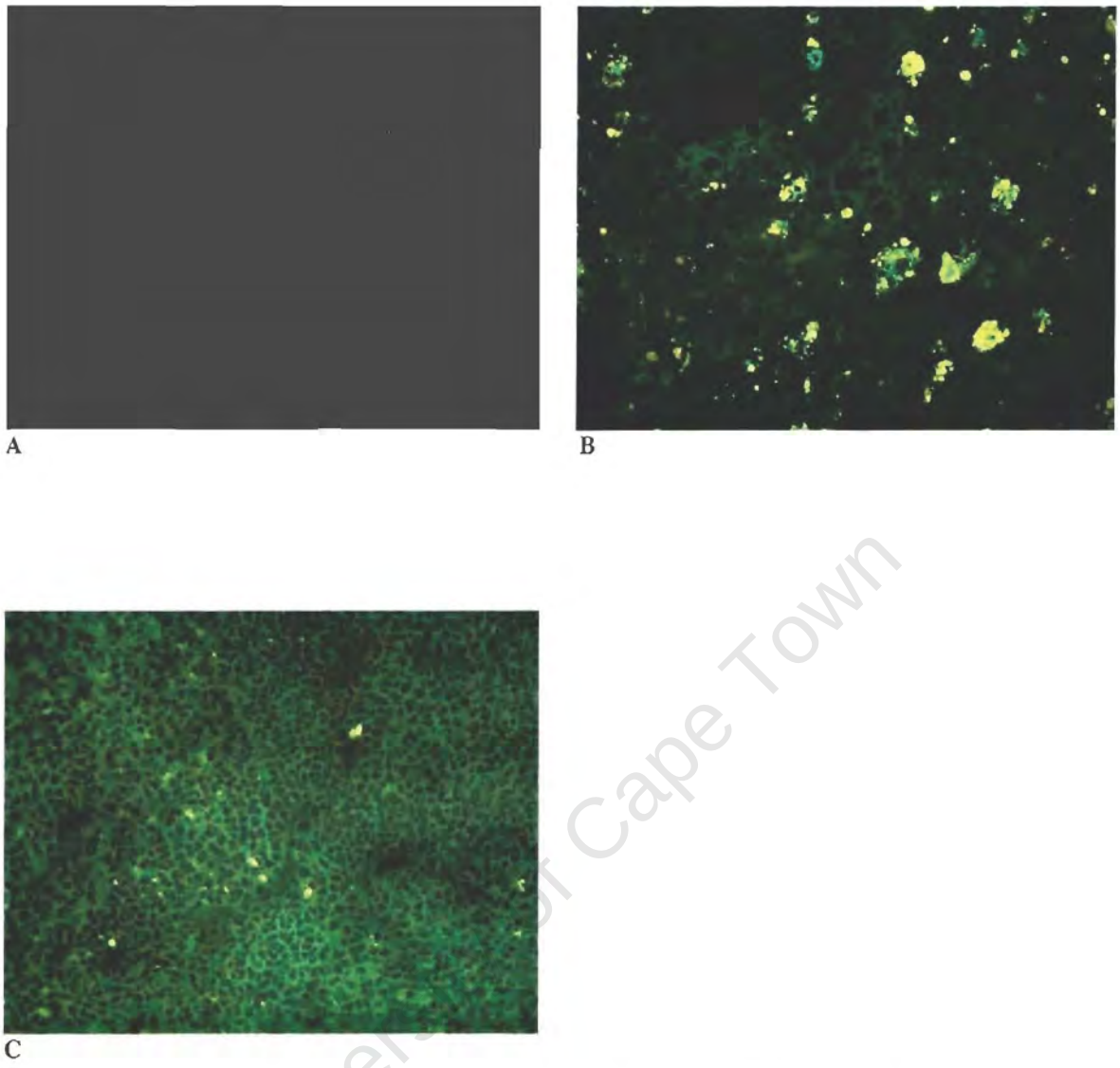

Figure 4.11: No CD 8+ cells were found in either (A) Ctrl or (B) MCDD livers. (C) Murine spleen serves as positive control. Immunofluorescent stains using antibody to CD8, 40x objective.

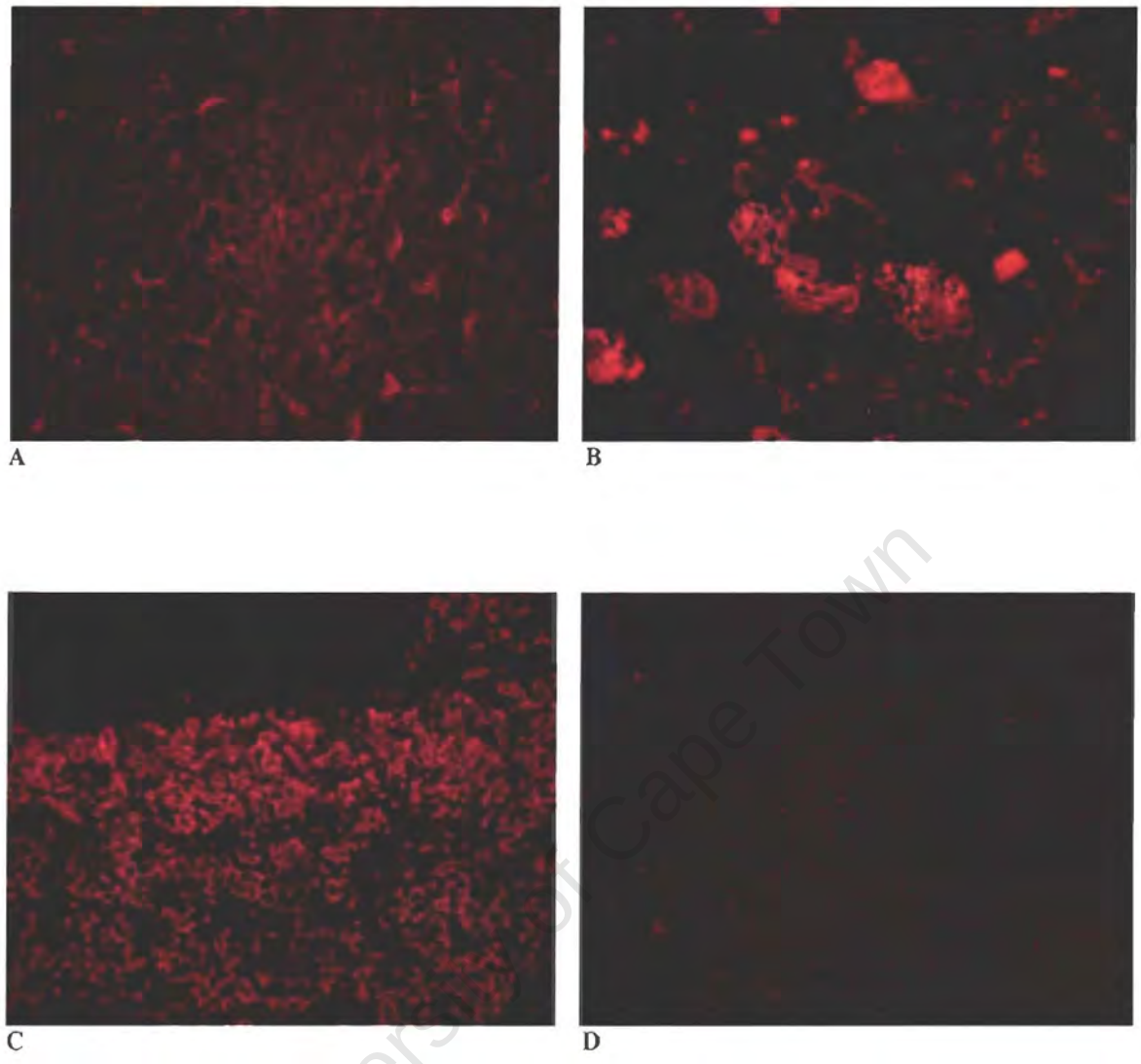

Figure 4.12: (A) Resident Kupffer cells in sinusoids of Ctrl liver (B) Enlarged Kupffer cells containing lipid droplets and lipofuscin are a feature exclusive to MCD liver (C) Spleen injected with red cells, positive control (D) Negative control, liver section stained using PBS in place of F4/80 as primary antibody. Immunofluorescent stain using antibody to F4/80, 40x objective.

4.6 Biochemical Measurement of Fibrosis

The quantity of collagen, as indicated by measurement of hydroxyproline, showed increased levels of this imino acid in LTS animals receiving the MCDD relative to Ctrl, p=0.0732 (Figure 4.13). However, although alcohol consumption appeared to enhance hydroxyproline in Ctrl mice (p=0.0403), MCD treated animals did not reflect this alcohol-mediated increase. Raw data is presented in Appendix 2.5.

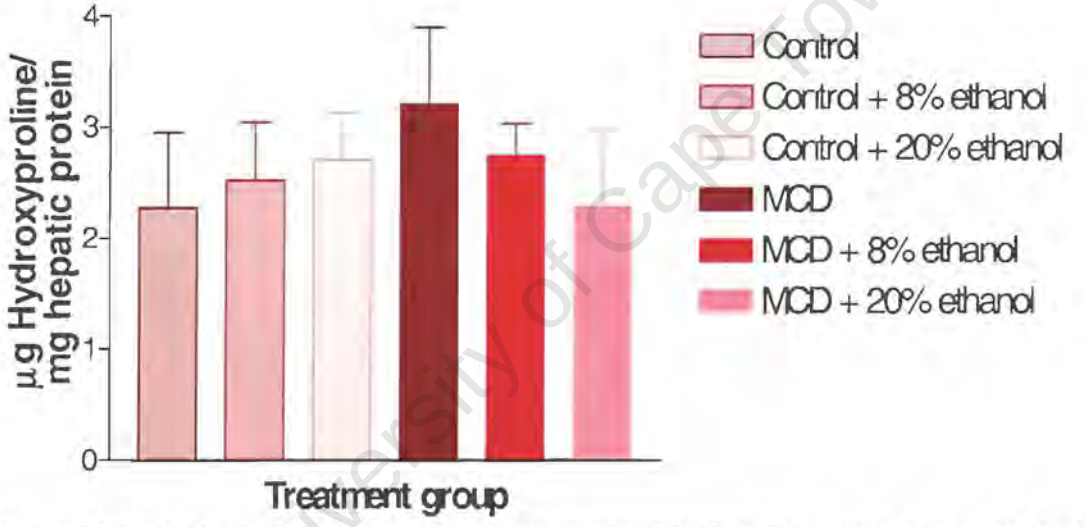

Figure 4.13: Hydroxyproline content in treatment groups of LTS is increased as a result of alcohol consumption in Ctrl groups but not MCD. MCD vs Ctrl p=0.0732, Ctrl + alcohol p=0.0403, MCD + alcohol p=0.2455.

4.7 Hepatic and Serum TG, Hepatic Phosphatidylcholine and Lipid Peroxidation

These measurements were taken with the intention of creating a profile of the biochemical alterations occurring over a time course on a lipotrope-deficient diet. Interpreted in conjunction with histochemical and immunocytochemical findings, such a profile was expected to shed some light on the basis for hepatic dysfunction resulting from lipid accumulation. Raw data for lipid measurements and LP indices are presented in Appendices 2.6-2.12 (LTS), and Appendices 3.1-3.4 (STS).

It is crucial to note that because sacrifice started ~2h after commencement of the light cycle, animals may not have been sufficiently fasted, and TG levels and LP measurements may be elevated, reflecting this. However, as the sacrifice regimen was identical for all groups in all studies, it is believed that the group *trends* for lipid measurements remain valid.

4.7.1 Factors affecting TG accumulation

Hepatic TG accumulation as a result of MCDD was noted at the earliest time point (Figure 4.14, MCD versus Ctrl p=0.0022), and continued in the long term (Figure 4.15A, MCD versus Ctrl p=0.0027). Although it is believed this was a consequence of decreased export of hepatic TG, serum TG did not appear to differ in the long term (Figure 4.15B).

Alcohol consumption increased hepatic TG in all treatment groups. Although alcohol-mediated changes in liver TG were not always incremental, increases in hepatic TG reached statistical significance in both STS Ctrl and MCD groups (Ctrl p=0.0445, MCD p=0.0017) and in LTS Ctrl (p= 0.0044). Changes were not statistically significant in LTS MCD groups (p=0.7033).

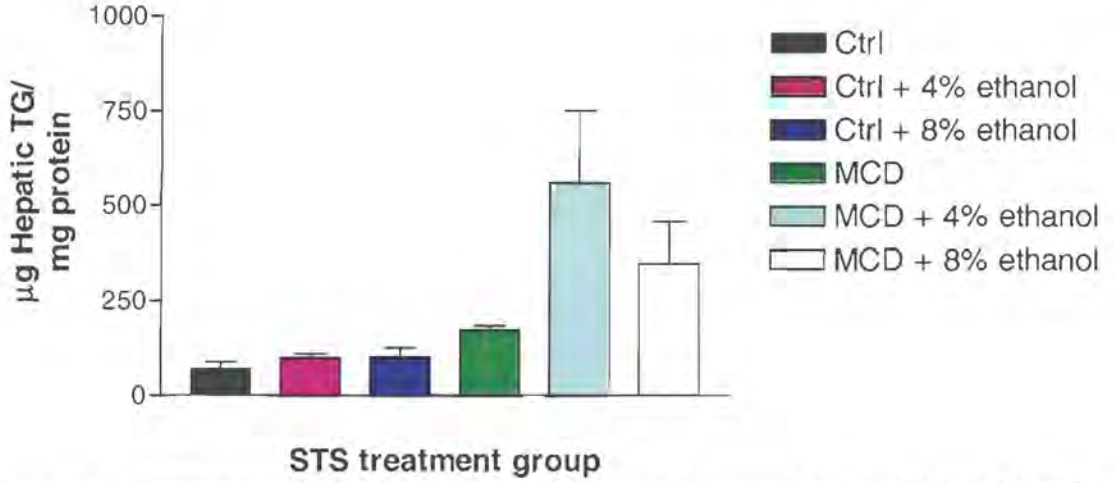

Figure 4.14: Hepatic triglyceride content in STS study (4 weeks) is increased by the MCDD. MCD vs Ctrl p=0.0022; Ctrl + alcohol p=0.0445; MCD + alcohol p=0.0017

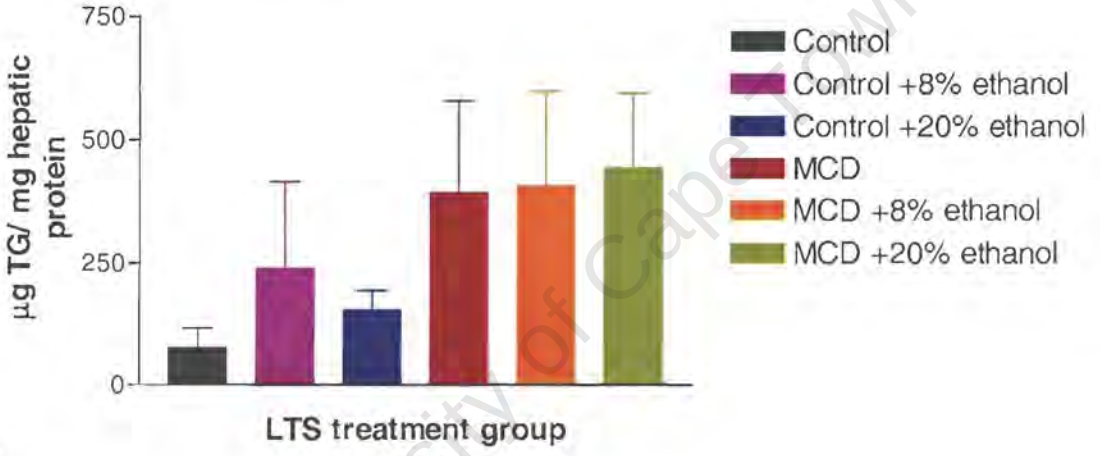

A

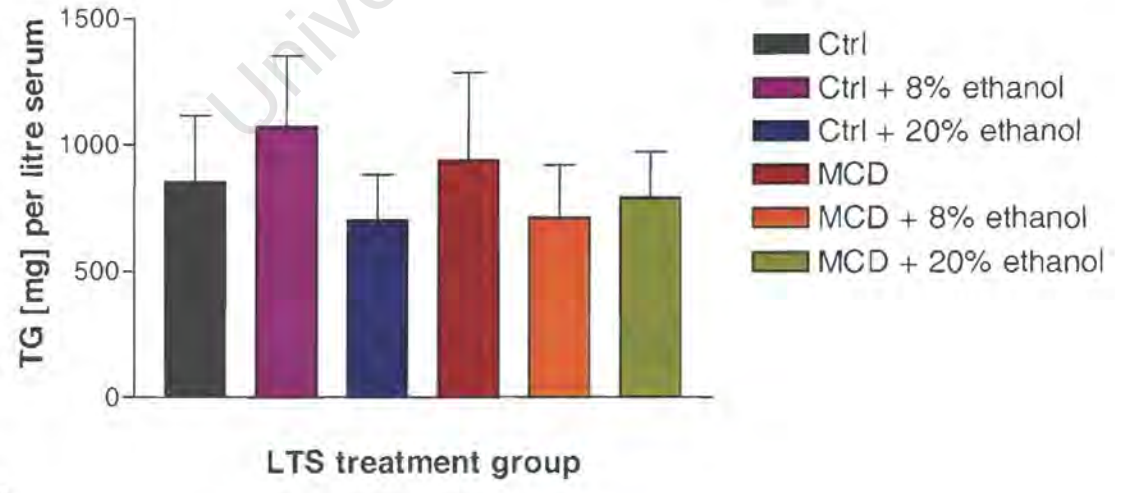

B

Figure 4.15: (A) Hepatic TG content after 8 weeks (LTS) MCDD is significantly higher than in Ctrl. MCD vs Ctrl p=0.0027; Ctrl + alcohol p=0.0044; MCD + alcohol p=0.7033. (B) Serum TG levels in treatment groups of LTS do not reflect hepatic TG values. MCD vs Ctrl p=1.000; Ctrl + alcohol p=0.0563; MCD + alcohol p=0.2893.

4.7.2 Phosphatidylcholine

Phosphatidylcholine (PC) is a major component of VLDL, which is required for export of hepatic TG (see **2.1**). The mechanism by which the MCDD causes steatosis was confirmed by comparison of PC levels in the LTS for animals receiving MCDD versus Ctrl counterparts. Due to technical difficulties, PC levels were not measured for the STS.

In the LTS, PC was always reduced in MCD mice; furthermore, alcohol consumption appeared to further abrogate PC synthesis (Figure 4.16). The results were statistically significant between MCD and Ctrl ($p<0.0001$), but alcohol consumption did not cause significant changes for either MCD ($p=0.1418$) or Ctrl ($p=0.5540$).

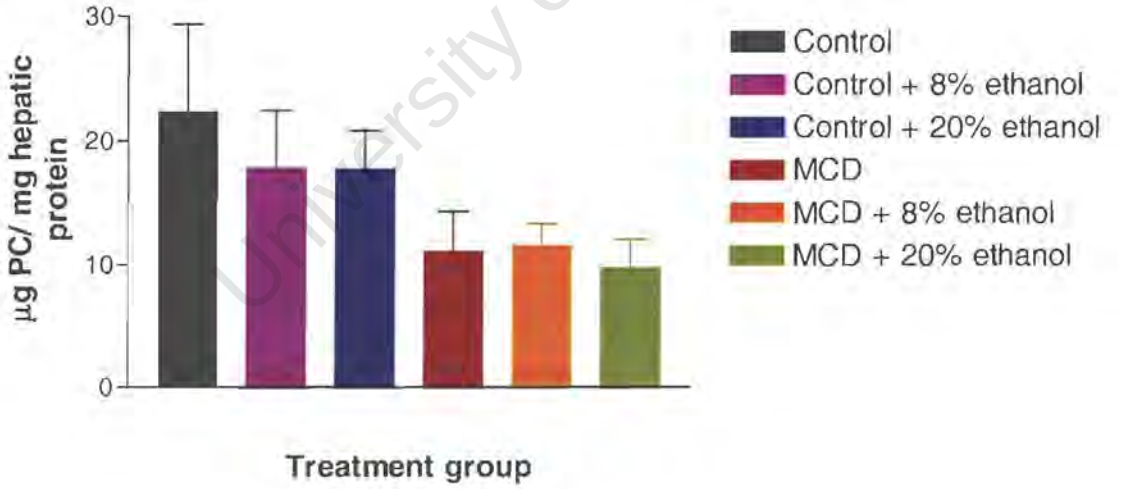

Figure 4.16: PC synthesis in MCD groups of the LTS is inhibited in the absence of methionine and choline, and may be further reduced by alcohol intoxication. MCD vs Ctrl $p<0.0001$; Ctrl + alcohol $p=0.5540$; MCD + alcohol $p=0.1418$

4.7.3 Lipid peroxidation (LP)

The MCDD consistently increased indices of LP (Figures 4.17 and 4.18). However, the following points should be noted while interpreting the data:

- Differences were most notable in CD (early indicator of LP) and TBARS (late LP products), but were not dramatic in mid-stage products (LOOH).
- While total TBARS (tTBARS, denoting the total possible TBARS in the system) were always markedly elevated in MCD versus Ctrl, and increased further following alcohol consumption, differences in free TBARS (fTBARS, measured in the presence of an antioxidant and therefore a better indicator of the actual value present at time of sacrifice, see **3.6.5**) were less stark.

CD were significantly elevated by the MCDD (STS MCD vs Ctrl p=0.0411; LTS MCD vs Ctrl p=0.0008). Although alcohol also elevated CD, the change increased consistently with alcohol concentration and was statistically significant only in the STS (STS Ctrl p=0.0181, MCD p=0.0066; LTS Ctrl p=0.1421, MCD p=0.0649).

Although LOOH were measured for the STS, levels were unreliable due to an unanticipated technical fault (which was rectified for the LTS). STS data for LOOH have therefore been omitted. In the LTS, levels of LOOH were minimal for all groups. The effect of the MCDD was not statistically significant (MCD vs Ctrl p=0.5000). The effect of alcohol was statistically significant in the Ctrl group (p=0.0027) but not in the MCD group (p=0.1045).

FTBARS were always significantly raised by the MCDD (STS MCD vs Ctrl p=0.0022; LTS MCD vs Ctrl p=0.0025). Alcohol also elevated fTBARS in the STS (Ctrl p=0.0067, MCD p=0.0025); in the LTS, it caused a decrease in Ctrl mice (p=0.0054), and an increase in MCD mice (p=0.0010). As expected, levels of tTBARS were higher than fTBARS. In the STS, the MCDD caused a significant increase in tTBARS (MCD vs Ctrl p=0.0019); alcohol caused an

additional increase in both Ctrl and MCD livers, however this was only significant in the Ctrl group (Ctrl p=0.0019 and MCD p=0.0600). On the contrary, although long term administration of the MCDD caused increased tTBARS in MCD relative to Ctrl mice (p<0.0001), the level of tTBARS was not significantly affected by alcohol in either Ctrl (p=0.4516) or MCD (p=0.0527) groups.

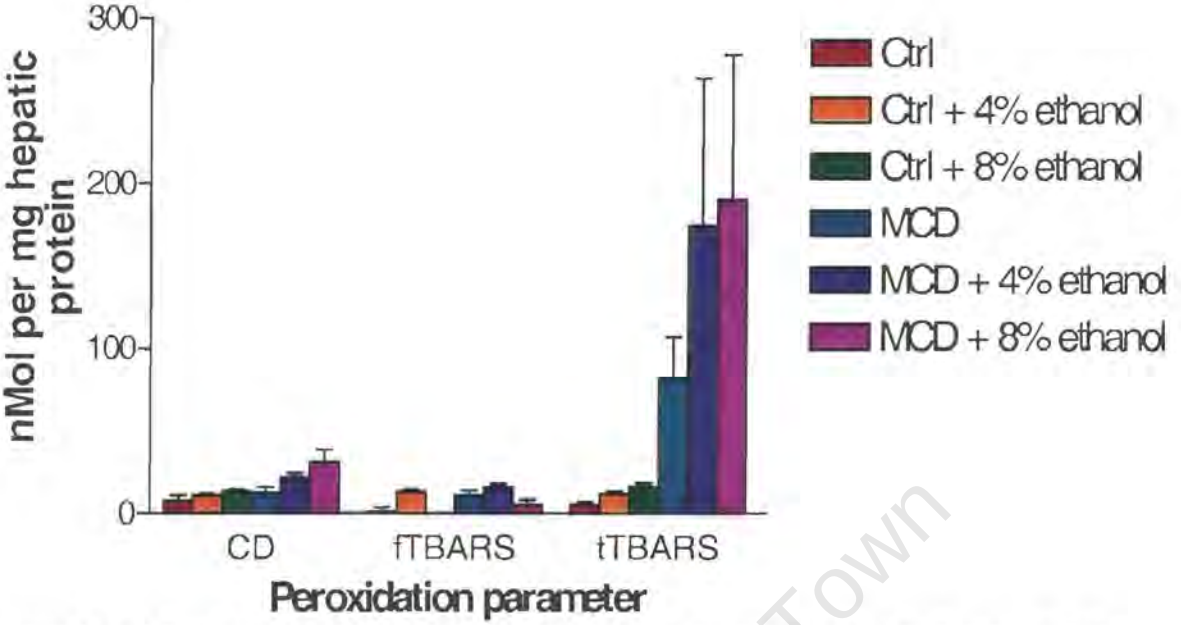

Figure 4.17: A profile of LP in the STS indicates early and late LP products in the STS were increased by the MCDD (CD, MCD vs Ctrl p=0.0411; fTBARS, MCD vs Ctrl p=0.0022; tTBARS, MCD vs Ctrl p=0.0019). Alcohol also caused significant increases in CD (Ctrl p=0.0181, MCD p=0.0066), fTBARS (Ctrl p=0.0067, MCD p=0.0025), but the alcohol-mediated increase in tTBARS only reached statistical significance in Ctrl + alcohol (p=0.0019).

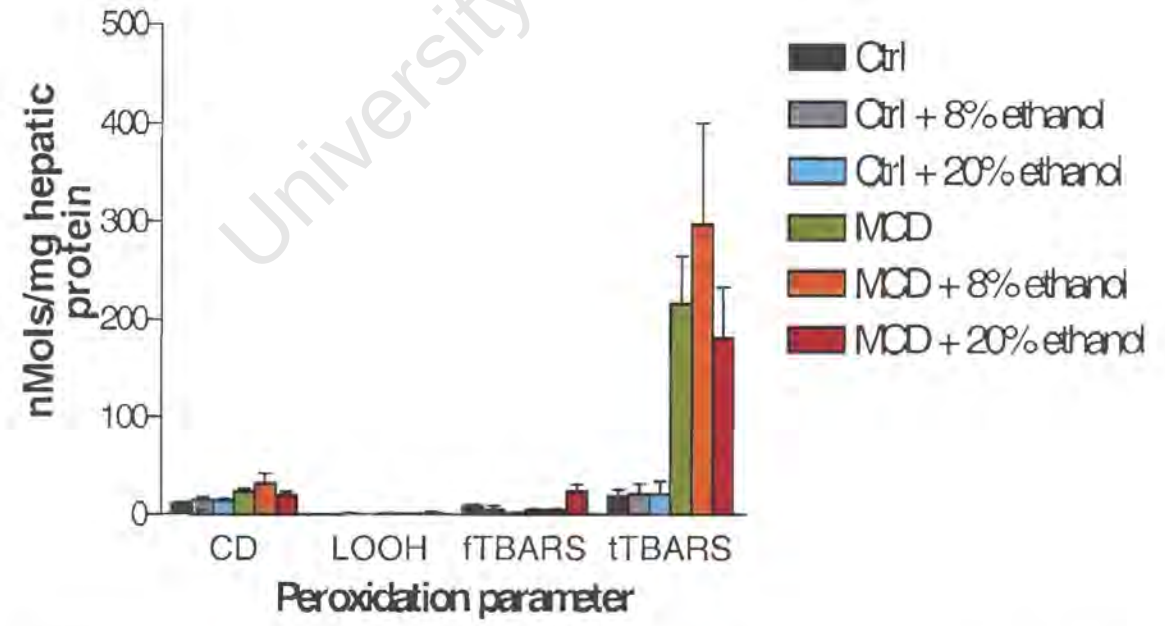

Figure 4.18: Profile of LP in treatment groups of the LTS. CD are significantly elevated by the MCDD (MCD vs Ctrl p=0.0008) but not noticeably affected by added alcohol. LOOH are minimal in all groups, and only significantly affected by alcohol addition in the Ctrl (p=0.0027). fTBARS are elevated by MCDD (MCD vs Ctrl p=0.0025) and by alcohol (Ctrl p=0.0054, MCD p=0.0010). tTBARS are significantly affected by MCDD (MCD vs Ctrl p<0.0001) but do not show significant change with added alcohol in either Ctrl or MCD groups.

The LP profile is alternatively represented in Tables 4.2 and 4.3 as a *ratio* of LP indices, with the mean nMol of early LP "products" (CD) always given a value of 1.0, and all other values presented as a ratio of nMol of CD measured. Table 4.2 shows that in the STS Ctrl, addition of alcohol drives LP to the right, generating increased levels of late LP products relative to early products. Also, addition of 8% alcohol *decreases the proportion* of fTBARS generated ber nMol of CD, yet the proportion of tTBARS continues to *increase.* In MCD groups, although addition of alcohol appears to increase *absolute values* of indices of LP (Figure 4.17), Table 4.2 indicates that the *proportion* of late products to early products measured is actually *decreased* by addition of alcohol.

In the LTS (Table 4.3) alcohol appeared to increase the proportion of mid-stage products (LOOH) generated per mean nMol CD, in both Ctrl and MCD groups. However, the effect of alcohol in the Ctrl group is similar to that seen in the STS, with proportion of fTBARS declining, while paradoxically proportion of tTBARS still continues to increase. In the MCD group, alcohol addition (8% group) initially favours generation of a high proportion of tTBARS while fTBARS are comparatively low. However, high levels of alcohol (20%) increase the proportion of fTBARS.

Table 4.2: Ratio of LP indices in STS.

Treatment Group	Ratio of LP products CD:fTBARS:tTBARS
Ctrl	1:1.30:0.68
Ctrl + 4% ethanol	1:1.24:1.12
Ctrl + 8% ethanol	1:0.02:1.21
MCD	1:0.93:6.76
MCD + 4% ethanol	1:0.73:8.05
MCD + 8% ethanol	1:0.18:6.11

*Value of CD always taken as 1.0

Table 4.3: Ratio of LP indices in LTS.

Treatment Group	Ratio of LP products CD:LOOH:fTBARS:tTBARS
Ctrl	1:0.04:0.73:1.19
Ctrl + 8% ethanol	1:0.05:0.34:1.41
Ctrl + 20% ethanol	1:0.21:0.08:1.48
MCD	1:0.04:0.21:9.35
MCD + 8% ethanol	1:0.04:0.14:9.45
MCD + 20% ethanol	1:0.09:1.21:9.28

*Value of CD always taken as 1.0

After observing increased hepatic LP with administration of the MCDD, immunohistochemical stains were conducted to determine the localization of this process. 4-hydroxy-2-nonenal (4-HNE) is a stable late-stage LP product and has been implicated in biochemical processes instrumental in liver disease (see **2.2.1**). Interestingly, in MCD groups of the LTS, 4-HNE-protein adducts were found exclusively in the same enlarged, lipid-laden Kupffer cells responsible for clearance of cellular debris, identified earlier by D/PAS (Figure 4.7). Ctrl mice receiving water showed no 4-HNE staining, however occasional Kupffer cells in Ctrl mice on 8% and 20% alcohol were positive. With few exceptions (Figure 4.19, E) hepatocytes did not stain positively for 4-HNE adducts (Figure 4.19).

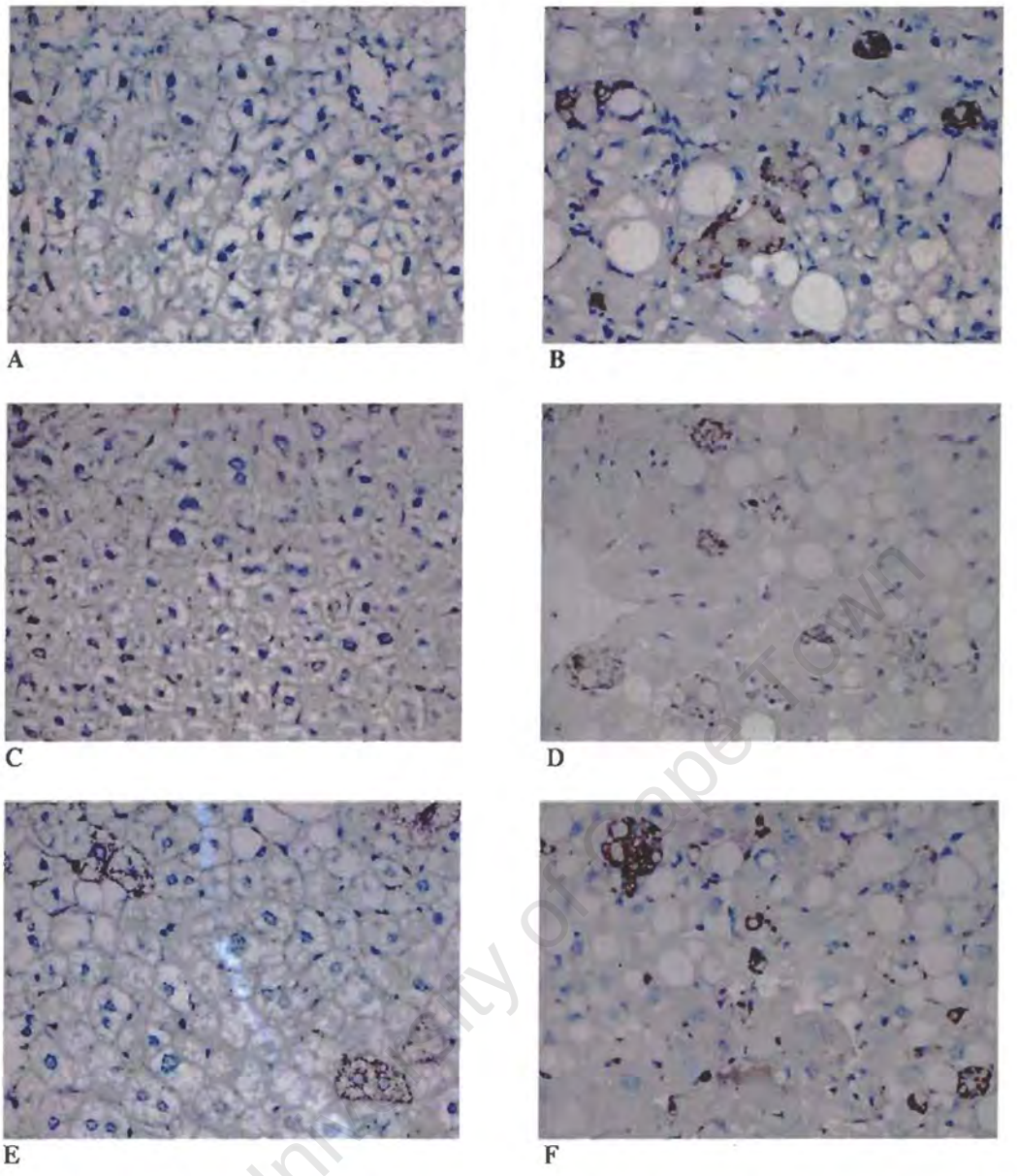

Figure 4.19: 4-HNE staining in the LTS (A) Ctrl – no 4-HNE detected (B) MCD – 4-HNE adducts are detected in enlarged Kupffer cells (C) Ctrl + 8% ethanol – no 4-HNE detected (D) MCD + 8% ethanol – 4-HNE adducts are seen in enlarged Kupffer cells (E) Ctrl + 20% ethanol, infrequent positive staining for 4-HNE-adducts identified in hepatocytes (F) MCD + 20% ethanol – 4-HNE adducts seen in enlarged Kupffer cells. Immunohistochemistry using antibody to 4-HNE protein adducts. 20x objective.

4.8 CYP2E1 Activity in the Rodent Nutritional Model of NASH

Because CYP2E1 has been implicated as a potential catalyst of LP (Weltman *et al.*, 1996; Leclercq *et al.*, 2000), we investigated activity of CYP2E1 in interactive hepatoxicity. However, on the basis of reports documenting loss of activity of this cytochrome during cold storage (Pearce *et al.*, 1996), initial investigations concentrated on assessing the accuracy of readings obtainable from our samples, some of which had been at -80^0C for more than a year.

As shown in Figure 4.20, CYP2E1 activity was best assessed in fresh liver, though it was comparable in liver frozen at -80^0C for 14 days. Activity was greatly diminished if tissue was homogenized prior to storage.

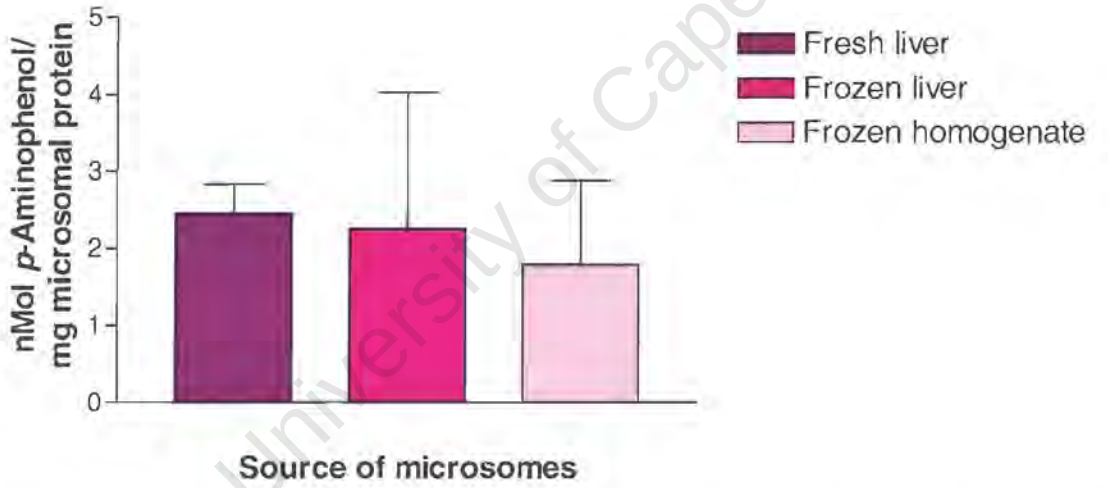

Figure 4.20: CYP2E1 activity in microsomes from liver tissue subjected to different storage conditions. Assays are best conducted on fresh liver, however comparable results are obtained from liver frozen for short periods. If liver tissue is disrupted or homogenised prior to storage, CYP2E1 activity is lost.

In accordance with previous reports, CYP2E1 activity was upregulated by the MCDD (MCD vs Ctrl p=0.0295, Figure 4.21). Although ethanol consumption elevated CYP2E1 activity in the MCD group, the effect was not statistically significant (p=0.5947); this may be attributable to the wide spread of data. Ethanol consumption did not appear to affect CYP2E1 activity in Ctrl groups. Raw data is presented in Appendix 2.13.

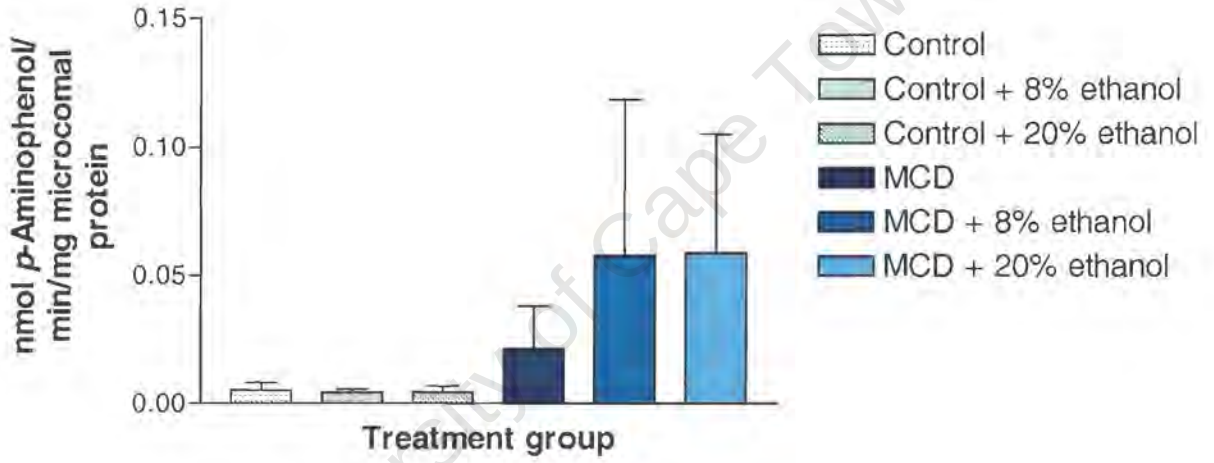

Figure 4.21: Activity of CYP2E1 is enhanced by the MCDD and alcohol. MCD vs Ctrl p=0.0295; Ctrl + alcohol p=0.7114, MCD + alcohol p=0.5947.

In conclusion, the MCDD causes hepatic damage, indicated by elevated aminotransferases and alterations at the light microscopic level, lipid accumulation, LP and increased CYP2E1 activity; these effects are exacerbated by alcohol consumption. Tables 4.4 (a and b) and 4.5 (a and b) summarise the biochemical effects of short and long term administration of the MCDD and alcohol.

Table 4.4 (a): Summary of biochemical effects of alcohol and/or the MCDD in the STS, with Ctrl + water used as baseline. All values are expressed as per cent [%] of the mean of baseline.

	Hepatic TG	CD	fTBARS	tTBARS
Ctrl + 4% alcohol	139	137	1022	227
Ctrl + 8% alcohol	139	171	17	307
MCD + water	240	157	870	1563
MCD + 4% alcohol	784	281	1230	3331
MCD + 8% alcohol	486	403	403	3628

Mean values of baseline: Hepatic TG 71.64µg/mg; **CD** 7.72nMol/mg; **fTBRARS** 1.29nMol/mg; **tTBARS** 5.24nMol/mg.

Table 4.4 (b): Summary of biochemical effects of alcohol on a fatty liver in the STS, MCD + water used as baseline. All values are expressed as per cent [%] of the mean of baseline.

	Hepatic TG	CD	FTBARS	tTBARS
MCD + 4% alcohol	327	179	141	213
MCD + 8% alcohol	202	257	46	232

Mean values of baseline: Hepatic TG ; **CD** 12.12nMol/mg; **fTBRARS** 11.22nMol/mg; **tTBARS** 81.88nMol/mg.

Table 4.5 (a): Summary of biochemical effects of long term administration of alcohol and/or MCDD, Ctrl + water used as baseline. All values are per cent [%] of the mean of baseline.

	ALT	AST	Hydroxyproline	Hepatic TG	Serum TG	PC	CD	LOOH	fTBARS	tTBARS	CYP2E1
Ctrl + 8% alcohol	51	320	111	326	125	83	116	170	54	112	80
Ctrl + 20% alcohol	67	97	119	200	82	79	112	63	12	112	80
MCD + water	240	312	141	513	110	50	184	208	48	1167	420
MCD + 8% alcohol	407	414	120	531	83	52	251	238	49	1607	1160
MCD + 20% alcohol	490	446	101	578	92	44	156	388	257	979	1180

Mean values of baseline: ALT 38U/L; **AST** 40U/L; **Hydroxyproline** 2.27µg/mg; **Hepatic TG** 76.44µg/mg; **Serum TG** 853.89mg/L; **PC** 22.31µg/mg; **CD** 12.48nMol/mg; **LOOH** 0.48 nMol/mg; **fTBARS** 9.15 nMol/mg; **tTBARS** 18.44 nMol/mg; **CYP2E1** 0.005nMol *p*-Aminophenol/mg/min.

Table 4.5 (b): Summary of biochemical effects of alcohol on a fatty liver in the LTS. MCD + water is used as baseline. All values are per cent [%] of the mean of baseline.

	ALT	AST	Hydroxyproline	Hepatic TG	Serum TG	PC	CD	LOOH	FTBARS	TTBARS	CYP2E1
MCD + 8% alcohol	170	133	85	103	76	104	136	114	103	138	276
MCD + 20% alcohol	204	143	71	113	84	88	85	186	538	84	281

Mean values of baseline: ALT 91.2U/L; **AST** 124.8U/L; **Hydroxyproline** 3.21µg/mg; **Hepatic TG** 392.41µg/mg; **Serum TG** 936.64 mg/L; **PC** 11.09µg/mg; **CD** 23.01nMol/mg; **LOOH** 1.00nMol/mg; **fTBARS** 4.38nMol/mg; **tTBARS** 215.16nMol/mg; **CYP2E1** 0.021nMol *p*-Aminophenol/mg/min.

Chapter 5

Animal Studies of Interactive Hepatoxicity II:

Role of TNFα

Studies were conducted with the approval of the UCT Ethics Committee for Research on Animals, and in compliance with the standards of the Medical Research Council (MRC).

5.1.1 Study 1: Tumour necrosis factor alpha (TNFα) knockout study (TNFS)

TNFα has been implicated in the pathogenesis of ASH, and is believed to be a critical factor which drives the pathogenesis NASH (Tilg and Diehl, 2000). However, there appear to be no studies documenting progression of NAFLD in TNFα knockout, to support the putative central role of this cytokine in NAFLD/NASH. This study was therefore conducted to investigate the role of TNFα in progression of the nutritional model of NAFLD.

12 wild type (wt) and 12 TNFα knockout (ko) male C57BL6 mice were allowed two weeks acclimatisation under sterile conditions in the UCT SPF Unit. Thereafter mice were placed on MCDD or Ctrl diets and water *ad libitum* for 28 and 30 days (MCDD and Ctrl respectively). Diets were irradiated and water was autoclaved. Mice were on a diurnal 12h light/dark cycle, and were weighed weekly.

Experimental design

6 wt mice
6 ko mice
} MCDD

6 wt mice
6 ko mice
} CTRL

Mice were sacrificed by cardiac puncture and exsanguination under ether anaesthetic. Livers were weighed and divided into lobes as described in **4.1.2**.

5.1.2 Study 2: Endotoxin study (LPSS)

Endotoxin (lipopolysaccharide, LPS) constitutes a potentially important candidate as one of the "second hits" driving benign fatty liver to the constellation of hepatic alterations constituting NASH (see **2.2.2**). This study was conducted to evaluate the role of LPS (via induction of TNFα) in pathogenesis of the rodent nutritional model of NASH.

32 male C57BL6 mice were given 2 weeks to acclimatise in the UCT Animal Facility, then allowed water and MCDD or Ctrl diet freely for 28 days. Animals were weighed weekly. 24h prior to sacrifice, half of each group was given intraperitoneal (i.p.) LPS (0.5μg/g body weight) in 100μl 0.9% sterile saline, or just saline, viz

Ctrl + saline
Ctrl + LPS
} n= 8/group { MCDD + saline
MCDD + LPS

Sacrifice and tissue harvest were as described above.

5.2 Body and Liver Weight

As in previous studies, animals on the MCDD experienced lethargy and weight loss compared to controls (Figures 5.1A, 5.1B), although this state did not appear to be a consequence of starvation. Livers of MCD animals were significantly smaller than control counterparts, however when adjusted to body weight (i.e. liver weight per gram body weight) to correct for weight loss on the MCDD, liver:body weight was similar in all groups (Figure 5.2A, 5.2B). In the TNFS, knockout animals (ko) had smaller ratios than their wild type (wt) counterparts, regardless of treatment, though the differences were not statistically significant (Ctrl p= 0.5887, MCD p=0.3524). Raw data for weights is presented in Appendices 4.1 and 5.1.

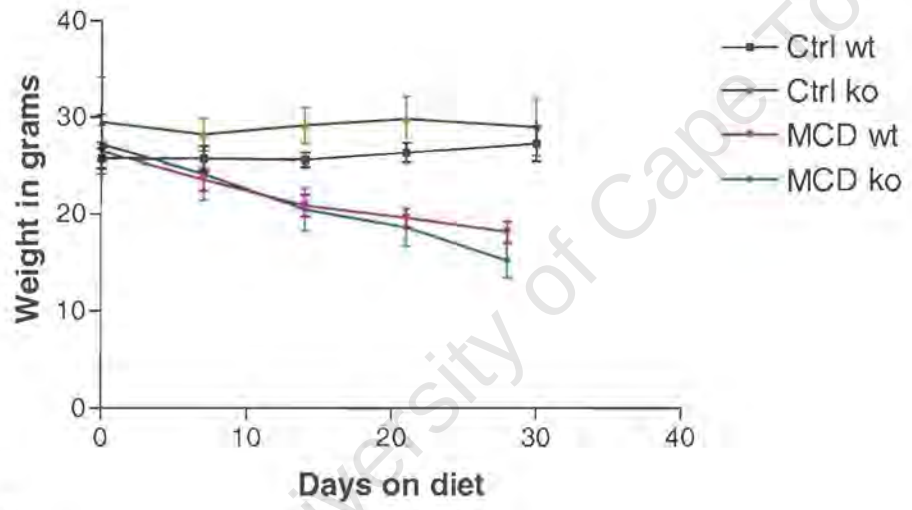

A

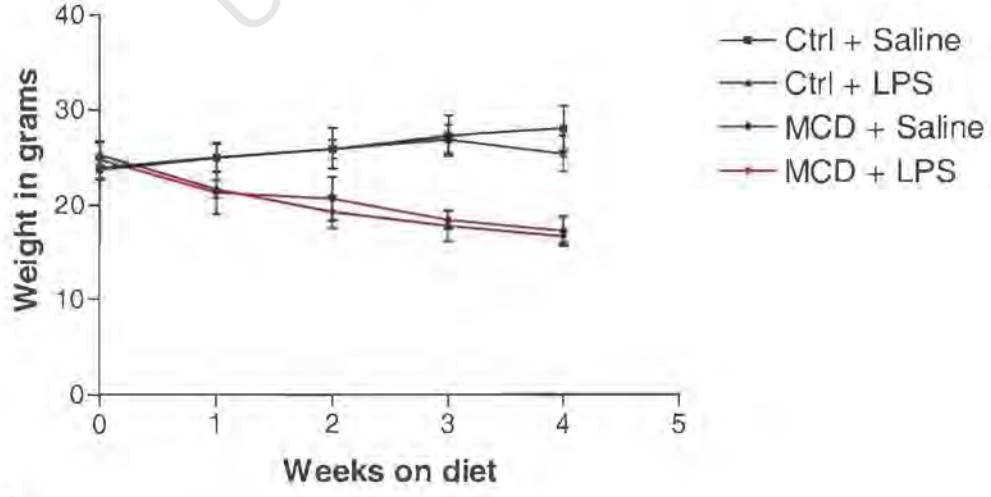

B

Figure 5.1: Body weight over the course of studies (A) TNFS and (B) LPSS. In both studies, the MCDD causes a rapid decline in body weight.

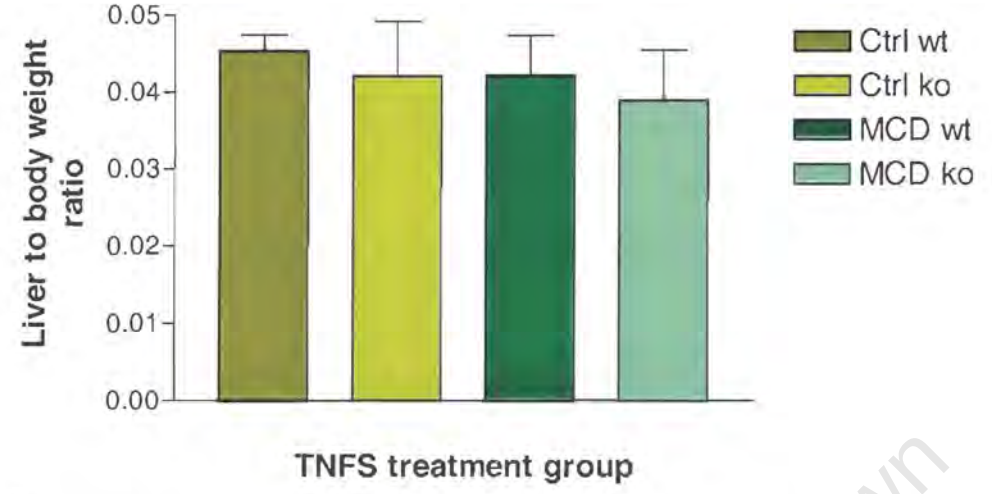

A

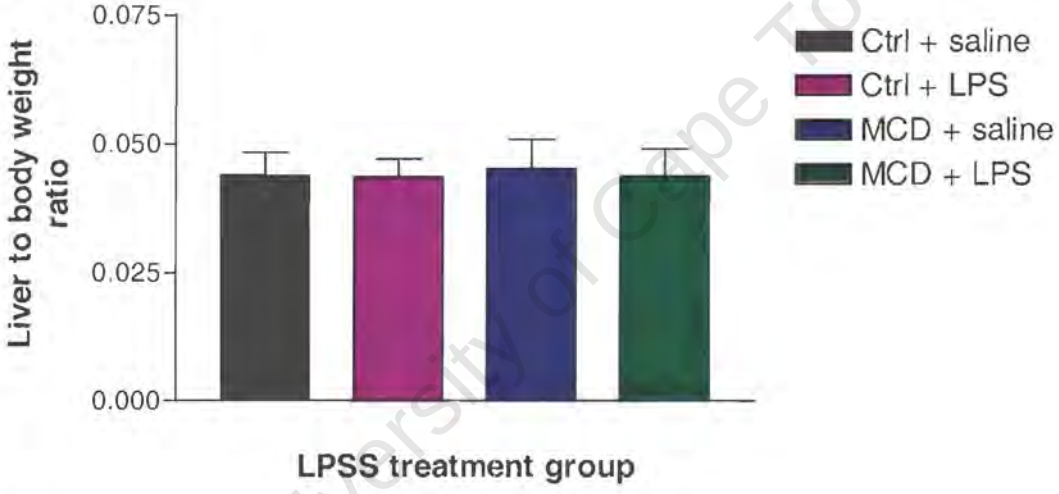

B

Figure 5.2: Liver weight:body weight for (A) TNFS and (B) LPSS. In the TNFS, the ratio is slightly but insignificantly less in ko mice relative to wt counterparts (Ctrl p= 0.5887, MCD p=0.3524). In both studies, the ratios for MCD and Ctrl mice are comparable.

5.3 Aminotransferases

ALT levels in TNFS (Figure 5.3A) were elevated in MCD versus Ctrl (wt versus wt p=0.0022, ko versus ko p=0.0095). In Ctrl groups, ko levels of ALT were also raised relative to wt (p=0.0152). In contrast to this, TNFα ko dampened ALT levels in mice receiving MCDD (p=0.2571) When TNFα was induced by LPS administration, ALT levels were markedly increased relative to Ctrl and MCDD counterparts on i.p. saline (Figure 5.3 B; Ctrl p=0.0002, MCD p=0.0002). Raw data is presented in appendices 4.2 and 5.2.

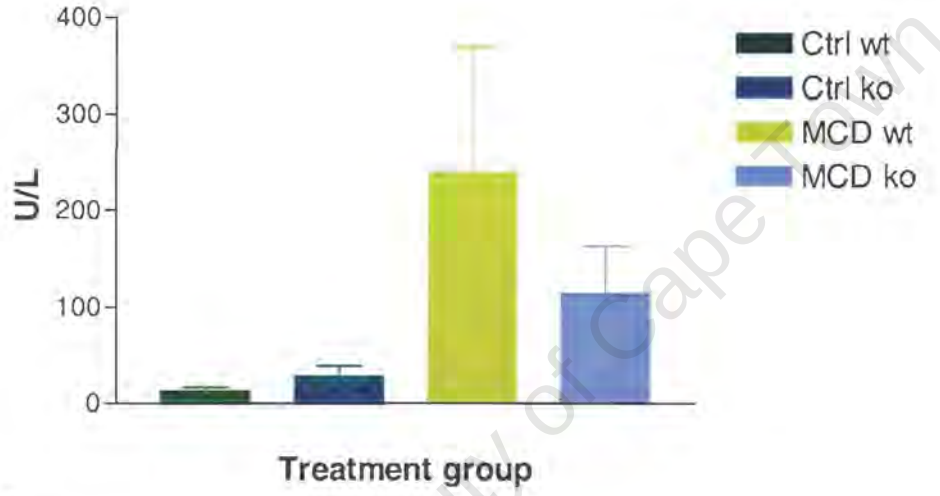

A

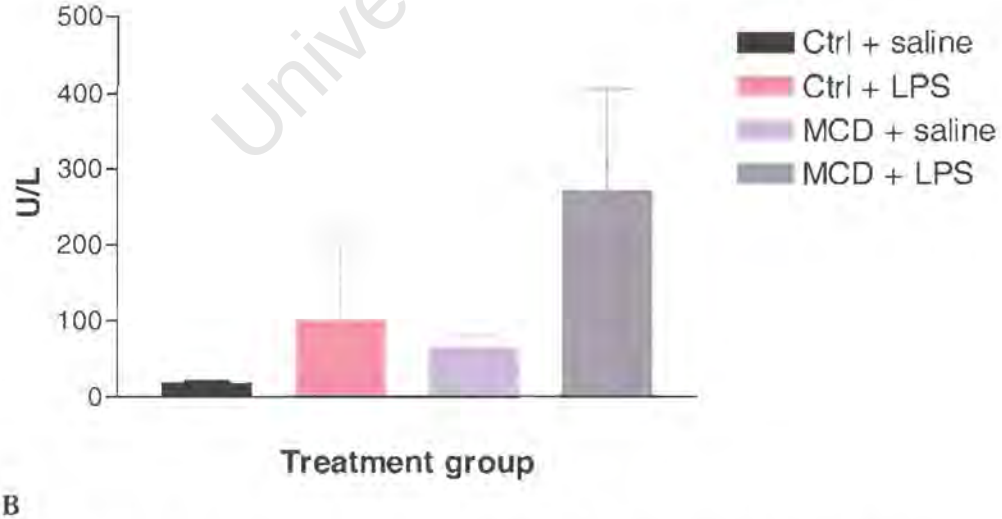

B

Figure 5.3: (A) ALT levels in the TNFS are elevated in Ctrl ko but reduced in MCD ko mice (Ctrl wt vs ko p=0.0152; MCD wt vs ko p=0.2571). (B) ALT levels in the LPSS are enhanced by LPS challenge (Ctrl p=0.0002, MCD p=0.0002).

5.4 Histopathology

5.4.1 Steatosis

There was an impression of smaller lipid droplets or scantier distribution of lipid in some MCD ko mice, which may suggest an inhibitory effect of TNFα on hepatic fat accumulation (Figure 5.4). However this did not translate to a smaller mean score (Table 5.1). Steatosis was primarily macrovesicular, but most livers also showed some microvesicular steatosis. In some mice (wt and ko), steatosis involved some hepatocytes in each of the zones and had no zonal predominance; in these mice, steatosis was either grade 1 or 2.

Although TNFα induction as a result of i.p. LPS administration caused a minor increase in hepatic TG of Ctrl mice, this increase did not occur in MCD mice (Figure 5.5).

5.4.2 Inflammation

Lobular inflammation was a feature in all MCDD groups, and foci contained mainly PMN with lesser numbers of mononuclear cells. In response to LPS treatment, variable numbers of large areas of confluent necrosis, with an associated infiltrate of PMNs, were seen, as well as occasional apoptotic cells.

Interestingly, the livers of MCDD mice injected with LPS showed increased numbers of necroinflammatory foci, compared to livers from mice injected with saline. However, the large areas of confluent necrosis seen in Ctrl mice challenged with LPS were not seen.

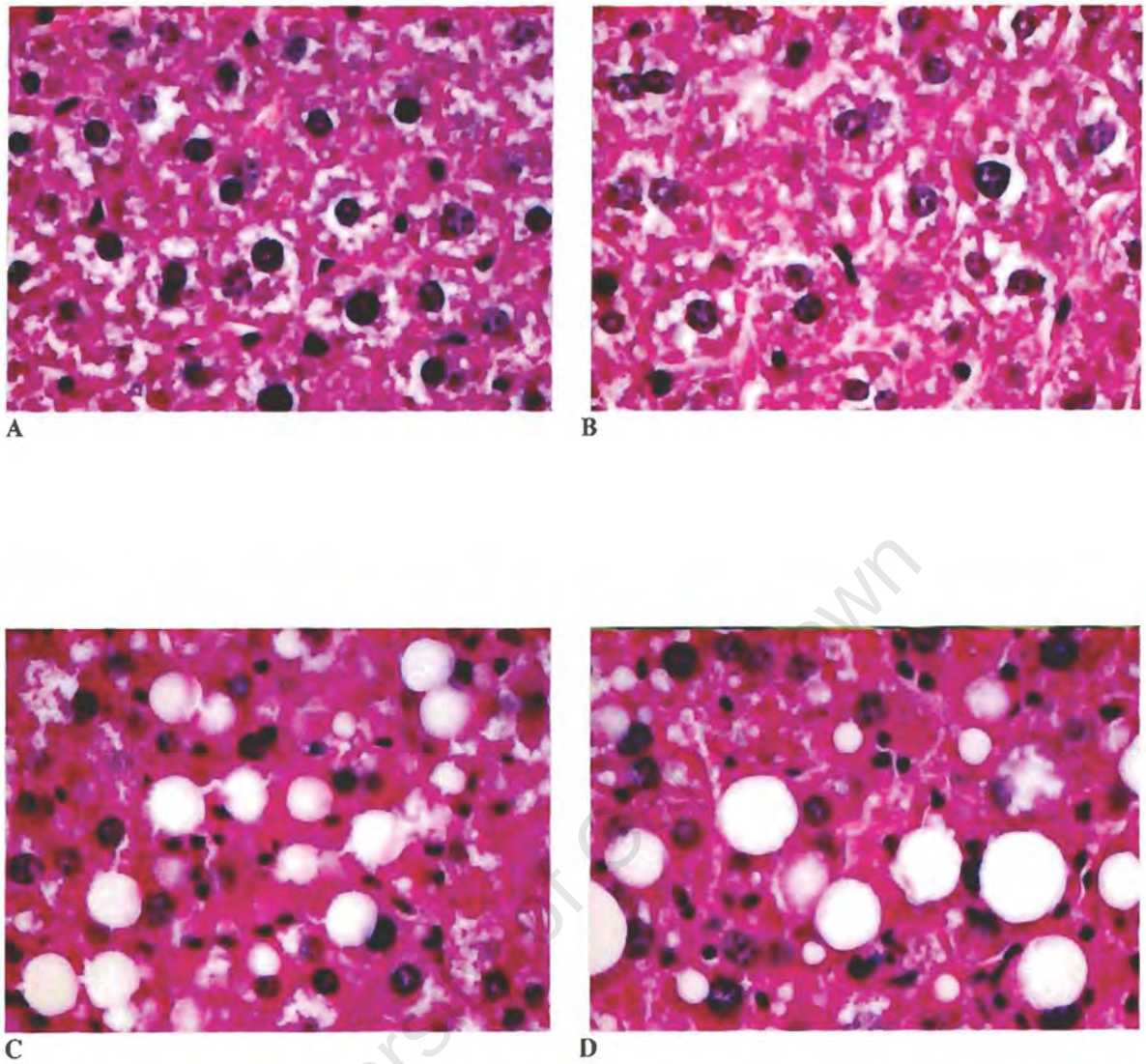

Figure 5.4: Liver sections from TNFS. Sections from (A) Ctrl wt and (B) Ctrl ko appear histologically normal. However, liver sections from (C) MCD wt and (D) MCD ko, show macrovesicular steatosis and scattered mononuclear cells. Necroinflamatory foci were present in both these treatment groups, but are not shown in these figures. H&E, 40x objective.

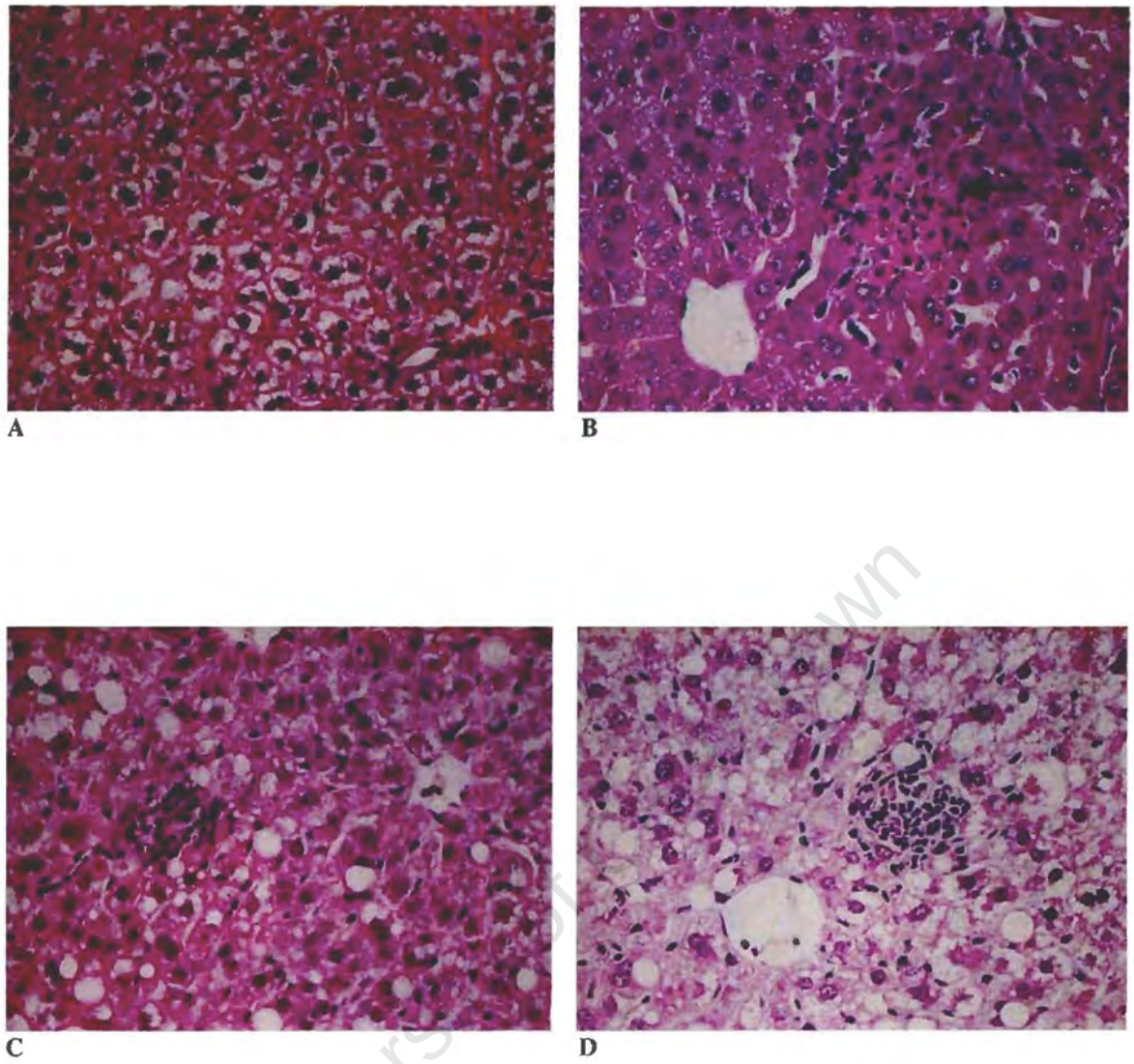

Figure 5.5: Liver sections from LPSS. (A) Ctrl + saline, normal liver (B) Ctrl + LPS, the arrow indicates a necroinflammatory focus. (C) MCD + saline and (D) MCD + LPS showing macrovesicular steatosis and necroinflammatory foci containing PMN and mononuclear cells. H&E, 20x objective.

Table 5.1: Histolofical features of livers of the TNFS

Treatment	Fat score	Distribution	Inflammatory foci (score)	Inflammatory foci (number)	Macrophage (D/PAS) score*	Macrophage (D/PAS) number*
Ctrl wt	0.0±0.0	-	0.0±0.0	1.17±1.17	0.0±0.0	0.0±0.0
Ctrl ko	0.0±0.0	-	0.0±0.0	1.0±0.89	0.0±0.0	0.0±0.0
MCD wt	1.67±1.21	**	1.52±0.84	11.5±5.82	0.0±0.0	0.0±0.0
MCD ko	2.0±1.0	**	2.75±0.50	21.67±5.77	0.0±0.0	0.0±0.0

Classification terms: **Distribution:** Zonal distribution of hepatocytes containing lipid; **Score:** Mean score (± standard deviation) per group, as outlined in **3.3**; **Number:** Refers to average number (± standard deviation) of inflammatory foci or D/PAS macrophages in 20hpf. ***D/PAS Macrophage numbers and scores** based on numbers of enlarged macrophages. **Zonal distribution showed great inter-animal variation.
See Appendix 4.3 for raw data

Table 5.2: Histological features of LPSS livers

Treatment	Fat score	Distribution	Inflammatory foci (score)	Inflammatory foci (number)	D/PAS macrophage (score)*	D/PAS macrophage (number)*
Ctrl + Saline	0.0±0.0	-	0.13±0.35	1.5±2.0	0.0±0.0	0.0±0.0
Ctrl + LPS	0.0±0.0	-	1.88±0.35	12.5±3.82	0.0±0.0	0.5±0.76
MCD + Saline	1.33±0.52	Zone 1	2.14±0.69	15.57±8.66	0.29±0.76	3.0±7.07
MCD + LPS	1.06±0.56	Zone 1	2.13±0.64	16.88±6.53	0.0±0.0	0.13±0.35

Classification terms: **Distribution:** Zonal distribution of hepatocytes containing lipid; **Score:** Mean score (± standard deviation) per group, as outlined in **3.3**; **Number:** Refers to average number (± standard deviation) of inflammatory foci or D/PAS macrophages in 20hpf. ***D/PAS Macrophage numbers and scores** based on numbers of enlarged macrophages.
See Appendix 5.3 for raw data

5.5 Characterization of the Inflammatory Infiltrate

TNFS

Due to unexpected ill health of ko mice, termination of the TNFS had to be conducted on a public holiday, and materials for cryopreservation of tissue were unavailable. Immunocytochemical analyses for this study were therefore not possible.

LPSS

NK and B cells were not stained for in this study, as they were absent in the LTS. Stains for CD4+ and CD8+ cells were conducted, but as in the LTS, none were detected. Kupffer cells detected by an antibody to F4/80 were found in all liver sections from this study. In saline treated samples, they were always spindle shaped and were in the sinusoids (Fig 5.6), though MCD mice had greater numbers than Ctrl. Following LPS challenge, there was no apparent change in morphology of Kupffer cells, however there was a marked increase in the number of macrophages (Fig 5.6). Lipid-laden Kupffer cells and lipofuscin were not features in this study.

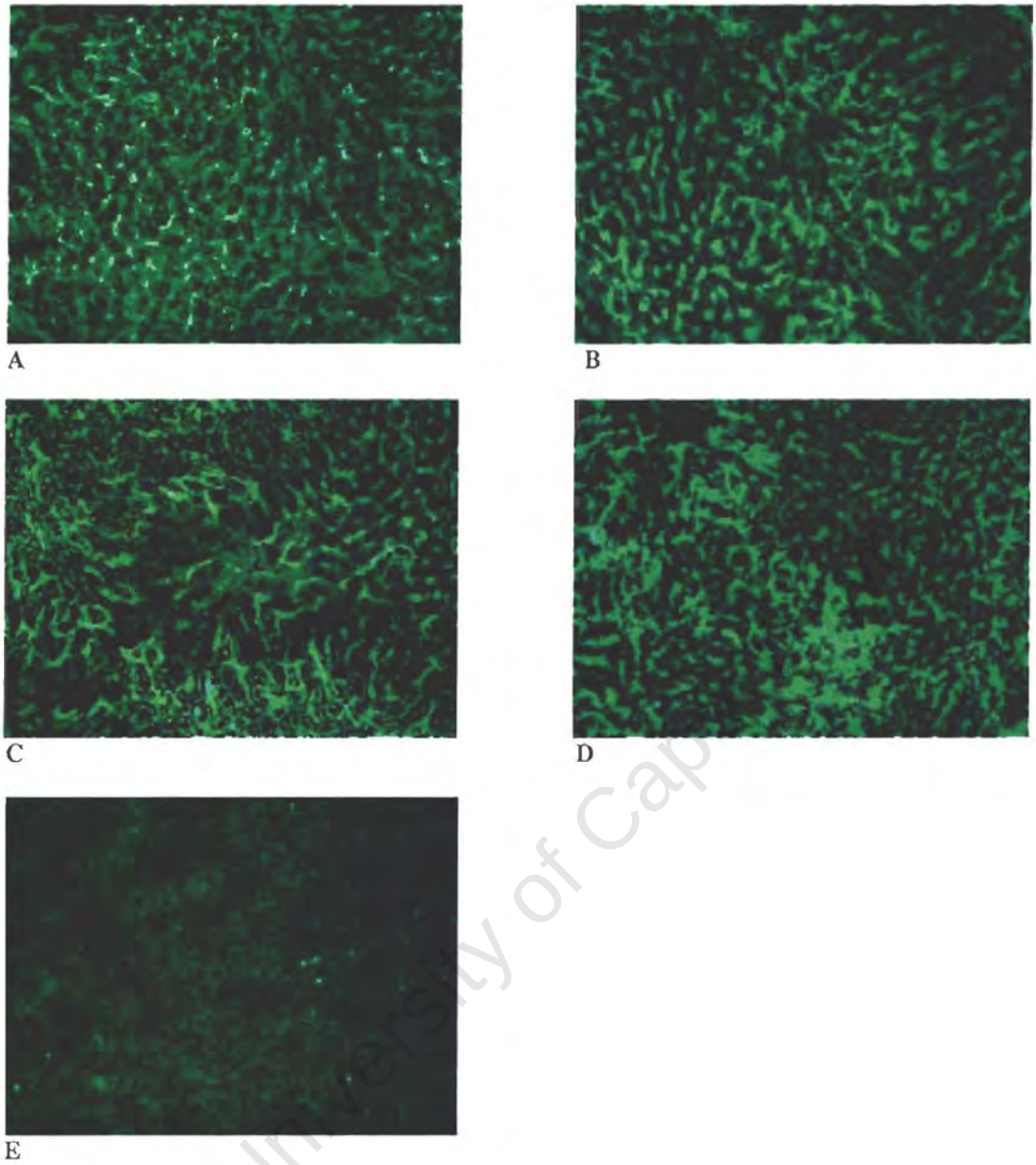

Figure 5.6: Antibody to F4/80 was used to detect Kupffer cells in the LPS study. (A) Kupffer cells in sinusoids of Ctrl mice + saline,
(C) MCD + saline
Increased numbers of Kupffer cells are seen after LPS challenge in (B) Ctrl mice (D) MCD mice
(E) Negative control, using PBS in place of F480 primary antibody. Immunofluorescence, 40x objective.

5.6 Histological Assessment and Biochemical Measurement of Fibrosis

SR stains on liver sections from the LPSS and TNFS showed no fibrosis in liver samples of either study. To assess subtle changes in collagen deposition which may not be observed at the level of light microscopy, the effect of TNFα on fibrosis was measured biochemically by assessment of hydroxyproline in the TNFS (see **3.4**). As shown in Figure 5.7, absence of TNFα appeared to significantly decrease hydroxyproline content in Ctrl animals (p=0.0043); but contrary to expectations, hydroxyproline deposition was enhanced in the absence of TNFα when animals received MCDD, though the change was only mild and did not reach statistical significance (p=0.9143). Raw data is presented in Appendix 4.4.

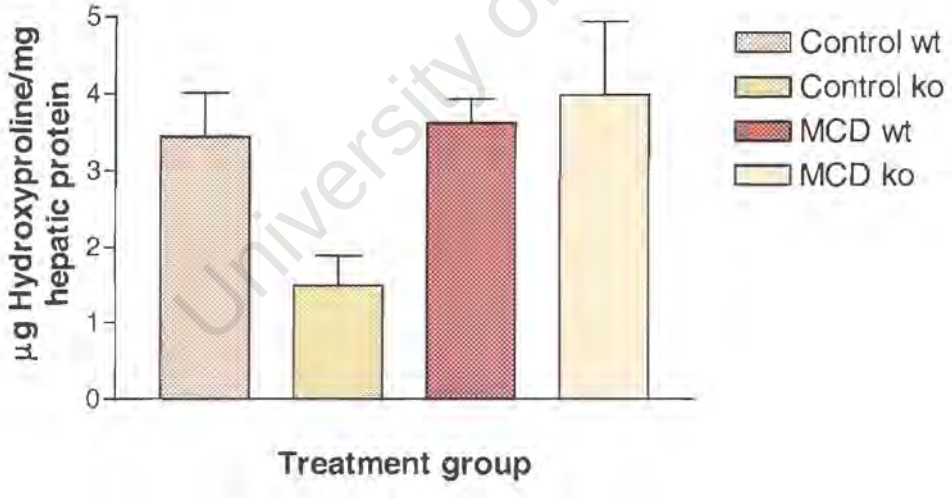

Figure 5.7: Hydroxyproline content in treatment groups of TNFS is slightly enhanced in MCD ko mice, though it is significantly reduced in Ctrl ko mice relative to Ctrl wt (p=0.0043).

5.7 Hepatic and Serum TG, and LP

5.7.1 Factors affecting TG accumulation

The MCDD always caused hepatic TG accumulation (Figures 5.8A and 5.8C); this was due to reduced TG export, as indicated by lower serum TG in mice receiving the MCDD versus Ctrl (Figure 5.8B, MCD wt vs Ctrl wt p=0.0022). Hepatic TG accumulation was mitigated, but not abolished, however by knocking out TNFα (Figure 5.8A, Ctrl wt versus ko p=0.3290; MCD wt versus ko p=0.9143). This concurs with findings at the light microscopic level, and may involve increased export of hepatic TG in ko mice, as shown by slight increases in serum TG for ko animals of both treatment groups, though these increases are not statistically signficant (Figure 5.8B, Ctrl wt vs ko p=0.3939, MCD wt vs ko p=1.000).

In the LPSS, induction of TNFα appeared to have a slight influence on hepatic TG accumulation in the 24h between LPS challenge and sacrifice for Ctrl (p=0.5737), but not MCD, mice (Figure 5.8C). Serum TG levels were unavailable for this study, as serum was utilised for measurement of serum TNFα. Raw data for hepatic and serum TG measurements in the TNFS and LPSS are presented in Appendices 4.5, 4.6 and 5.4.

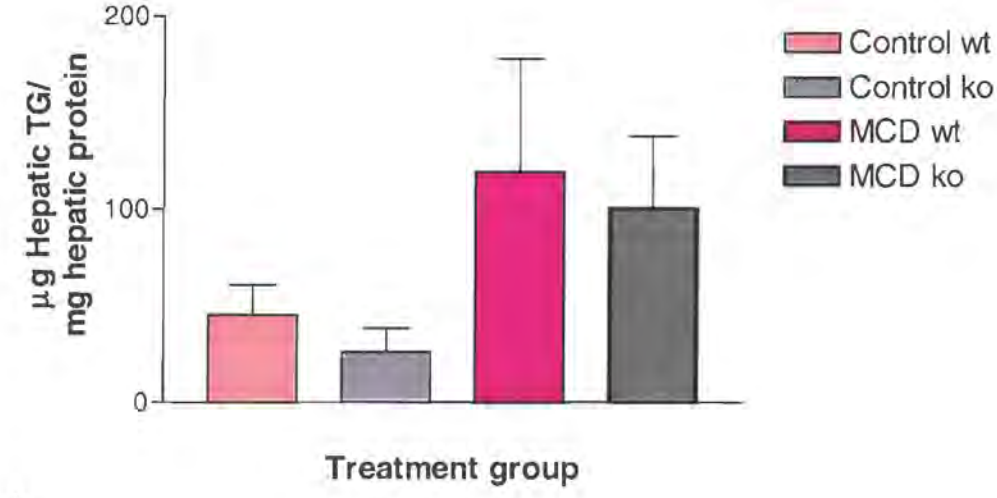

A

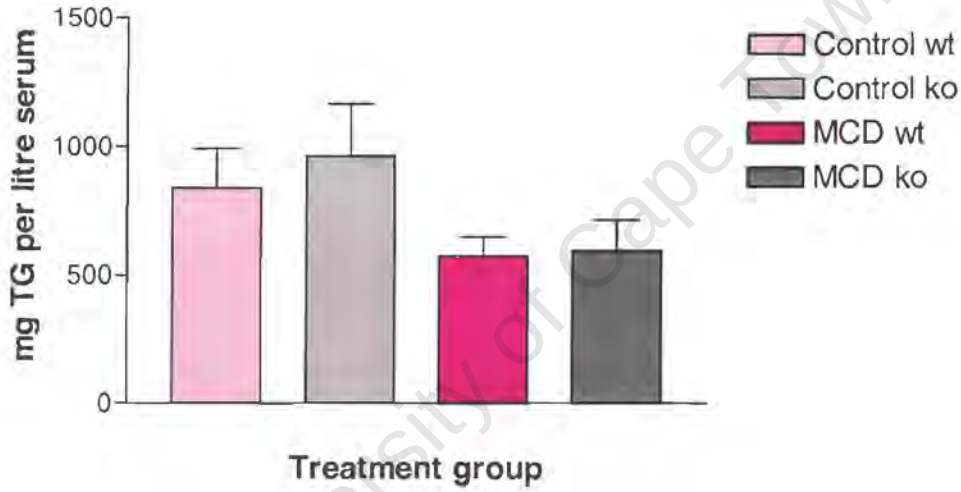

B

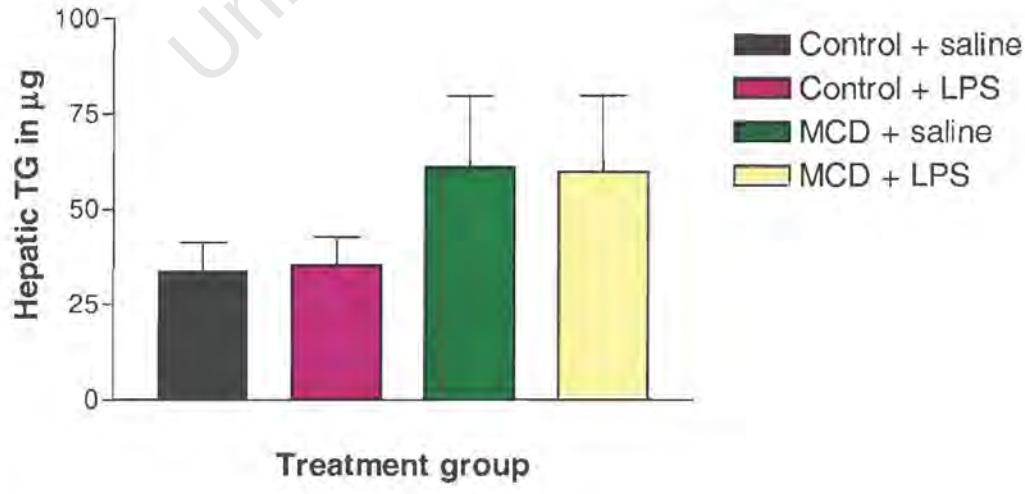

C

Figure 5.8: (A) Hepatic TG content in TNFS is increased by MCDD, but is always less in ko mice relative to wt counterparts, regardless of treatment (Ctrl wt versus ko p=0.3290; MCD wt versus ko p=0.9143) (B) Serum TG in TNFS is reduced by MCDD (p=0.0022), but is higher in ko versus wt in both MCD and Ctrl groups. (C) In the LPSS, hepatic TG is slightly elevated in Ctrl (but not MCD) group after LPS challenge.

5.7.2 Phosphatidylcholine

Due to technical difficulties, PC values were unreliable for TNFS and LPS and are not reported in the thesis.

5.7.3 Effect of TNFα on LP

All animals on the MCDD showed evidence of LP in the TNFS (Figure 5.9). Contrary to expectation, knocking out TNFα enhanced rather than ameliorated LP. Although Ctrl ko mice had similar levels of CD to Ctrl wt, ko mice receiving the MCDD had higher levels of CD than MCD wt (p=0.1714). LOOH levels were negligible in all groups. With regard to fTBARS, ko mice expressed significantly higher levels than wt counterparts (Ctrl p=0.0022, MCD p=0.0095). TTBARS were also elevated in ko mice versus wt, though the changes did not reach statistical significance (Ctrl p=0.0649; MCD p=0.2571). The ratio of mean values of LP indices was calculated as an alternative view of the LP profile in the TNFS (Table 5.3). In Ctrl ko, although LP is enhanced, there is a preference for late products; thus the proportion of LOOH generated per nMol of CD is only marginally higher than Ctrl wt, while the proportions of late products (fTBARS, tTBARS) are markedly increased. In MCD mice, though higher *absolute values* of LOOH are produced by ko relative to wt mice (Figure 5.9), the *proportion* of LOOH generated per unit of CD is less than in wt mice. The proportion of late products (fTBARS and tTBARS) however is increased in MCD ko mice relative to wt.

Induction of TNFα also increased LP (Figure 5.10), though in Ctrl mice challenged with LPS this was only noted at the level of tTBARS (p=0.0002). Mice which received the MCDD and LPS had higher levels of CD (p=0.1949), fTBARS (p=0.0207) and tTBARS (p=0.3823) than those in the MCD-saline treatment group. Interestingly, the ratio of LP products (Table 5.4) indicates that despite higher absolute values of LP products in mice challenged with LPS, the proportion of LP products generated per nMol of CD is only higher in Ctrl mice receiving LPS (relative to saline Ctrl) at the level of fTBARS and tTBARS. In MCD mice, differences

in absolute values are also not adequately reflected in the proportion of LP products generated per nMol of CD; thus MCD mice challenged with LPS generate comparable proportion of LOOH, higher proportion of fTBARS, and lower proportion of tTBARS relative to MCD mice which received i.p. saline. Raw data is presented in Appendices 4.7-4.10, and 5.5-5.8.

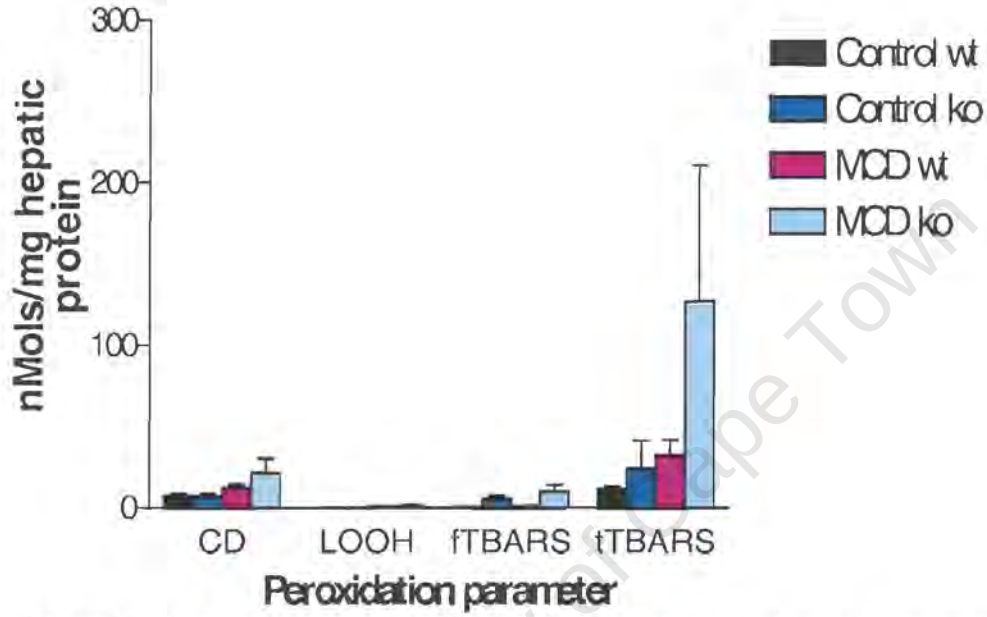

Figure 5.9: In Ctrl mice, late LP indices in the TNFS are elevated in ko relative to wt mice, while MCD ko mice had higher levels of early and late LP products relative to wt. Ctrl fTBARS p=0.0022, tTBARS p=0.0649. MCD CD p=0.1714, fTBARS p=0.0095, tTBARS p=0.2571.

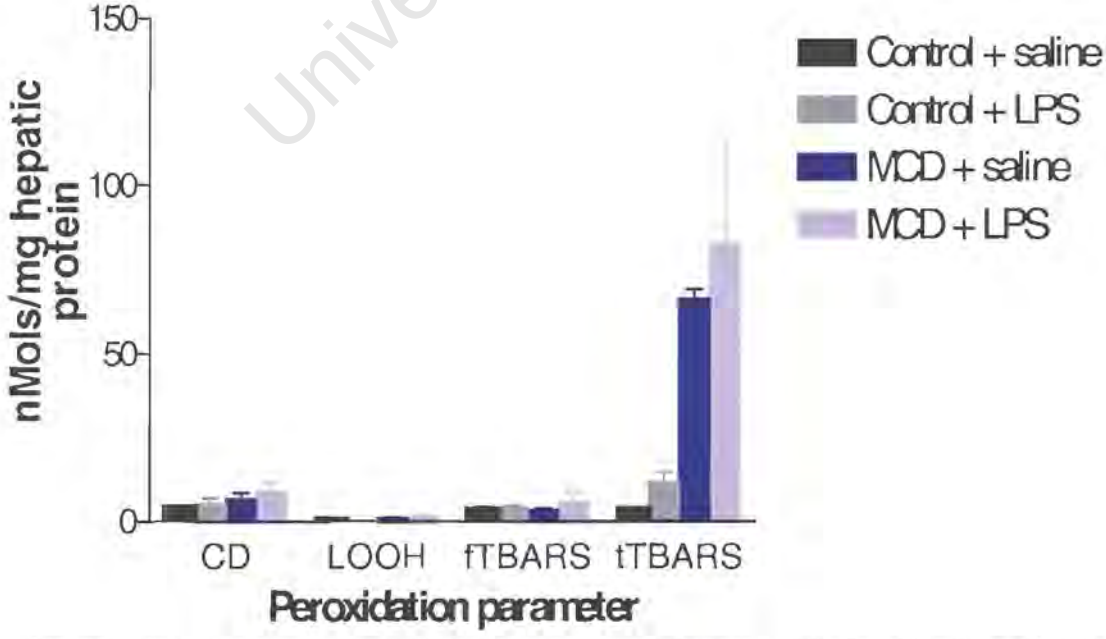

Figure 5.10: TNFα induction by LPS challenge enhances LP in the LPSS. Ctrl tTBARS p=0.0002; MCD CD p=0.1949, fTBARS p=0.0207 and tTBARS p=0.3823.

Table 5.3: Ratio of LP indices in TNFS.

Treatment Group	Ratio of mean LP products CD:LOOH:fTBARS:tTBARS
Ctrl wt	1.0:0.02:0.08:1.68
Ctrl ko	1.0:0.03:0.80:3.50
MCD wt	1.0:0.07:0.09:2.68
MCD ko	1.0:0.04:0.47:5.87

*Value of CD always taken as 1.0

Table 5.4: Ratio of LP indices in LTS.

Treatment Group	Ratio of mean LP products CD:LOOH:fTBARS:tTBARS
Ctrl + Saline	1.0:0.09:0.77:0.84
Ctrl + LPS	1.0:0.09:0.81:2.24
MCD + Saline	1.0:0.15:0.51:10.09
MCD + LPS	1.0:0.14:0.65:9.18

*Value of CD always taken as 1.0

Because the enlarged D/PAS positive Kupffer cells (presumed to be responsible for generation of 4-HNE in the LTS) are absent in short term studies, the main source of 4-HNE in short term administration of the MCDD was queried, especially in interesting scenarios where changes in LP are rapid (such as following LPS administration), or steatosis is mitigated (such as with TNFα ko).

When coded sections were examined, it was impossible to distinguish Ctrl wt from Ctrl ko, as livers from both groups showed positive staining in some but not all of the small, inactivated Kupffer cells. Occasional normal hepatocytes also showed positive cytoplasmic staining

(Figure 5.11 A and C). Similarly, livers from wt and ko mice receiving the MCDD could not be distinguished from one another (but were distinct from Ctrl livers). Greater numbers of both hepatocytes and Kupffer cells showed positive cytoplasmic staining, compared to Ctrl livers (Figure 5.11 B and D). Staining was strongest in macrophages that were seen in the necroinflammatory foci. In all treatment groups, there was considerable inter-animal variation in the number of positive cells.

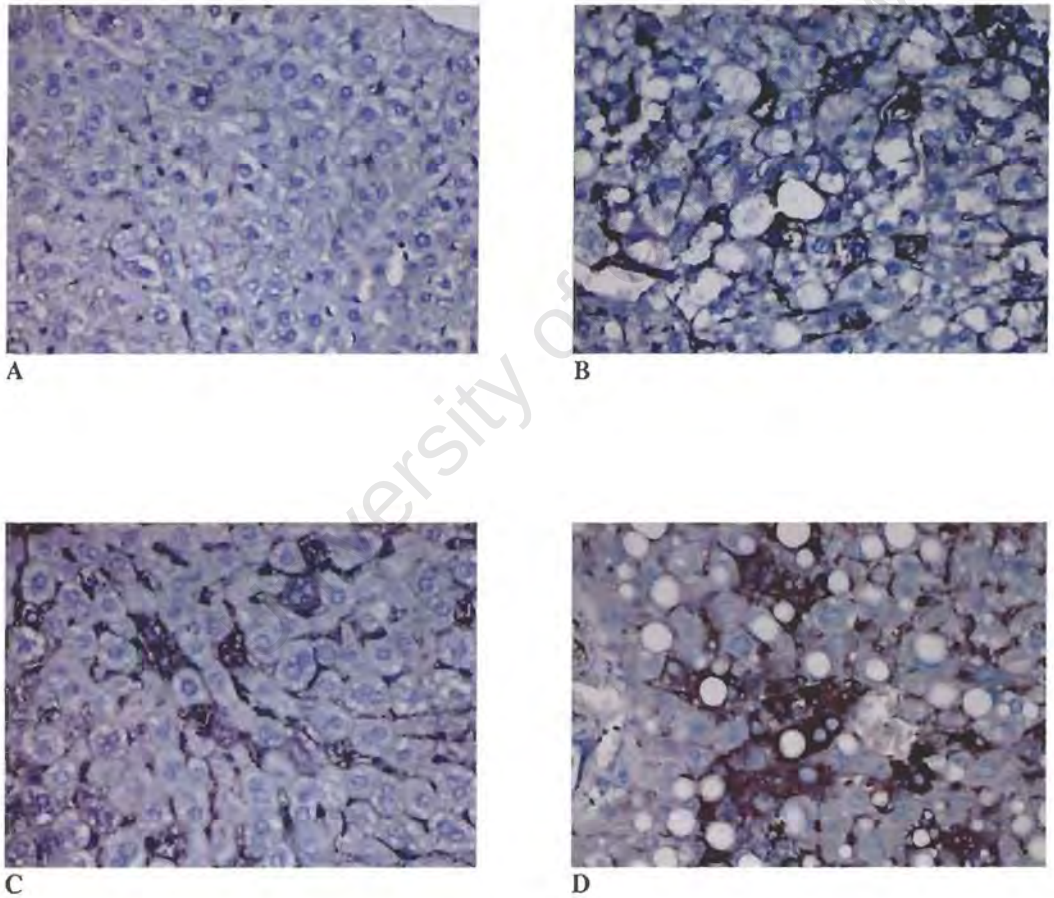

Figure 5.11: 4-HNE-protein adducts are detected in hepatocytes of the TNFS (A) Ctrl wt (B) MCD wt (C) Ctrl + ko (D) MCD ko. Kupffer cells in sinusoids can also be seen staining positive for protein adducts of 4-HNE. 20x objective.

5.8 Relationship Between CYP2E1 Activity and TNFα in the Rodent Nutritional Model of NASH

Because of the unexpected effects of TNFα knockout on LP, and the role of CYP2E1 as a catalyst of microsomal LP (Weltman *et al.*, 1996; Leclercq *et al.*, 2000), CYP2E1 activity in the presence and absence of this cytokine was investigated. Consistent with the findings of increased LP in ko mice, abolition of TNFα also increased CYP2E1 activity (Figure 5.12). Although the change was negligible in Ctrl mice, it was striking in MCD ko versus wt (p=0.1143). Raw data is presented in Appendix 4.11.

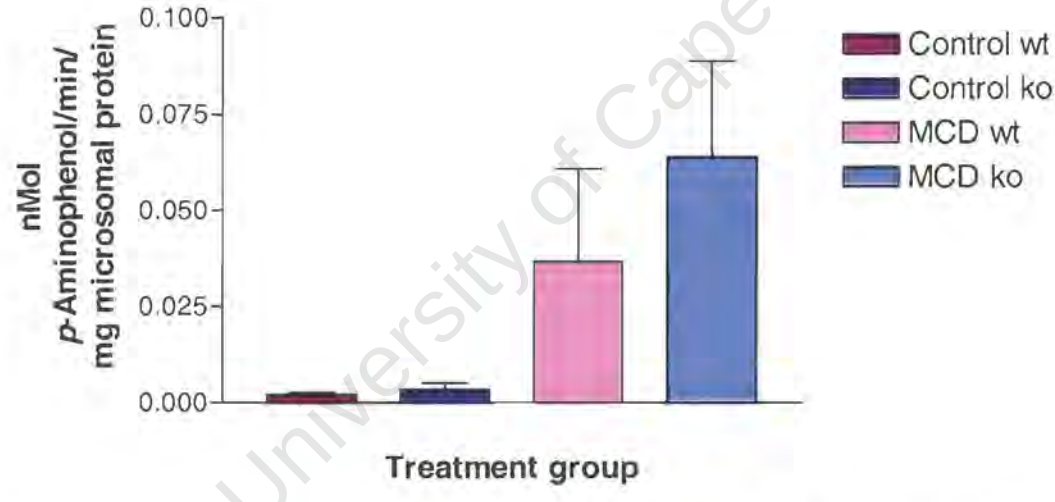

Figure 5.12: CYP2E1 activity is enhanced in TNFα ko mice relative to wt, however this difference is only noteworthy in animals receiving the MCDD (p=0.1143)

5.9 Serum TNFα

TNFα was measured in serum from the LPSS, diluted ½, $^1/_3$, and $^1/_9$. These dilutions proved too low for detection of TNFα on the standard curve. There was no remaining neat serum for repetition of the assay.

The effects of TNFα on biochemical measurements of liver dysfunction are summarised in Tables 5.5 and 5.6. Based on the data presented, it is possible to conclude that, while TNFα may play a role in progression of NAFLD in the MCD model, it does not appear to be essential for development of NAFLD.

Table 5.5 (a): Summary of effect of knocking out TNFα on biochemical measurements of hepatic dysfunction. Values are per cent [%] of mean of baseline (i.e. Ctrl wt)

	ALT	Hydroxyproline	Hepatic TG	Serum TG	CD	LOOH	fTBARS	tTBARS	CYP2E1
Ctrl ko	225	43	51	115	100	200	964	208	150
MCD wt	1912	105	245	68	173	755	198	277	1850
MCD ko	914	116	218	71	309	973	1762	1084	3200

Mean values of baseline: ALT 12.5U/L; **Hydroxyproline** 3.45µg/mg; **Hepatic TG** 45.97µg/mg; **Serum TG** 839.16mg/L; **CD** 7.01nMol/mg; **LOOH** 0.11nMol/mg; **fTBARS** 0.58nMol/mg; **tTBARS** 11.73nMol/mg; **CYP2E1** 0.002nMol *p*-Aminophenol/mg/min.

Table 5.5 (b): Summary of effect of knocking out TNFα on biochemical markers of MCDD-induced NAFLD. Values are expressed as % of mean of baseline, MCD wt is baseline.

	ALT	Hydroxyproline	Hepatic TG	Serum TG	CD	LOOH	FTBARS	tTBARS	CYP2E1
MCD ko	48	110	89	104	178	129	889	392	173

Mean values of baseline: ALT 239U/L; **Hydroxyproline** 3.62µg/mg; **Hepatic TG** 112.40µg/mg; **Serum TG** 572.76mg/L; **CD** 12.13 nMol/mg; **LOOH** 0.83nMol/mg; **fTBARS** 1.15nMol/mg; **tTBARS** 32.46nMol/mg; **CYP2E1** 0.037nMol *p*-Aminophenol/mg/min.

Table 5.6 (a): Summary of effect of TNFα induction on biochemical markers of hepatic dysfunction. Ctrl + saline serves as baseline, and values are expressed as % of mean of baseline.

	ALT	Hepatic TG	CD	LOOH	fTBARS	tTBARS
Ctrl + LPS	563	104	120	113	126	319
MCD + Saline	360	180	153	250	100	1828
MCD + LPS	1524	177	210	310	175	2279

Mean values of baseline: ALT 17.75U/L; **Hepatic TG** 33.78µg/mg; **CD** 4.29nMol/mg; **LOOH** 0.40nMol/mg; **fTBARS** 3.34nMol/mg; **tTBARS** 3.62nMol/mg.

Table 5.6 (b): Summary of effect of TNFα induction on progression of MCDD-induced NAFLD. Values are expressed as % of mean of baseline. MCD + saline is baseline.

	ALT	Hepatic TG	CD	LOOH	fTBARS	tTBARS
MCD + LPS	423	98	137	124	176	125

Mean values of baseline: ALT 63.88U/L; **Hepatic TG** 60.92µg/mg; **CD** 6.56nMol/mg; **LOOH** 1.00nMol/mg; **fTBARS** 3.33nMol/mg; **tTBARS** 66.19nMol/mg.

Chapter Six

Discussion and Conclusions

Investigations utilizing animal models to draw conclusions relevant to a human system suffer numerous drawbacks. The shortcomings of the MCD model of NASH have been discussed in some detail (see **2.1**); however, animal models remain the most realistic means of conducting in depth investigations, which are impossible using human subjects. In most studies, the MCD model lacks the features required for designation as NAFLD Types 3 or 4/NASH (Matteoni *et al.*, 1999) such as ballooning degeneration and significant fibrosis, and thus more appropriately describes derangements present in NAFLD Type 2. Nevertheless, because some features prominent in the MCD model, which are probably responsible for the observed hepatic injury (TG accumulation and lobular inflammation including PMN, increased CYP2E1 activity) are also present in human NAFLD Types 2 to 4, it seems likely that some of the same mechanisms at play in this model are relevant to human NASH.

The findings of four studies using the MCD model are discussed below. Since all studies were concerned with the concept of *interactive* hepatoxicity, implications of all findings are brought together in a single chapter, rather than discussed at the end of preceding chapters. While interpreting the results, three factors must be underscored. Firstly, due to the small sample size of each study, the values recorded may sometimes not accurately reflect true population means (μ), or adequately describe real trends and relationships between treatment groups. In spite of this, it is possible to speculate on the implications of findings within the studies, especially where the trends are clear, and consistent with current scientific ideas of the pathogenesis of NAFLD/NASH. Secondly, because of disparate storage conditions between LTS samples (which were stored at -80^{0}C for a few months at most), and livers from the STS (which were stored at -80^{0}C for up to a year), direct comparisons between the STS and LTS should be conducted with caution, especially when analysing potentially unstable products such as those of LP, some of which (LOOH) are known to be stable for ~14 days at -20^{0}C (D. Marais, personal communication). To the knowledge of this investigator, long term stability at lower temperatures has not been documented. Finally, tissue for the LTS,

TNFS and LPSS were collected in a pre-determined fashion, with different lobes allocated to specific assays (see **4.1**). However, livers were not stored in this fashion for preceding analyses, as the STS sacrifice was conducted previously by colleagues in the UCT NASH Research Group. While spatial variations in the biochemical indices measured are unlikely to be significant, this represents another difference between the LTS and STS.

Weight loss as a result of the MCDD was apparent within the first week of feeding in all experiments. Although the caloric intake of animals was not monitored, this did not appear to be the result of feed refusal until late in the LTS, when animals appeared too lethargic to accept feed. NASH has been linked to rapid weight loss in humans (see **1.1**), and in this context is believed to be a consequence of significant influx of FA as a result of adipocyte lipolysis. Rapid and profound weight loss may contribute to steatosis in human NASH and may well be a contributing factor in the pathogenesis of the MCD model.

NASH requires, by definition, that the suspected patient consume "insignificant" amounts of alcohol, yet there is little consensus with regard to the exact quantity to which this refers. Some authors considered values of ≥20g/day to be excessive (Bacon *et al.*, 1994), while others found 20g/day (Brunt *et al.*, 1999) and 210g/week acceptable (Teli *et al.*, 1995). There appears to be no laboratory data indicating at what level, if any, alcohol begins to contribute to development of fatty liver disease in the putative non-drinker. The purpose of the STS and LTS was therefore to investigate the effect of short and long term alcohol consumption (low to high concentration) on MCDD-induced fatty liver in a rodent model of NAFLD.

Aminotransferases, elevated levels of which are indicative of liver injury, were always elevated by the MCDD. While Ctrl mice in the LTS displayed no definite association between aminotransferase levels and alcohol concentration, the effect of the MCDD on liver enzymes was enhanced when mice received alcohol in addition to the deficient diet, indicating increased hepatic injury. An AST/ALT ratio less than 1 is believed to be

suggestive of NASH rather than ASH (Zamin *et al.*, 2002); a high AST/ALT is thought to be indicative of ASH, and in addition identifies patients at risk for fibrosis (Angulo *et al.*, 1999). The ratio of AST to ALT was slightly greater than 1 in all groups but Ctrl, Ctrl plus 8% ethanol and MCDD, but was roughly 1 in all other groups. These ratios show no correlation with the treatments administered, thus it is uncertain as to whether the ratio of liver enzymes can be used to as an indicator of the presence, or type, of NAFLD in the MCD model.

Light microscopy showed steatosis as a result of the MCDD; the pattern of steatosis was predominantly macrovesicular, however in some animals receiving alcohol in addition to the deficient diet, steatosis was micro- and macrovesicular. In addition, in Ctrl animals, the fat score was slightly higher when mice received 8% alcohol, and mild microvesicular steatosis as a result of alcohol intake was seen in Ctrl mice receiving 20% alcohol. This suggests that the levels of alcohol used in the LTS are sufficient to cause some hepatic dysfunction, even in the absence of a lipotrope deficient diet, and should probably not be considered "insignificant" in the context of NAFLD. Steatosis was seen in all zones of the liver but did not always involve all of the zone 3 regions. This apparent sparing of some zone 3 hepatocytes was due, in part, to the presence of necroinflammatory foci immediately adjacent to the veins but could also be due to the fact that some of the hepaocytes in these regions were recently regenerated cells.

Biochemical measurements of TG showed a 139% increase in hepatic TG in STS Ctrl mice receiving both 4% and 8% alcohol, compared to the overall baseline (i.e. Ctrl + water). The MCDD enhanced the TG content to 240% above the overall baseline, and when the MCDD was consumed with alcohol, it caused further increases of 784% and 486% (4% and 8% alcohol, respectively). In the LTS, TG levels were typically higher than in the STS, perhaps suggesting a cumulative effect of the high fat diets on lipid accumulation over time. TG levels also correlated roughly with fat scores at the light microscopic level. Alcohol supplementation increased hepatic TG in both Ctrl and MCD. As in the STS, LTS Ctrl mice

failed to show a dose-dependent correlation between TG content and alcohol concentration, potentially suggesting that on alcohol alone the maximum possible level of hepatic TG is quickly reached. On a lipotrope deficient diet, this "ceiling" is necessarily higher, and because of the putative exacerbating effect of alcohol on fatty liver, further increases in hepatic TG are also possible, which may correlate with alcohol concentration. Although it is possible to challenge this hypothesis on the basis of the unusually high levels of hepatic TG in MCD + 4% alcohol mice in the STS, it must be noted that for this assay, the standard deviation for mice in this group is relatively high in comparison to other animals in the study, thus a few unusually high values may skew the mean. Again, this reflects a flaw in using small sample sizes to draw conclusions which are subsequently extended to the behaviour of populations.

Steatosis as a result of the MCDD was believed to be due to PC deficiency, which would lead to deficient VLDL synthesis. Although levels of serum TG in the LTS were comparable in all treatment groups, apparently challenging this view, it is likely that the high levels of serum TG in MCD mice simply represents increased (albeit inadequate) TG transport from a significantly larger hepatic lipid pool than in Ctrl mice. The role of the MCDD in lipid accumulation was in fact confirmed by PC values of ~50% of Ctrl baseline in MCD groups of the LTS. However, although MCD mice receiving alcohol had hepatic TG increases of 103% and 113% relative to MCD mice receiving water (i.e. the MCD baseline), hepatic PC was elevated to 104% of MCD baseline in mice on the deficient diet and 8% alcohol, but reduced to 88% of the MCD baseline when mice received 20% alcohol in addition to the MCDD. This suggests that the mechanism for hepatic lipid accumulation as a result of alcohol consumption is distinct from the pathway for hepatic TG trapping resulting from a lipotrope deficient diet.

Several explanations for the effect of alcohol on TG accumulation have been proposed. Initially, steatosis is believed to be the result of an increased $NADH/NAD^+$ ratio, which

enhances glycerol 3-phospate, a principal substrate for TG esterification (Casini, 2000). This imbalance is attenuated with time, however, and other factors become operative in long-term alcohol abuse. These include increases in activity of phosphatidate phosphohydrolase (which catalyses dephosphorylation of phosphatidic acid to diacylglycerol) and diacylglycerol acyltransferase (which increases esterification of TG), increased fatty acid binding protein expression and decreased VLDL secretion of TG (Day and Yeaman, 1994; Eaton *et al.*, 1997). The latter does not appear to be linked exclusively to direct effects on PC, since alcohol consumption did not incrementally lower hepatic PC in the LTS. Finally, alcohol is also believed to drive steatosis by decreasing β-oxidation, although this has been debated (Eaton *et al.*, 1997). The hepatoxic effect of alcohol is exacerbated by a lipid-rich diet, since alcohol enhances FA uptake, and FFA are potentially cytotoxic due to detergent effects on cellular and organellar membranes (Day and Yeaman, 1994; Casini, 2002). Thus in the rodent model of interactive hepatoxicity described by the STS and LTS, the various effects of alcohol on lipid metabolism, the effects of a high fat diet (alone and in association with alcohol), and lipotrope deficiency, work in concert to drive lipid accumulation and concomitant hepatic dysfunction.

Inflammation was present in the livers of mice receiving the MCDD, however the inflammatory score appeared to correlate neither with fat score nor concentration of alcohol consumed. H&E stains indicated that foci were composed of both PMN leukocytes and mononuclear cells, which were thought to be mainly lymphocytes; D/PAS stains showed large numbers of foamy macrophages in MCD livers. In an attempt to understand the role of inflammation in pathogenesis of the animal model of NAFLD, the phenotypes of cells comprising the inflammatory infiltrate in the LTS were characterized. Immunocytochemistry on frozen tissue revealed no NK or B cells in Ctrl or MCD livers, which is consistent with human NASH. However, CD4+ and CD8+ positive cells, which have been described in human NASH (Lefkowitch *et al.*, 2002), were also not detected. Due to limitations of immunocytochemistry, it is conceivable that a small number of each T cell subtype could

escape detection. Staining for CD3+ cells would detect T lymphocytes irrespective of subclass, and since this collective number may exceed the number of each type that is separately detectable, the presence of T cells may thus be established. Alternatively, flow cytometry (FACS) is a sensitive technique which would analyse and sort lymphocte subpopulations in the infiltrate.

Immunocytochemistry did, however, show the presence of macrophages/Kupffer cells. Since Kupffer cells are normal resident cells of the liver, they were also detected in Ctrl samples, where they were usually spindle shaped and located in the sinusoids. In livers from MCD mice, Kupffer cells were numerous, enlarged and irregular, and contained lipid droplets and lipofuscin. The presence of PMNs and Kupffer cells in the MCD model of NAFLD is unsurprising. Imminent LP is indicated by elevated levels of CD within 1 day of feeding the MCDD (Rushmore *et al.*, 1984). Since LP products upregulate adhesion molecules and are chemoattractant for neutrophils (Pessayre *et al.*, 1999), the peroxidative process may be at least partly responsible for recruitment of PMN populations seen in the MCD model and human NASH. Kupffer cells are instrumental in ingestion and processing of cellular debris and, with PMN, are also a source of oxidative stress. Finally, inflammatory cells are also key players in the initiation of the cytokine cascade, and although cytokine production is intended to be hepatoprotective, it may contribute to liver injury.

The MCDD and alcohol also elevated LP in the rodent nutritional model of NASH. LP is currently believed to be a driving force behind a diverse array of diseases. But since (1) antioxidant defences (in the way of non-enzymatic radical scavengers such as glutathione and α-tocopherol, and enzymes such as MnSOD and catalase) normally exist to counteract the effects of cellular oxidative stress, and (2) assessment of LP in all studies required mechanical tissue disruption (thereby bringing into contact peroxidizable substrates, lipoxygenases and free radicals), the levels of LP presented in all studies may not be an accurate representation of *in vivo* LP in the MCD model. Furthermore, while differences did

exist between animals receiving MCDD and Ctrl counterparts with respect to CD and free TBARS, the most striking change resulting from administration of MCDD often occurred at the level of total TBARS. The TBARS assay is, however, fundamentally flawed. The pink chromogen resulting from reaction of late LP products with thiobarbituric acid (TBA) must be generated by heating samples at 100^{0}C for 15min (see **3.5.7**), and heat drives LP. In addition, although the assay is often used as a measure of the scission product malondialdehyde (MDA), two molecules of which react with TBA to yield the stable pink chromogen, TBA reacts with a considerable number of other compounds, including pyrimidine, 2-aminopyrimidine and sulfadiazine; unsaturated aldehydes (alone or in the presence of a sugar), and saturated aldehydes in the presence of sugars. TBA also reacts with oxidised 2-deoxyribose (Knight *et al.*, 1988). It is acknowledged that some of these reactions may not be relevant in a system utilising hepatic lipid rather than the popularly preferred tissue homogenate; however, the assay for total TBARS (tTBARS), though accepted in the field as a legitimate tool, is still dubious. Since it does not incorporate an antioxidant, it measures not only hepatic TBARS present at time of sacrifice but also TBARS generated during subsequent tissue processing and heating of extracted lipid. Thus the remarkable levels of total TBARS recorded for all studies are, to a large extent, artefact. The levels of free TBARS (fTBARS), which are measured in the presence of an antioxidant, may be more realistic (and are understandably much lower), however even these may be hampered by cross-reaction of TBA with other molecules; in addition, some small molecules of fTBARS may be potentially volatile and reactive (D. Marais, personal communication).

Although the cytotoxic and profibrogenic effects of LP products have been described (see **2.2.1**), the issues discussed above demand that the role of LP in the MCD model be scrutinized more critically. More sophisticated methods for measurement of *in vivo* and *in vitro* LP would reveal the level of meaningful peroxidation occurring during progressive liver disease. A time course of LP, generated and analysed alongside other markers of hepatic

damage, would also shed some light on the interplay between LP and other factors driving pathogenesis.

In spite of the conceptual and technical concerns detailed above, there is no doubt that LP does occur during liver injury, and may be a driving force behind this. In the STS, consumption of alcohol alone elevated CD more than 130% above the Ctrl baseline. In MCD mice, CD were elevated to 157% above baseline, and in mice consuming 4% and 8% alcohol in addition to the deficient diet CD increased further, to 179% and 257% respectively above levels recorded for mice on MCDD alone. The absolute value and proportion of tTBARS generated per nMol of CD were predictably increased by the MCDD; the absolute value of tTBARS also correlated directly with alcohol concentration both in MCD and Ctrl mice. In the case of fTBARS, however, although there was an initial increase in Ctrl mice on 4% alcohol, consumption of 8% reduced fTBARS to a staggering 17% of the Ctrl baseline; the proportion of fTBARS generated per nMol of CD also decreased with increased alcohol concentration. A similar but less striking trend was seen in MCD mice. Co-administration of the MCDD and 4% alcohol raised fTBARS to 141% of the level of the MCD baseline, however in mice receiving the MCDD and 8%, fTBARS dropped to 46% of the MCD baseline. The nMols of fTBARS generated per nMol of CD was also inversely proportional to alcohol concentration.

In the LTS, LP products were in general elevated relative to the STS; this may suggest either a time-dependent increase in LP and/or accumulation of LP products in the LTS, or degradation of LP products in the stored STS tissue. In Ctrl mice, CD were elevated relative to the overall baseline when alcohol was consumed, however this appeared to be at a steady state, beyond which further increases were not possible. This was the case also for absolute value of tTBARS, though a profile of the ratio of tTBARS to CD indicates that the nMols of tTBARS generated per nMol of CD actually continues to increase with increased alcohol concentration. Mid-stage LP products (LOOH) were never prominent in any group. In Ctrl

mice, absolute values of LOOH displayed the same unexpected pattern seen for fTBARS in the STS; thus consumption of 8% alcohol elevated LOOH to 170% above baseline, but consumption of 20% alcohol decreased LOOH to 63% of baseline. However, as with tTBARS, the nMols of LOOH generated per nMol of CD continued to increase in proportion to alcohol concentration. FTBARS showed a concentration-dependent decline in Ctrl mice, both in terms of absolute value and proportion of fTBARS generated per nMol of CD. The MCDD alone significantly elevated all indices of LP except fTBARS (which were unexpectedly reduced), relative to the overall baseline. In mice consuming alcohol and the MCDD, CD levels were elevated to 136% above the MCD baseline (8% alcohol), but dropped to 86% of the MCD baseline when mice consumed 20% alcohol. A similar pattern was seen for tTBARS. Absolute values of LOOH and fTBARS, however, showed an alcohol concentration-dependent increase in mice on the MCDD and alcohol.

If it is assumed that the LP assays are essentially a valid indication of the status of LP, as well as the profile of LP products in the MCD model, the data presented strongly suggests that, although LP may be upregulated by alcohol and/or a lipotrope deficient diet, these interventions cause different fluxes in the LP pathway. In short, different treatments may favour generation of different types of products at the expense of others. Further studies are required to understand the implications of these findings.

A common late LP product, 4-HNE, is stable and can diffuse to sites distant from the point of origin. The effects of 4-HNE include inhibition of RNA and DNA synthesis, modification of proteins, stimulation of neutrophil migration, enzyme inhibition and activation of stress-signalling pathways (Luckey and Petersen, 2001). To investigate the source of this cytotoxic product of LP, immunohistochemistry was conducted to detect protein adducts of 4-HNE. The results showed that in the LTS, D/PAS positive Kupffer cells appeared to be the source of 4-HNE. The enlarged D/PAS positive Kupffer cells in the LTS probably represent a reaction to significant hepatic damage, at which time they are responsible for phagocytosis and

processing of cellular debris at sites of hepatocyte necrosis and/or apoptosis (Vrba and Modriansky, 2002). The presence of 4-HNE adducts in Kupffer cells suggests that they may also inadvertently contribute to pathogenesis of NAFLD. Enlarged 'activated' Kupffer cells were not present at earlier time points, and normal Kupffer cells did not appear to express 4-HNE.

Finally, activity of CYP2E1 in the LTS was investigated. Enhanced CYP2E1 activity in the MCD model of NASH has been described, and roles for CYP2E1 and CYP4A as catalysts of microsomal LP have been demonstrated (Weltman *et al.*, 1996; Leclercq *et al.*, 2000; Robertson *et al.*, 2001; see **2.2.7**). The findings obtained from the LTS, which show CYP2E1 activity to be enhanced 420% above Ctrl baseline in MCD mice, are consistent with the findings of these authors. CYP2E1 is also involved in the microsomal pathway of ethanol metabolism, and thus, as expected, activity of this enzyme was further upregulated by ethanol consumption in the LTS (to 276% above the MCD baseline by 8% alcohol, and 281% above the MCD baseline by 20% alcohol). Because significantly higher concentrations of alcohol do not cause a proportional increase in CYP2E1 activity, however, it can be assumed that a moderate amount of alcohol is sufficient to elevate enzyme activity to maximum, steady state levels, beyond which marked increases are no longer possible. Despite its known role as a catalyst of microsomal LP, however, CYP2E1 activity did not correlate with CD ($r=0.6000$, $p=0.2417$), LOOH ($r=0.8286$, $p=0.0583$), fTBARS ($r=0.3714$, $p=0.4972$) or tTBARS ($r=0.6571$, $p=0.1750$) in the LTS.

The implications of the findings in the alcohol/MCDD interactive hepatoxicity studies can be summarised by the following conclusions:

1. The MCDD causes TG accumulation (as a result of PC deficiency) and oxidative stress due to increased LP.

2. The MCDD is associated with inflammation, comprised mainly of PMN and macrophages/Kupffer cells, the latter of which are demonstrably a source of a cytotoxic LP product, 4-HNE.
3. MCDD resulted in only mild pericellular fibrosis in zone 3. Contrary to expectation, this was not enhanced by the addition of alcohol in either the STS or LTS.
4. Alcohol consumption aggravates NAFLD, as indicated by elevated aminotransferases, increased lipid accumulation and decreased TG export. Alcohol consumption also favours enhancement of some indices of LP.

However, because minor signs of alcohol-induced hepatic damage are evident even in Ctrl animals, the levels of alcohol utilised in the STS and LTS cannot be considered "insignificant". Although metabolic differences discourage direct comparisons between the effect of alcohol consumption on rodents and humans, the results of the STS and LTS raise the possibility that so-called "insignificant" amounts of alcohol consumed by some patients with NAFLD may in fact be contributing to the liver injury that is currently designated as "non-alcoholic". However, verification of this theory will require further analyses, which would whittle down boundaries in order to establish the threshold, if one exists, at which alcoholic liver injury becomes superimposed on hepatic injury of non-alcoholic aetiology. For example, future studies could investigate the effect of very low alcohol levels on NAFLD. However, it is likely that other factors will continue to affect the way an individual reacts to alcohol in the context of NAFLD. For example, the rate of alcohol metabolism, and clearance of the toxic product aceltaldehyde, varies from individual to individual (Boggan, 2003). This may be affected by such factors as polymorphisms in the genes for alcohol dehydrogenase (ADH), which catalyses the reaction

$$CH_3CH_2OH + NAD^+ \longrightarrow CH_3CHO + NADH + H^+$$

The effects on lipid metabolism of a homeostatic imbalance introduced by excess reducing equivalents (NADH) have been previously discussed. In addition, the well-documented intolerance to alcohol in some Asian populations due to alleles of ADH2

and ADH3 that rapidly generate acetaldehyde, supports the theory that there may therefore exist no "magic number" that describes a one-size-fits-all level of alcohol consumption that is universally insignificant. In the context of NAFLD, it may be safer to diagnose "NASH" only in non-drinkers, however, this "all or nothing" proposition is both simplistic and unrealistic. The role of alcohol in NAFLD therefore requires critical scrutiny.

5. The MCDD upregulates activity of CYP2E1, and this is further enhanced by alcohol. The deleterious effects of this induction may derive from increased microsomal LP, and possibly increased ω-oxidation (catalysed by CYP2E1). This process generates dicarboxylic acids, which are toxic to mitochondria (Day and Yeaman, 1994).

TNFα is known to be play a role in the pathogenesis of ASH, and is currently believed to be pivotal in the development and progression of NASH (Tilg and Diehl, 2000). The fact that this cytokine is capable of mediating a number of the cytotoxic effects associated with fatty liver disease, supporting a pro-inflammatory cascade that enhances hepatic damage, and driving IR, appears to support this belief. However, while studies on the effect of TNFα *induction* abound, there are insufficient investigations of the effect of TNFα *abrogation* to circumstantiate the hypothesis that this cytokine is indeed critical or even essential for development of NAFLD. The aim of the TNFS was to compare progression of the rodent nutritional model of NAFLD/NASH in a setting in which TNFα regulation was "normal", versus a setting in which expression of the cytokine had been genetically abolished. This was accomplished by placing wt and TNFα ko mice on MCDD or Ctrl diets. Liver histology, serum ALT, indices of LP and CYP2E1 activity were assessed as indicators of the extent of hepatic dysfunction.

The LPSS study served as an adjunct to the TNFS, and was conducted to assess the effect of TNFα induction (due to LPS challenge) on MCDD-induced NAFLD. The effects of this induction were gauged by assessment of liver histology, measurement of serum ALT and LP. This study was also conducted to characterise inflammatory cells present during short term MCDD administration, and to compare these to those present in the LTS. Although the implications of results of the TNFS and LPSS must necessarily be brought together to form a more comprehensive picture of the role of TNFα in liver injury, direct comparisons of absolute values from both studies are discouraged. Because animals lacking TNFα are unable to mount an adequate response to infections requiring a full pro-inflammatory cytokine cascade, the TNFS was conducted in a sterile environment; water was autoclaved and chow was irradiated for all animals. The experimental diets have a high fat content: 10% by mass of the diet is corn oil. Although this oil contains a relatively high quantity of sterols and its unsaturated fatty acids are generally believed to have good oxidative stability (D. Marais, personal communication), the effects of gamma irradiation on the constituent double bounds of corn oil, and on other non-lipid components of the diet, are unknown.

Aminotransferase levels were elevated in Ctrl ko mice relative to wt counterparts, perhaps suggesting that even when they are transcriptionally silent, functional TNFα genes may be essential for homeostasis. In mice receiving the MCDD, however, ko mice had lower levels of ALT than wt, supporting the belief that TNFα may aggravate liver injury. Confirmation of this belief was obtained from the LPSS, where induction of TNFα by LPS challenge consistently increased ALT levels in both Ctrl and MCD mice.

Although steatosis still occurred in MCD mice of the TNFS, knocking out TNFα decreased absolute values of hepatic TG. Serum TG in Ctrl ko were increased to 115% of Ctrl wt (the overall baseline for the TNFS), and in MCD ko they were elevated to 104% of the value for MCD wt; this suggests that reduced hepatic lipid accumulation in ko mice may be the result

of increased hepatic TG export. The effects on TG accumulation can be explained by the effect of TNFα on lipid metabolism. 60-90min after administration of low doses of this cytokine, incorporation of glycerol into hepatic TG is increased 57%. *De novo* FA synthesis and TG export are also acutely increased (Feingold *et al.*, 1989; Feingold *et al.*, 1990). Other studies found that if TNFα was stimulated by LPS administration, serum TG levels were increased 62%, serum cholesterol increased 41%, hepatic TG was increased 2.7-fold and hepatic cholesterol was increased 8.6-fold (Memon *et al.*, 1993). At high doses of LPS, TG synthesis remains high, but clearance of TG by VLDL is decreased, further increasing hepatic TG accumulation (Feingold *et al.*, 1992).

The rapid increase in hepatic TG in response to LPS challenge described by other authors (Memon *et al.*, 1993) was not seen in the LPSS, although Ctrl mice receiving LPS did have slightly elevated levels of hepatic TG relative to saline controls. Mice receiving the MCDD and LPS had slightly lower levels of hepatic TG than MCDD mice that received saline. This may be related to the ability of excess TNFα coupled with a high fat diet to inhibit gastric clearance, leading to malabsorption of fat (Feingold *et al.*, 1990).

In human NASH, the inflammatory infiltrate consists of PMN, Kupffer cells and lymphocytes (Brunt, 2001; Lefkowitch, 2002), in contrast to the Kupffer cell rich composition of the LTS. To investigate this, immunocytochemistry was conducted on liver samples from the LPSS. This study maintained mice on Ctrl and MCDD for the same duration (4 weeks) as mice on the STS, on which the above hypothesis was based. H&E stains showed the presence of both PMN and mononuclear cells in the LPSS, thus immunocytochemistry was conducted to assess the phenotype of the mononuclear cell component. Although no CD4+ or CD8+ cells were observed, antibodies to F4/80 detected Kupffer cells in both Ctrl and MCD samples of the LPSS. In all treatment groups of the LPSS, these cells were morphologically similar to F4/80 positive cells identified in Ctrl samples of the LTS, and did not contain lipid or lipofuscin, as

seen in MCD samples in the LTS. As expected, however, the number of Kupffer cells was increased by LPS challenge.

Contrary to expectations, however, knocking out TNFα did not protect against LP. In Ctrl ko mice, CD levels were the same as in wt. However, although levels of LOOH minimal in all groups, these products were increased 200% in Ctrl ko, while fTBARS and tTBARS were elevated 964% and 208% above baseline, respectively. LP products were unilaterally increased in Ctrl ko mice, with increased generation of LOOH, fTBARS and tTBARS per nMol CD, compared to Ctrl ko. In comparison to MCD wt, MCD ko mice had elevated levels of CD (178%), LOOH (129%), fTBARS (889%) and tTBARS (392%). However, although the proportion of fTBARS and tTBARS generated per nMol of CD was also elevated in MCD ko relative to wt, the nMols of LOOH generated per nMol CD was *less* in MCD ko than wt. It is not known whether this reflects an inhibitory effect on lipooxygenases.

LPS challenge of Ctrl mice caused modest and consistent changes in absolute values of CD (120%), LOOH (113%) and fTBARS (126%), though tTBARS were strikingly elevated (319%) compared to baseline. In addition, proportion of LOOH produced per nMol of CD remained the same in Ctrl/LPS mice, while fTBARS only showed a moderate increase. The proportion of tTBARS generated per nMol CD reflected absolute values and was much higher than in Ctrl/saline mice. This data may suggest that TNFα induction generates a "controlled" peroxidative process. In MCD mice, absolute value of all LP products were also enhanced by TNFα induction, though as with Ctrl mice, the proportion all these products produced per nMol of CD was not significantly different from MCD/saline. The effect of LPS on LP has been documented (Basu and Eriksson, 2000; Bochkov *et al.*, 2002), and is believed to be due in part to LPS-induced nitric oxide synthase activity (Basu and Eriksson, 2000). It has been suggested (Bochkov *et al.*, 2002) that the enhanced LP is due to rapid oxidation of PL (in part

due to the oxidative burst), and that these oxidised PL products actually enter a feedback loop to moderate or blunt the inflammatory response to LPS, thus averting septic shock.

LP is widely considered to be a direct, deleterious consequence of TG accumulation. Although the TNFS and LPSS both documented an increase in indices of LP in fatty liver, the data suggests that a significant and direct role of TG accumulation in hepatic LP is questionable. In the TNFS, for example, ko animals consistently displayed elevated LP relative to wt counterparts, despite lower hepatic TG. In the LPSS, increased LP after LPS challenge was also not associated with a noticeable increase in hepatic TG. Furthermore, Rushmore *et al.* (1984) observed elevated CD (indicative of an imminent peroxidative process) within 1 day of feeding the MCDD, before significant TG accumulation occurs. This suggests the surprising possibility that LP in a fatty liver is not exclusively a consequence of peroxidation of accumulated TG. Clearly, however, the two processes are linked: ROS and free radicals generated during peroxisomal oxidation, and by inflammatory cells, may initiate LP in TG by attack on polyunsaturated FA side chains attached to glycerol, though lipoxygenases (which catalyse formation of LOOH) cannot (Spiteller, 2002). Since in LP it is not so much the *nature* of the initiation process that counts, this is sufficient to set in motion a chain of events that generate and further propagate LP. Polyunsaturated membrane PL in the vicinity of these LP products, which are readily accessible and highly susceptible to attack, would soon become the preferred peroxidation substrates. This two-step peroxidative process would explain the absence of a direct correlation between hepatic TG content and LP seen in our studies. The higher LP indices in ko mice could be a possible result of an undescribed role for TNFα in recruiting antioxidant defence mechanisms that normally confer some protective function on membranes against LP.

Because D/PAS positive Kupffer cells were absent in the TNFS and LPSS, the source of the late LP product, 4-HNE, during short term administration of the MCDD was investigated. Although positive staining for 4-HNE-protein adducts was not prominent in any treatment

group, hepatocytes and Kupffer cells in the sinusoids were the source of 4-HNE in the TNFS. Hepatocytes containing 4-HNE were more prominent in livers of mice receiving the MCDD, however they were also occasionally found in livers of ko and wt mice on the Ctrl diet.

There are at least two possible scenarios explaining the presence of 4-HNE in hepatocytes of the TNFS, but not LTS. Firstly, it is conceivable 4-HNE may be generated after long term administration of the MCDD from reaction of ingested, peroxidized hepatocyte membrane lipids with D/PAS Kupffer cell membranes, as well as ROS produced as a consequence of the oxidative burst. The second scenario, described below, involves the ability of Kupffer cells to metabolise 4-HNE.

The absence of 4-HNE in hepatocytes of MCD mice of the LTS may be due to the ability of hepatocytes to detoxify and metabolise this compound using alcohol dehydrogenase (ADH), aldehyde dehydrogenase (ALDH) and, especially, glutathione S-transferase (GST) enzymatic pathways (Luckey and Petersen, 2001). In response to LP, it is possible that these pathways may be upregulated in hepatocytes, leading to more efficient disposal of 4-HNE with time. Kupffer cells, however, have 45 times lower cellular glutathione levels than hepatocytes, and these levels diminish significantly after exposure to 4-HNE due to limited Kupffer cell capacity to metabolise this compound. Viewed in terms of efficiency, Kupffer cells are 100-fold less efficient than isolated hepatocytes at metabolising 4-HNE (Luckey and Petersen, 2001). Thus, it is also conceivable that the observed staining in the LTS is the result of prolonged build-up of this compound in Kupffer cells.

With regard to CYP2E1, the interesting finding in this project was the unexpected relationship between this enzyme and TNFα. As discussed, CYP2E1 is upregulated in human NAFLD/NASH, which is also associated with increased levels of TNFα. The motivation for measurement of CYP2E1 activity in the TNFS was the hypothesis that abolition of TNFα

would mitigate features of hepatic injury, and it was expected that this could be reflected in terms of reduced CYP2E1 activity. However, knocking out TNFα *increased* CYP2E1 activity. This may correlate with the finding that TNFα ko mice also have elevated levels of hepatic LP in the MCD model of NASH. Although the exact reasons for the elevated CYP2E1 activity in TNFα ko mice are currently unclear, a recent study of Fao rat hepatoma cells (which constitutively express CYP2E1) suggests that proinflammatory cytokines (IL1β, IL-6 and TNFα) have a rapid (within 24h) and strong inhibitory effect on CYP2E1 transcription. Levels of CYP2E1 protein are also decreased, however this effect is not observed until 72h after cytokine administration (Hakkola *et al.*, 2003). Whether this is relevant in the MCD model is not known, and investigations of CYP2E1 activity were not conducted on the LPSS. This was due to the preconceived misconception at the start of this study that TNFα was pivotal in liver injury, and that therefore TNFα induction would simply enhance all markers and contributors to liver injury, including CYP2E1. However, the results of the TNFS study clearly challenge this hypothesis, and the effects of LPS on CYP2E1 are in fact extensively documented in the literature (Saitoh *et al.*, 1999; Renton and Nicholson, 2000; Cheng *et al.*, 2003). A recent report documented downregulation of CYP2E1 transcriptional activity in rats to 10% of controls after LPS administration (Cheng *et al.*, 2003). LPS injection into the lateral ventricle was also accompanied by loss of CYP2E1 activity in an earlier study (Renton and Nicholson, 2000). Due to various constraints, it is not possible at this time to investigate CYP2E1 activity in an LPSS, however it is presumed that if conducted, future analyses will corroborate the findings of Cheng *et al.* (2003).

Serum TNFα could not be detected in the LPSS because samples were too dilute, however TNFα upregulation is a well known consequence of LPS challenge, and is in fact responsible for many of the negative effects of LPS (Raeburn *et al.*, 2002; Ulmer *et al.*, 2002). In a study using rats, TNFα was elevated as a result of the MCDD, and further increased after LPS administration (Chawla *et al.*, 1998). In another study on rats receiving the MCDD and LPS,

administration of exogenous *S*-adenosylmethionine (adomet, a necessary metabolic intermediate in the transsulfuration pathway which is formed from methionine and ATP in a reaction catalysed by methionine adenosyltransferase) attenuated LPS-induced TNFα expression and mitigated LPS-induced liver injury (Watson *et al.*, 1999).

In conclusion, the findings of both the TNFS and LPSS suggest the following:

1. TNFα exacerbates liver injury in the rodent nutritional model of NAFLD. However, because liver injury still occurs in the absence of this cytokine, it is neither pivotal nor essential for development or progression of NAFLD. Furthermore, the role of TNFα in liver disease is likely to be highly complex, and it may even be required for moderation, as well as controlled induction of, LP.
2. Although TNFα and CYP2E1 have both been implicated in the pathogenesis of NASH, TNFα expression downregulates CYP2E1 activity. The complex and seemingly paradoxical relationship between this cytokine and enzyme merit further investigation.
3. LP, which is commonly believed to be a direct consequence of peroxidation of TG in fatty liver, is the result of more complex interactions that are possibly only initiated by hepatocellular lipid accumulation. Furthermore, the cell types responsible for generation of certain LP products, such as 4-HNE, may vary with time and/or severity of disease.

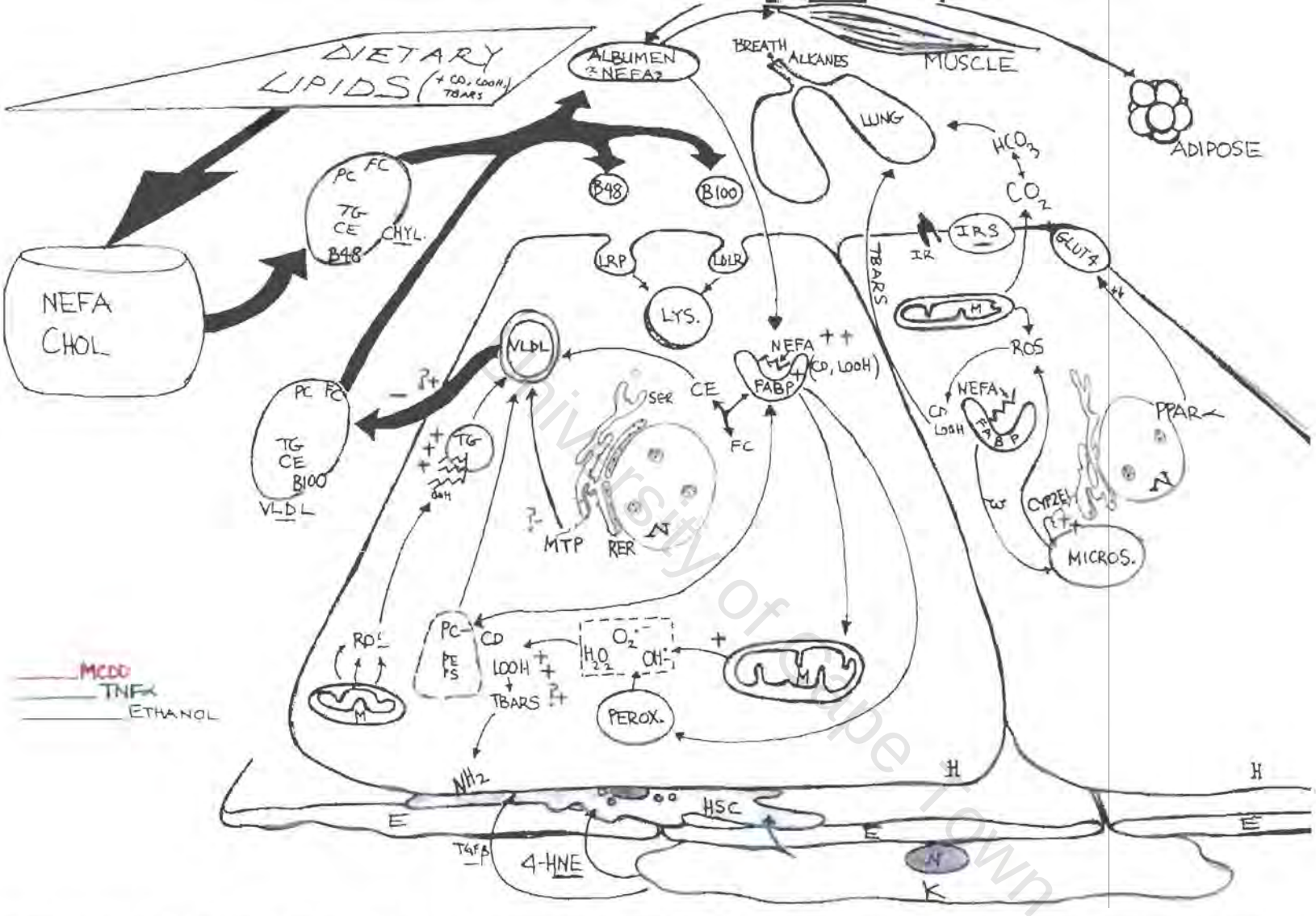

Figure 6.1: Simplified schematic diagram of the interplay of pathogenic mechanisms in NAFLD. The effects of MCDD, TNFα and ethanol, as suggested by data in this project, are indicated. **CE:** Cholesterol ester; **Chol.:** Cholesterol; **E:** Endothelial cells; **FABP:** Fatty acid binding protein; **FC:** Free cholesterol; **H:** Hepatocytes; **HSC:** Hepatic stellate cell; **IR:** Insulin receptor; **IRS:** Insulin receptor substrate; **K:** Kupffer cell; **LDLR:** Low density lipoprotein receptor; **Lys.:** Lysosome; **M:** Mitochondria; **Micros:** Microsome; **MTP:** Mitochondrial triglyceride transfer protein; **N:** Nuclei; **NEFA:** Non-esterified fatty acids; **PE:** Phosphatidylethanolamine; **PS:** Phosphatidylserine; **RER:** Rough endoplasmic reticulum; **SER:** Smooth endoplasmic reticulum; **ω:** ω-oxidation.
Diagram adapted and modified with permission from a diagram by D. Marais. Information represented encompasses both data from existing literature, and from this project.

Concluding remarks

There was a time when fatty liver was overlooked as an insignificant finding with "benign" outcome. However, since the landmark paper by Ludwig *et al.*(1980) circumscribed the constellation of findings (macrovesicular steatosis, lobular necroinflammation, and even Mallory bodies) under the name "nonalcoholic steatohepatits", and linked them to metabolic disturbances in nondrinkers such as obesity and diabetes mellitus II, NASH has come to hold a place of prominence. This has been aided by the understanding that, while extensive and nonprogressive fatty liver may and does exist for long periods, for example in kwashiorkor (Day and Yeaman, 1994), steatosis with inflammation (steatohepatitis) can lead to development of advanced pathology, and progress to fibrosis, cirrhosis, liver failure and even hepatocellular carcinoma. NAFLD/NASH can no longer constitute an obscure finding, but a potentially serious form of chronic liver disease which now ranks among the most common liver-related conditions in the world.

The exact reasons determining disease progression are not clearly understood, however a "two hit" hypothesis has been proposed (Day and James, 1998). According to this model, steatosis (the first "hit") renders a liver vulnerable to the effects of second "hits" such as enhanced LP and oxidative stress, upregulation of and/or increased sensitivity to TNFα, progressive IR, and other factors associated with lipotoxicity, all of which drive hepatic dysfunction. The results of this project also strongly suggest that consumption of even low levels of alcohol could contribute to further liver injury, and should thus be discouraged in patients with NASH.

Numerous animal models, as well as some human studies, have attempted to understand what appears to be an increasingly complex picture of the pathogenic mechanisms of NASH. Although these investigations have identified a number of factors, many of which are associated with control of lipid metabolism, insulin action and immunomodulation, a concise

pathogenic model for NASH is still lacking. Indeed, what has emerged so far resembles more a tangle of intriguing and sometimes contradictory information.

As a case in point, TNFα was, until recently, considered by some parties to be a pivotal player in the development of NASH. However, the findings in this project suggest that, while TNFα is important in development of liver injury, its role is neither vital nor unique. A recent study of NASH patients also revealed no TNFα (Perrella *et al.*, 2003), in contrast to other studies where significant upregulation of this cytokine was associated with NASH (Crespo *et al.*, 2001; Wigg *et al.*, 2001; Kugelmas *et al.*, 2003).

Much remains to be clarified about the true meaning of, and mechanisms driving the pathogenesis of, NASH. Such an understanding will be instrumental for development of safe and effective treatment options. It may well be that in the future, the term NASH will be essentially abandoned for the more appropriate term "NAFLD", which represents a more comprehensive description encompassing the spectrum from fatty liver alone to NASH with fibrosis/cirrhosis (Matteoni *et al.*, 1999). It is also possible that NASH/NAFLD may ultimately be inadequate to describe a single, universal entity, but rather is the end result of many potential initiating and interacting causes. In the same vein, the pathogenic mechanisms at play in each "subtype" of NAFLD would then come to reflect the initiating causes or "hits", with diagnosis (1) based on correlation of laboratory and histopathological findings with the accepted standards for NAFLD, and (2) an account of the relevant factors suspected to be responsible for disease initiation and progression. Treatment would then be tailored to counteract these factors.

Although no type of liver injury may necessarily be summarised by a simple formula such that Factor A + Factor B always equals Factor C, the scenario described above would explain

the disparate findings from different studies, and may help clinicians provide more suitable treatment options for affected patients.

Future work will hopefully establish the following

1. A better animal model of NAFLD/NASH, possessing more key features relevant to human NASH.
2. The role of alcohol, and the stage at which it exerts an effect on fatty liver disease of supposedly non-alcoholic aetiology.
3. The level of LP occurring *in vivo*, the lipid subclasses (TG and/or PL) affected, and negative and/or positive effects of this process.
4. The role of TNFα, and the validity of treating certain "types" of NASH/NAFLD with antibodies to TNFα.
5. The role of CYP2E1 and its relationship to TNFα in pathogenesis of NAFLD/NASH.
6. The role of isotypes of PPAR.
7. The role of leptin: Leptin expression is increased in the obese NASH patient; however, although studies of rodents lacking functional leptin expression or signalling indicate that it is *essential* for development of fibrosis (suggesting for a moment that this may be the critical "missing link" explaining progressive liver disease), leptin expression does not in fact correlate with fibrotic severity in humans (Chitturi *et al.*, 2002). To further confound the investigator, leptin, which is also induced by TNFα, is also now believed to exert protective effects against TNFα-mediated toxicity (Takahashi *et al.*, 1999)! The complex roles of leptin (both beneficial and detrimental) remain to be elucidated.
8. The role of transcription factors: Nuclear factor kappa beta (NFκβ). Because of its antiapoptotic effects, this transcription factor enjoyed a moment in the limelight when it was considered a possible key to the toxic effects of TNFα (Tilg and Diehl, 2000). According to a version of the "two hit" hypothesis in which the role of TNFα is considered central (Tilg and Diehl, 2000), hepatocytes become sensitised to the effects of

TNFα during the progression of liver disease as a result of "hits" such as loss of NFκβ induction or activity. Thus, in chronic liver disease, hepatocytes react adversely to levels of TNFα that would encourage proliferation rather than cell death in healthy parenchymal cells (Tilg and Diehl, 2000). Although this theory is tempting and elegantly simple, subsequent investigations in *ob/ob* mice indicated that fatty liver remained vulnerable to damage despite NFκβ induction (Yang *et al.*, 2001). Furthermore, NFκβ has now emerged as a transcription factor which is silent in healthy HSC but active when these cell types become non-quiescent (Mann and Smart, 2002), perhaps suggesting a role in fibrosis.

Finally, it is important to bear in mind that NASH is in many ways a disease of affluence. It is therefore essential, above all, to devote efforts not just to finding pharmacological or invasive solutions to this disease, but to drawing the attention of consumers and patients, in these days of excess, to the benefits of healthy lifestyle habits and exercise.

Bibliography

Angulo P. 2002a. "Nonalcoholic fatty liver disease." *N. Engl. J. Med* **346(16):** 1221-1231.

Angulo P. 2002b. "Treatment of nonalcoholic fatty liver disease." *Annals Hepatol.* **1(1):** 12-19.

Angulo P., Keach J.C., Batts K.P., Lindor K.D. 1999. "Independent predictors of liver fibrosis in patients with nonalcoholic steatohepatitis." *Hepatology* **30:** 1356-1362.

Aranda A., Pascual A. 2001. "Nuclear hormone receptors and gene expression." *Physiol. Rev.* **81:** 1269-1304.

Asakawa T., Matsushita S. 1979. "Colouring conditions of thiobarbituric acid test for detecting lipid hydroperoxides." *Lipids* **15(3):** 137-140.

Ayata G., Gordon F.D., Lewis W.D., Pomfret E., Pompselli J.J., Jenkins R.L., Khettry U. 2002. "Cryptogenic cirrhosis: Clinicopathologic findings at and after liver transplantation." *Hum. Pathol.***33:** 1098-1104.

Bacon B.R., Farahvash M.J., Janney C.G., Neuschwander-Tetri B.A. 1994. "Nonalcoholic steatohepatitis: an expanded clinical entity." *Gastroenterology* **107:** 1103-1109.

Bao L., Zhu Y., Elhassan A.M., Wu Q., Xiao B., Zhu J., Lindgren J.U. 2001. "Adjuvant-induced arthritis: IL-1, IL-6 and TNFα are upregulated in spinal cord." *Neuroreport* **12(18):** 3905-3908.

Barzilai N. 2002. "Insulin resistance and the adipose tissue." *Proceedings of the Clinical Research Single Topic Conference, Atlanta.* Pp 26-28.

Basu S., Eriksson M. 2000. "Lipid peroxidation induced by an early inflammatory response in endotoxaemia." *Acta Anaesthesiol. Scand.* **44(1):** 17-23.

Bedossa P., Houglum K., Trautwein C, Holstege A., Chojkier M. 1994. "Stimulation of collagen α_1 (I) gene expression is associated with lipid peroxidation in hepatocellular injury: a link to tissue fibrosis?" *Hepatology* **19:** 1262-1271.

Bernard S., Touzet S., Personne I., Lapras V., Bondon P.J., Berthezene F., Moulin P. 2000. "Association between microsomal triglyceride transfer protein gene polymorphism and the biological features of liver steatosis in patients with type II diabetes." *Diabetologia* **43(8):** 995-999.

Black S.D., Coon M.J. 1987. "P-450 cytochromes: Structure and function." *Adv. Enzymol.* **60:** 35-87.

Bligh E.G., Dyer J. 1959. "A rapid method of total lipid extraction and purification." *Can. J Biochem.* **31:** 911-917.

Bochkov V.N., Kadl A., Huber J., Gruber F., Binder B.R., Leitinger N. 2002. "Protective role of phospholipid oxidation products in endotoxin-induced tissue damage." *Nature* **419:** 77-81.

Boggan B. 2003. "Alcohol, chemistry and you: Metabolism of ethyl alcohol in the body." Retrieved October, 2003 from `http://chemcases.com/alcohol/alc-06.htm`.

Boulangé A., Planche E., de Gasquet P. 1979. "Onset of genetic obesity in the absence of hyperphagia during the first week of life in the Zucker rat (*fa/fa*)." *J. Lip. Res.* **20:** 857-864.

Bowie A.G., Moynagh P.N., O'Neill L.A. 1997. "Lipid peroxidation is involved in the activation of NF-Kappa beta by tumor necrosis factor but not interleukin-1 in the human endothelial cell line ECV304. Lack of involvement of H_2O_2 in NF-Kappa beta activation by either cytokine in primary and transformed endothelial cells." *J Biol Chem.* **272(41):** 25941-25950.

Brunt E.M. 2001. "Nonalcoholic steatohepatitis: Definition and pathology." *Sem. Liv. Dis.* **21:** 3-16.

Brunt E.M. 2002. "Pathology of non-alcoholic steatohepatitis." *Proceedings of the Clinical Research Single Topic Conference, Atlanta.* Pp 2-10.

Brunt E.M., Janney C.G., di Bisceglie A.M., Neuschwander-Tetri B.A., Bacon B.R. 1999. "Nonalcoholic steatohepatitis: A proposal for grading and staging the histological lesions." *Am. J. Gastroenterol.* **94(9):** 2467-2474.

Bugianesi E., Leone N., Vanni E., Marchesini G., Brunello F., Carucci P., Musso A., de Paolis P., Capussotti L., Salizzoni M., Rizzetto M. 2002. "Expanding the natural history of nonalcoholic steatohepatitis: from cryptogenic cirrhosis to hepatocellular carcinoma." *Gastroenterology.* **123:** 134-140.

Burt A.D., Mutton A., Day C. 1998. "Diagnosis and interpretation of steatosis and steatohepatitis." *Sem. Diagn. Pathol.* **15:** 246-258.

Caldwell S.H., Swerdlow R.H., Khan E.M., Iezzoni J.C., Hespenheide E.E., Parks J.E., Parker W.D. 1999. "Mitochondrial abnormalities in nonalcoholic steatohepatitis." *J. Hepatol.* **31:** 430-434.

Caldwell, S.H. 2002. "The mitochondria in NAFLD/NASH." *Proceedings of the Clinical Research Single Topic Conference, Atlanta.* Pp 86-94.

Casini A. 2002. "Alcohol-induced fatty liver and inflammation: where do kupffer cells act?" *J. Hepatol.* **32:** 1026-1030.

Chalasani N., Deeg M.A., Persohn S., Crabb D.W. 2003. "Metabolic and anthropometric evaluation of insulin resistance in nondiabetic patients with nonalcoholic steatohepatitis." *Am. J. Gastroenterol.* **98(8):** 1849-1855.

Charlton M., Sreekumar R., Rasmussen D., Lindor K., Nair K.S. 2002. "Apoliprotein synthesis in nonalcoholic steatohepatitis." *Hepatology* **35:** 898-904.

Chawla R.K., Watson W.H., Eastin C.E., Lee E.Y., Schmidt J., McClain C.J. 1998. "*S*-adenosylmethionine deficiency and TNFα in lipopolysaccharide-induced hepatic injury." *Am. J Physiol. Gastrointest. Liver Physiol.* **38:** G125-129.

Cheng P.Y., Wang M., Morgan E.T. 2003. "Rapid transcriptional suppression of rat cytochrome P450 genes by endotoxin treatment, and its inhibition by curcumin." *J. Pharmacol. Exp. Ther.* **307(3):** 1205-1212.

Cheung AT, Ree D, Kolls JK, Fuselier J, Coy DH, Bryer-Ash M. 1998. "An in vivo model for elucidation of the mechanism of tumor necrosis factor-alpha (TNF-alpha)-induced insulin

resistance: evidence for differential regulation of insulin signaling by TNF-alpha." *Endocrinology* **139(12):** 4928-4935.

Chitturi S., Farrell G., Frost L., Kriketos A., Lin R., Liddle C., Samarasinghe D., George J. 2002. "Serum leptin in NASH correlates with hepatic steatosis but not fibrosis: A manifestation of lipotoxicity?" *Hepatology* **36:** 403-409.

Chitturi S., Farrell G.C. 2001. "Etiopathogenesis of nonalcoholic steatohepatitis." *Sem. Liv. Dis.* **21(1):** 27-41.

Chitturi S., Weltman M., Farrell G.C., McDonald D., Liddle C., Samarasinghe D., Lin R., Abeygunasekera S., George J. 2002. "HFE mutations, hepatic iron, and fibrosis: Ethnic-specific association of NASH with C282Y but no association with fibrotic severity." *Hepatology* **36(1):** 142-149.

Cigolini M., Targher O., Agostino G., Tonoli M., Muggeo M., De Sandre O. 1996. "Liver steatosis and its relation to plasma haemostatic factors in apparently healthy men. Role of the metabolic syndrome." *Thromb. Haemost.* **76:** 69-73.

Clarke S.D. 2001. "Nonalcoholic steatosis and steatohepatitis I. Molecular mechanism for polyunsaturated fatty acid regulation of gene transcription." *Am. J. Physiol. Gastrointest. Liver Physiol.* **281:** G865-869.

Coligan J.E., Kruisbeek A., Margulies D.H., Shecach E.M., Strober W. 1994. "Current protocols in Immunology, Volume 1." Wiley Interscience.

Cortez-Pinto H., Diehl A.M. 2002. "ATP homeostasis and MR spectroscopy in NASH." *Proceedings of the Clinical Research Single Topic Conference, Atlanta.* Pp 46-53.

Costet P., Legendre C., Moore J., Edgar A., Galtier P., Pineau T. 1998. "Peroxisome proliferator-activated receptor alpha-isoform deficiency leads to progressive dyslipidemia with sexually dimorphic obesity and steatosis." *J. Biol. Chem.* **273:** 29577-29585.

Crespo J., Cayón A., Fernández-Gil P., Hernández-Guerra M., Mayorga M., Domínguez-Díez A., Fernández-Escalante J.C., Pons-Romero F. 2001. "Gene expression of tumor necrosis factor α and TNF-receptors, p55 and p75, in nonalcoholic steatohepatitis patients." *Hepatology* **34:** 1158-1163.

Day C.P. 2002a. "Pathogenesis of steatohepatitis." *Best Prac. Res. Clin. Gastroenterol.* **16(5):** 663-678.

Day C.P. 2002b. "Genetic polymorphisms and susceptibility to liver inflammation in NASH and related diseases." *Proceedings of the Clinical Research Single Topic Conference, Atlanta.* Pp 77-85.

Day C.P. 2002c. "Non-alcoholic steatohepatitis (NASH): where are we now and where are we going?" *Gut.* **50:** 585-588.

Day C.P., James O.F.W. 1998. "Steatohepatitis: a tale of two 'hits'?" *Gastroenterology* **114(4):** 842-845.

Day C.P., Yeaman S.J. 1994. "The biochemistry of alcohol-induced fatty liver." *Bioch. Biophys. Acta* **1215:** 33-48.

Diehl A.M. 2002. "Nonalcoholic liver disease lessons from animal models." *Proceedings of the Clinical Research Single Topic Conference, Atlanta.* Pp 64-68.

Diehl A.M. 2002. "Nonalcoholic steatosis and seatohepatitis IV. Nonalcoholic fatty liver disease abnormalities in macrophage function and cytokines." *Am. J. Physiol. Gastrointest. Liver Physiol.* **282:** G1-G5.

Dixon J.B., Bhathal P.S., O'Brien P.E. 2003. "Problems with NASH? HAIR is some help." *Am. J. Gastroenterol.* **98(2):** 500.

Doldi S.B. 1998. "Surgery of morbid obesity: intestinal bypass to adjustable gastric banding." *Ann. Chir.* **52(2):** 125-131.

Donato M.T., Castell J.V., Gómez-Lechón M.J. 1999. "Characterization of drug metabolizing activities in pig hepatocytes for use in bioartificial liver devices: comparison with other hepatic cellular models." *J. Hepatol.* **31:** 542-549.

Eaton S., Record C.O., Bartlett K. 1997. "Multiple biochemical effects in the pathogenesis of alcoholic fatty liver." *Eur. J. Clin. Invest.* **27:** 719-722.

Emery M.G., Fisher J.M., Chien J.Y., Kharasch E.D., Dellinger E.P., Kowdley K.V., Thummel K.E. 2003. "CYP2E1 activity before and after weight loss in morbidly obese subjects with nonalcoholic fatty liver disease." *Hepatology* **38:** 428-435.

Fargion S., Mattioli M., Francanzani A.L., Sampietro M., Tavazzi D., Fociani P., Taioli E., Valenti L., Fiorelli G. 2001. "Hyperferriteinemia, iron overload, and multiple metabolic alterations identify patients at risk for nonalcoholic steatohepatitis." *Am. J. Gastroenterol.* **96(8):** 2448-2455.

Farrell G.C., Phung N., Ip E., de la Peña A., Robertson G., Pera N., George J., Leclercq I. 2002. "Sources of oxidant stress in fatty liver disorders. Interactive mechanisms, and relevance to fibrosing steatohepatitis." *Proceedings of the Clinical Research Single Topic Conference, Atlanta.* Pp 69-76.

Feingold K.R., Serio M.K., Adi S., Moser A.H., Grunfeld C. 1989. "Tumor necrosis factor stimulates hepatic lipid synthesis and secretion." *Endocrinology* **124(5):** 2336-2342.

Feingold K.R., Soued M., Serio M.K., Adi S., Mser A.H., Grunfeld C. 1990. "The effect of diet on tumor necrosis factor stimulation of hepatic lipogenesis." *Metabolism* **39(6):** 623-632.

Feingold K.R., Staprans I., Memon R.A., Moser A.H., Shigenaga J.K., Doerrler W., Dinarelloo C.A., Grunfeld C. 1992. "Endotoxin rapidly induces changes in lipid metabolism that produce hypertriglyceridemia: Low doses stimulate hepatic triglyceride production while high doses inhibit clearance." *J. Lipid Research.* **33:** 1765-1776.

Fernández-Real J-M., Ricart-Engel W., Arroyo E., Blança R., Casamitjana-Abella R., Cabrero D., Fernández-Castañer M. Soler J. 1998. "Serum ferritin as a component of the insulin resistance syndrome." *Diabetes Care* **21(1):** 62-68.

Folch J., Lees M., Sloane-Stanley G.A. 1957. "A simple method for the isolation and purification of total lipids from animal tissues." *J. Biol. Chem.* **226:** 497-509.

Friedman J.M., Halaas J.L. 1998. "Leptin and the regulation of body weight in mamals." *Nature* **395:** 763-770.

Friedman S.L. 1993. "The cellular basis of hepatic fibrosis." *N. Engl. J. Med.* **328(25):** 1828-1835.

Friedman S.L. 2003. "Liver fibrosis – from bench to bedside." *J. Hepatol.* **38:** S38-S53.

Garcia-Monzon C., Martin-Perez E., Iacono O.L., Fernandez Bermejo M., Majano P.L., Apolinario A., Larranga E., Moreno-Otero R. 2000. "Characterization of pathogenic and prognostic factors of nonalcoholic steatohepatitis associated with obesity." *J. Hepatol.* **33:** 716-724.

Garg A., Misra A. 2002. "Hepatic steatosis, insulin resistance and adipose tissue disorders." *Proceedings of the Clinical Research Single Topic Conference, Atlanta.* Pp 35-39.

George D.K., Goldwurm S., Macdonald G.A., Cowley L.L., Walker N.I., Ward P.J., Jazwinska E.C., Powell L.W.. 1998. "Increased hepatic iron concentration in nonalcoholic steatohepatitis is associated with increased fibrosis." *Gastroenterology* **114:** 311-318.

Gholam P.M., Kotler D.P., Flancbaum L.J. 2002. "Liver pathology in morbidly obese patients unergoing Roux-en-Y gastric bypass surgery." *Obes. Surg.* **12(1):** 49-51.

Ghoshal A.K., Ahluwalia M., Farber E. 1983. "The rapid induction of liver cell death in rats fed a choline-deficient methionine-low diet." *Am. J. Pathol.* **113:** 309-314.

Ghoshal A.K., Farber E. 1993. "Choline deficiency, lipotrope deficiency and the development of liver disease including liver cancer: A new perspective." *Lab. Invest.* **68(3):** 255-260.

Gurr M.I., Harwood J.L. 1991. "Lipid biochemistry: An introduction." 4th Edition, St Edmundsbury Press.

Hakkola J., Hu Y., Ingelman-Sundberg M. 2003. "Mechanisms of down-regulation of CYP2E1 expression by inflammatory cytokines in rat hepatoma cells." *J. Pharmacol. Exp. Ther.* **304(3):** 1048-1054.

Harrison S.A., Diehl A.M. 2002. "Fat and the liver – A molecular overview." *Sem. Gastrointest. Dis.* **13(1):** 3-16.

Harrison S.A., Kadakia S., Lang K.A., Schenker S. 2002. "Nonalcoholic steatohepatitis: what we know in the new millenium." *Am. J. Gastroenterol.* **97(11):** 2714-2724.

Ikejima K., Honda H., Yoshikawa M., Hirose M., Kitamura T., Takei Y., Sato N. 2001. "Leptin augments inflammatory and profibrogenic responses in the murine liver induced by hepatotoxic chemicals." *Hepatology* **34:** 288-297.

Imai Y., Ito A., Sato R. 1966. "Evidence for biochemically different types of vesicles in the hepatic microsomal fraction." *J. Biochem* (Tokyo) **60(4):** 417-428.

Ip E., Farrell G.C., Robertson G., Hall P., Kirsch R., Leclercq I. 2003. "Central role of PPARα-dependent hepatic lipid turnover in dietary steatohepatitis in mice." *Hepatology* **38:** 123-132.

Itoh S. Yogel T., Kawagoe K. 1987. "Comparison between nonalcoholic steatohepatitis and alcoholic hepatitis." *Am. J. Gastroenterol.* **82:** 650-654.

James O.F.W., Day C.P. 1998. "Nonalcoholic steatohepatitis (NASH): a disease of emerging identity and importance." *J. Hepatol.* **29:** 495-501.

Järveläinen H.A., Fang C., Ingelman-Sundberg M., Lukkari T.A., Sippel H., Lindros K.O. 2000. "Kupffer cell inactivation alleviates ethanol-induced steatosis and CYP2E1 induction but not inflammatory responses in rat liver." *J. Hepatol.* **32:** 900-910.

Jiang G., Dallas-Yang Q., Biswas S., Li Z., Zhang B.B. 2004. "Rosiglitazone, an agonist of peroxisomal proliferator activated receptor gamma (PPAR gamma), reduces inhibitory serine phosphorylation of IRS1 in vitro and in vivo." *Biochem J* **377(2):** 339-346.

Jiang Z., Hunt J.V., Wolff S.P. 1992. "Ferrous ion oxidation in the presence of xylenol orange for detection of lipid hydroperoxide in low density lipoprotein." *Anal. Biochem.* **202:** 384-389.

Jiang Z., Wollard A.C.S., Wolff S.P. 1991. "Lipid hydroperoxide measurement by oxidation of Fe^{++} in the presence of xylenol orange. Comparison with the TBA assay and iodometric method." *Lipids* **26:** 853-856.

Kersten, S. 2002. "Peroxisome proliferator activated receptors and obesity." *Eur. J. Pharmacol.* **440:** 223-234.

Khan B., Flier J.S. 2000. "Obesity and insulin resistance." *J. Clin. Invest.* **106(4):** 473-481.

Kim H., Haluzik M., Asghar Z., Yau D., Joseph J.W., Fernandez A.M., Reitman M.L., Yakar S., Stunnard B., Milhavet L., Wheeler M.B., Le Roith D. 2003. "Peroxisome proliferator-activated receptor α agonist treatment in a transgenic model of type 2 diabetes reverses the lipotoxic state and improves glucose homeostasis." *Diabetes* **52:** 1770-1778.

Kim J.H., Taylor P.N., Young D., Karst S.Y., Nishina, Naggert J.K. 2003. "New leptin receptor mutations n mice: $Lepr^{db\text{-}rtmd}$, $Lepr^{db\text{-}dmpg}$, $Lepr^{db\text{-}rlpy}$." *J. Nutr.* **133:** 1265-1271.

Kirsch R., Clarkson V., Shephard E.G., Marais A.D., Jaffer M.A., Woodburne V.E., Kirsch R.E., Hall P. de la M. 2003. "Rodent nutritional model of non-alcoholic steatohepatitis: Species, strain and sex difference studies." *J. Gastroenterol. Hepatol.* **18(11):** 1272-1282.

Knight J.A., Pieper R.K., McClellan L. 1988. "Specificity of the thiobarbituric acid reaction: It use in studies of lipid peroxidation." *Clin. Chem.* **34(12):** 2433-2438.

Knobler H., Schattner A., Zhornicki T., Malnick S.D.H., Keter D., Sokolovskaya N., Lurie Y., Bass D.D. 1999. "Fatty liver — an additional and treatable feature of the insulin resistance syndrome." *Q. J. Med.* **92:** 73-79.

Koetish A., Diehl A.M. 2002. "Animal models of steatohepatitis." *Best Prac. Res. Clin. Gastroenterol.* **16(5):** 679-690.

Koop D.R., Tierney D.J. 1990. "Multiple mechanisms in the regulation of ethanol-inducible cytochrome P450IIE1". *Bioessays* **12(9):** 429-435.

Koruk M., Savas M.C., Yilmaz O., Taysi S., Karakok M., Gundogdu C., Yilmaz A. 2003. "Serum lipids, lipoproteins and apoliproteins levels in patients with nonalcoholic steatohepatitis." *J. Clin. Gastroenterol.* **37(2):** 177-182.

Kugelmas M., Hill D.B., Vivian B., Marsano L., McClain C.J. 2003. "Cytokines and NASH: A pilot study of the effects of lifestyle modification and vitamin E." *Hepatology* **38:** 413-419.

Langman G., Hall de la M P., Todd G. 2001. "Role of nonalcoholic steatohepatitis in methotrexate-induced liver injury." *J. Gastroenterol. Hepatol.* **16:** 1395-1401.

Laurin J. 2002. "Motion – All patients with NASH need to have a liver biopsy: Arguments against the motion." *Can. J. Gastroenterol.* **16(10):** 722-726.

Lavine J.E. 2002. "Paediatric aspects of NASH." *Proceedings of the Clinical Research Single Topic Conference, Atlanta.* Pp 20-23.

Le Roith D., Zick Y. 2001. "Recent advances in our understanding of insulin action and insulin resistance." *Diabetes Care* **24(3):** 588-597.

Lean M.E.J., Han T.S., Morrison C.E. 1995. "Waist circumference as a measure for indicating need for weight management." *Br. Med. J.* **311:** 158-161.

Leclercq I.A., Farrell G.C., Field J., Cell D.R., Gonzalez F.J., Robertson G.R. 2000. "CYP2E1 and CYP4A as microsomal catalysts of lipid peroxides in murine nonalcoholic steatohepatitis." *J. Clin. Invest.* **105:** 1067-1075.

Leclercq I.A., Farrell G.C., Schriemer R., Robertson G.R. 2002. "Leptin is essential for the hepatic fibrogenic response to chronic liver injury." *J.Hepatol.* **37:** 206-213.

Lee G.H., Proenca R., Montez J.M., Carroll K.M., Darvishzadeh J.G., Lee J.I., Friedman J.H. 1996. "Abnormal splicing of the leptin receptor in diabetic mice." *Nature* **379:** 632-635.

Lee Y., Wang M-Y., Kakuma T.,Wang Z-W., Babcock E., McCorkle K., Higa M., Zhou Y.T., Unger R.H. 2001. "Liporegulation in diet-induced obesity." *J. Biol. Chem.* **276(8):** 5629-5635.

Lefkowitch J.H, Haythe J.H., Regent N. 2002. "Kupffer cell aggregation and perivenular distribution in steatohepatitis." *Mod. Pathol.* **15(7):** 699-704.

Leist M., Gantner F., Bohlinger I., Germann P.G., Tiegs G., Wendel A. 1994. "Murine hepatocyte apoptosis induced *in vitro* and *in vivo* by TNFα requires transcriptional arrest." *J. Immunol.* **153:** 1778-1788.

Lettéron P., Fromenty B., Terris B., Degott C., Pessayre D. 1996. "Acute and chronic hepatic steatosis lead to *in vivo* lipid peroxidation in mice." *J. Hepatol.* **24:** 200-208.

Li Z., Hin H., Yang S., Diehl A.M. 2002. "Murine leptin deficiency alters kupffer cell production of cytokines that regulate the innate immune system." *Gastroenterology* **123:** 1304-1310.

Li Z., Yang S., Lin H., Huang J., Watkins P.A., Moser A.B., Desimone C. Song X.Y., Diehl A.M. 2003. "Probiotics and antibodies to TNF inhibit inflammatory activity and improve non-alcoholic fatty liver disease." *Hepatology* **37:** 343-350.

Lieber C.S. 2002. "S-Adenosyl-L-methionine: its role in the reatment of liver disorders." *Am. J.Clin. Nutr.* **76(Suppl):** 1183S-1187S.

Lieber C.S., Packer L. 2002. "S-Adenosylmethionine: molecular, biological, and clinical aspects – an introduction." *Am. J. Clin. Nutr.* **76(Suppl):** 1148S-1150S.

Lin H.Z., Yang S.Q., Chuckaree C., Kuhajda F., Ronnet G., Diehl A.M. 2000. "Metformin reverses fatty liver disease in obese, leptin-deficient mice." *Nat. Med.* **6(8):** 998-1003.

Loffreda S., Yang S.Q., Lin H.Z., Karp C.L., Bergman M.L., Wang D.J., Klein A.S., Bulkley G.B., Bao C., Noble P.W., Lane M.D., Diehl A.M. 1998. "Leptin regulates proinflammatory immune responses." *FASEB J.* **12:** 57-65.

Lonardo A. 1999. "Fatty liver and nonalcoholic steatohepatitis. Where do we stand and where are we going?" *Dig. Dis.* **17(2):** 80-89.

Lowry O.H., Rosebrough A.J., Farr A., Randall R.J. 1951. "Protein measurement with the folin phenol reagent." *J. Biol. Chem.* **193:** 265-275.

Luckey S.W., Petersen D.R. 2001. "Metabolism of 4-hydroxynonenal by rat kupffer cells." *Arch. Bioch. Biophys.* **389(1):** 77-83.

Ludwig J., McGill D.B., Lindor K.D. 1997. "Metabolic liver diseases. Review: Nonalcoholic steatohepatitis." *J. Gastroenterol. Hepatol.* **12:** 398-405.

Ludwig J., Viggiano T.R., McGill D.B., Ott B.J. 1980. "Mayo clinic experiences with a hitherto unnamed disease." *Mayo Clin. Proc.* **55:** 434-438.

Luyckx F.H., Desaive C., Thiry A. Dewe W., Scheen A.J., Gielen J.E., Lefebvre P.J. 1998. "Liver abnormalities in severely obese subjects: effect of drastic weight loss after gastroplasty." *Int. J Obes. Relat. Metab. Disord.* **22(3):** 222-226.

Luyckx F.H., Lefebvre P.J., Scheen A.J. 2000. "Nonalcoholic steatohepatitis: association with obesity and insulin resistance, and influence of weight loss." *Diabetes Metab.* **26(2):** 98-106.

Mach T. 2000. "Fatty liver -- Current look at the old disease." *Med. Sci. Monit.* **6(1):** 209-216.

Mann D.A., Smart D.E. 2002. "Transcriptional regulation of hepatic stellate cell activation." *Gut* **50:** 891-896.

Marceau P., Biron S., Hould F.-S., Marceau S., Simard S., Thung S.N. 1999. "Liver pathology and the metabolic syndrome X in severe obesity." *J. Clin. Endocrinol. Metab.* **84 (5):** 1513-1517.

Markwell M.A.K., Haas S.M., Bieber L.L., Tobert N.E. 1978. "A modification of the Lowry procedure to simplify protein determination in membrane and lipoprotein samples." *Anal. Bioch.* **87:** 206-210.

Matteoni C.A., Younossi Z.M., Gramlich T., Boparai N., Liu Y.C., McCullogh A.J. 1999. "Nonalcoholic fatty liver disease: A spectrum of clinical and pathological severity." *Gastroenterology* **116:** 1413-1419.

McGowan M.W., Artiss J.D., Strandbergh D.R., Zak B. 1983. "A peroxidase-coupled method for the colorimetric determination of serum triglycerides." *Clin. Chem.* **29(3):** 538-542.

McMahon K.E., Farrell P.M. 1986. "Effect of choline deficiency on lung phospholipid concenration in the rat." *J. Nutr.* **116(6):** 936-943.

Mead J.F., Alfin-Slater P.B., Howton D.R., Popják G. 1986. "Lipids: Chemistry, biochemistry and nuitrition." New York: Plenum Press.

Mehta K., Thiel D.H., Shah N., Mobarhan S. 2002. "Nonalcoholic fatty liver disease: pathogenesis and the role of antioxidants." *Nutr. Rev.* **60(9):** 289-293.

Memon R.A., Grunfeld C., Moser A.H., Feingold K.R. 1993. "Tumor necrosis factor mediates the effect of endotoxin on cholesterol and triglyceride metabolism in mice." *Endocrinology* **132(5):** 2246-2253.

Molloy R.M., Komorowski R., Varma R.R. 1997. "Recurrent nonalcoholic steatohepatitis and cirrhosis after liver transplantation." *Liver Transpl. Surg.* **3(2):** 177-178.

Moran J.R., Ghishan F.K., Halter S.A., Greene H.L. 1983. "Steatohepatitis in obese children: a cause of chronic liver dysfunction." *Am. J. Gastroenterol.* **78:** 374-377.

Morio L.A., Chiu H., Sprowles K.A., Zhour P., Heck D.E., Gordon M.K., Laskin D.L. 2001. "Distinct role of tumor nectosis factor alpha and nitric oxide in acute liver injury induced by carbon tetrachloride in mice." *Toxicol. Appl. Pharmacol.* **172(1):** 44-51.

Muriel P., Escobar Y. 2003. "Kupffer cells are responsible for liver cirrhosis induced by carbon tetrachloride." *J. Appl. Toxicol.* **23(2):** 103-108.

Nelson, D. 2001. "Cytochrome P450s in humans." Retrieved October 2003 from `http://drnelson.utmem.edu/P450lect.html`

Neuschwander-Tetri B.A. 2001. "A resistance movement in NASH." *Am. J. Gastroenterol.* **96(10):** 2813-2814.

Neuschwander-Tetri B.A., Brunt E.M., Wehmeier K.R., Oliver D., Bacon B.R. 2003. "Improved nonalcoholic steatohepatitis after 48 weeks of treatment with the PPAR-gamma ligand rosiglitazone." *Hepatology* **38(4):** 1008-17.

Neuschwender-Tetri B.A., Caldwell S.H. 2003. "Nonalcoholic steatohepatitis: Summary of an AASLD Single Topic Conference." *Hepatology* **32:** 1202-1219.

Oben J.A., Roskams T., Yang S., Lin H., Sinelli N., Li Z., Torbenson M., Thomas S.A., Diehl A.M. 2003. "Norepinephrine induces hepatic fibrogenesis in leptin deficient *ob/ob* mice." *Biochem. Biophys. Res. Comm.* **308:** 284-292.

Paradis V., Perlemuter G., Bonvoust F., Dargere D., Parfait B., Vidaud M., Conti M., Huet S., Ba N., Buffet C., Bedossa P. 2002. "High glucose and hyperinsulinemia stimulate connective tissue growth factor expression: a potential mechanism involved in progression to fibrosis in nonalcoholic seatohepatitis." *Hepatology* **34(4):** 738-744.

Parola M., Pinzani M., Casini A., Albano E., Poli G., Gentilini A., Gentilini P., Dianzani M.U. 1993. "Stimulation of lipid peroxidation or 4-hydroxynonenal treatment increases procollagen α_1 gene expression in human liver fat-storing cells." *Bioch Biophys. Res. Comm.* **194(3):** 1044-1050.

Parola M., Robino G. 2001. "Oxidative stress-related molecules and liver fibrosis." *J. Hepatol.* **35:** 297-306.

Pearce R.E., McIntyre C.J., Madan A., Sanzgiri U., Draper A.J., Bullock P.L., Cook D.C., Burton L.A., Latham J., Nevins C., Parkinson A. 1996. "Effects of freezing, thawing, and

storing human liver microsomes on cytochrome P450 activity." *Arch. Bioch. Biophys.* **331(2):** 145-169.

Perrella A., Tarantino G., Borgia G., Conca P., Sorrentino P., Ragucci P., Vecchione R., Perrella O. 2003. "Cytokine network during NASH and possible treatment selection." *Hepatology* **38(2):** 530.

Pessayre D., Mansouri A., Haouzi D., Fromenty B. 1999. "Hepatotoxicity due to mitochondrial dysfunction." *Cell Biol. Toxicol.* **15:**: 367-373.

Peters R.L., Gay T., Reynolds T.B. 1975. "Post-jejunoileal bypass hepatic disease. Its similarity to alcoholic hepatic disease." *Am. J. Clin. Pathol.* **63:** 318-331.

Pinto H.C., Baptista A., Camilo M.E., Valente A., Saragoca A., de Moura M.C. 1996. "Nonalcoholic steatohepatitis: clinicopathologic comparison with alcoholic hepatitis in amulatory and hopitalized patients." *Dig. Dis. Sci.* **41:** 172-179.

Raeburn C.D., Sheappard F., Barsness K.A., Arya J., Harken A.H. 2002. "Cytokines for surgeons." *Am. J. Surg.* **183:** 268-273.

Randle P.J., Garland P.B., Hales C.N., Newshomlme E.A. 1963. "The glucose fatty acid cycle: its role in insulin sensitivity and the metabolic disturbances of diabetes mellitus." *Lancet* **1:** 785-789.

Ranlov I., Hardt F. 1990. "Regression of liver steatosis following gastroplasty or gastric bypass for morbid obesity." *Digestion.* **47(4):** 208-214.

Rao M.S., Papreddy K., Musunuri S., Okonkwo A. 2002. "Prevention/Reversal of choline deficiency-induced steatohepatitis by a peroxisome proliferator-activated receptor α ligand in rats." *In vivo* **16:** 145-152.

Raschid, M., Roberts E.A. 2000. "Nonalcoholic steatohepatitis in children." *J. Paedr. Gastroenterol. Nutr.* **30:** 48-53.

Ratziu V., Giral P., Charlotte F., Bruckert E., Thibault V., Theodorou I., Khalil L., Turpin G., Opolon P. 2000. "Liver fibrosis in overweight patients." *Gastroenterology* **118:** 1117-1123.

Recknagel R.O., Glende E.A. 1984. "Spectrophotometric detection of lipid conjugated dienes." *Meth. Enzymol.* **105:** 331-337.

Reddy G.K., Enwemeka C.S. 1996. "A simplified method for the analysis of hydroxyproline in biological tissues." *Clin. Biochem.* **29:** 225-229.

Reid, A.E. 2001. "Nonalcoholic steatohepatitis." *Gastroenterology* **121:** 710-723.

Renton K.W., Nicholson T.E. 2000. "Hepatic and central nervous system cytochrome P450 are downregulated during lipopolysaccharide-evoked localised inflammation in brain." *J. Pharmacol. Exp. Ther.* **294(2):** 524-530.

Roberts B.J., Shoaf S.E., Song B.J. 1995. "Rapid changes in cytochrome P4502E1 (CYP2E1) activity and other P450 isoenzymes following ethanol withdrawal in rats." *Biochem. Pharmacol.* **49(11):** 1665-1673.

Robertson G., Leclercq I., Farrell G.C. 2001. "Nonalcoholic steatosis and steatohepatitis II. Cytochrome P-450 enzymes and oxidative stress." *Am. J Physiol. Gastrointest. Liver Physiol.* **281:** G1135-G1139.

Rodríguez-Antona C., Donato M.T., Pareja E., Gómez-Lehón M-J., Castell J.V. 2001. "Cytochrome P-450 mRNA expression in human liver and is relationship with enzyme activity." *Arch. Biochem. Biophys.* **393(2):** 308-315.

Rushmore T.H., Lim Y.P., Farber E., Ghoshal A.K. 1984. "Rapid lipid peroxidation in the nuclear fraction of rat liver induced by a diet deficient in choline and methionine." *Cancer Lett.* **24(3):** 251-255.

Saadeh S., Younossi Z.M., Remer E.M., Gramlich T., Ong J.P., Hurley M., Mullen K.D., Cooper J.N., Sheridan M.J. 2002. "The utility of radiological imaging in nonalcoholic fatty liver disease." *Gastroenterology* **123(3):** 745-750.

Saitoh T., Kokue E., Shimoda M. 1999. "The suppressive effects of lipopolysaccharide-induced acute phase response on hepatic cytochrome P450-dependent drug metabolism in rats." *J. Vet. Pharmacol. Ther.* **22(2):** 87-95.

Sanyal A.J. 2001. "Insulin resistance and nonalcoholic steatohepatitis: fat or fiction?" *Am. J. Gastroenterol.* **96(2):** 274-276.

Saxena N.K., Ikeda K., Rockey D.C., Friedman S.L., Anania F.A. "Leptin in hepatic fibrosis: evidence for increased collagen production in stellate cells and lean littermates of *ob/ob* mice." *Hepatology* **35:** 762-771.

Schoon K., Staels B., Auwerx J. 1996. "Role of the peroxisome proliferator-activated receptor (PPAR) in mediating the effects of fibrates and fatty acid gene expression." *J. Lipid Research* **37:** 907-925.

Schulman G.I. 2000. "Cellular mechanisms of insulin resistance." *J Clin. Invest.* **106(2):** 171-176.

Shaffer E.A. 2002. "Nonalcoholic steatohepatitis: more than just being fat." *Can. J. Gastroenterol.* **16(5):** 318-321.

Shi Z., Wakil A.E., Rockey D.C. 1997. "Strain-specific differences in mouse hepatic wound healing are mediated by divergent T helper cytokine responses." *Proc. Nat. Aacd. Sci. USA* **94:** 10663-10668.

Shimada M., Hashimoto E., Kaneda H., Noguchi S., Hayashi N. 2002a. "Nonalcoholic steatohepatitis: risk factors for liver fibrosis." *Hepatol. Res.* **24(4):** 429-438.

Shimada M., Hashimoto E., Taniai M., Hasegawa K., Okuda H., Hayashi N., Takasaki K., Ludwig J. 2002b. "Hepatocellular carcinoma in patients with nonalcoholic steatohepatitis." *J. Hepatol.* **37:** 154-160.

Spiteller G. 2002. "Do changes in the cell membrane structure induce the generation of lipid peroxidation products which serve as first signalling molecules in cell to cell communication?" *Prost. Leuk. Essent. Fatty Acids.* **67(2-3):** 151-162.

Sreekumar R., Rosado B., Rasmussen D., Charlton M. 2003. "Hepatic gene expression in histologically progressive nonalcoholic steatohepatitis." *Hepatology* **38(1):** 244-251.

Sumida Y., Nakashima T., Yoh T., Furutani M., Hirohama A., Kakisaka Y., Nakajima Y., Ishikawa H., Mitsuyoshi H., Okanoue T., Kashima K., Nakamura H., Yodoi J. 2003. "Serum thioredoxin levels as a predictor of steatohepatitis in patients with nonalcoholic fatty liver disease." *J. Hepatol.* **38:** 32-38.

Szekanecz Z., Halloran M.M., Volm M.V., Woods J.M. 2000. "Temporal expression of inflammatory cytokines and chemokines in rat adjuvant-induced arthritis." *Arthritis Rheum.* **43(6):** 1266-1277.

Takahashi N., Waelput W., Guisez Y. 1999. "Leptin is an endogenous protective protein against the toxicity exerted by tumor necrosis factor." *J. Exp. Med.* **189(1):** 207-212.

Takahashi T., Lasker J.M., Rosman A.S., Lieber C.S. 1993. "Induction of cytochrome P-4502E1 in human liver by ethanol is caused by a corresponding increase in encoding messenger RNA." *Hepatology* **17:** 236-245.

Takaya K., Ogawa Y., Isse N., Okazaki T., Satoh N., Masuzaki H., Mori K., Tamura N., Hosoda K., Nakawa K. 1996. "Molecular Cloning of rat leptin receptor isoform complementary DNAs – identification of a missense mutation in Zucker fatty (*fa/fa*) rats." *Bioch. Biophys. Res. Comm.* **225:** 75-83.

Talwalkar J.A. 2002. "Motion – All patients with NASH need to have a liver biopsy: Arguments for the motion." *Can. J. Gastroenterol.* **16(10):** 718-721.

Teli M.R., James O.F.W., Buurt A.D., Bennett M.K., Day C.P. 1995. "The natural history of nonalcoholic fatty liver: a follow-up study." *Hepatology* **22:** 1714-1719.

Tessitore L., Sesca E., Greco M., Pani P., Dianzini M.U. 1995. "Sexually differentiated response to choline in choline deficiency and ethionine intoxication." *Intl. Exp. Pathol.* **76(2):** 125-129.

Thaler H. 1971. "Morphologische befunde bei chronischer Alkoholintoxikation." In: Gerok V., Sickinger K., Hennkeuser HH. *Alkohol und Leber.* 257-265. Stuttgart: Schattauer Verlag.

Tietz N. 1987. "Fundamentals of Clinical Chemistry". (3rd ed.) W.B. Saunders Company.

Tilg H., Diehl A. 2000. "Cytokines in alcoholic and nonalcoholic steatohepatitis." *N. Engl. J. Med.* **343:** 1467-1476.

Tinoco J., Endemann G., Medwadowski B., Miljanich P., Williams M. 1979. "Ethanolamine kinase activity and compositions of diacylglycerol, phosphatidylcholines and phosphatidylethanolamines in liver of choline-deficient rats." *Lipids* **14(2):** 968-974.

Tsukamoto H., Towner S.J., Ciofalo L.M., French S.W. 1986. "Ethanol-induced liver fibrosis in rats fed high fat diets." *Hepatology* **6:** 814-822.

Tsutsui H., Matsui K., Kawada N., Hyodo Y., Hayashi N., Okamura H., Higashino K., Nakanishi K. 1997. "IL-18 accounts for both TNFα- and Fas Ligand-mediated hepatotoxic pathways in endotoxin-induced liver injury in mice." *Immunology* **159:** 3961-3967.

Turlin B., Mendler M.H., Moirand R., Guyader D., Guillygomarc'h A., Deugnier Y. 2001. "Histologic features of the liver in insulin resistance-associated iron overload. A study of 139 patients." *Am. J. Clin. Pathol.* **116:** 263-270.

Ulmer A.J., Reitschel E.Th., Zähringer U., Heine H. 2002. "Lipopolysaccharide: Structure, bioactivity, receptors and signal transduction." *Trends Glycosc. Clycotech.* **14(76):** 53-68.

Valenti L., Fracanzani A.L., Dongiovanni P., Santorelli G., Branchi A., Taioli E., Fiorelli G., Fargion S. 2002. "Tumor necrosis factor α promoter polymorphisms and insulin resistance in nonalcoholic fatty disease." *Gastroenterology* **122:** 274-280.

Van Gossum A., Decuyper J. 1989. "Breath alkanes as an index of lipid peroxidation." *Eur. Respr. J.* **2:** 787-791.

Vasankari T., Urho K., Olli H., Kapanen J., Markku A. 1995. "Measurement of serum lipid peroxidation during exercise using three different methods : diene conjugation, thiobarbituric acid reactive material and fluorescent chromolipids." *Clin. Chim. Acta* **234:** 63-69.

Videla L.A., Fernandez V., Tapia G., Varela P. 2003. "Oxidative stress-mediated hepatotoxicity of iron and copper: role of Kupffer cells." *Biometals* **16(1):** 103-111.

Vrba J., Modriansky M. 2002. "Oxidative burst of Kupffer cells: Target for liver injury treatment." *Biomed. Papers* **146(2):** 15-20.

Wanless I.R., Lentz J.S. 1990. "Fatty liver hepatitis (steatohepatitis) and obesity: an autopsy study with analysis of risk factors." *Hepatology* **12:** 1106-1110.

Watson W.H., Zhao Y., Chawla R.K. 1999. "*S*-adenosylmethionine attenuates the lipopolysaccharide-induced expression of the gene for tumour necrosis factor α." *Biochem. J.* **342:** 21-25.

Weltman M.D., Farrell G.C., Hall P., Ingelman-Sundberg M., Liddle C. 1998. "Hepatic cytochrome P450 2E1 is increased in patients with nonalcoholic steatohepatitis." *Hepatology* **27:** 128-133.

Weltman M.D., Farrell G.C., Liddle C. 1996. "Increased hepatocyte CYP2E1 expression in a rat nutritional model of hepatic steatosis with inflammation." *Gastroenterology* **111:** 1645-1653.

Wheatly R.A. 2000. "Some recent trends in the analytical chemistry of lipid peroxidation." *Trends Anal. Chem.* **19(10):** 617-628.

Wigg A.J., Roberts-Thomson I.C., Dymock R.B., McCarthy P.J., Grose R.H., Cummins A.G. 2001. "The role of small intestinal bacterial overgrowth, intestinal permeability, endotoxaemia, and tumor α in the pathogenesis of nonalcoholic steatohepatitis." *Gut* **48:** 206-211.

Wolff S.P., Garner A., Dean R.T. 1986. "Free radicals, lipids and protein degradation." *Trends Bioch. Sci.* **11:** 27-31.

Woodcroft K.J., Hafner M.S., Novak R.F. 2002. "Insulin signaling in the transcriptional and posttranscriptional regulation of CYP2E1 expression." *Hepatology* **35:** 263-273.

Yang S., Lin H., Diehl A.M. 2001. "Fatty liver vulnerability to endotoxin-induced damage despite NFκβ induction and inhibited caspase 3 activation." *Am. J. Gastrointest. Liver Physiol.* **281:** G382-G392.

Yang S., Lin H.Z., Hwang J., Chacko V.O., Diehl A.M. 2001. "Hepatic hyperplasia in noncirrhotic fatty livers: Is obesity-related hepatic steatosis a premalignant condition?" *Can. Res.* **61:** 5016-5023.

Younossi Z.M., Gramlich G., Bacon B.R., Matteoni C.A., Boparai N., O'Neill R.O., McCullough A.J. 1999. "Hepatic iron and nonalcoholic fatty liver disease." *Hepatology* **30:** 847-950.

Yu A.S., Keefe A.B. 2002. "Nonalcoholic fatty liver disease." *Rev. Gastroenterol. Disord.* **2(1):** 11-19.

Zamin J.I., de Mattos A.A., Perin C., Ramos G.Z. 2002. "The importance of AST/ALT rate in nonalcoholic steatohepatitis." *Arq. Gastroenterol.* **39(1):** 22-26.

Zheng J. 1998. "Immunohistochemistry and immunocytochemistry." In: Methods in Molecular Biology. Humana press, New Jersey.

Appendices

Appendix 1(a)
Composition of custom methionine choline deficient diet (ICN Biomedicals)

Component	Quantity in 7kg diet [g]
Sucrose	3152
Corn starch	1400
Corn oil	700
Alphacell non-nutritive bulk	210
AIN mineral mix	245
Dicalcium phosphate	21
L-Alanine	24.5
L-Arginine HCl	84.7
L-Asparagine monohydrate	42
L-Aspartic acid	24.5
L-Cystine	24.5
L-Glutamic acid	280
Glycine	163.1
L-Histidine HCl	31.5
L-Isoleucine	57.4
L-Lysine HCl	77.7
L-Phenylalanine	126
L-Proline	52.5
L-Serine	24.5
L-Threonine	24.5
L-Tryptophan	12.6
L-Tyrosine	35
L-Valine	57.4
D-, L-α Tocopherol acetate (250U/g)	3.388
Vitamin A palmitate (250 000U/g)	0.554
Vitamin D3 (400 000U/g)	0.039
Ethyoxyquin	0.14
Biotin	0.003
D-Calcium pantothenate	0.463
Folic acid	0.014
Inositol	0.771
Menadione	0.347
Niacin	0.694
P-aminobenzoic acid	0.771
Pyridoxine HCl	0.154
Riboflavin	0.154
Thiamine HCl	0.154
Vitamin B12	0.208
Ascorbic acid	7.116
Corn starch	24.152

***Ctrl diet is supplemented with choline chloride (14g) and D-,L-methionine (21g)**

Appendix 1(b): TG values in MCD and Ctrl diets (70mg/2ml SEAP)

MCD diet 10ul	2.37µg
MCD diet 30ul	3.92µg
Ctrl diet 10ul	1.60µg
Ctrl diet 30ul	4.70µg

Appendix 2
Raw Data: Long Term Study

Appendix 2.1: Weights [g] during LTS

	Cage #	Treatment	Mass at Week 0	Mass at Week 1	Mass at Week 2	Mass at Week 3	Mass at Week 4	Mass at Week 5
Mouse # 1	1	MCD/water	30.4	30.5	32.0	32.1	23.8	23.0
Mouse # 2	1	MCD/water	25.8	26.5	27.7	27.5	25.9	21.8
Mouse # 1	2	MCD/water	27.6	28.0	28.3	28.4	24.6	21.8
Mouse #2	2	MCD/water	27.6	27.2	28.0	27.2	23.3	21.7
Mouse #1	3	MCD/water	26.5	27.3	28.1	27.9	22.5	20.5
Mouse #2	3	MCD/water	29.4	29.4	31.4	30.5	25.4	23.6
Mouse #1	4	MCD/water	27.6	27.9	28.5	27.7	23.7	21.7
Mouse #2	4	MCD/water	26.4	27.5	28.0	27.3	22.7	21.2
Mouse #1	5	MCD/water	28.6	29.2	30.0	30.0	29.0	29.9
Mouse #1	6	MCD/water	30.7	31.4	31.6	32.8	32.1	33.2
Mouse #1	7	MCD/water	26.9	27.2	28.0	27.0	27.3	28.2
Mouse #1	8	MCD/water	26.6	27.2	28.1	28.8	27.8	30.0
Mouse #1	9	MCD/water	28.2	28.5	30.8	31.0	31.1	31.3
Mouse #2	9	MCD/water	29.4	29.7	31.5	31.0	32.0	32.5
Mouse #3	9	MCD/water	27.4	28.1	29.4	28.1	30.0	30.5
Mouse #4	9	MCD/water	22.4	22.1	23.4	23.4	23.0	23.5
Mouse #1	1	MCD/8%	26.8	29.4	30.9	31.1	25.8	23.5
Mouse #2	1	MCD/8%	28.9	27.0	28.4	29.3	23.9	21.5
Mouse #3	1	MCD/8%	25.2	25.5	27.2	27.9	23.7	21.7
Mouse #1	2	MCD/8%	23.8	24.0	24.9	24.8	21.4	20.1
Mouse #1	3	MCD/8%	26.6	27.0	29.4	29.4	23.2	21.4
Mouse #2	3	MCD/8%	27.4	26.4	27.4	27.8	23.5	21.8
Mouse #3	3	MCD/8%	27.1	27.1	28.8	28.5	24.2	22.5
Mouse #4	3	MCD/8%	26.8	27.4	28.4	29.2	23.9	21.6
Mouse #1	4	MCD/8%	26.8	26.9	27.6	27.5	24.1	22.6
Mouse #1	5	MCD/8%	32.9	32.9	34.3	34.8	35.7	36.1
Mouse #2	5	MCD/8%	29.7	30.1	31.2	31.6	31.9	31.7
Mouse #3	5	MCD/8%	24.6	24.9	25.1	25.4	25.9	26.1
Mouse #1	6	MCD/8%	31.7	31.6	33.3	33.4	33.4	33.4
Mouse #2	6	MCD/8%	30.4	31.3	33.0	33.1	33.8	33.8

	Cage #	Treatment	Mass at Week 0	Mass at Week 1	Mass at Week 2	Mass at Week 3	Mass at Week 4	Mass at Week 5
Mouse #3	6	MCD/8%	30.9	31.4	32.9	31.9	32.0	33.0
Mouse #1	7	MCD/8%	28.6	29.4	29.8	29.4	30.6	30.3
Mouse #1	1	MCD/20%	29.9	30.1	30.0	31.8	26.2	24.1
Mouse #1	2	MCD/20%	29.5	29.9	30.2	30.0	25.6	23.6
Mouse #1	3	MCD/20%	26.2	26.4	26.5	27.5	23.0	21.0
Mouse #1	4	MCD/20%	27.0	27.6	28.6	27.5	24.5	22.1
Mouse #2	4	MCD/20%	26.9	26.8	28.4	28.2	23.9	22.3
Mouse #1	5	MCD/20%	24.4	24.5	25.4	26.3	26.8	26.8
Mouse #2	5	MCD/20%	26.6	26.2	27.2	26.9	27.3	27.9
Mouse #3	5	MCD/20%	27.7	27.9	29.2	29.2	29.7	29.5
Mouse #1	6	MCD/20%	27.6	28.3	29.1	28.7	29.0	30.3
Mouse #1	7	MCD/20%	23.1	23.1	23.4	24.4	24.5	24.6
Mouse #2	7	MCD/20%	25.0	26.4	27.3	27.5	27.7	28.6
Mouse #1	8	MCD/20%	28.3	29.2	29.2	29.5	29.2	30.5
Mouse #1	9	MCD/20%	28.4	27.8	30.1	29.3	29.5	30.3
Mouse #2	9	MCD/20%	29.2	27.5	29.3	28.4	30.2	30.7
Mouse #3	9	MCD/20%	28.2	27.8	30.1	30.8	30.7	32.2
Mouse #1	10	MCD/20%	29.2	29.2	30.1	30.2	30.8	31.0
Mouse #2	10	MCD/20%	26.7	27.2	27.2	27.2	27.2	27.4
Mouse #1	1	Ctrl/Water	27.9	28.9	30.2	29.4	33.3	34.3
Mouse #2	1	Ctrl/Water	24.3	24.3	25.4	25.9	28.4	29.8
Mouse #3	1	Ctrl/Water	27.6	27.5	27.9	27.5	30.1	32.3
Mouse #1	2	Ctrl/Water	25.3	25.8	27.4	27.2	28.8	28.8
Mouse #2	2	Ctrl/Water	27.1	28.2	29.5	29.4	33.3	33.8
Mouse #3	2	Ctrl/Water	26.3	26.4	28.0	27.9	29.1	28.4
Mouse #1	3	Ctrl/Water	27.6	29.4	29.6	29.3	30.5	30.5
Mouse #1	4	Ctrl/Water	30.1	30.3	29.5	30.2	32.2	33.4
Mouse #1	5	Ctrl/Water	21.9	22.4	22.9	23.2	23.6	23.8
Mouse #2	5	Ctrl/Water	22.2	22.9	24.1	24.1	24.4	25.0
Mouse #3	5	Ctrl/Water	24.5	25.1	25.9	26.9	27.6	28.4

	Cage #	Treatment	Mass at Week 0	Mass at Week 1	Mass at Week 2	Mass at Week 3	Mass at Week 4	Mass at Week 5
Mouse #4	5	Ctrl/Water	26.6	27.2	28.5	29.1	30.4	31.3
Mouse #1	6	Ctrl/Water	28.4	29.5	29.9	30.5	30.3	30.8
Mouse #1	7	Ctrl/Water	21.8	25.4	25.5	25.2	25.3	25.7
Mouse #1	8	Ctrl/Water	28.9	29.9	30.7	31.6	31.6	31.6
Mouse #1	1	Ctrl/8%	27.3	28.4	28.8	29.1	29.0	29.0
Mouse #1	2	Ctrl/8%	26.7	26.2	27.6	26.2	28.6	28.8
Mouse #2	2	Ctrl/8%	24.8	24.9	26.1	26.2	27.9	29.9
Mouse #3	2	Ctrl/8%	25.8	26.8	27.3	27.1	29.2	30.6
Mouse #4	2	Ctrl/8%	27.1	27.1	29.1	28.3	27.9	27.9
Mouse #1	3	Ctrl/8%	24.4	24.0	25.0	26.1	28.2	29.3
Mouse #2	3	Ctrl/8%	22.8	22.6	23.8	24.1	26.4	26.8
Mouse #3	3	Ctrl/8%	26.0	25.4	26.1	27.1	28.5	29.0
Mouse #4	3	Ctrl/8%	24.2	24.1	24.4	24.4	26.1	27.4
Mouse #1	4	Ctrl/8%	25.5	26.4	27.5	27.5	30.0	30.4
Mouse #2	4	Ctrl/8%	24.1	25.0	25.5	25.0	26.9	27.5
Mouse #3	4	Ctrl/8%	21.1	21.8	22.7	22.6	22.8	23.6
Mouse #1	5	Ctrl/8%	22.5	23.7	24.4	24.3	25.2	25.6
Mouse #2	5	Ctrl/8%	24.8	26.2	27.1	26.1	27.0	27.4
Mouse #1	6	Ctrl/8%	29.7	29.9	30.8	30.7	30.5	31.6
Mouse #1	7	Ctrl/8%	32.1	33.8	32.5	33.9	33.5	35.0
Mouse #1	8	Ctrl/8%	23.7	24.2	24.4	24.9	25.1	25.7
Mouse #1	1	Ctrl/20%	30.0	30.4	31.1	31.2	34.5	35.5
Mouse #1	2	Ctrl/20%	27.0	25.3	25.6	26.0	30.0	31.8
Mouse #2	2	Ctrl/20%	24.2	24.2	28.6	28.0	29.0	29.8
Mouse #3	2	Ctrl/20%	24.9	24.9	25.7	26.8	28.1	29.4
Mouse #4	2	Ctrl/20%	24.7	24.4	25.6	26.3	28.2	28.8
Mouse #1	3	Ctrl/20%	27.1	27.9	28.0	26.1	29.0	29.8
Mouse #1	4	Ctrl/20%	29.4	29.7	30.2	30.6	33.5	34.0
Mouse #1	5	Ctrl/20%	25.6	25.8	26.8	27.4	27.4	27.1
Mouse #1	6	Ctrl/20%	22.6	23.0	23.6	24.0	24.6	25.2
Mouse #2	6	Ctrl/20%	24.3	25.4	26.3	26.1	27.3	27.7
Mouse #3	6	Ctrl/20%	23.4	24.1	24.6	25.0	26.0	26.6
Mouse #1	7	Ctrl/20%	27.5	27.0	28.9	28.7	29.2	29.3
Mouse #2	7	Ctrl/20%	29.6	29.2	31.0	30.3	31.4	32.1
Mouse #3	7	Ctrl/20%	25.6	26.2	28.6	28.6	29.9	29.6
Mouse #4	7	Ctrl/20%	24.2	24.5	25.4	24.8	25.5	25.9

Weeks 6-9

	Cage #	Treatment	Mass at Week 6	Mass at Week 7	Mass at Week 8	Mass at Week 9
Mouse # 1	1	MCD/water	***Sacrificed on Monday, June 24 2002 for preliminary assessment of hepatic changes***			
Mouse # 2	1	MCD/water				
Mouse # 1	2	MCD/water	20.4	19.6	18.8	18.4
Mouse #2	2	MCD/water	20.9	20.0	19.6	19.1
Mouse #1	3	MCD/water	19.3	18.7	17.6	17.1
Mouse #2	3	MCD/water	22.5	21.8	21.1	21.1
Mouse #1	4	MCD/water	19.3	19.4	18.9	18.6
Mouse #2	4	MCD/water	20.1	18.7	17.3	16.7
Mouse #1	5	MCD/water	24.6	22.3	21.4	20.1
Mouse #1	6	MCD/water	27.9	24.9	23.3	22.4
Mouse #1	7	MCD/water	23.0	21.1	20.0	18.9
Mouse #1	8	MCD/water	25.0	23.6	21.6	20.4
Mouse #1	9	MCD/water	26.4	23.8	22.3	21.0
Mouse #2	9	MCD/water	26.9	24.2	23.3	22.6
Mouse #3	9	MCD/water	24.3	22.1	21.0	19.9
Mouse #4	9	MCD/water	19.9	18.0	17.2	16.3
Mouse #1	1	MCD/8%	20.4	21.1	20.2	19.8
Mouse #2	1	MCD/8%	20.0	18.9	18.3	17.3
Mouse #3	1	MCD/8%	22.7	19.4	18.4	18.0
Mouse #1	2	MCD/8%	18.9	18.0	17.1	17.0
Mouse #1	3	MCD/8%	20.3	19.5	18.4	17.9
Mouse #2	3	MCD/8%	20.6	19.8	19.4	18.2
Mouse #3	3	MCD/8%	21.0	20.1	19.1	18.3
Mouse #4	3	MCD/8%	20.4	19.1	18.7	18.4
Mouse #1	4	MCD/8%	21.5	19.8	18.6	18.0
Mouse #1	5	MCD/8%	29.4	26.8	25.2	23.9
Mouse #2	5	MCD/8%	26.9	23.5	22.7	21.5
Mouse #3	5	MCD/8%	21.8	20.0	18.6	17.7
Mouse #1	6	MCD/8%	28.2	24.8	22.8	21.6
Mouse #2	6	MCD/8%	27.7	24.6	23.3	22.0

	Cage #	Treatment	Mass at Week 6	Mass at Week 7	Mass at Week 8	Mass at Week 9
Mouse #3	6	MCD/8%	27.5	24.1	22.0	21.0
Mouse #1	7	MCD/8%	25.8	27.4	23.3	21.9
Mouse #1	1	MCD/20%	22.8	21.0	20.7	20.4
Mouse #1	2	MCD/20%	22.4	21.3	19.4	19.9
Mouse #1	3	MCD/20%	19.0	18.4	17.6	17.2
Mouse #1	4	MCD/20%	20.6	19.7	18.9	18.4
Mouse #2	4	MCD/20%	21.5	20.4	19.6	18.9
Mouse #1	5	MCD/20%	22.7	20.3	18.9	18.0
Mouse #2	5	MCD/20%	24.4	22.4	21.1	20.1
Mouse #3	5	MCD/20%	25.8	22.6	21.0	20.3
Mouse #1	6	MCD/20%	26.8	24.7	23.5	22.3
Mouse #1	7	MCD/20%	21.7	19.8	18.3	17.8
Mouse #2	7	MCD/20%	23.8	21.8	20.4	20.0
Mouse #1	8	MCD/20%	25.6	24.0	22.1	20.9
Mouse #1	9	MCD/20%	25.5	23.0	20.5	20.0
Mouse #2	9	MCD/20%	25.1	24.4	21.5	20.3
Mouse #3	9	MCD/20%	26.9	23.1	22.4	21.5
Mouse #1	10	MCD/20%	25.2	22.6	20.8	19.7
Mouse #2	10	MCD/20%	23.6	21.7	20.6	19.9
Mouse #1	1	Ctrl/Water	33.0	39.2	40.3	42.0
Mouse #2	1	Ctrl/Water	30.3	30.8	31.5	32.1
Mouse #3	1	Ctrl/Water	36.3	35.1	35.9	36.0
Mouse #1	2	Ctrl/Water	29.4	31.8	31.6	33.7
Mouse #2	2	Ctrl/Water	29.0	36.1	35.8	38.7
Mouse #3	2	Ctrl/Water	35.4	31.0	31.0	33.4
Mouse #1	3	Ctrl/Water	31.4	32.0	33.1	33.5
Mouse #1	4	Ctrl/Water	33.4	34.7	35.4	37.4
Mouse #1	5	Ctrl/Water	25.8	27.8	28.9	30.2
Mouse #2	5	Ctrl/Water	26.2	26.7	27.6	27.8
Mouse #3	5	Ctrl/Water	28.7	29.1	29.6	30.7

	Cage #	Treatment	Mass at Week 6	Mass at Week 7	Mass at Week 8	Mass at Week 9
Mouse #4	5	Ctrl/Water	33.0	33.6	34.8	37.5
Mouse #1	6	Ctrl/Water	33.5	35.5	38.8	40.5
Mouse #1	7	Ctrl/Water	26.0	26.2	27.4	27.8
Mouse #1	8	Ctrl/Water	36.5	38.5	41.3	42.6
Mouse #1	1	Ctrl/8%	29.0	28.7	20.1	30.4
Mouse #1	2	Ctrl/8%	29.9	29.5	29.4	30.2
Mouse #2	2	Ctrl/8%	30.4	31.5	32.2	33.0
Mouse #3	2	Ctrl/8%	32.6	32.4	33.2	34.0
Mouse #4	2	Ctrl/8%	27.5	28.1	28.2	29.2
Mouse #1	3	Ctrl/8%	27.4	28.7	28.4	29.8
Mouse #2	3	Ctrl/8%	29.8	31.0	31.0	31.5
Mouse #3	3	Ctrl/8%	29.2	30.1	30.9	31.7
Mouse #4	3	Ctrl/8%	27.6	29.0	30.1	31.0
Mouse #1	4	Ctrl/8%	28.7	29.9	29.9	33.4
Mouse #2	4	Ctrl/8%	31.7	31.8	31.9	32.0
Mouse #3	4	Ctrl/8%	24.5	25.8	25.3	27.2
Mouse #1	5	Ctrl/8%	26.5	26.6	277.6	27.4
Mouse #2	5	Ctrl/8%	27.8	27.5	29.4	29.5
Mouse #1	6	Ctrl/8%	33.9	34.7	35.7	37.1
Mouse #1	7	Ctrl/8%	38.3	39.6	42.5	42.9
Mouse #1	8	Ctrl/8%	26.5	26.9	28.1	30.6
Mouse #1	1	Ctrl/20%	36.5	38.2	38.0	39.5
Mouse #1	2	Ctrl/20%	32.9	32.1	33.4	34.3
Mouse #2	2	Ctrl/20%	31.0	30.5	30.7	30.3
Mouse #3	2	Ctrl/20%	30.4	30.0	31.8	32.5
Mouse #4	2	Ctrl/20%	28.1	26.6	29.4	29.8
Mouse #1	3	Ctrl/20%	***Found dead Tuesday July 02, 2002***			
Mouse #1	4	Ctrl/20%	34.0	35.4	35.7	36.8
Mouse #1	5	Ctrl/20%	28.4	28.9	30.9	31.8
Mouse #1	6	Ctrl/20%	26.5	27.0	27.8	28.5
Mouse #2	6	Ctrl/20%	29.1	29.3	30.5	31.1
Mouse #3	6	Ctrl/20%	28.3	29.2	31.3	31.6
Mouse #1	7	Ctrl/20%	30.2	30.2	31.3	31.0
Mouse #2	7	Ctrl/20%	31.8	32.6	34.7	35.6
Mouse #3	7	Ctrl/20%	30.0	30.0	31.6	34.4
Mouse #4	7	Ctrl/20%	25.7	25.8	27.3	28.5

Weeks 10-14

	Cage #	Treatment	Mass at Week 10	Mass at Week 11	Mass at Week 12	Mass at Week 13	Mass at Week 14
Mouse # 1	1	MCD/water	***Sacrificed June 24, 2002 for preliminary***				
Mouse # 2	1	MCD/water	***assessment of liver changes***				
Mouse # 1	2	MCD/water	17.6	16.9			
Mouse #2	2	MCD/water	18.5	18.5			
Mouse #1	3	MCD/water	16.6	16.0	***Sacrificed July 30, 2002***		
Mouse #2	3	MCD/water	20.6	20.4			
Mouse #1	4	MCD/water	18.1	18.9			
Mouse #2	4	MCD/water	15.8	14.3	***Found eaten July 30, 2002***		
Mouse #1	5	MCD/water	19.7	18.6		18.1	
Mouse #1	6	MCD/water	21.5	21.1		20.0	
Mouse #1	7	MCD/water	17.8	16.8		16.1	
Mouse #1	8	MCD/water	-	18.5		18.1	***Sacr. 15.08.02***
Mouse #1	9	MCD/water	20.4	19.7		19.1	
Mouse #2	9	MCD/water	21.7	21.1		20.8	
Mouse #3	9	MCD/water	19.1	18.8		18.2	
Mouse #4	9	MCD/water	15.6	15.2		15.0	
Mouse #1	1	MCD/8%	19.1	18.7			
Mouse #2	1	MCD/8%	17.1	16.6			
Mouse #3	1	MCD/8%	17.3	16.9	***Sacrificed July 30, 2002***		
Mouse #1	2	MCD/8%	16.1	15.6			
Mouse #1	3	MCD/8%	18.6	17.9			
Mouse #2	3	MCD/8%	***Found (eaten) July 16, 2002***				
Mouse #3	3	MCD/8%	20.0	18.3	***Sacrificed July 30, 2002***		
Mouse #4	3	MCD/8%	18.5	17.9			
Mouse #1	4	MCD/8%	17.5	16.9		16.4	
Mouse #1	5	MCD/8%	22.7	21.6		20.0	
Mouse #2	5	MCD/8%	20.6	19.6		19.2	***Sacr. 15.08.02***
Mouse #3	5	MCD/8%	16.8	16.5		16.1	
Mouse #1	6	MCD/8%	20.3	19.2		18.7	
Mouse #2	6	MCD/8%	20.7	19.9		19.1	

	Cage #	Treatment	Mass at Week 10	Mass at Week 11	Mass at Week 12	Mass at Week 13	Mass at Week 14
Mouse #3	6	MCD/8%	19.8	19.1		18.7	*Sacr. 15.08.02*
Mouse #1	7	MCD/8%	21.1	20.4		19.8	
Mouse #1	1	MCD/20%	19.5	18.9	*Sacrificed July 30, 2002*		
Mouse #1	2	MCD/20%	18.7	17.5			
Mouse #1	3	MCD/20%	15.9	16.0			
Mouse #1	4	MCD/20%	17.8	17.2			
Mouse #2	4	MCD/20%	16.2	17.8			
Mouse #1	5	MCD/20%	17.4	16.7			
Mouse #2	5	MCD/20%	19.0	17.9			
Mouse #3	5	MCD/20%	19.0	18.1			
Mouse #1	6	MCD/20%	21.3	21.2		20.2	
Mouse #1	7	MCD/20%	16.9	16.1		16.0	*Sacr. 15.08.02*
Mouse #2	7	MCD/20%	18.6	17.5		17.1	
Mouse #1	8	MCD/20%	19.9	19.3		18.9	
Mouse #1	9	MCD/20%	19.0	18.3		*Found eaten August 05, 2002*	
Mouse #2	9	MCD/20%	19.6	19.0		18.7	
Mouse #3	9	MCD/20%	20.4	19.5		19.1	*Sacr. 15.08.02*
Mouse #1	10	MCD/20%	19.0	18.2		17.7	
Mouse #2	10	MCD/20%	19.7	18.7		18.2	
Mouse #1	1	Ctrl/Water	40.4	*Sacrificed July 24, 2002*			
Mouse #2	1	Ctrl/Water	30.7				
Mouse #3	1	Ctrl/Water	34.2				
Mouse #1	2	Ctrl/Water	33.7				
Mouse #2	2	Ctrl/Water	38.9				
Mouse #3	2	Ctrl/Water	33.7				
Mouse #1	3	Ctrl/Water	33.8				
Mouse #1	4	Ctrl/Water	32.3				
Mouse #1	5	Ctrl/Water	28.4	27.6		31.5	*Found dead 12.08.02*
Mouse #2	5	Ctrl/Water	26.1	25.9		29.4	
Mouse #3	5	Ctrl/Water	28.2	27.4		30.6	

	Cage #	Treatment	Mass at Week 10	Mass at Week 11	Mass at Week 12	Mass at Week 13	Mass at Week 14
Mouse #4	5	Ctrl/Water	35.2	34.2		36.2	*Found dead 12.08.02*
Mouse #1	6	Ctrl/Water	39.8	38.7		39.1	*Sacr. 13.08.02*
Mouse #1	7	Ctrl/Water	28.3 *Severe hair loss*	26.3		28.4	
Mouse #1	8	Ctrl/Water	41.6	38.6		43.7	
Mouse #1	1	Ctrl/8%	30.5	*Sacrificed July 24, 2002*			
Mouse #1	2	Ctrl/8%	29.3				
Mouse #2	2	Ctrl/8%	32.2				
Mouse #3	2	Ctrl/8%	33.2				
Mouse #4	2	Ctrl/8%	27.8				
Mouse #1	3	Ctrl/8%	28.7				
Mouse #2	3	Ctrl/8%	30.9				
Mouse #3	3	Ctrl/8%	31.3				
Mouse #4	3	Ctrl/8%	30.1				
Mouse #1	4	Ctrl/8%	33.3	31.5		35.5	*Sacr. 13.08.02*
Mouse #2	4	Ctrl/8%	30.8	28.7		33.7	
Mouse #3	4	Ctrl/8%	28.2	25.7		29.7	
Mouse #1	5	Ctrl/8%	27.0	27.0		29.2	
Mouse #2	5	Ctrl/8%	30.0	29.7		32.1	
Mouse #1	6	Ctrl/8%	36.3	36.0		37.3	
Mouse #1	7	Ctrl/8%	42.2	40.9		42.3	
Mouse #1	8	Ctrl/8%	29.5	29.8		31.2	
Mouse #1	1	Ctrl/20%	39.3	*Sacrificed July 24, 2002*			
Mouse #1	2	Ctrl/20%	33.8				
Mouse #2	2	Ctrl/20%	28.7				
Mouse #3	2	Ctrl/20%	31.8				
Mouse #4	2	Ctrl/20%	27.4				
Mouse #1	3	Ctrl/20%	*Found dead Tuesday July 02, 2002*				
Mouse #1	4	Ctrl/20%	36.8	*Sacrificed July 24, 2002*			
Mouse #1	5	Ctrl/20%	31.6				
Mouse #1	6	Ctrl/20%	30.8	29.9		30.3	*Sacr. 13.08.02*
Mouse #2	6	Ctrl/20%	31.9	29.8		32.0	
Mouse #3	6	Ctrl/20%	28.4	31.6		34.3	
Mouse #1	7	Ctrl/20%	29.8	27.7		31.8	
Mouse #2	7	Ctrl/20%	34.6	32.7		36.5	
Mouse #3	7	Ctrl/20%	34.2	31.8		36.0	
Mouse #4	7	Ctrl/20%	28.1	26.5		30.7	

Appendix 2.2: Sacrifce details (liver weight, body weight) for Group 1 (tissue used in assays, ALT and AST) and Group 2 (serum used for serum TG measurement)

Sacrifice Details for Group 1 Mice

New no.		Cage #	Treatment	Weight at Week 10 [g]	Weight of liver	Body weight [g]
1	Mouse #1	1	Ctrl/Water	40.4	2.2	41
2	Mouse #2	1	Ctrl/Water	30.7	1.4	32
3	Mouse #3	1	Ctrl/Water	34.2	1.8	36
4	Mouse #1	2	Ctrl/Water	33.7	1.8	30
5	Mouse #2	2	Ctrl/Water	38.9	1.8	34.4
6	Mouse #3	2	Ctrl/Water	33.7	1.4	27.4
7	Mouse #1	3	Ctrl/Water	33.8	2.0	34.0
8	Mouse #1	4	Ctrl/Water	32.3	2.0	37.0
9	Mouse #1	1	Ctrl/8%	30.5	1.4	30.6
10	Mouse #1	2	Ctrl/8%	29.3	1.4	28.8
11	Mouse #2	2	Ctrl/8%	32.2	1.6	31.8
12	Mouse #3	2	Ctrl/8%	33.2	1.6	32.6
13	Mouse #4	2	Ctrl/8%	27.8	1.4	27.4
14	Mouse #1	3	Ctrl/8%	28.7	1.4	28.0
15***	Mouse #2	3	Ctrl/8%	30.9	1.0* *Fatty?	28.0
16	Mouse #3	3	Ctrl/8%	31.3	1.6	30.6
17	Mouse #4	3	Ctrl/8%	30.1	1.2	29.4
18	Mouse #1	1	Ctrl/20%	39.3	2.0	39.0
19	Mouse #1	2	Ctrl/20%	33.8	1.6	33.6
20	Mouse #2	2	Ctrl/20%	28.7	1.4	28.6
21	Mouse #3	2	Ctrl/20%	31.8	1.4	31.0
22	Mouse #4	2	Ctrl/20%	27.4	1.4	27.0
23	Mouse #1	4	Ctrl/20%	36.8	2.0	27.2
24	Mouse #1	5	Ctrl/20%	31.6	2.0	33.2
25	Mouse # 1	2	MCD/water	16.9	0.8	16.6
26	Mouse #2	2	MCD/water	18.5	0.6	17.8
27	Mouse #1	3	MCD/water	16.0	0.6	15.6
28	Mouse #2	3	MCD/water	20.4	0.8	19.8
29	Mouse #1	4	MCD/water	18.9	0.8	20.0
30	Mouse #2	4	MCD/water	14.3	**Found eaten**	
31	Mouse #1	1	MCD/8%	18.7	1.0	18.0
32	Mouse #2	1	MCD/8%	16.6	0.8	16.2
33	Mouse #3	1	MCD/8%	16.9	1.0	16.6
34	Mouse #1	2	MCD/8%	15.6	0.8	15.2
35	Mouse #1	3	MCD/8%	17.9	0.8	16.8
36	Mouse #3	3	MCD/8%	18.3	0.8	17.4
37	Mouse #4	3	MCD/8%	17.9	0.8	17.2
38	Mouse #1	1	MCD/20%	18.9	1.0	18.6
39	Mouse #1	2	MCD/20%	17.5	1.0	17.4
40	Mouse #1	3	MCD/20%	16.0	0.8	15.6
41	Mouse #1	4	MCD/20%	16.6	1.0	17.2
42	Mouse #2	4	MCD/20%	17.6	0.8	17.8
43	Mouse #1	5	MCD/20%	16.7	0.8	16.2
44	Mouse #2	5	MCD/20%	17.9	1.0	17.4
45	Mouse #3	5	MCD/20%	18.1	0.8	17.6

Sacrifice Details for Group 2 Mice

New No.		Cage #	Treatment	Wght. at Week 13	Body Weight	Weight of liver
	Mouse #1	5	Ctrl/Water	31.5	*Found dead Monday August 13, 2002*	
	Mouse #2	5	Ctrl/Water	29.4		
	Mouse #3	5	Ctrl/Water	30.6		
	Mouse #4	5	Ctrl/Water	36.2		
50	Mouse #1	6	Ctrl/Water	39.1	33.8	0.8
51	Mouse #1	7	Ctrl/Water	28.4	36.4	1.2
49	Mouse #1	8	Ctrl/Water	43.7	33.8	0.8
52	Mouse #1	4	Ctrl/8%	35.5	31.2	1.6
53	Mouse #2	4	Ctrl/8%	33.7	30.6	1.0
54	Mouse #3	4	Ctrl/8%	29.7	27.2	1.2
55	Mouse #1	5	Ctrl/8%	29.2	29.4	1.0
56	Mouse #2	5	Ctrl/8%	32.1	32.4	1.4
57	Mouse #1	6	Ctrl/8%	37.3	37.4	1.4
58	Mouse #1	7	Ctrl/8%	42.3	42.6	1.4
59	Mouse #1	8	Ctrl/8%	31.2	31.0	1.2
60	Mouse #1	6	Ctrl/20%	30.3	28.8	1.4
61	Mouse #2	6	Ctrl/20%	32.0	31.2	1.4
62	Mouse #3	6	Ctrl/20%	34.3	32.6	1.4
63	Mouse #1	7	Ctrl/20%	31.8	28.0	1.6
64	Mouse #2	7	Ctrl/20%	36.5	33.6	1.6
65	Mouse #3	7	Ctrl/20%	36.0	33.4	2.0
66	Mouse #4	7	Ctrl/20%	30.7	28.4	1.8
67	Mouse #1	5	MCD/water	18.1	18.4	0.6
68	Mouse #1	6	MCD/water	20.0	19.0	1.0
69	Mouse #1	7	MCD/water	16.1	15.0	0.6
70	Mouse #1	8	MCD/water	18.1	16.0	0.8
71	Mouse #1	9	MCD/water	19.1	18.0	0.8
72	Mouse #2	9	MCD/water	20.8	18.6	1.0
74	Mouse #3	9	MCD/water	15.0	14.0	0.6
73	Mouse #4	9	MCD/water	18.2	17.2	0.6
75	Mouse #1	4	MCD/8%	16.4	15.8	1.0
76	Mouse #1	5	MCD/8%	20.0	19.6	1.2
77	Mouse #2	5	MCD/8%	19.2	17.8	1.0
78	Mouse #3	5	MCD/8%	16.1	14.6	0.8
79	Mouse #1	6	MCD/8%	18.7	17.6	0.8
80	Mouse #2	6	MCD/8%	19.1	19.8	1.0
81	Mouse #3	6	MCD/8%	18.7	19.0	0.8
82	Mouse #1	7	MCD/8%	19.8	18.0	1.2
83	Mouse #1	6	MCD/20%	20.2	18.6	1.2
84	Mouse #1	7	MCD/20%	16.0	14.4	0.8
85	Mouse #2	7	MCD/20%	17.1	15.4	0.8
86	Mouse #1	8	MCD/20%	18.9	17.4	1.0
87	Mouse #2	9	MCD/20%	18.7	19.0	0.8
88	Mouse #3	9	MCD/20%	19.1	20.0	1.0
89	Mouse #1	10	MCD/20%	17.7	16.2	0.8
90	Mouse #2	10	MCD/20%	18.2	16.6	0.8

Appendix 2.3.1: ALT and AST levels in the LTS, given in U/L

Mouse #	Treatment	AST	ALT	AST/ALT
1	Ctrl/water	18	37	0.49
2	Ctrl/water	38	40	0.95
3	Ctrl/water	37	28	1.32
4	Ctrl/water	98	38	2.58
5	Ctrl/water	20	33	0.61
6	Ctrl/water	31	27	1.15
7	Ctrl/water	42	88	0.48
8	Ctrl/water	26	13	2.00
9	Ctrl/8%	28	14	2.00
10	Ctrl/8%	36	12	3.00
11	Ctrl/8%	33	22	1.50
12	Ctrl/8%	18	16	1.13
13	Ctrl/8%	34	20	1.70
14	Ctrl/8%	30	20	1.50
15	Ctrl/8%	791	238	3.32
16	Ctrl/8%	51	37	1.38
17	Ctrl/20%	56	13	4.31
18	Ctrl/20%	26	29	0.90
19	Ctrl/20%	24	16	1.50
20	Ctrl/20%	N/a	N/a	N/a
21	Ctrl/20%	42	37	1.14
22	Ctrl/20%	18	42	0.43
23	Ctrl/20%	17	14	1.21
24	Ctrl/20%	11	15	0.73
25	MCD/water	121	196	0.62
26	MCD/water	190	97	1.96
27	MCD/water	170	46	3.70
28	MCD/water	114	48	2.38
29	MCD/water	79	69	1.14
31	MCD/8%	71	44	1.61
32	MCD/8%	68	61	1.11
33	MCD/8%	96	68	1.41
34	MCD/8%	164	117	1.40
35	MCD/8%	296	304	0.97
36	MCD/8%	170	199	0.85
37	MCD/8%	200	290	0.69
38	MCD/20%	332	298	1.11
39	MCD/20%	235	265	0.89
40	MCD/20%	180	132	1.36
41	MCD/20%	150	154	0.97
42	MCD/20%	165	94	1.76
43	MCD/20%	182	190	0.96
44	MCD/20%	30	88	0.34
45	MCD/20%	307	268	1.15

Appendix 2.3.2: Mean, Standard deviation (SD) for ALT, AST, AST/ALT

		MEAN	SD
ALT	CTRL	38	20.54
	CTRL 8%	19.25	7.53
	CTRL 20%	25.5	11.18
	MCD	91.2	55.53
	MCD 8%	154.71	101.79
	MCD 20%	186.13	77.08
AST	CTRL	40	22.92
	CTRL 8%	128	180.48
	CTRL 20%	38.83	38.01
	MCD	124.8	47.76
	MCD 8%	165.67	73.69
	MCD 20%	178.43	78.16
RATIO	CTRL	1.64	0.85
	CTRL 8%	1.62	0.69
	CTRL 20%	1.01	0.50
	MCD	1.96	1.06
	MCD 8%	1.15	0.31
	MCD 20%	1.07	0.38

Appendix 2.4 (a): Liver pathology in the Long Term Study, Ctrl samples

Mouse #	Treatment	Fat (score)	Fat (distribution)	Inflammatory foci score	No. foci	D/PAS Macrophages (score)	No. macs	Fibrosis (Score)	Fibrosis (distribution)
1	Ctrl/water	0	N/A	1	4	0	0	0	0
2	Ctrl/water	0	N/A	0	1	0	0	0	0
3	Ctrl/water	0	N/A	0	0	0	0	0	0
4	Ctrl/water	0	N/A	0	3	0	0	0	0
5	Ctrl/water	0	N/A	0	0	0	0	0	0
6	Ctrl/water	0	N/A	0	1	0	0	0	0
7	Ctrl/water	0	N/A	0	1	0	0	0	0
8	Ctrl/water	0	N/A	0	1	0	0	0	0
9	Ctrl/8%	0	N/A	1	5	0	0	0	0
10	Ctrl/8%	0	N/A	0	1	0	0	0	0
11	Ctrl/8%	0	N/A	0	0	0	0	0	0
12	Ctrl/8%	0	N/A	0	0	0	0	0	0
13	Ctrl/8%	0	N/A	0	1	0	0	0	0
14	Ctrl/8%	0	N/A	0	3	0	0	0	0
15	Ctrl/8%	IGNORE, MOUSE WAS ILL							
16	Ctrl/8%	0	N/A	0	2	0	0	0	0
17	Ctrl/20%	1	N/A	1	4	0	0	0	0
18	Ctrl/20%	1	random	0	1	0	0	0	0
19	Ctrl/20%	1	N/A	0	1	0	0	0	0
20	Ctrl/20%	1	N/A	1	5	0	0	0	0
21	Ctrl/20%	1	N/A	0	2	0	0	0	0
22	Ctrl/20%	0	N/A	0	3	0	0	0	0
23	Ctrl/20%	1	N/A	1	4	0	0	0	0
24	Ctrl/20%	1	N/A	1	4	0	0	0	0

Macs: Macrophages. ***D/PAS numbers and scores are based on counts of enlarged macrophages.***
Random indicates that some fat was found in all zones, with no zonal predominance.
All assessments conducted on 20 high power fields (40x objective)

Appendix 2.4 (b): Liver Pathology in the Long Term Study, MCD samples

Mouse #	Treatment	Fat (score)	Fat (distribution)	Inflammatory foci score	No. foci	D/PAS Macrophages (score)	No. macs	Fibrosis (Score)	Fibrosis (distribution)
25	MCD/water	3	Z1 to z3	3	55	3	110	1	PC
26	MCD/water	3	Z1 to z2	3	35	3	51	0	
27	MCD/water	3	Z1 to z2	3	30	3	57	0	
28	MCD/water	3	Z1 to z3	3	65	3	175	1	PC
29	MCD/water	2 ↓	Z2	Query 2		3	42	1 ↓	PC
30	MCD/8%	3	Z1 to z3						
31	MCD/8%	3	Z1 to z3	3	33	3	42	0	
32	MCD/8%	3	Z1 to z2	3	33	3	71	1	PC
33	MCD/8%	3	Z1 to z2	3	33	3	61	1	PC
34	MCD/8%	3	Z1 to z3	3	23	3	45	0	
35	MCD/8%	3 ↓, query 2	Z2	3	40	3	84	1	PC
36	MCD/8%	3	Z1 to z2	3	46	3	110	1	PC
37	MCD/8%	3	Z1 to z2	3	58	3	100	1	PC
38	MCD/20%	3	Query z1to z3	3	44	3	132	0	
39	MCD/20%	3	Z1 to z2	3	59	3	93	1	PC
40	MCD/20%	3	Z1 to z3	3	29	3	35	1	
41	MCD/20%	3	Z1 to z2	3	28	3	104	1	PC
42	MCD/20%	3	Z1 to z2	3	46	3	146	1	PC
43	MCD/20%	3	Z1 to z2	3	37	3	84	1	PC
44	MCD/20%	3	Z1 to z2	3	45	3	65	1 ↓	PC
45	MCD/20%	3	Z1 to z2	3	55	3	127	1	PC

Macs: Macrophages. ***D/PAS numbers and scores are based on counts of enlarged macrophages.*** **PC:** Pericellular; **Z:** Zones.
All assessments conducted on 20 high power fields (40x objective)

Appendix 2.5: Raw data for hydroxyproline (Hyp) showing mean, SD

Mouse #	Treatment	Hyp from curve [ug]	Hyp in sample [ug]	Total Protein [mg]	Hyp per mg protein
1	Ctrl/water	1.94	16.20	10.18	1.59
2	Ctrl/water	1.59	13.24	8.92	1.49
3	Ctrl/water	3.05	25.38	7.25	3.50
4	Ctrl/water	N/a			
5	Ctrl/water	N/a			
6	Ctrl/water	3.44	28.65	10.87	2.64
7	Ctrl/water	2.65	22.10	9.81	2.25
8	Ctrl/water	2.14	17.83	8.19	2.18
9	Ctrl/8%	3.20	26.63	12.31	2.16
10	Ctrl/8%	4.03	33.57	12.95	2.59
11	Ctrl/8%	4.46	37.18	11.24	3.31
12	Ctrl/8%	3.28	27.34	9.60	2.85
13	Ctrl/8%	2.65	22.10	12.63	1.75
14	Ctrl/8%	3.16	26.36	8.24	3.20
15	Ctrl/8%	N/a		8.918	
16	Ctrl/8%	2.89	24.06	10.08	2.39
17	Ctrl/8%	3.01	25.05	11.14	2.25
18	Ctrl/20%	N/a		9.18	
19	Ctrl/20%	3.16	26.36	11.03	2.39
20	Ctrl/20%	4.42	36.85	11.67	3.16
21	Ctrl/20%	N/a		10.552	
22	Ctrl/20%	3.87	32.26	10.02	3.22
23	Ctrl/20%	3.24	27.02	12.69	2.13
24	Ctrl/20%	3.40	28.33	10.82	2.62
25	MCD/water	3.56	29.64	9.50	3.12
26	MCD/water	3.71	30.95	11.30	2.74
27	MCD/water	3.99	33.24	10.34	3.22
28	MCD/water	5.05	42.10	9.39	4.48
29	MCD/water	3.56	29.64	11.99	2.47
31	MCD/8%	3.67	30.62	11.46	2.67
32	MCD/8%	3.44	28.65	11.88	2.41
33	MCD/8%	2.57	21.44	8.60	2.49
34	MCD/8%	2.77	23.08	9.02	2.56
35	MCD/8%	3.32	27.67	10.08	2.75
36	MCD/8%	4.26	35.54	11.56	3.07
37	MCD/8%	4.11	34.23	10.55	3.24
38	MCD/20%	3.87	32.26	12.26	2.63
39	MCD/20%	2.69	22.43	13.71	1.64
40	MCD/20%	2.57	21.44	11.78	1.82
41	MCD/20%	3.48	28.98	9.97	2.91
42	MCD/20%	2.65	22.10	13.55	1.63
43	MCD/20%	2.26	18.82	13.01	1.45
44	MCD/20%	4.38	36.52	10.98	3.33
45	MCD/20%	3.24	27.02	9.34	2.89
		MEAN	SD		
	CTRL/WATER	2.27	0.68		
	CTRL/8%	2.52	0.52		
	CTRL/20%	2.70	0.43		
	MCD/WATER	3.21	0.69		
	MCD/8%	2.74	0.29		
	MCD/20%	2.29	0.68		

Appendix 2.6: Raw data for hepatic triglycerides (TG) showing mean, SD

Mouse #	Treatment	TG from curve [ug]	TG per ml [ug]	Total TG [ug]	Total protein [mg]	TG [ug] per mg protein
1	Ctrl/water	7.37	0.74	1474.76	10.18	144.85
2	Ctrl/water	3.25	0.32	649.12	8.92	72.79
3	Ctrl/water	3.70	0.37	740.86	7.25	102.20
4	Ctrl/water	N/a	N/a	N/a	N/a	N/a
5	Ctrl/water	3.09	0.31	618.54	9.29	66.62
6	Ctrl/water	N/a	N/a	N/a	N/a	N/a
7	Ctrl/water	4.32	0.43	863.18	9.81	87.97
8	Ctrl/water	2.48	0.25	496.22	8.19	60.62
9	Ctrl/8%	12.60	1.26	2520.40	12.31	204.74
10	Ctrl/8%	15.12	1.51	3024.80	12.95	233.50
11	Ctrl/8%	14.22	1.42	2844.60	11.24	253.03
12	Ctrl/8%	4.77	0.48	953.40	9.60	99.30
13	Ctrl/8%	8.23	0.82	1646.20	12.63	130.33
14	Ctrl/8%	29.33	2.93	5865.80	8.24	712.04
15	Ctrl/8%	8.08	0.81	1615.80	8.92	181.18
16	Ctrl/8%	11.07	1.11	2213.00	10.08	219.63
17	Ctrl/8%	6.34	0.63	1268.20	11.14	113.88
18	Ctrl/20%	7.60	0.76	1520.20	9.18	165.60
19	Ctrl/20%	9.65	0.96	1929.60	11.03	174.96
20	Ctrl/20%	6.66	0.67	1331.20	11.67	114.09
21	Ctrl/20%	6.34	0.63	1268.20	10.55	120.19
22	Ctrl/20%	6.97	0.70	1394.20	10.02	139.10
23	Ctrl/20%	7.76	0.78	1551.60	12.69	122.32
24	Ctrl/20%	12.64	1.26	2527.80	10.82	233.69
25	MCD/water	16.89	1.69	3378.20	9.50	355.75
26	MCD/water	11.85	1.19	2370.40	11.30	209.84
27	MCD/water	27.91	2.79	5582.40	10.34	539.88
28	MCD/water	8.86	0.89	1772.20	9.39	188.71
29	MCD/water	40.04	4.00	8007.20	11.99	667.88
31	MCD/8%	21.14	2.11	4228.40	11.46	369.13
32	MCD/8%	39.88	3.99	7975.80	11.88	671.25
33	MCD/8%	20.67	2.07	4133.80	8.60	480.45
34	MCD/8%	7.44	0.74	1488.60	9.02	164.98
35	MCD/8%	12.48	1.25	2496.40	10.08	247.76
36	MCD/8%	13.74	1.37	2748.40	11.56	237.71
37	MCD/8%	35.31	3.53	7062.60	10.55	669.31
38	MCD/20%	22.40	2.24	4480.20	12.26	365.55
39	MCD/20%	17.05	1.70	3409.60	13.71	248.73
40	MCD/20%	26.02	2.60	5204.60	11.78	442.00
41	MCD/20%	25.55	2.56	5110.00	9.97	512.54
42	MCD/20%	14.37	1.44	2874.20	13.55	212.18
43	MCD/20%	35.94	3.59	7188.40	13.01	552.61
44	MCD/20%	38.78	3.88	7755.20	10.98	706.56
45	MCD/20%	23.19	2.32	4637.80	9.34	496.66
			MEAN	SD		
		CTRL/WATER	89.18	28.47		
		CTRL/8%	238.63	175.08		
		CTRL/20%	152.85	39.42		
		CTRL/8%-15	245.81	184.44		
		MCD/WATER	392.41	186.44		
		MCD/8%	405.80	192.00		
		MCD/20%	442.10	152.56		

Appendix 2.7: Serum TG raw data, mean and SD (Group2 mice)

Mouse #	Treatment	Serum TG from curve [ug]	TG [mg] per L serum
50	Ctrl/Water	9.82	490.93
51	Ctrl/Water	19.33	966.36
49	Ctrl/Water	22.09	1104.38
52	Ctrl/8%	12.73	636.62
53	Ctrl/8%	16.72	836.00
54	Ctrl/8%	21.47	1073.71
55	Ctrl/8%	24.69	1234.74
56	Ctrl/8%	20.86	1043.04
57	Ctrl/8%	21.78	1089.05
58	Ctrl/8%	33.44	1671.83
59	Ctrl/8%	19.63	981.69
60	Ctrl/20%	16.87	843.67
61	Ctrl/20%	15.03	751.65
62	Ctrl/20%	20.55	1027.70
63	Ctrl/20%	9.67	483.26
64	Ctrl/20%	10.59	529.27
65	Ctrl/20%	11.05	552.27
66	Ctrl/20%	14.11	705.64
67	MCD/water	21.01	1050.71
68	MCD/water	14.57	728.64
69	MCD/water	35.28	1763.85
70	MCD/water	20.86	1043.04
71	MCD/water	14.57	728.64
72	MCD/water	17.49	874.34
74	MCD/water	10.43	521.60
73	MCD/water	15.65	782.32
75	MCD/8%	20.40	1020.03
76	MCD/8%	15.34	766.98
77	MCD/8%	19.94	997.03
78	MCD/8%	12.58	628.96
79	MCD/8%	7.52	375.91
80	MCD/8%	9.67	483.26
81	MCD/8%	13.65	682.63
82	MCD/8%	14.42	720.97
83	MCD/20%	20.40	1020.03
84	MCD/20%	17.49	874.34
85	MCD/20%	19.48	974.03
86	MCD/20%	11.20	559.94
87	MCD/20%	18.41	920.35
88	MCD/20%	15.95	797.66
89	MCD/20%	9.67	483.26
90	MCD/20%	13.50	674.97
		MEAN	SD
	CTRL/WATER	853.89	262.77
	CTRL/8%	1070.84	283.02
	CTRL/20%	699.07	180.74
	MCD/WATER	936.64	352.68
	MCD/8%	709.47	209.83
	MCD/20%	788.07	184.11

Appendix 2.8: Raw data, mean and SD for hepatic phosphatidylcholine (PC)

Mouse #	Treatment	PC from curve [ug]	PC in sample [ug]	Total protein [mg]	PC per mg protein
1	Ctrl/water	5.63	140.68	10.18	13.82
2	Ctrl/water	9.77	244.15	8.92	27.38
3	Ctrl/water	10.00	250.00	7.25	34.49
4	Ctrl/water	6.60	165.08	8.71	18.95
5	Ctrl/water	9.92	248.05	9.29	26.72
6	Ctrl/water	6.99	174.83	10.87	16.08
7	Ctrl/water	5.59	139.70	9.81	14.24
8	Ctrl/water	8.79	219.75	8.19	26.84
9	Ctrl/8%	8.01	200.23	12.31	16.27
10	Ctrl/8%	8.05	201.20	12.95	15.53
11	Ctrl/8%	N/a	N/a	N/a	N/a
12	Ctrl/8%	N/a	N/a	N/a	N/a
13	Ctrl/8%	4.38	218.79	12.63	17.32
14	Ctrl/8%	4.69	234.73	8.24	28.49
15	Ctrl/8%	4.85	121.35	8.92	13.61
16	Ctrl/8%	7.65	191.35	10.08	18.99
17	Ctrl/8%	6.56	164.03	11.14	14.73
18	Ctrl/20%	8.52	212.97	9.18	23.20
19	Ctrl/20%	7.68	191.91	11.03	17.40
20	Ctrl/20%	8.52	212.97	11.67	18.25
21	Ctrl/20%	7.61	190.21	10.55	18.03
22	Ctrl/20%	7.63	190.78	10.02	19.03
23	Ctrl/20%	8.20	205.00	12.69	16.16
24	Ctrl/20%	5.17	129.31	10.82	11.95
25	MCD/water	6.11	152.65	9.50	16.07
26	MCD/water	4.26	106.55	11.30	9.43
27	MCD/water	5.04	125.90	10.34	12.18
28	MCD/water	4.31	107.69	9.39	11.47
29	MCD/water	3.01	75.25	11.99	6.28
31	MCD/8%			11.46	
32	MCD/8%	6.47	161.75	11.88	13.61
33	MCD/8%	4.83	120.78	8.60	14.04
34	MCD/8%	4.88	121.92	9.02	13.51
35	MCD/8%	5.56	138.99	10.08	13.79
36	MCD/8%	4.56	113.95	11.56	9.86
37	MCD/8%	4.33	108.26	10.55	10.26
38	MCD/20%	5.49	137.28	12.26	11.20
39	MCD/20%	3.69	92.32	13.71	6.73
40	MCD/20%	4.40	109.96	11.78	9.34
41	MCD/20%	5.22	130.45	9.97	13.08
42	MCD/20%	5.67	141.83	13.55	10.47
43	MCD/20%	3.28	82.08	13.01	6.31
44	MCD/20%	3.58	89.48	10.98	8.15
45	MCD/20%	4.63	115.66	9.34	12.39
		MEAN	SD		
	CTRL/WATER	22.31	7.08		
	CTRL 8%	17.85	4.64		
	CTRL 20%	17.72	3.11		
	MCD/WATER	11.09	3.23		
	MCD 8%	11.57	1.75		
	MCD 20%	9.71	2.35		

Appendix 2.9: Raw data, mean and SD for Conjugated dienes (CD)

Mouse #	Treatment	OD 234	CD [nMol]	Total protein [mg]	CD per mg protein
1	Ctrl/water	0.141	119.49	10.18	11.74
2	Ctrl/water	0.132	111.86	8.92	12.54
3	Ctrl/water	0.105	88.98	7.25	12.28
4	Ctrl/water	0.137	116.10	8.71	13.33
5	Ctrl/water	0.142	120.34	9.29	12.96
6	Ctrl/water	0.127	107.63	10.87	9.90
7	Ctrl/water	0.169	143.22	9.81	14.60
8	Ctrl/water	0.121	102.54	8.19	12.53
9	Ctrl/8%	0.287	243.22	12.31	19.76
10	Ctrl/8%	0.175	148.31	12.95	11.45
11	Ctrl/8%	0.17	144.07	11.24	12.82
12	Ctrl/8%	0.137	116.10	9.60	12.09
13	Ctrl/8%	0.0945	160.17	12.63	12.68
14	Ctrl/8%	0.091	154.24	8.24	18.72
15	Ctrl/8%	0.294	249.15	8.92	27.94
16	Ctrl/8%	0.182	154.24	10.08	15.31
17	Ctrl/8%	0.183	155.08	11.14	13.93
18	Ctrl/20%	0.186	157.63	9.18	17.17
19	Ctrl/20%	0.177	150.00	11.03	13.60
20	Ctrl/20%	0.187	158.47	11.67	13.58
21	Ctrl/20%	0.15	127.12	10.55	12.05
22	Ctrl/20%	0.178	150.85	10.02	15.05
23	Ctrl/20%	0.207	175.42	12.69	13.83
24	Ctrl/20%	0.161	136.44	10.82	12.61
25	MCD/water	0.307	260.17	9.50	27.40
26	MCD/water	0.33	279.66	11.30	24.76
27	MCD/water	0.23	194.92	10.34	18.85
28	MCD/water	0.257	217.80	9.39	23.19
29	MCD/water	0.295	250.00	11.99	20.85
31	MCD/8%	0.198	167.80	11.46	14.65
32	MCD/8%	0.324	274.58	11.88	23.11
33	MCD/8%	0.292	247.46	8.60	28.76
34	MCD/8%	0.264	223.73	9.02	24.80
35	MCD/8%	0.532	450.85	10.08	44.74
36	MCD/8%	0.612	518.64	11.56	44.86
37	MCD/8%	0.479	405.93	10.55	38.47
38	MCD/20%	0.277	234.75	12.26	19.15
39	MCD/20%	0.214	181.36	13.71	13.23
40	MCD/20%	0.288	244.07	11.78	20.73
41	MCD/20%	0.224	189.83	9.97	19.04
42	MCD/20%	0.252	213.56	13.55	15.77
43	MCD/20%	0.356	301.69	13.01	23.19
44	MCD/20%	0.251	212.71	10.98	19.38
45	MCD/20%	0.279	236.44	9.34	25.32
				MEAN	SD
			CTRL/WATER	12.48	1.26
			CTRL /8%	16.08	5.01
			CTRL/20%	13.98	1.57
			CTRL/8%-15	14.59	2.91
			MCD/WATER	23.01	2.98
			MCD/8%	31.34	10.75
			MCD/20%	19.48	3.58

Appendix 2.10: Raw data, mean and SD for lipid hydroperxides (LOOH)

Mouse #	Treatment	LOOH from curve [nMol]	LOOH in sample [nMol]	Total protein [mg]	LOOH per mg protein
1	Ctrl/water	0.125	3.13	10.18	0.31
2	Ctrl/water	0.100	2.50	8.92	0.28
3	Ctrl/water	0.033	0.83	7.25	0.11
4	Ctrl/water	N/a	N/a	N/a	N/a
5	Ctrl/water	0.587	14.68	9.29	1.58
6	Ctrl/water	0.209	5.23	10.87	0.48
7	Ctrl/water	0.017	0.43	9.81	0.04
8	Ctrl/water	0.184	4.60	8.19	0.56
9	Ctrl/8%	2.446	61.15	12.31	4.97
10	Ctrl/8%	0.293	7.33	12.95	0.57
11	Ctrl/8%	0.251	6.28	11.24	0.56
12	Ctrl/8%	0.301	7.53	9.60	0.78
13	Ctrl/8%	0.167	8.35	12.63	0.66
14	Ctrl/8%			8.24	
15	Ctrl/8%	1.091	27.28	8.92	3.06
16	Ctrl/8%	0.249	6.23	10.08	0.62
17	Ctrl/8%	0.785	19.63	11.14	1.76
18	Ctrl/20%			9.18	
19	Ctrl/20%	0.203	5.08	11.03	0.46
20	Ctrl/20%	0.092	2.30	11.67	0.20
21	Ctrl/20%	0	0.00	10.55	0.00
22	Ctrl/20%	0.166	4.15	10.02	0.41
23	Ctrl/20%	0.092	2.30	12.69	0.18
24	Ctrl/20%	0.101	2.53	10.82	0.23
25	MCD/water	0.553	13.83	9.50	1.46
26	MCD/water	0.049	1.23	11.30	0.11
27	MCD/water	0.041	1.03	10.34	0.10
28	MCD/water	1.186	29.65	9.39	3.16
29	MCD/water	0.09	2.25	11.99	0.19
31	MCD/8%	0.132	3.30	11.46	0.29
32	MCD/8%	0.305	7.63	11.88	0.64
33	MCD/8%	0.222	5.55	8.60	0.65
34	MCD/8%	0.379	9.48	9.02	1.05
35	MCD/8%	0.802	20.05	10.08	1.99
36	MCD/8%	0.844	21.10	11.56	1.82
37	MCD/8%	0.661	16.53	10.55	1.57
38	MCD/20%	1.058	26.45	12.26	2.16
39	MCD/20%	0.505	12.63	13.71	0.92
40	MCD/20%	0.956	23.90	11.78	2.03
41	MCD/20%	0.82	20.50	9.97	2.06
42	MCD/20%	1.591	39.78	13.55	2.94
43	MCD/20%	0.633	15.83	13.01	1.22
44	MCD/20%	0.489	12.23	10.98	1.11
45	MCD/20%	0.913	22.83	9.34	2.44
		MEAN	SD		
	CTRL/WATER	0.48	0.48		no 4
	CTRL/8%	0.82	0.43		outliers 9, 15; no 14
	CTRL/20%	0.30	0.12		outlier 21
	MCD/WATER	1.00	1.13		
	MCD/8%	1.14	0.61		
	MCD/20%	1.86	0.66		

Appendix 2.11(a): Raw data for free thiobarbituric acid reactive substances (fTBARS)

Mouse #	Treatment	OD 540	fTBARS [nMol]	Total protein [mg]	fTBARS per mg protein
1	Ctrl/water	0.032	63.12	10.18	6.20
2	Ctrl/water	0.029	57.20	8.92	6.41
3	Ctrl/water	0.035	69.04	7.25	9.52
4	Ctrl/water	0.048	94.68	8.71	10.87
5	Ctrl/water	0.056	110.46	9.29	11.90
6	Ctrl/water	0.054	106.51	10.87	9.80
7	Ctrl/water	0.05	98.62	9.81	10.05
8	Ctrl/water	0.035	69.04	8.19	8.43
9	Ctrl/8%	0.048	94.68	12.31	7.69
10	Ctrl/8%	0.061	120.32	12.95	9.29
11	Ctrl/8%	0.049	96.65	11.24	8.60
12	Ctrl/8%	0.048	94.68	9.60	9.86
13	Ctrl/8%	0.003	11.83	12.63	0.94
14	Ctrl/8%	0.001	3.94	8.24	0.48
15	Ctrl/8%	0.02	39.45	8.92	4.42
16	Ctrl/8%	0.009	17.75	10.08	1.76
17	Ctrl/8%	0.006	11.83	11.14	1.06
18	Ctrl/20%	0.008	15.78	9.18	1.72
19	Ctrl/20%	0.006	11.83	11.03	1.07
20	Ctrl/20%	0.009	17.75	11.67	1.52
21	Ctrl/20%	0.007	13.81	10.55	1.31
22	Ctrl/20%	0.005	9.86	10.02	0.98
23	Ctrl/20%	0.005	9.86	12.69	0.78
24	Ctrl/20%	0.002	3.94	10.82	0.36
25	MCD/water	0.022	43.39	9.50	4.57
26	MCD/water	0.024	47.34	11.30	4.19
27	MCD/water	0.019	37.48	10.34	3.62
28	MCD/water	0.032	63.12	9.39	6.72
29	MCD/water	0.017	33.53	11.99	2.80
31	MCD/8%	0.014	27.61	11.46	2.41
32	MCD/8%	0.022	43.39	11.88	3.65
33	MCD/8%	0.022	43.39	8.60	5.04
34	MCD/8%	0.027	53.26	9.02	5.90
35	MCD/8%	0.024	47.34	10.08	4.70
36	MCD/8%	0.024	47.34	11.56	4.09
37	MCD/8%	0.03	59.17	10.55	5.61
38	MCD/20%	0.139	274.17	12.26	22.37
39	MCD/20%	0.208	410.28	13.71	29.93
40	MCD/20%	0.095	187.39	11.78	15.91
41	MCD/20%	0.196	386.61	9.97	38.78
42	MCD/20%	0.102	201.19	13.55	14.85
43	MCD/20%	0.143	282.06	13.01	21.68
44	MCD/20%	0.13	256.42	10.98	23.36
45	MCD/20%	0.102	201.19	9.34	21.55

Appendix 2.11(b): Mean and SD for fTBARS

	MEAN	SD
CTRL/WATER	9.15	1.89
CTRL/8%	4.90	3.73
CTRL/20%	1.11	0.42
CTRL/8%-15	4.96	3.95
MCD/WATER	4.38	1.31
MCD/8%	4.49	1.12
MCD/20%	23.55	7.21

Appendix 2.12(a): Raw data for total thiobarbituric acid reactive substances (tTBARS)

Mouse #	Treatment	OD 540	tTBARS [nMol]	Total Protein [mg]	tTBARS per mg protein
1	Ctrl/water	0.106	209.08	10.18	20.54
2	Ctrl/water	0.094	185.41	8.92	20.79
3	Ctrl/water	0.092	181.47	7.25	25.03
4	Ctrl/water	0.08	157.80	8.71	18.12
5	Ctrl/water	0.144	284.04	9.29	30.59
6	Ctrl/water	0.067	132.16	10.87	12.16
7	Ctrl/water	0.047	92.71	9.81	9.45
8	Ctrl/water	0.045	88.76	8.19	10.84
9	Ctrl/8%	0.139	274.17	12.31	22.27
10	Ctrl/8%	0.113	222.89	12.95	17.21
11	Ctrl/8%	0.137	270.23	11.24	24.04
12	Ctrl/8%	0.117	230.78	9.60	24.04
13	Ctrl/8%	0.022	86.79	12.63	6.87
14	Ctrl/8%	0.033	130.18	8.24	15.80
15	Ctrl/8%	0.995	1962.61	8.92	220.07
16	Ctrl/8%	0.221	435.92	10.08	43.26
17	Ctrl/8%	0.065	128.21	11.14	11.51
18	Ctrl/20%	0.169	333.35	9.18	36.31
19	Ctrl/20%	0.105	207.11	11.03	18.78
20	Ctrl/20%	0.199	392.52	11.67	33.64
21	Ctrl/20%	0.192	378.72	10.55	35.89
22	Ctrl/20%	0.049	96.65	10.02	9.64
23	Ctrl/20%	0.037	72.98	12.69	5.75
24	Ctrl/20%	0.028	55.23	10.82	5.11
25	MCD/water	1.246	2457.71	9.50	258.81
26	MCD/water	1.248	2461.65	11.30	217.92
27	MCD/water	1.119	2207.20	10.34	213.46
28	MCD/water	1.246	2457.71	9.39	261.71
29	MCD/water	0.753	1485.28	11.99	123.89
31	MCD/8%	1.465	2889.68	11.46	252.26
32	MCD/8%	1.579	3114.54	11.88	262.12
33	MCD/8%	1.679	3311.79	8.60	384.91
34	MCD/8%	2.346	4627.43	9.02	512.85
35	MCD/8%	1.229	2424.17	10.08	240.59
36	MCD/8%	1.256	2477.43	11.56	214.27
37	MCD/8%	1.11	2189.45	10.55	207.49
38	MCD/20%	1.133	2234.82	12.26	182.34
39	MCD/20%	1.107	2183.53	13.71	159.29
40	MCD/20%	0.671	1323.53	11.78	112.40
41	MCD/20%	1.474	2907.43	9.97	291.62
42	MCD/20%	1.001	1974.45	13.55	145.76
43	MCD/20%	1.01	1992.20	13.01	153.15
44	MCD/20%	0.984	1940.92	10.98	176.83
45	MCD/20%	1.058	2086.88	9.34	223.48
				MEAN	SD
			CTRL/WATER	18.44	6.88
			CTRL/8%	42.79	63.43
			CTRL/20%	20.73	13.28
			CTRL/8%-15	20.63	10.28
			MCD/WATER	215.16	49.83
			MCD/8%	296.36	103.90
			MCD/20%	180.61	51.54

Appendix 2.13: Raw data, mean and SD for CYP2E1 activity, indicated by rate of generation of *p*-Aminophenol (*p*-AP)

Mouse #	Treatment	nMols *p*-AP from curve	nMols *p*-AP per ul	nMols *p*-AP in 120 ul	Microsomal protein [mg]	nMols *p*-AP/mg protein/min
1	Ctrl/water	0.375	0.008	0.900	5.141	0.003
2	Ctrl/water	0.437	0.009	1.049	5.047	0.003
3	Ctrl/water	0.375	0.008	0.900	3.464	0.004
4	Ctrl/water	0.437	0.009	1.049	2.857	0.006
5	Ctrl/water	0.395	0.008	0.948	4.439	0.004
6	Ctrl/water	1.636	0.033	3.926	5.109	0.013
7	Ctrl/water	0.620	0.012	1.488	6.208	0.004
8	Ctrl/water	0.620	0.012	1.488	5.364	0.005
9	Ctrl/8%	0.312	0.006	0.749	6.016	0.002
10	Ctrl/8%	0.500	0.010	1.200	6.973	0.003
11	Ctrl/8%	0.312	0.006	0.749	3.580	0.003
12	Ctrl/8%	0.496	0.010	1.190	3.177	0.006
13	Ctrl/8%	0.395	0.008	0.948	5.601	0.003
14	Ctrl/8%	0.790	0.016	1.896	5.252	0.006
15	Ctrl/8%	3.954	0.079	9.490	3.766	0.042
16	Ctrl/8%	0.902	0.018	2.165	4.212	0.009
17	Ctrl/8%	0.564	0.011	1.354	5.276	0.004
18	Ctrl/20%	0.500	0.010	1.200	6.651	0.003
19	Ctrl/20%	0.375	0.008	0.900	6.877	0.002
20	Ctrl/20%	0.312	0.006	0.749	4.040	0.003
21	Ctrl/20%	0.425	0.009	1.020	1.807	0.009
22	Ctrl/20%	0.959	0.019	2.302	5.743	0.007
23	Ctrl/20%	0.564	0.011	1.354	6.155	0.004
24	Ctrl/20%	0.508	0.010	1.219	6.993	0.003
25	MCD/water	1.437	0.029	3.449	1.843	0.031
26	MCD/water	0.375	0.008	0.900	3.621	0.004
27	MCD/water	0.437	0.009	1.049	2.433	0.007
28	MCD/water	0.922	0.018	2.213	2.621	0.014
29	MCD/water	4.463	0.089	10.711	3.621	0.049
31	MCD/8%	15.732	0.315	37.757	3.336	0.189
32	MCD/8%	0.500	0.010	1.200	2.107	0.009
33	MCD/8%	0.250	0.005	0.600	3.390	0.003
34	MCD/8%	1.874	0.037	4.498	2.564	0.029
35	MCD/8%	1.064	0.021	2.554	2.371	0.018
36	MCD/8%	6.900	0.138	16.560	3.150	0.088
37	MCD/8%	5.539	0.111	13.294	3.263	0.068
38	MCD/20%	0.375	0.008	0.900	3.857	0.004
39	MCD/20%	0.375	0.008	0.900	6.129	0.002
40	MCD/20%					
41	MCD/20%	1.064	0.021	2.554	2.697	0.016
42	MCD/20%	4.973	0.099	11.935	2.477	0.080
43	MCD/20%	9.400	0.188	22.560	3.111	0.121
44	MCD/20%	5.199	0.104	12.478	2.477	0.084
45	MCD/20%	5.823	0.116	13.975	2.235	0.104
			MEAN	SD		
		CTRL	0.005	0.003		
		CTRL/8%	0.004	0.001	(excl no. 15)	
		CTRL/20%	0.004	0.002		
		MCD	0.021	0.017		
		MCD/8%	0.058	0.061		
		MCD/20%	0.059	0.046		

Appendix 3
Raw Data: Short Term Study

Appendix 3.1: Raw data, mean and SD of hepatic TG

Mouse #	Treatment	TG from curve	TG per ul sample	Total TG in sample [ug]	Trigs. per mg protein [ug/mg]	Total protein [mg]
73	Ctrl	5.82	0.58	1163.04	71.82	16.20
74	Ctrl	7.90	0.79	1580.86	94.24	16.78
75	Ctrl	7.42	0.74	1484.44	83.41	17.80
76	Ctrl	7.26	0.73	1452.30	83.32	17.43
77	Ctrl	3.89	0.39	777.37	54.95	14.15
78	Ctrl	5.98	0.60	1195.18	42.14	28.37
85	Ctrl+4%	4.44	0.44	887.20	104.99	8.45
87	Ctrl+4%	4.23	0.42	845.20	99.44	8.50
88	Ctrl+4%	3.24	0.32	648.60	86.48	7.50
89	Ctrl+4%	5.46	0.55	1091.80	116.15	9.40
90	Ctrl+4%	3.76	0.38	751.00	90.48	8.30
98	Ctrl+8%	4.69	0.47	938.07	111.74	8.40
99	Ctrl+8%	5.49	0.55	1098.76	127.73	8.60
100	Ctrl+8%	4.53	0.45	905.93	121.48	7.46
101	Ctrl+8%	2.44	0.24	488.11	58.51	8.34
102	Ctrl+8%	4.85	0.49	970.21	85.35	11.37
109	MCD	11.12	1.11	2223.66	168.65	13.19
110	MCD	11.60	1.16	2320.08	186.54	12.44
111	MCD	15.78	1.58	3155.71	174.40	18.10
112	MCD	7.26	0.73	1452.30	185.36	7.84
113	MCD	10.15	1.02	2030.82	147.86	13.74
114	MCD	12.56	1.26	2512.92	169.25	14.85
121	MCD+4%	25.23	2.52	5045.80	731.28	6.90
122	MCD+4%	12.11	1.21	2421.20	410.37	5.90
123	MCD+4%	6.82	0.68	1364.40	209.91	6.50
124	MCD+4%	19.95	1.99	3989.20	664.87	6.00
125	MCD+4%	23.01	2.30	4602.60	626.20	7.35
126	MCD+4%	24.55	2.45	4909.40	727.32	6.75
133	MCD+8%	9.19	0.92	1837.98	292.91	6.28
134	MCD+8%	17.22	1.72	3444.97	558.12	6.17
135	MCD+8%	11.28	1.13	2255.80	340.37	6.63
136	MCD+8%	6.94	0.69	1388.02	238.70	5.82
137	MCD+8%	8.23	0.82	1645.14	248.04	6.63
138	MCD+8%	12.24	1.22	2448.64	410.33	5.97
					MEAN	SD
				Ctrl	71.64	17.96
				Ctrl+4%	99.51	10.57
				Ctrl+8%	100.96	25.69
				MCD	172.01	12.89
				MCD+4%	561.66	190.46
				MCD+8%	348.08	110.35

Appendix 3.2: Raw data, mean and SD of CD

Mouse #	Treatment	OD 234	CD [nMol]	CD per mg protein	Total protein [mg]
73	Ctrl	0.118	100.00	6.17	16.20
74	Ctrl	0.117	99.15	5.91	16.78
75	Ctrl	0.167	141.53	7.95	17.80
76	Ctrl	0.279	236.44	13.57	17.43
77	Ctrl	0.146	123.73	8.75	14.15
78	Ctrl	0.133	112.71	3.97	28.37
85	Ctrl+4%	0.099	83.90	9.93	8.45
87	Ctrl+4%	0.094	79.66	9.37	8.50
88	Ctrl+4%	0.1	84.75	11.30	7.50
89	Ctrl+4%	0.118	100.00	10.64	9.40
90	Ctrl+4%	0.115	97.46	11.74	8.30
98	Ctrl+8%	0.139	117.80	14.03	8.40
99	Ctrl+8%	0.113	95.76	11.13	8.60
100	Ctrl+8%	0.133	112.71	15.11	7.46
101	Ctrl+8%	0.133	112.71	13.51	8.34
102	Ctrl+8%	0.164	138.98	12.23	11.37
109	MCD	0.143	121.19	9.19	13.19
110	MCD	0.255	216.10	17.38	12.44
111	MCD	0.226	191.53	10.58	18.10
112	MCD	0.157	133.05	16.98	7.84
113	MCD	0.162	137.29	10.00	13.74
114	MCD	0.151	127.97	8.62	14.85
121	MCD+4%	0.156	132.20	19.16	6.90
122	MCD+4%	0.127	107.63	18.24	5.90
123	MCD+4%	0.19	161.02	24.77	6.50
124	MCD+4%	0.159	134.75	22.46	6.00
125	MCD+4%	0.205	173.73	23.64	7.35
126	MCD+4%	0.174	147.46	21.85	6.75
133	MCD+8%	0.223	188.98	30.12	6.28
134	MCD+8%	0.338	286.44	46.41	6.17
135	MCD+8%	0.229	194.07	29.28	6.63
136	MCD+8%	0.218	184.75	31.77	5.82
137	MCD+8%	0.186	157.63	23.77	6.63
138	MCD+8%	0.178	150.85	25.28	5.97
				MEAN	SD
			Ctrl	7.72	3.03
			Ctrl + 4%	10.60	0.87
			Ctrl+8%	13.20	1.39
			MCD	12.12	3.63
			MCD + 4%	21.69	2.32
			MCD+8%	31.10	7.38

Appendix 3.3: Raw data, mean and SD for fTBARS

Mouse #	Treatment	OD 540	fTBARS [nMol]	fTBARS per mg protein	Total protein [mg
73	Ctrl	0.004	7.89	0.49	16.20
74	Ctrl	0	0.00	0.00	16.78
75	Ctrl	0	0.00	0.00	17.80
76	Ctrl	0	0.00	0.00	17.43
77	Ctrl	0.001	1.97	0.14	14.15
78	Ctrl	0.102	201.19	7.09	28.37
85	Ctrl+4%	0.057	112.43	13.31	8.45
87	Ctrl+4%	0.046	90.73	10.67	8.50
88	Ctrl+4%	0.053	104.54	13.94	7.50
89	Ctrl+4%	0.07	138.07	14.69	9.40
90	Ctrl+4%	0.056	110.46	13.31	8.30
98	Ctrl+8%	0.001	1.97	0.23	8.40
99	Ctrl+8%	0	0.00	0.00	8.60
100	Ctrl+8%	0.002	3.94	0.53	7.46
101	Ctrl+8%	0	0.00	0.00	8.34
102	Ctrl+8%	0.002	3.94	0.35	11.37
109	MCD	0.082	161.74	12.27	13.19
110	MCD	0.099	195.28	15.70	12.44
111	MCD	0.078	153.85	8.50	18.10
112	MCD	0.051	100.60	12.84	7.84
113	MCD	0.071	140.05	10.20	13.74
114	MCD	0.059	116.38	7.84	14.85
121	MCD+4%	0.048	94.68	13.72	6.90
122	MCD+4%	0.045	88.76	15.04	5.90
123	MCD+4%	0.041	80.87	12.44	6.50
124	MCD+4%	0.052	102.57	17.09	6.00
125	MCD+4%	0.07	138.07	18.79	7.35
126	MCD+4%	0.062	122.29	18.12	6.75
133	MCD+8%	0.019	37.48	5.97	6.28
134	MCD+8%	0.027	53.26	8.63	6.17
135	MCD+8%	0.032	63.12	9.52	6.63
136	MCD+8%	0.003	5.92	1.02	5.82
137	MCD+8%	0.007	13.81	2.08	6.63
138	MCD+8%	0.012	23.67	3.97	5.97
		MEAN	SD		
	Ctrl	1.29	2.60		
	Ctrl + 4%	13.18	1.35		
	Ctrl+8%	0.22	0.20		
	MCD	11.22	2.70		
	MCD + 4%	15.87	2.31		
	MCD+8%	5.20	3.16		

Appendix 3.4: Raw data, mean and SD for tTBARS

Mouse #	Treatment	OD 540	tTBARS [nMol]	tTBARS per mg protein	Total protein [mg]
73	Ctrl	0.027	53.26	3.29	16.20
74	Ctrl	0.041	80.87	4.82	16.78
75	Ctrl	0.033	65.09	3.66	17.80
76	Ctrl	0.041	80.87	4.64	17.43
77	Ctrl	0.052	102.57	7.25	14.15
78	Ctrl	0.112	220.92	7.79	28.37
85	Ctrl+4%	0.06	118.35	14.01	8.45
87	Ctrl+4%	0.049	96.65	11.37	8.50
88	Ctrl+4%	0.05	98.62	13.15	7.50
89	Ctrl+4%	0.053	104.54	11.12	9.40
90	Ctrl+4%	0.041	80.87	9.74	8.30
98	Ctrl+8%	0.074	145.96	17.39	8.40
99	Ctrl+8%	0.069	136.10	15.82	8.60
100	Ctrl+8%	0.071	140.05	18.78	7.46
101	Ctrl+8%	0.07	138.07	16.55	8.34
102	Ctrl+8%	0.068	134.13	11.80	11.37
109	MCD	0.338	666.70	50.56	13.19
110	MCD	0.703	1386.65	111.49	12.44
111	MCD	1.085	2140.14	118.27	18.10
112	MCD	0.286	564.13	72.00	7.84
113	MCD	0.553	1090.78	79.42	13.74
114	MCD	0.448	883.67	59.52	14.85
121	MCD+4%	0.558	1100.64	159.51	6.90
122	MCD+4%	0.22	433.94	73.55	5.90
123	MCD+4%	0.198	390.55	60.08	6.50
124	MCD+4%	0.606	1195.32	199.22	6.00
125	MCD+4%	0.887	1749.59	238.04	7.35
126	MCD+4%	1.0845	2139.15	316.91	6.75
133	MCD+8%	0.709	1398.49	222.87	6.28
134	MCD+8%	0.98	1933.03	313.17	6.17
135	MCD+8%	0.952	1877.80	283.33	6.63
136	MCD+8%	0.297	585.83	100.74	5.82
137	MCD+8%	0.274	540.46	81.49	6.63
138	MCD+8%	0.421	830.41	139.16	5.97
		MEAN	SD		
	Ctrl	5.24	1.70		
	Ctrl + 4%	11.88	1.52		
	Ctrl+8%	16.07	2.35		
	MCD	81.88	25.12		
	MCD + 4%	174.55	89.85		
	MCD+8%	190.13	88.78		

Appendix 4
Raw Data: TNFα Knockout Study

Appendix 4.1: Weights [g] in TNFS

Mouse #	Day 0	Day 7	Day 14	Day 21	Day 28 23.09.02 Sacr,	Day 30 25.09.02 Sacr.
1	27.45	28.30	29.51	30.74		32.0 liv wt 1.6
2	27.85	28.27	28.95	30.53		31.4 liv wt 1.6
25	27.36	27.45	28.97	30.36		26.2 liv wt 0.8
26	25.03	25.22	25.35	25.62		25.2 liv wt 1.0
5 4	29.27 39.45	31.06	31.04	32.49		26.4 liv wt 1.0
6	29.48	28.57	30.73	32.66		32.2 liv wt 1.4
7	24.94	22.05	19.12	17	16.0 liv wt 0.6	
8	32.15	28.65	24.22	21.93	17.2 liv wt 0.6	
9	29.32	25.67	21.22	19.37	Killed 22.09.02 14.22	
10	25.11	23.02	19.41	17.86	16.0 liv wt 0.8	
11	24.14	20.97	17.87	16.39	12.0 liv wt. 0.4	
12	21.48	20.56	17.34	15.93	F/d 22.09.02 11.25	
13	25.44	26.30	25.70	25.85		27.8 liv wt 1.2
14	27.46	27.95	26.63	28.09		30.2 liv wt 1.4
15	26.88	26.20	25.81	25.67		27.2 liv wt 1.2
16	25.04	25.05	25.17	26.32		25.2 liv wt 1.2
17	25.01	24.35	24.25	25.08		25.0 liv wt 1.2
18	24.63	24.35	25.91	26.87		28.0 liv wt 1.2
19	25.21	25.31	19.51	18.97	17.8 liv wt 0.8	
20	26.81	21.77	21.49	20.14	18.8 liv wt 0.8	
21	26.67	23.90	21.33	19.68	18.4 liv wt 0.8	
22	27.36	24.39	22.46	21.10	19.8 liv wt 1.0	
23	27.22	23.23	20.86	19.32	16.6 liv wt 0.6	
24	25.18	22.48	19.23	18.06	17.0 liv wt 0.6	

Liv wt: liver weight

Appendix 4.2: ALT levels, mean (U/L) and SD for TNFS

Mouse #	Treatment	ALT
1	CTRL/KO	38
2	CTRL/KO	24
25	CTRL/KO	42
26	CTRL/KO	34
4	CTRL/KO	14
6	CTRL/KO	17
7	MCD/KO	177
8	MCD/KO	75
10	MCD/KO	145
11	MCD/KO	60
13	CTRL/WT	6
14	CTRL/WT	9
15	CTRL/WT	12
16	CTRL/WT	17
17	CTRL/WT	16
18	CTRL/WT	15
19	MCD/WT	118
20	MCD/WT	140
21	MCD/WT	110
22	MCD/WT	252
23	MCD/WT	368
24	MCD/WT	446
	MEAN	SD
CTRL/WT	12.5	3.95
CTRL/KO	28.17	10.53
MCD/WT	239	129.58
MCD/KO	114.25	48.39

Appendix 4.3: Liver pathology in the Tumor necrosis factor α study

Mouse #	Treatment	Fat (score)	Fat (distribution)	Inflammatory foci score	No. foci	D/PAS Macs (score)	No. macs
1	Ctrl ko	0	N/A	0	1	0	0
2	Ctrl ko	0	N/A	0	0	0	0
25	Ctrl ko	0	N/A	0	2	0	0
26	Ctrl ko	0	N/A	0	1	0	0
4	Ctrl ko	0	N/A	0	2	0	0
6	Ctrl ko	0	N/A	0	0	0	0
7	MCD ko	2, query1↑	Random	3	25	0	0
8	MCD ko	2	Random	2	15	0	0
10	MCD ko	3↓	Random	3	25	0	0
11	MCD ko	1	Random	2	12		
13	Ctrl wt	0	N/A	0	0	0	
14	Ctrl wt	0	N/A	0	2	0	0
15	Ctrl wt	0	N/A	0	0	0	0
16	Ctrl wt	0	N/A	0	1	0	0
17	Ctrl wt	0	N/A	0	1	0	0
18	Ctrl wt	0	N/A	0	3	0	0
19	MCD wt	3	Zones 1 to 3	1	8	0	0
20	MCD wt	1↓	Random	0	2	0	0
21	MCD wt	2, query 1↑	Zone 1? Query random	2	18	0	0
22	MCD wt	3↓	Zones 1 to 3	2	15	0	0
23	MCD wt	1	Random	2	15	0	0
24	MCD wt	2	Zones 1 to 3	2	11	0	0

Macs: Enlarged macrophages; **Random** indicates some fat was found in all zones with no zonal predominance.
All scores and numbers based on counts in 20hpf.

Appendix 4.4: Raw data, mean and SD for Hyp measurements

Mouse #	Treatment	Hyp from curve [ug]	Hyp in sample [ug]	Total protein [mg]	Hyp per mg protein
1	CTRL/KO	0.82	16.38	11.52	1.42
2	CTRL/KO	1.10	21.94	18.22	1.20
25	CTRL/KO	0.65	13.04	10.05	1.30
26	CTRL/KO	N/a	N/a	N/a	N/a
4	CTRL/KO	0.99	19.72	15.43	1.28
6	CTRL/KO	1.54	30.84	13.58	2.27
7	MCD/KO	1.76	35.29	8.69	4.06
8	MCD/KO	2.88	57.54	10.54	5.46
10	MCD/KO	2.54	50.87	14.24	3.57
11	MCD/KO	1.88	37.52	13.12	2.86
13	CTRL/WT	2.77	55.32	16.94	3.26
14	CTRL/WT	1.76	35.29	14.96	2.36
15	CTRL/WT	3.04	60.88	15.53	3.92
16	CTRL/WT	2.82	56.43	16.16	3.49
17	CTRL/WT	3.21	64.22	15.58	4.12
18	CTRL/WT	2.82	56.43	16.05	3.52
19	MCD/WT	3.04	60.88	12.82	4.75
20	MCD/WT	2.88	57.54	14.24	4.04
21	MCD/WT	2.82	56.43	16.21	3.48
22	MCD/WT	2.60	51.98	14.24	3.65
23	MCD/WT	2.49	49.75	15.95	3.12
24	MCD/WT	2.38	47.53	12.42	3.83
			MEAN	SD	
		CTRL/KO	1.49	0.39	
		MCD/KO	3.99	0.95	
		CTRL/WT	3.45	0.56	
		MCD/WT	3.62	0.31	

Appendix 4.5: Raw data, mean and SD for hepatic TG

Mouse #	Treatment	TG from curve [ug]	TG in sample [ug]	Total protein [mg]	TG per mg protein
1	CTRL/KO	1.89	378.79	11.52	32.88
2	CTRL/KO	0.75	150.48	18.22	8.26
25	CTRL/KO	6.13	1226.80	10.05	122.10
26	CTRL/KO	N/a	N/a	N/a	N/a
4	CTRL/KO	3.04	607.10	15.43	39.36
6	CTRL/KO	0.92	183.10	13.58	13.49
7	MCD/KO	4.67	933.25	8.69	107.35
8	MCD/KO	6.46	1292.03	10.54	122.63
10	MCD/KO	8.91	1781.26	14.24	125.08
11	MCD/KO	3.04	607.10	13.12	46.27
13	CTRL/WT	3.20	639.71	16.94	37.75
14	CTRL/WT	3.69	737.56	14.96	49.30
15	CTRL/WT	2.38	476.64	15.53	30.69
16	CTRL/WT	2.87	574.48	16.16	35.56
17	CTRL/WT	5.81	1161.56	15.58	74.55
18	CTRL/WT	3.85	770.18	16.05	47.98
19	MCD/WT	5.16	1031.10	12.82	80.43
20	MCD/WT	4.67	933.25	14.24	65.54
21	MCD/WT	22.93	4586.20	16.21	282.96
22	MCD/WT	9.40	1879.11	14.24	131.96
23	MCD/WT	3.69	737.56	15.95	46.25
24	MCD/WT	4.18	835.41	12.42	67.27
	MCD diet 10ul	2.37			
	MCD diet 30ul	3.92			
	Ctrl diet 10ul	1.60			
	Ctrl diet 30ul	4.70			
			MEAN	SD	
		Ctrl KO	23.49	41.11	
		MCD KO	100.33	31.95	
		Ctrl WT	45.97	14.38	
		MCD WT	112.40	80.73	

Appendix 4.6: Raw data, mean and SD for serum TG

Mouse #	Treatment	Serum TG [ug]	TG [mg] in 1L serum
1	CTRL/KO	22.74	1136.98
2	CTRL/KO	25.76	1287.78
25	CTRL/KO	19.42	971.11
26	CTRL/KO	13.39	669.52
4	CTRL/KO	17.16	858.01
6	CTRL/KO	17.16	858.01
7	MCD/KO	10.53	526.26
8	MCD/KO	15.80	790.15
10	MCD/KO	9.47	473.48
11	MCD/KO	11.88	594.12
13	CTRL/WT	20.78	1038.96
14	CTRL/WT	14.60	729.83
15	CTRL/WT	21.38	1069.12
16	CTRL/WT	15.50	775.07
17	CTRL/WT	14.75	737.37
18	CTRL/WT	13.69	684.60
19	MCD/WT	11.88	594.12
20	MCD/WT	8.72	435.78
21	MCD/WT	11.58	579.04
22	MCD/WT	10.53	526.26
23	MCD/WT	12.49	624.28
24	MCD/WT	13.54	677.06
		MEAN	SD
	CTRL/WT	839.16	154.44
	CTRL/KO	963.57	201.66
	MCD/WT	572.76	76.32
	MCD/KO	596.00	119.97

Appendix 4.7: Raw data, mean and SD for CD

Mouse #	Treatment	OD 234	CD [nMol]	Total protein [mg]	CD per mg protein
1	CTRL/KO	0.101	85.59	11.52	7.43
2	CTRL/KO	0.099	83.90	18.22	4.60
25	CTRL/KO	0.167	141.53	10.05	14.09
26	CTRL/KO	0.151	127.97	13.83	9.25
4	CTRL/KO	0.142	120.34	15.43	7.80
6	CTRL/KO	0.09325	79.03	13.58	5.82
7	MCD/KO	0.335	283.90	8.69	32.66
8	MCD/KO	0.324	274.58	10.54	26.06
10	MCD/KO	0.306	259.32	14.24	18.21
11	MCD/KO	0.149	126.27	13.12	9.62
13	CTRL/WT	0.099	83.90	16.94	4.95
14	CTRL/WT	0.1185	100.42	14.96	6.71
15	CTRL/WT	0.102	86.44	15.53	5.57
16	CTRL/WT	0.13	110.17	16.16	6.82
17	CTRL/WT	0.188	159.32	15.58	10.23
18	CTRL/WT	0.147	124.58	16.05	7.76
19	MCD/WT	0.174	147.46	12.82	11.50
20	MCD/WT	0.174	147.46	14.24	10.35
21	MCD/WT	0.164	138.98	16.21	8.57
22	MCD/WT	0.212	179.66	14.24	12.62
23	MCD/WT	0.27	228.81	15.95	14.35
24	MCD/WT	0.225	190.68	12.42	15.35
				MEAN	SD
			CTRL/KO	6.98	1.61
			MCD/KO	21.64	8.62
			CTRL/WT	7.01	1.70
			MCD/WT	12.13	2.30

Appendix 4.8: Raw data, mean and SD for LOOH

Mouse #	Treatment	LOOH from curve [nMol]	LOOH in sample [nMol]	Total protein [mg]	LOOH per mg protein
1	CTRL/KO	0.08	2.10	11.52	0.18
2	CTRL/KO	0.07	1.64	18.22	0.09
25	CTRL/KO	0.26	6.48	10.05	0.64
26	CTRL/KO	0.18	4.44	13.83	0.32
4	CTRL/KO	0.17	4.21	15.43	0.27
6	CTRL/KO	0.13	3.27	13.58	0.24
7	MCD/KO	0.23	5.65	8.69	0.65
8	MCD/KO	0.42	10.54	10.54	1.00
10	MCD/KO	1.24	31.08	14.24	2.18
11	MCD/KO	0.24	6.08	13.12	0.46
13	CTRL/WT	N/a	N/a	N/a	N/a
14	CTRL/WT	0.05	1.17	14.96	0.08
15	CTRL/WT	0.08	1.96	15.53	0.13
16	CTRL/WT	0.08	2.09	16.16	0.13
17	CTRL/WT	0.07	1.77	15.58	0.11
18	CTRL/WT	0.07	1.64	16.05	0.10
19	MCD/WT	0.57	14.30	12.82	1.12
20	MCD/WT	0.54	13.59	14.24	0.95
21	MCD/WT	0.39	9.83	16.21	0.61
22	MCD/WT	0.70	17.60	14.24	1.24
23	MCD/WT	0.35	8.66	15.95	0.54
24	MCD/WT	0.27	6.79	12.42	0.55
			MEAN	SD	
		CTRL/KO	0.22	0.08	
		MCD/KO	1.07	0.67	
		CTRL/WT	0.11	0.02	
		MCD/WT	0.83	0.28	

Appendix 4.9: Raw data, mean and SD for fTBARS

Mouse #	Treatment	OD 540	fTBARS [nMol]	Total protein [mg]	fTBARS per mg protein
1	CTRL/KO	0.025	49.31	11.52	4.28
2	CTRL/KO	0.027	53.26	18.22	2.92
25	CTRL/KO	0.1405	277.13	10.05	27.58
26	CTRL/KO	0.047	92.71	13.83	6.70
4	CTRL/KO	0.07	138.07	15.43	8.95
6	CTRL/KO	0.035	69.04	13.58	5.08
7	MCD/KO	0.071	140.05	8.69	16.11
8	MCD/KO	0.062	122.29	10.54	11.61
10	MCD/KO	0.055	108.49	14.24	7.62
11	MCD/KO	0.037	72.98	13.12	5.56
13	CTRL/WT	0.004	7.89	16.94	0.47
14	CTRL/WT	0.006	11.83	14.96	0.79
15	CTRL/WT	0.005	9.86	15.53	0.64
16	CTRL/WT	0.005	9.86	16.16	0.61
17	CTRL/WT	0.002	3.94	15.58	0.25
18	CTRL/WT	0.006	11.83	16.05	0.74
19	MCD/WT	0.007	13.81	12.82	1.08
20	MCD/WT	0.008	15.78	14.24	1.11
21	MCD/WT	0.013	25.64	16.21	1.58
22	MCD/WT	0.007	17.02	14.24	1.20
23	MCD/WT	0.008	15.78	15.95	0.99
24	MCD/WT	0.006	11.83	12.42	0.95
			MEAN	SD	
		Ctrl/KO	5.59	2.08	*Mouse 25 excluded
		MCD/KO	10.22	4.03	
		Ctrl/WT	0.58	0.18	
		MCD/WT	1.15	0.21	

Appendix 4.10: Raw data, mean, SD of tTBARS

Mouse #	Treatment	OD 540	tTBARS [nMol]	Total protein [mg]	tTBARS per mg protein
1	CTRL/KO	0.139	274.17	11.52	23.80
2	CTRL/KO	0.083	163.72	18.22	8.98
25	CTRL/KO	0.272	536.51	10.05	53.40
26	CTRL/KO	0.198	390.55	13.83	28.23
4	CTRL/KO	0.124	244.59	15.43	15.86
6	CTRL/KO	0.133	262.34	13.58	19.32
7	MCD/KO	1.055	2080.96	8.69	239.37
8	MCD/KO	0.533	1051.33	10.54	99.79
10	MCD/KO	1.149	2266.38	14.24	159.15
11	MCD/KO	0.068	134.13	13.12	10.22
13	CTRL/WT	0.103	203.17	16.94	11.99
14	CTRL/WT	0.09	177.52	14.96	11.87
15	CTRL/WT	0.092	181.47	15.53	11.69
16	CTRL/WT	0.111	218.94	16.16	13.55
17	CTRL/WT	0.071	140.05	15.58	8.99
18	CTRL/WT	0.1	197.25	16.05	12.29
19	MCD/WT	0.248	489.17	12.82	38.16
20	MCD/WT	0.277	546.38	14.24	38.37
21	MCD/WT	0.197	388.58	16.21	23.97
22	MCD/WT	0.271	658.85	14.24	46.27
23	MCD/WT	0.153	301.79	15.95	18.93
24	MCD/WT	0.183	360.96	12.42	29.07
			AVG	STD	
		Ctrl/KO	24.39	17.16	
		MCD/KO	127.13	83.72	
		Ctrl/WT	11.73	1.37	
		MCD/WT	32.46	9.35	

Appendix 4.11: Raw data, mean and SD for CYP2E1 activity

Mouse #	Treatment	nMols *p*-AP from curve	nMols *p*-AP per ul	nMols *p*-AP in 120 ul	Microsomal protein [mg]	nMols p-AP/mg protein/min
1	CTRL/KO	0.24	0.005	0.582	7.00	0.001
2	CTRL/KO	0.36	0.007	0.873	8.53	0.002
25	CTRL/KO	0.73	0.015	1.747	5.99	0.005
26	CTRL/KO	1.03	0.021	2.475	6.72	0.006
4	CTRL/KO	0.67	0.013	1.601	7.12	0.004
6	CTRL/KO	0.49	0.010	1.165	8.09	0.002
7	MCD/KO	6.56	0.131	15.743	4.40	0.060
8	MCD/KO	3.03	0.061	7.282	4.81	0.025
10	MCD/KO	8.75	0.175	21.001	4.41	0.079
11	MCD/KO	7.59	0.152	18.225	3.32	0.091
13	CTRL/WT	0.36	0.007	0.873	8.11	0.002
14	CTRL/WT	0.49	0.010	1.165	7.84	0.002
15	CTRL/WT	0.36	0.007	0.873	8.86	0.002
16	CTRL/WT	0.55	0.011	1.310	7.24	0.003
17	CTRL/WT	0.42	0.008	1.019	8.11	0.002
18	CTRL/WT	0.24	0.005	0.582	7.61	0.001
19	MCD/WT	2.18	0.044	5.242	5.24	0.017
20	MCD/WT	3.34	0.067	8.011	5.74	0.023
21	MCD/WT	2.49	0.050	5.971	6.84	0.015
22	MCD/WT	3.88	0.078	9.323	6.19	0.025
23	MCD/WT	7.65	0.153	18.371	4.04	0.076
24	MCD/WT	8.51	0.170	20.416	5.24	0.065
					MEAN	SD
				CTRL/KO	0.003	0.002
				MCD/KO	0.064	0.025
				CTRL/WT	0.002	0.001
				MCD/WT	0.037	0.024

Appendix 5
Raw Data: LPS Study

Appendix 5.1: Weights [g] during the LPSS

Mouse # on cage	Treatment	Weight at Wk 0	Wk 1	Wk 2	Wk 3	Sacrifice (wk 4)	Liver wt [g]	New No.
1	MCD/LPS	25.0	21.5	19.8	17.9	16.6	0.6	9
2	MCD/LPS	26.6	22.7	17.4	15.8	16.8	0.8	10
3	MCD/LPS	27.1	22.0	19.3	18.0	16.8	0.8	11
4	MCD/LPS	25.6	21.6	19.0	17.7	16.6	0.6	12
5	MCD/LPS	24.9	21.2	18.6	17.1	17.4	0.8	13
6	MCD/LPS	26.0	22.1	16.4	15.2	17.4	0.8	14
7	MCD/LPS	23.4	19.5	22.3	20.6	15.4	0.6	15
8	MCD/LPS	23.8	22.5	20.9	19.3	15.8	0.8	16
1	MCD/Saline	26.0	22.3	19.6	18.2	17.0	0.8	17
2	MCD/Saline	22.7	18.9	21.4	19.9	15.6	0.6	18
3	MCD/Saline	24.3	20.7	20.3	18.6	17.4	0.8	19
4	MCD/Saline	24.2	20.9	20.0	18.9	17.4	1.0	20
5	MCD/Saline	23.7	19.7	19.9	18.3	16.4	0.8	21
6	MCD/Saline	22.2	18.5	20.7	18.9	14.8	0.6	22
7	MCD/Saline	28.2	23.9	18.2	16.3	19.6	0.8	23
8	MCD/Saline	26.9	25.5	19.5	17.7	19.2	0.8	24
1	Ctrl/LPS	23.9	25.2	25.9	27.1	25.6	1.0	25
2	Ctrl/LPS	24.4	25.4	26.2	26.9	25.4	1.0	26
3	Ctrl/LPS	23.5	23.8	24.5	24.8	26.0	1.2	27
4	Ctrl/LPS	23.7	24.8	26.0	27.3	23.8	1.2	28
5	Ctrl/LPS	24.9	26.5	26.3	28.4	26.8	1.2	29
6	Ctrl/LPS	25.0	27.2	27.8	29.1	28.8	1.2	30
7	Ctrl/LPS	22.0	23.7	24.6	27.4	23.8	1.0	31
8	Ctrl/LPS	22.3	22.7	25.2	23.6	22.4	1.0	32
1	Ctrl/Saline	24.6	26.0	28.1	28.9	29.2	1.2	1
2	Ctrl/Saline	23.3	23.9	24.2	25.3	25.4	1.2	2
3	Ctrl/Saline	23.4	25.8	27.5	28.9	30.4	1.2	3
4	Ctrl/Saline	25.3	25.1	27.3	27.6	28.6	1.2	4
5	Ctrl/Saline	24.8	26.1	23.5	27.0	28.2	1.4	5
6	Ctrl/Saline	25.0	26.7	28.5	30.1	31.4	1.2	6
7	Ctrl/Saline	21.4	21.6	22.6	23.0	23.8	1.2	7
8	Ctrl/Saline	23.7	25.5	26.0	27.5	27.4	1.2	8

Appendix 5.2: ALT

Mouse #	Treatment	ALT (U/ml)	
1	Ctrl/Saline	20	
2	Ctrl/Saline	22	
3	Ctrl/Saline	17	
4	Ctrl/Saline	18	
5	Ctrl/Saline	13	
6	Ctrl/Saline	22	
7	Ctrl/Saline	17	
8	Ctrl/Saline	13	
9	MCD/LPS	177	
10	MCD/LPS	239	
11	MCD/LPS	353	
12	MCD/LPS	93	
13	MCD/LPS	368	
14	MCD/LPS	218	
15	MCD/LPS	549	
16	MCD/LPS	167	
17	MCD/Saline	59	
18	MCD/Saline	85	
19	MCD/Saline	45	
20	MCD/Saline	65	
21	MCD/Saline	46	
22	MCD/Saline	90	
23	MCD/Saline	54	
24	MCD/Saline	67	
25	Ctrl/LPS	24	
26	Ctrl/LPS	36	
27	Ctrl/LPS	70	
28	Ctrl/LPS	364	
29	Ctrl/LPS	33	
30	Ctrl/LPS	66	
31	Ctrl/LPS	40	
32	Ctrl/LPS	166	
		MEAN	SD
	Ctrl	17.75	3.31
	Ctrl/LPS	99.88	108.44
	MCD/LPS	270.50	136.28
	MCD/Saline	63.88	15.56

Appendix 5.3: Liver Pathology in the Lipopolysaccharide Study

No.	Treatment	Fat (score)	Fat (distribution)	Inflammatory foci score	No. foci	D/PAS macs (score)	No. macs	Fibrosis (Score)
1	Ctrl/Saline	0	N/A	1	6	0	0	0
2	Ctrl/Saline	0	N/A	0	1	0	0	0
3	Ctrl/Saline	0	N/A	0	0	0	0	0
4	Ctrl/Saline	0	N/A	0	1	0	0	0
5	Ctrl/Saline	0	N/A	0	0	0	0	0
6	Ctrl/Saline	0	N/A	0	0	0	0	0
7	Ctrl/Saline	0	N/A	0	2	0	0	0
8	Ctrl/Saline	0	N/A	0	2	0	0	0
9	MCD/Saline	3	Zone 1	1	4	0	0	0
10	MCD/Saline	1	Zone 1	2	18	0	0	0
11	MCD/Saline	2	Zone 1	3	24	2	19	0
12	MCD/Saline	1↑	Zone 1	2	11	0	1	0
13	MCD/Saline	N/A	N/A	N/A	N/A	N/A	N/A	N/A
14	MCD/Saline	2↑, Query 3	Zone 1	2	10	0	0	0
15	MCD/Saline	1	Zone 1	3	29	0	0	0
16	MCD/Saline	1	Zone 1	2	13	0	1	0
17	MCD/LPS	1	Zone 1	2	19	0	1	0
18	MCD/LPS	2	Zone 1	2	16	0	0	0
19	MCD/LPS	1	Zone 1	2	15	0	0	0
20	MCD/LPS	2↓ or 1↑	Zone 1	2	17	0	0	0
21	MCD/LPS	1	Zone 1	3	20	0	0	0
22	MCD/LPS	1↓	Zone 1	3	29	0	0	0
23	MCD/LPS	0	Zone 1	1	6	0	0	0
24	MCD/LPS	1	Zone 1	2	13	0	0	0
25	Ctrl/LPS	0	N/A	2	19	0	0	0
26	Ctrl/LPS	0	N/A	2	11	0	0	0
27	Ctrl/LPS	0	N/A	2	10	0	0	0
28	Ctrl/LPS	0	N/A	2	11	0	1	0
29	Ctrl/LPS	0	N/A	2	10	0	0	0
30	Ctrl/LPS	0	N/A	2	18	0	2	0
31	Ctrl/LPS	0	N/A	2	12	0	0	0
32	Ctrl/LPS	0	N/A	1	9	0	1	0

Macs: Enlarged macrophages; **Random** indicates some fat was found in all zones with no zonal predominance.
All scores and numbers based on counts in 20hpf.

Appendix 5.4: Raw data, mean and SD for hepatic TG

Mouse #	Treatment	TG from curve [ug]	TG in sample [ug]	Total protein [mg]	TG per mg protein
1	Ctrl/Saline	3.92	784.02	18.02	43.51
2	Ctrl/Saline	2.03	405.74	17.68	22.95
3	Ctrl/Saline	2.37	474.52	15.99	29.68
4	Ctrl/Saline	3.40	680.85	21.94	31.03
5	Ctrl/Saline	2.89	577.68	18.77	30.78
6	Ctrl/Saline	3.58	715.24	18.02	39.69
7	Ctrl/Saline	2.72	543.29	19.52	27.83
8	Ctrl/Saline	4.26	852.80	19.04	44.78
9	MCD/LPS	4.44	887.19	18.70	47.44
10	MCD/LPS	2.72	543.29	12.66	42.91
11	MCD/LPS	3.40	680.85	16.53	41.19
12	MCD/LPS	2.72	543.29	11.35	47.88
13	MCD/LPS	3.75	749.63	9.59	78.18
14	MCD/LPS	4.09	818.41	11.94	68.56
15	MCD/LPS	4.26	852.80	16.80	50.76
16	MCD/LPS	6.50	1299.86	12.73	102.14
17	MCD/Saline	4.09	818.41	10.95	74.71
18	MCD/Saline	5.64	1127.92	11.67	96.61
19	MCD/Saline	3.40	680.85	13.59	50.11
20	MCD/Saline	3.75	749.63	14.52	51.64
21	MCD/Saline	3.75	749.63	15.79	47.48
22	MCD/Saline	4.44	887.19	17.41	50.96
23	MCD/Saline	3.23	646.46	17.61	36.71
24	MCD/Saline	5.98	1196.69	15.12	79.16
25	Ctrl/LPS	3.75	749.63	21.81	34.38
26	Ctrl/LPS	3.58	715.24	20.70	34.56
27	Ctrl/LPS	3.58	715.24	18.98	37.69
28	Ctrl/LPS	2.03	405.74	19.80	20.49
29	Ctrl/LPS	2.89	577.68	15.92	36.28
30	Ctrl/LPS	3.40	680.85	20.28	33.57
31	Ctrl/LPS	4.26	852.80	17.41	48.99
32	Ctrl/LPS	4.09	818.41	22.50	36.37
			MEAN	SD	
		CTRL	33.78	7.39	
		CTRL/LPS	35.29	7.24	
		MCD	60.92	18.93	
		MCD/LPS	59.88	20.05	

Appendix 5.5: Raw data, mean and SD for CD

Mouse #	Treatment	OD 234	CD [nMol]	Total Protein [mg]	CD/mg total protein
1	Ctrl/Saline	0.0995	84.32	18.02	4.68
2	Ctrl/Saline	0.09	76.27	17.68	4.31
3	Ctrl/Saline	0.107	90.68	15.99	5.67
4	Ctrl/Saline	0.102	86.44	21.94	3.94
5	Ctrl/Saline	0.083	70.34	18.77	3.75
6	Ctrl/Saline	0.088	74.58	18.02	4.14
7	Ctrl/Saline	0.086	72.88	19.52	3.73
8	Ctrl/Saline	0.092	77.97	19.04	4.09
9	MCD/LPS	0.117	98.73	18.70	5.28
10	MCD/LPS	0.143	121.19	12.66	9.57
11	MCD/LPS	0.102	86.02	16.53	5.20
12	MCD/LPS	0.137	116.10	11.35	10.23
13	MCD/LPS	0.155	131.36	9.59	13.70
14	MCD/LPS	0.143	121.19	11.94	10.15
15	MCD/LPS	0.186	157.63	16.80	9.38
16	MCD/LPS	0.126	106.78	12.73	8.39
17	MCD/Saline	0.091	76.69	10.95	7.00
18	MCD/Saline	0.148	125.42	11.67	10.74
19	MCD/Saline	0.095	80.08	13.59	5.89
20	MCD/Saline	0.112	94.92	14.52	6.54
21	MCD/Saline	0.121	102.54	15.79	6.49
22	MCD/Saline	0.1165	98.73	17.41	5.67
23	MCD/Saline	0.099	83.90	17.61	4.76
24	MCD/Saline	0.096	80.93	15.12	5.35
25	Ctrl/LPS	0.087	73.31	21.81	3.36
26	Ctrl/LPS	0.101	85.59	20.70	4.14
27	Ctrl/LPS	0.203	172.03	18.98	9.07
28	Ctrl/LPS	0.112	94.92	19.80	4.79
29	Ctrl/LPS	0.089	75.42	15.92	4.74
30	Ctrl/LPS	0.122	103.39	20.28	5.10
31	Ctrl/LPS	0.119	100.85	17.41	5.79
32	Ctrl/LPS	0.115	97.46	22.50	4.33
			MEAN	SD	
		CTRL	4.29	0.60	
		CTRL/LPS	5.16	1.62	
		MCD/LPS	8.99	2.60	
		MCD/Saline	6.56	1.72	

Appendix 5.6: Raw data, mean and SD of LOOH

Mouse #	Treatment	LOOH from curve [nMol]	LOOH in sample [nMol]	Total protein [mg]	LOOH per mg protein
1	Ctrl/Saline	0.22	5.59	18.02	0.31
2	Ctrl/Saline	0.38	9.62	17.68	0.54
3	Ctrl/Saline	0.24	5.98	15.99	0.37
4	Ctrl/Saline	0.34	8.45	21.94	0.38
5	Ctrl/Saline	0.33	8.19	18.77	0.44
6	Ctrl/Saline	0.33	8.32	18.02	0.46
7	Ctrl/Saline	0.26	6.50	19.52	0.33
8	Ctrl/Saline	0.29	7.28	19.04	0.38
9	MCD/LPS	0.32	8.06	18.70	0.43
10	MCD/LPS	0.60	14.96	12.66	1.18
11	MCD/LPS	0.51	12.87	16.53	0.78
12	MCD/LPS	0.76	18.99	11.35	1.67
13	MCD/LPS	1.18	29.43	9.59	3.07
14	MCD/LPS	0.69	17.17	11.94	1.44
15	MCD/LPS	0.51	12.74	16.80	0.76
16	MCD/LPS	0.32	7.93	12.73	0.62
17	MCD/Saline	0.51	12.78	10.95	1.17
18	MCD/Saline	0.63	15.84	11.67	1.36
19	MCD/Saline	0.57	14.24	13.59	1.05
20	MCD/Saline	0.60	15.04	14.52	1.04
21	MCD/Saline	0.55	13.71	15.79	0.87
22	MCD/Saline	0.63	15.84	17.41	0.91
23	MCD/Saline	0.50	12.51	17.61	0.71
24	MCD/Saline	0.53	13.18	15.12	0.87
25	Ctrl/LPS	0.26	6.52	21.81	0.30
26	Ctrl/LPS	0.37	9.31	20.70	0.45
27	Ctrl/LPS	0.33	8.25	18.98	0.43
28	Ctrl/LPS	0.38	9.45	19.80	0.48
29	Ctrl/LPS	0.30	7.45	15.92	0.47
30	Ctrl/LPS	0.31	7.72	20.28	0.38
31	Ctrl/LPS	0.51	12.78	17.41	0.73
32	Ctrl/LPS	0.31	7.85	22.50	0.35
		MEAN	SD		
	CTRL	0.40	0.07		
	CTRL/LPS	0.45	0.12		
	MCD/LPS	1.24	0.79		
	MCD/Saline	1.00	0.19		

Appendix 5.7: Raw data, mean and SD for fTBARS

Mouse #	Treatment	OD 540	fTBARS [nMol]	Total protein [mg]	fTBARS/mg protein
1	Ctrl/Saline	0.018	35.50	18.02	1.97
2	Ctrl/Saline	0.029	57.20	17.68	3.24
3	Ctrl/Saline	0.0165	32.55	15.99	2.04
4	Ctrl/Saline	0.0405	79.89	21.94	3.64
5	Ctrl/Saline	0.033	65.09	18.77	3.47
6	Ctrl/Saline	0.0465	91.72	18.02	5.09
7	Ctrl/Saline	0.0345	68.05	19.52	3.49
8	Ctrl/Saline	0.0365	72.00	19.04	3.78
9	MCD/LPS	0.0495	97.64	18.70	5.22
10	MCD/LPS	0.0535	105.53	12.66	8.33
11	MCD/LPS	0.021	41.42	16.53	2.51
12	MCD/LPS	0.037	72.98	11.35	6.43
13	MCD/LPS	0.0455	89.75	9.59	9.36
14	MCD/LPS	0.033	65.09	11.94	5.45
15	MCD/LPS	0.031	61.15	16.80	3.64
16	MCD/LPS	0.0385	75.94	12.73	5.97
17	MCD/Saline	0.0195	38.46	10.95	3.51
18	MCD/Saline	0.0265	52.27	11.67	4.48
19	MCD/Saline	0.02	39.45	13.59	2.90
20	MCD/Saline	0.028	55.23	14.52	3.80
21	MCD/Saline	0.021	41.42	15.79	2.62
22	MCD/Saline	0.028	55.23	17.41	3.17
23	MCD/Saline	0.0245	48.33	17.61	2.74
24	MCD/Saline	0.026	51.28	15.12	3.39
25	Ctrl/LPS	0.05	98.62	21.81	4.52
26	Ctrl/LPS	0.0325	64.11	20.70	3.10
27	Ctrl/LPS	0.035	69.04	18.98	3.64
28	Ctrl/LPS	0.0515	101.58	19.80	5.13
29	Ctrl/LPS	0.0325	64.11	15.92	4.03
30	Ctrl/LPS	0.0425	83.83	20.28	4.13
31	Ctrl/LPS	0.042	82.84	17.41	4.76
32	Ctrl/LPS	0.0505	99.61	22.50	4.43
			MEAN	SD	
		CTRL	3.34	0.93	
		CTRL/LPS	4.22	0.60	
		MCD/LPS	5.86	2.11	
		MCD/Saline	3.33	0.57	

Appendix 5.8: Raw data, mean and SD for tTBARs

Mouse #	Treatment	OD 540	tTBARS [nMol]	Total protein [mg]	tTBARS/mg protein
1	Ctrl/Saline	0.0405	79.89	18.02	4.43
2	Ctrl/Saline	0.033	65.09	17.68	3.68
3	Ctrl/Saline	0.0315	62.13	15.99	3.89
4	Ctrl/Saline	0.0335	66.08	21.94	3.01
5	Ctrl/Saline	0.0355	70.02	18.77	3.73
6	Ctrl/Saline	0.033	65.09	18.02	3.61
7	Ctrl/Saline	0.0335	66.08	19.52	3.38
8	Ctrl/Saline	0.031	61.15	19.04	3.21
9	MCD/LPS	0.3235	638.10	18.70	34.12
10	MCD/LPS	0.393	775.18	12.66	61.23
11	MCD/LPS	0.371	731.79	16.53	44.27
12	MCD/LPS	0.654	1290.00	11.35	113.68
13	MCD/LPS	0.6125	1208.14	9.59	125.99
14	MCD/LPS	0.6605	1302.82	11.94	109.14
15	MCD/LPS	0.6005	1184.47	16.80	70.51
16	MCD/LPS	0.6515	1285.07	12.73	100.97
17	MCD/Saline	0.4845	955.67	10.95	87.24
18	MCD/Saline	0.893	1761.42	11.67	150.88
19	MCD/Saline	0.2355	464.52	13.59	34.19
20	MCD/Saline	0.484	954.68	14.52	65.76
21	MCD/Saline	0.5055	997.09	15.79	63.15
22	MCD/Saline	0.4575	902.41	17.41	51.84
23	MCD/Saline	0.233	459.59	17.61	26.10
24	MCD/Saline	0.386	761.38	15.12	50.36
25	Ctrl/LPS	0.136	268.26	21.81	12.30
26	Ctrl/LPS	0.1675	330.39	20.70	15.96
27	Ctrl/LPS	0.1455	287.00	18.98	15.12
28	Ctrl/LPS	0.062	122.29	19.80	6.18
29	Ctrl/LPS	0.078	153.85	15.92	9.66
30	Ctrl/LPS	0.127	250.50	20.28	12.35
31	Ctrl/LPS	0.0895	176.54	17.41	10.14
32	Ctrl/LPS	0.1225	241.63	22.50	10.74
			MEAN	SD	
		CTRL	3.62	0.41	
		CTRL/LPS	11.56	2.93	
		MCD/LPS	82.49	32.24	
		MCD/Saline	66.19	2.93	